NORTHEAST BC GEOLOGICAL CARBON CAPTURE AND STORAGE ATLAS

Geoscience BC Report 2023-04

January 2023
Canadian Discovery Ltd.

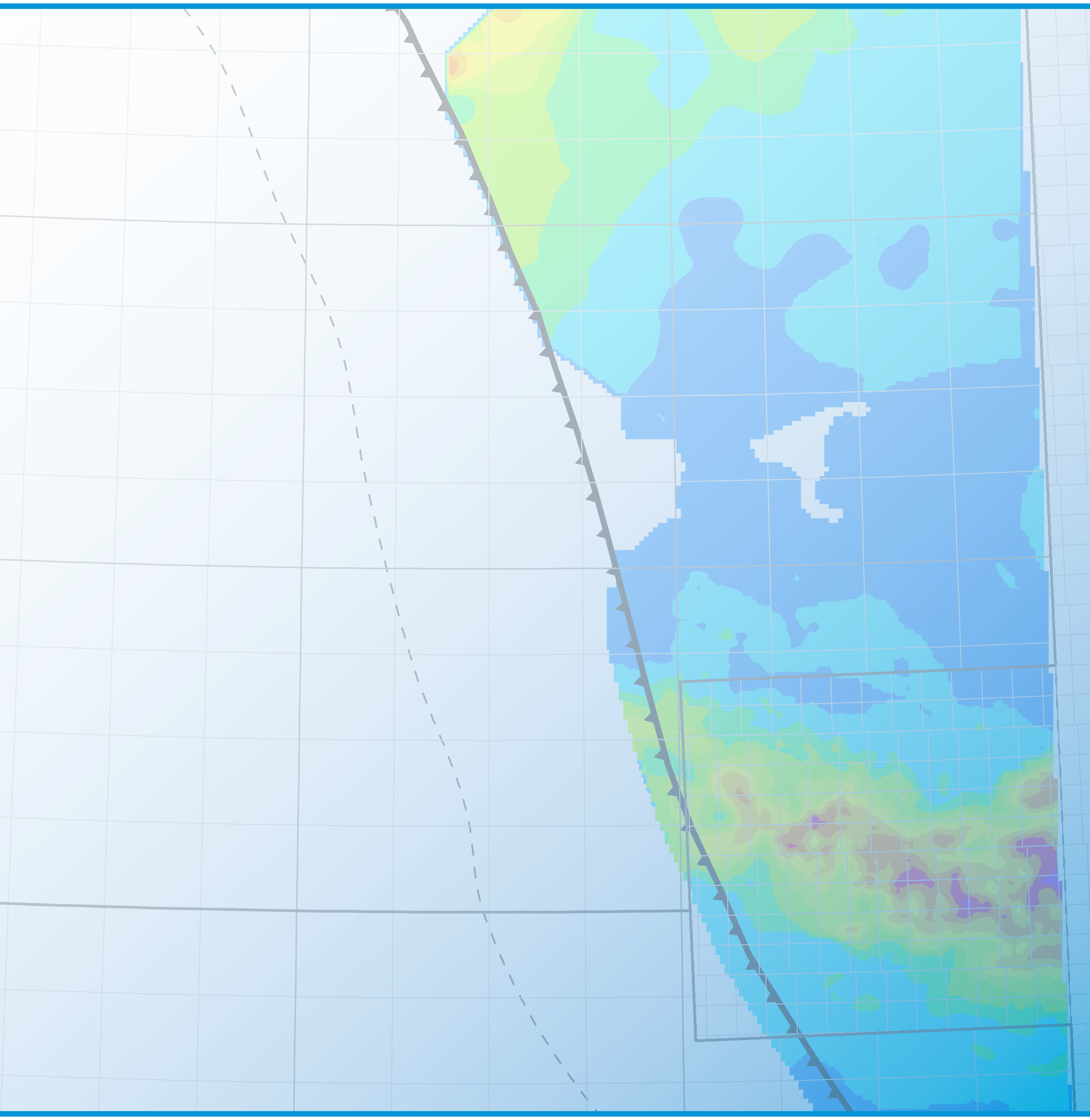

Geoscience BC
CICE B.C. CENTRE FOR INNOVATION & CLEAN ENERGY
BRITISH COLUMBIA
Canadian Discovery Ltd.

NORTHEAST BC GEOLOGICAL CARBON CAPTURE AND STORAGE ATLAS

Canadian Discovery Ltd.

JANUARY 2023

PREPARED FOR:
Geoscience BC

PREPARED BY:
Canadian Discovery Ltd.
APEGA Permit No. P09364

Tessa Wilson, M.Sc., P.Geo
Geologist

Natalie Sweet, P.Geo
Project Manager

PROFESSIONAL ENGINEER ALBERTA JOHN XIE

John Xie, P.Eng.
Evaluations Engineer

PROFESSIONAL GEOLOGIST ALBERTA ALLISON GIBBS

Allison Gibbs, P.Geol.
Senior Hydrodynamicist

W. Steven Donaldson, PhD, P. Geol.
Exploration Analyst

PROFESSIONAL GEOLOGIST ALBERTA MERIDEE FOCKLER

Meridee Fockler, P.Geol.
Technical Analysis Director

Geoscience BC   CICE B.C. CENTRE FOR INNOVATION & CLEAN ENERGY   BRITISH COLUMBIA   Canadian Discovery Ltd.

Table of Contents

1.0 EXECUTIVE SUMMARY 5
- Executive Summary 5
- Project Outcomes 7
- Acknowledgements 11

2.0 CARBON CAPTURE AND STORAGE (CCS) BASICS 12
- Introduction 12
- Carbon Capture 12
- Transportation 13
- Geological Storage Overview 14

3.0 CARBON STORAGE PROJECT CONSIDERATIONS 18
- Geological Carbon Storage Suitability Criteria 18
- Pressure, Temperature and Depth Requirements 18
- Potential CCS Risks and Risk Mitigation 18
- Hub Storage and Local Storage 19

4.0 ATLAS OVERVIEW 21
- Introduction to the Atlas 21
- Chapter Organization 21
- Formation Selection and Exclusion Criteria 21
- Atlas Components 22
- Carbon Storage Calculations 23

5.0 PEACE RIVER (PADDY/CADOTTE) FORMATION 24
- Peace River Overview 24
- Storage Complex 26
- Porosity-Permeability Correlations 30
- Hydrodynamics 30
- Carbon Storage Calculations 31

6.0 SPIRIT RIVER (NOTIKEWIN, FALHER) FORMATION 34
- Spirit River Overview 34
- Storage Complex 36
- Carbon Storage Calculations 38

7.0 BLUESKY FORMATION 41
- Bluesky Overview 41
- Storage Complex 43
- Porosity-Permeability Correlations 47
- Hydrodynamics 47
- Carbon Storage Calculations 48

8.0 CADOMIN-GETHING FORMATION 52
- Cadomin-Gething Overview 52
- Storage Complex 54
- Porosity-Permeability Correlations 58
- Hydrodynamics 58
- Carbon Storage Calculations 59

9.0 NIKANASSIN-DUNLEVY FORMATION ... 63
Nikanassin-Dunlevy Overview ... 63
Storage Complex ... 65
Porosity-Permeability Correlations ... 69
Hydrodynamics ... 70
Carbon Storage Calculations ... 71

10.0 BALDONNEL-PARDONET FORMATION ... 75
Baldonnel-Pardonet Overview ... 75
Storage Complex ... 77
Porosity-Permeability Correlations ... 81
Hydrodynamics ... 82
Carbon Storage Calculations ... 83

11.0 CHARLIE LAKE FORMATION ... 87
Charlie Lake Overview ... 87
Storage Complex ... 89
Carbon Storage Calculations ... 91

12.0 HALFWAY FORMATION ... 94
Halfway Overview ... 94
Storage Complex ... 96
Porosity-Permeability Correlations ... 100
Hydrodynamics ... 101
Carbon Storage Calculations ... 102

13.0 BELLOY FORMATION ... 106
Belloy Overview ... 106
Storage Complex ... 108
Porosity-Permeability Correlations ... 112
Hydrodynamics ... 113
Carbon Storage Calculations ... 114

14.0 DEBOLT FORMATION ... 118
Debolt Overview ... 118
Storage Complex ... 120
Porosity-Permeability Correlations ... 124
Hydrodynamics ... 124
Carbon Storage Calculations ... 125

15.0 JEAN MARIE FORMATION ... 128
Jean Marie Overview ... 128
Storage Complex ... 130
Carbon Storage Calculations ... 132

16.0 MIDDLE DEVONIAN CARBONATES ... 134
Middle Devonian Carbonates (Slave Point–Keg River) Overview ... 134
Storage Complex ... 136
Porosity-Permeability Correlations ... 141
Hydrodynamics ... 142
Carbon Storage Calculations ... 143

17.0 RECOMMENDATIONS ... 147
Recommendations ... 147
Next Steps ... 148
Proposed Future Areas of Study ... 150

Appendices

APPENDIX A 151
Regional Stratigraphy of NEBC 151
APPENDIX B 156
Carbon Storage Calculations 156
APPENDIX C 158
Pool Storage Database (Digital) 158
APPENDIX D 159
References and Resources 159
APPENDIX E 163
Maps, Shapefiles and List of Figures 163

Tables

Table 5.1 Peace River Favourability Attributes 24
Table 5.2 Depleted Peace River Pools 32
Table 5.3 Peace River Aquifers Properties and Storage Potential 32
Table 6.1 Spirit River Favourability Attributes 34
Table 6.2 Depleted Spirit River Pools 39
Table 7.1 Bluesky Favourability Attributes 41
Table 7.2 Top 25 Depleted Bluesky Pools 49
Table 7.3 Bluesky Aquifer Properties and Storage Potential 50
Table 8.1 Cadomin-Gething Favourability Attributes 52
Table 8.2 Top 25 Depleted Cadomin-Gething Pools 60
Table 8.3 Cadomin Aquifer Properties and Storage Potential 61
Table 9.1 Nikanassin-Dunlevy Favourability Attributes 63
Table 9.2 Top 25 Depleted Nikanassin-Dunlevy Pools 72
Table 9.3 Nikanassin-Dunlevy Aquifer Properties and Storage Potential 73
Table 10.1 Baldonnel-Pardonet Favourability Attributes 75
Table 10.2 Top 25 Depleted Baldonnel-Pardonet Pools 84
Table 10.3 Baldonnel-Pardonet Aquifer Properties and Storage Potential 85
Table 11.1 Charlie Lake Favourability Attributes 87
Table 11.2 Top 25 Depleted Charlie Lake Pools 92
Table 12.1 Halfway Favourability Attributes 94
Table 12.2 Top 25 Depleted Halfway Pools 103
Table 12.3 Halfway Aquifer Properties and Storage Potential 104
Table 13.1 Belloy Favourability Attributes 106
Table 13.2 Depleted Belloy Pools 115
Table 13.3 Belloy Aquifer Properties and Storage Potential 116
Table 14.1 Debolt Favourability Attributes 118
Table 14.2 Depleted Debolt Pools 126
Table 14.3 Debolt Aquifer Properties and Storage Potential 126
Table 15.1 Jean Marie Favourability Attributes 128
Table 15.2 Depleted Jean Marie Pool 132
Table 16.1 Middle Devonian Carbonates Favourability Attributes 134
Table 16.2 Top 25 Depleted Middle Devonian Carbonates Pools 144
Table 16.3 Middle Devonian Carbonates Aquifer Properties and Storage Potential 145

Figures

List of figures available in *Appendix E*

EXECUTIVE SUMMARY

Executive Summary

Carbon capture and storage (CCS) provides an opportunity to help British Columbia reach "net zero" carbon dioxide (CO_2) emissions by 2050 (CleanBC, 2018, 2021b). Permanent removal of excess CO_2, a greenhouse gas, from the atmosphere can be accomplished by safely storing CO_2 underground in rock units (geological storage) that are well below groundwater, with non-porous seals above, and in areas less prone to earthquake activity. This atlas study identifies and undertakes a preliminary quantification of the best CO_2 storage potential* locations in subsurface rock units in Northeastern British Columbia (NEBC), and is an important part of the information needed to assess the potential for CCS and hydrogen projects in the region (BC Hydrogen Strategy, 2021). Identifying areas with sufficient storage potential, in conjunction with knowledge of locations of stationary CO_2 emitters and existing infrastructure such as roads and pipelines, will assist in evaluation and decision making for potential carbon storage and hydrogen projects.

CO_2 storage is an important component of Canada's enhanced Paris targets (www.un.org), as well as the rapidly expanding low carbon intensity hydrogen energy sector. Hydrogen becomes a cost effective power solution in areas like NEBC where natural gas is plentiful and by-product CO_2 can be captured onsite and stored in geological reservoirs (NETL, 2021). This atlas can be used to high-grade prospective areas when considering future locations for CCS and hydrogen development.

Why NEBC? NEBC is a favourable area for CCS as the region has been an area of oil and gas exploration and development for decades, and as such, has a large amount of data that can be used to evaluate CCS opportunities. NEBC is part of the Western Canadian Sedimentary Basin and hosts many geological rock units (formations) that have favourable rock characteristics to safely store CO_2. This scoping technical atlas assesses the geological potential for CO_2 storage in the NEBC area and encompasses over 130,000 square kilometres *(figure 1.1)*. *Figure 1.1* also displays the location of First Nations communities, cities, towns, stationary CO_2 emitters, main transportation routes and primary pipeline infrastructure.

The atlas study provides a written report that summarizes the basics of carbon capture and storage (CCS) and types of sequestration (carbon storage), carbon storage project considerations, an atlas overview and formation (geological zone) summaries of zones that have storage potential. This atlas focuses on two main types of permanent geological storage:

- Saline aquifers
  - A saline aquifer is a geological formation of porous sedimentary rocks hosting salt water
- Depleted or nearly depleted natural gas pools
  - A depleted gas pool (or nearly depleted pool) is a subsurface reservoir that has produced all, or nearly all, of its natural gas.

In addition to the report, the study provides summary and formation maps, summary tables, shapefiles and a database that can be used to high-grade areas of storage potential.

The atlas evaluates the CO_2 storage potential by formation, or groups of formations in some cases, as well as providing a summary of overall CO_2 storage potential. The formation chapters provide an overview of the areal extent of favourable storage (reservoirs), pertinent reservoir characteristics, and estimated CO_2 storage potential, measured in megatonnes (Mt). A high level assessment of regional seal containment is discussed. These maps and data are intended as guides to assist in selecting areas with potential and are not intended to be used for specific CCS site selection. Specific site selection will require further detailed geological, hydrodynamic and engineering analyses.

* The term *storage potential* has recently replaced the term *storage capacity* when discussing the characterization of pore space at a scoping level. *Storage capacity* is now used as a resource term (SPE-SRMS, 2022) and reserved for pore space that is discovered, characterized, injectable and classified as commercially viable (Hares et al, 2022). *Storage potential* includes resources that are contingent (potentially accessible) and prospective (undiscovered and estimated). This atlas study assessed the overall storage potential of NEBC and further work is required to quantify projects with commercially viable *storage capacity*.

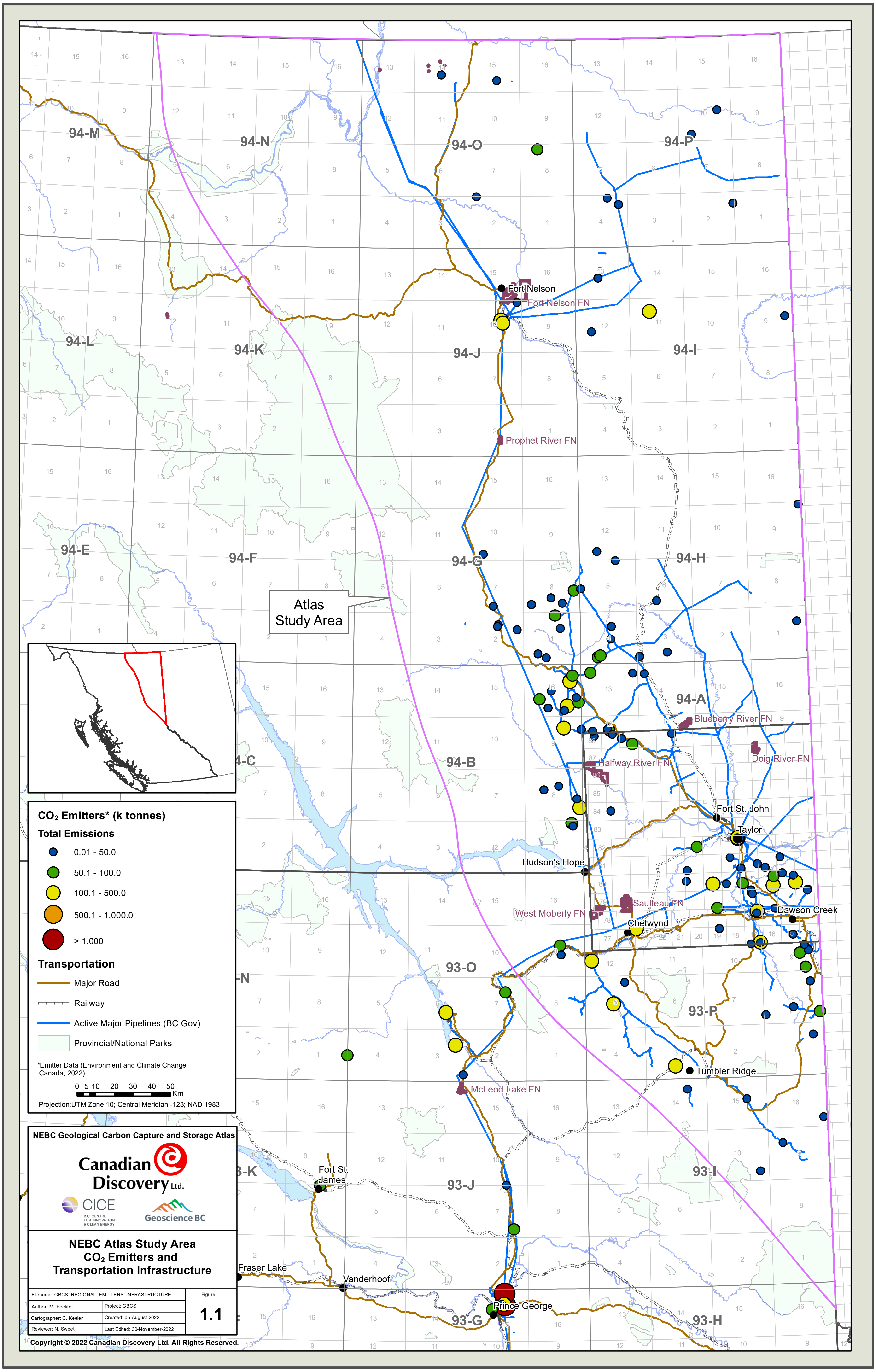

© Canadian Discovery Ltd. *Figure 1.1*

Project Outcomes

The study found that NEBC has numerous opportunities for geological carbon storage within a variety of depleted gas pools and saline aquifers, offering potential opportunities for small to large scale storage. More detailed information on storage potential calculations is provided in *Chapter 4*. *Figure 1.2* shows the distribution of estimated effective CO_2 storage potential by formation in depleted natural gas pools. *Figure 1.3* shows the distribution of the estimated effective storage potential of saline aquifers by formation on a P10 (small), P50 (median) and P90 (large) basis. Total estimated effective storage available in depleted pools in NEBC is approximately 1.2 Gt (gigatonne) (1,173 Mt), and total estimated effective P50 storage potential available in saline aquifers is 3.0 Gt (3,030 Mt), with a P10–P90 range of 0.758 Gt (758 Mt) to 8.2 Gt (8,182 Mt), respectively. Combined storage potential of depleted pools plus the total aquifers P50 calculation is estimated at 4.2 Gt (4,203 Mt). To put this in perspective, British Columbia's CO_2 emissions for 2020 were calculated by the provincial government to be 65.4 Mt (BC Government Climate Change, 2021a).

Recommended areas of focus are identified where there are multiple storage opportunities coincident with stationary emitters and infrastructure. *Figure 1.4* is a map of the study area highlighting areas of total estimated P50 effective CO_2 storage potential combined (stacked) for all aquifers. A clearly defined fairway of stacked aquifers with significant storage potential has been identified in the Peace River block near Fort St. John (PRA Stacked Aquifer Fairway). Another substantial aquifer fairway exists further north near Fort Nelson (Middle Devonian Carbonates Aquifer Fairway). *Figure 1.5* is a map of depleted gas pools with greater than 5 Mt of CO_2 calculated storage potential. Several depleted pools with greater than 25 Mt of storage potential occur in the Fort St. John area. For perspective, a depleted pool with 25 Mt of storage has the potential to sequester 1.2 Mt annually for 20 years.

Many storage options have been identified throughout the NEBC study area which will benefit from further evaluation. Depending on the storage and area needs, there are opportunities for small and large local CCS, as well as potential for hub model or cluster networks providing a variety of solutions in the NEBC region.

Readers are directed to *Appendix D* for a list of publications and websites for more information on carbon storage in NEBC.

1.2 Estimated Effective Storage Potential in Depleted Pools

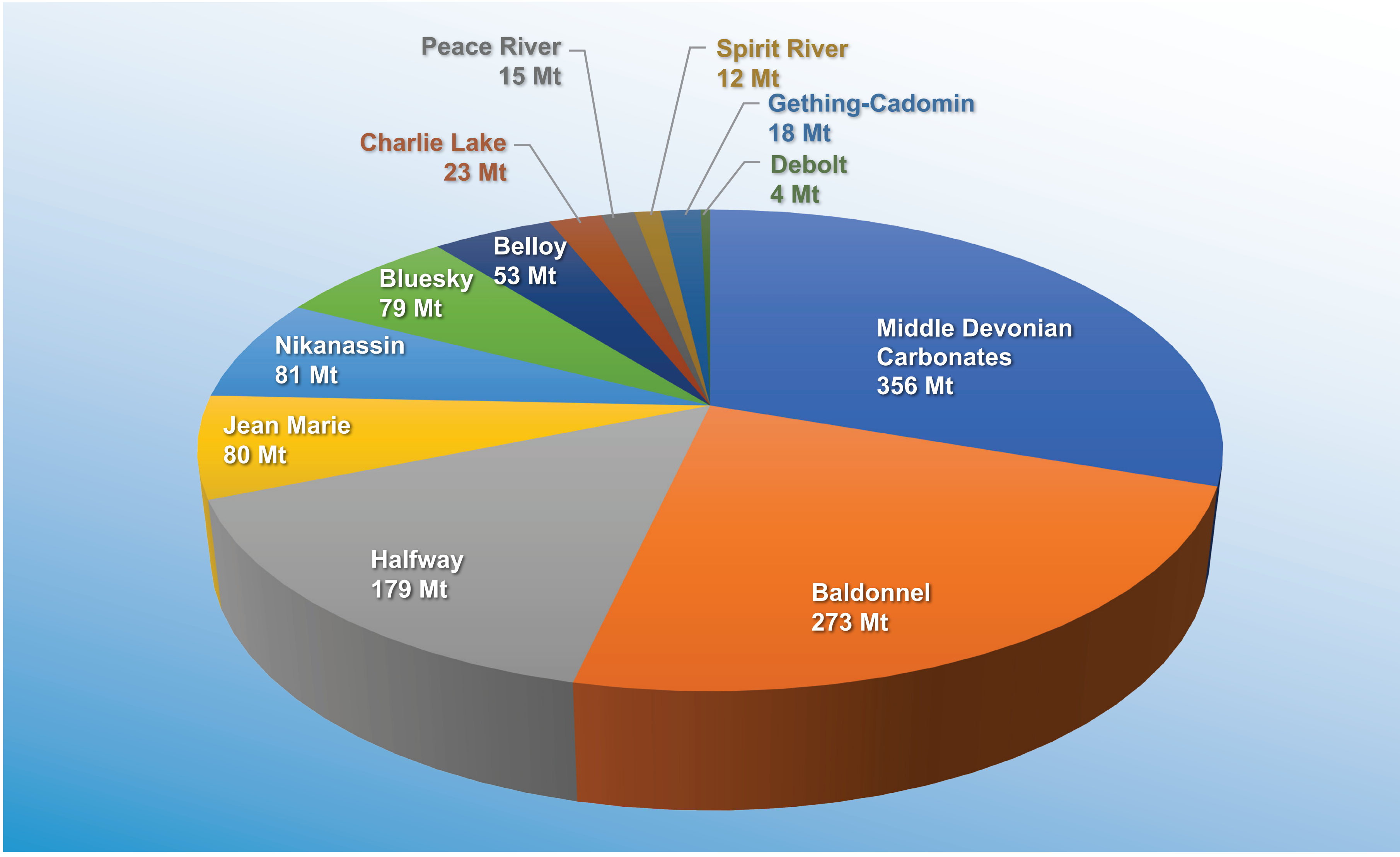

Figure 1.2

1.3 Estimated Effective Storage Potential in Saline Aquifers

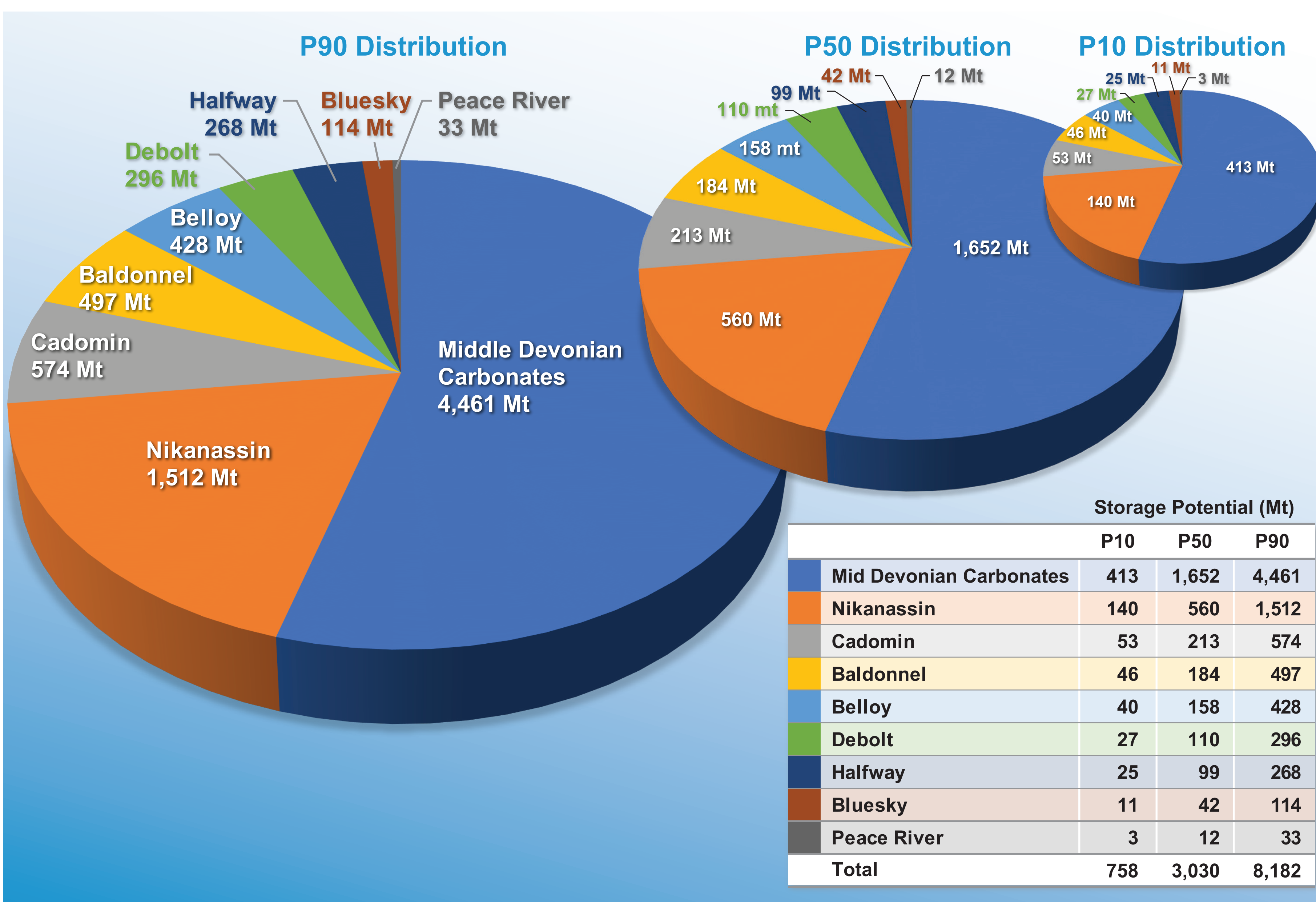

Storage Potential (Mt)

	P10	P50	P90
Mid Devonian Carbonates	413	1,652	4,461
Nikanassin	140	560	1,512
Cadomin	53	213	574
Baldonnel	46	184	497
Belloy	40	158	428
Debolt	27	110	296
Halfway	25	99	268
Bluesky	11	42	114
Peace River	3	12	33
Total	758	3,030	8,182

Figure 1.3

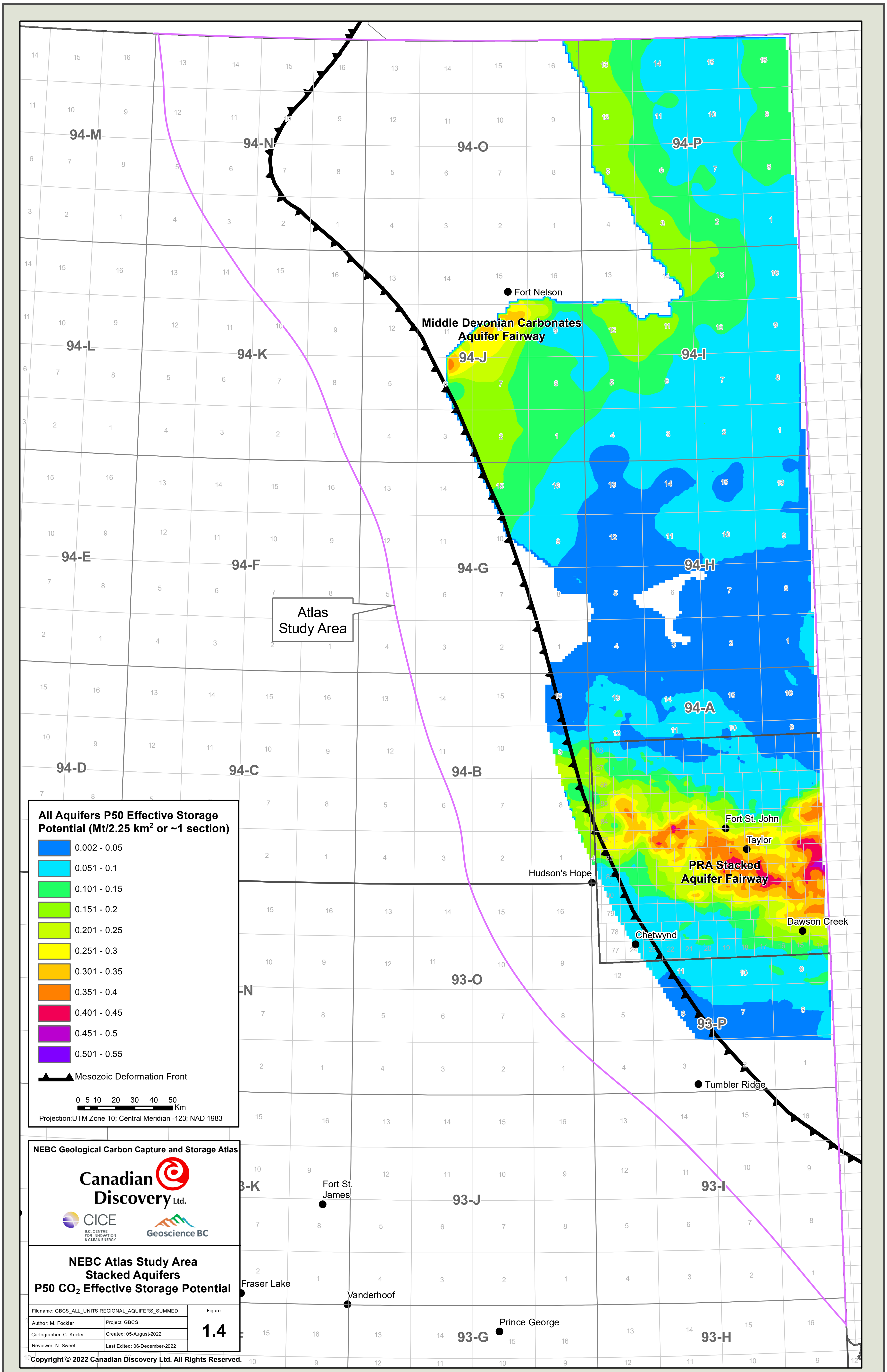
94-M
94-N
94-O
94-P
94-L
94-K
94-J
94-I
94-E
94-F
94-G
94-H
94-D
94-C
94-B
94-A
93-O
93-P
93-J
93-I
93-G
93-H
Fort Nelson
Middle Devonian Carbonates Aquifer Fairway
Atlas Study Area
Fort St. John
Taylor
PRA Stacked Aquifer Fairway
Hudson's Hope
Dawson Creek
Chetwynd
Tumbler Ridge
Fort St. James
Fraser Lake
Vanderhoof
Prince George
All Aquifers P50 Effective Storage Potential (Mt/2.25 km² or ~1 section)
0.002 - 0.05
0.051 - 0.1
0.101 - 0.15
0.151 - 0.2
0.201 - 0.25
0.251 - 0.3
0.301 - 0.35
0.351 - 0.4
0.401 - 0.45
0.451 - 0.5
0.501 - 0.55
Mesozoic Deformation Front
0 5 10 20 30 40 50 Km
Projection:UTM Zone 10; Central Meridian -123; NAD 1983
NEBC Geological Carbon Capture and Storage Atlas
Canadian Discovery Ltd.
CICE
Geoscience BC
NEBC Atlas Study Area
Stacked Aquifers
P50 CO2 Effective Storage Potential
Filename: GBCS_ALL_UNITS REGIONAL_AQUIFERS_SUMMED
Author: M. Fockler
Project: GBCS
Cartographer: C. Keeler
Created: 05-August-2022
Reviewer: N. Sweet
Last Edited: 06-December-2022
Figure
1.4
Copyright © 2022 Canadian Discovery Ltd. All Rights Reserved.

 Figure 1.4

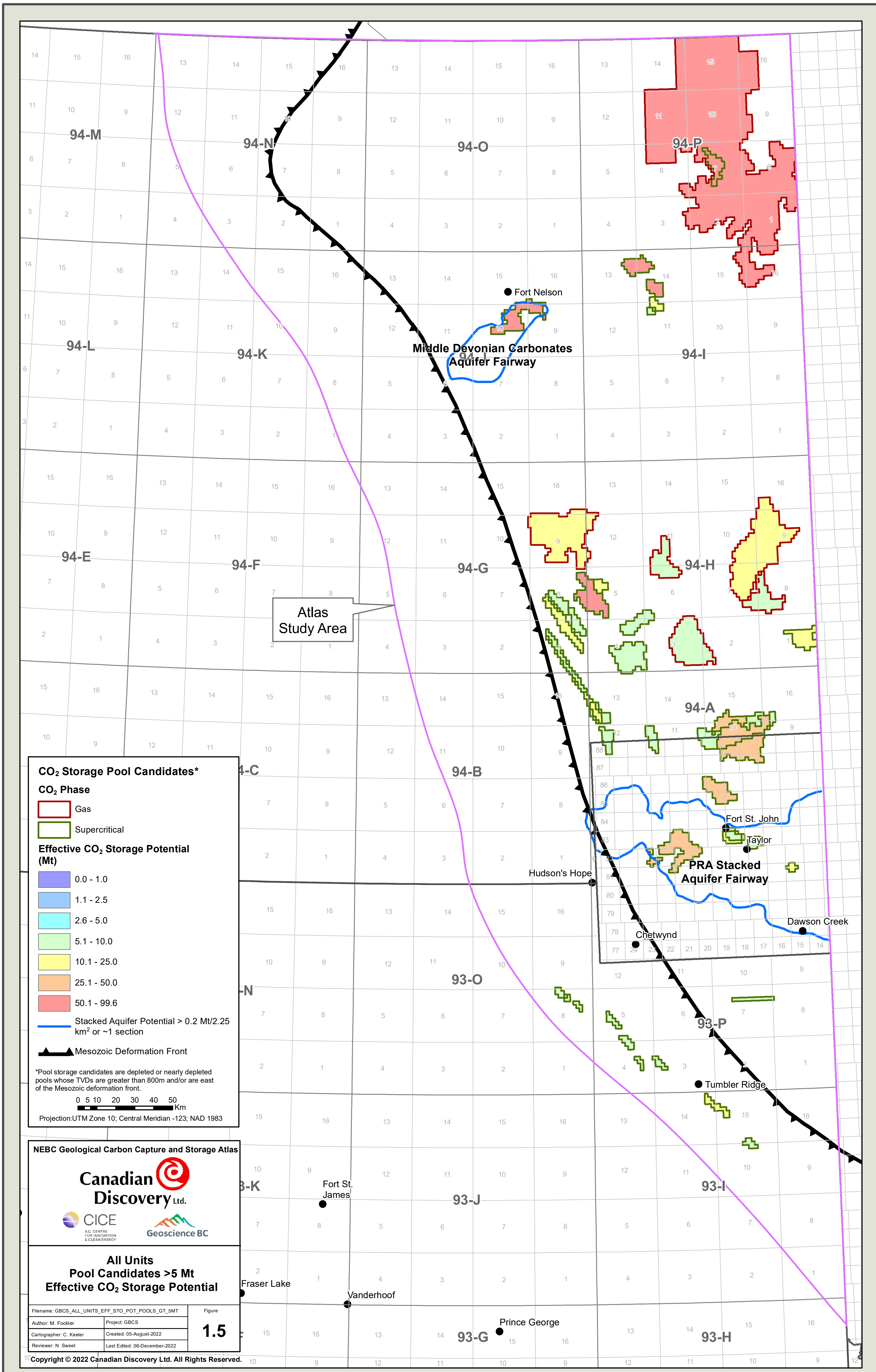

© Canadian Discovery Ltd. Figure 1.5

Acknowledgements

The project partners acknowledge that this research concerns the territory of the Treaty 8 First Nations of British Columbia. We encourage anyone considering new development or activities in their territories to engage early and engage often with appropriate Indigenous groups. The Province of British Columbia's Consultative Areas Database can be used to identify potentially impacted First Nations and their respective contacts. *(https://www2.gov.bc.ca/gov/content/data/geographic-data-services/land-use/contacts-for-first-nation-consultation-areas)*

We thank the project partners for their support of this project, including Geoscience BC, the BC Centre for Innovation & Clean Energy (CICE), and the BC Hydrogen Office. CICE and Geoscience BC are grateful to the Province of British Columbia for funding this project. This atlas had a Steering Committee and a Project Advisory Committee facilitated by Randy Hughes of Geoscience BC, and the project partners extend a sincere thank you to the anonymous peer reviewers and the following committee members for their time and valuable input.

Steering Committee

Yemi Adefulu	BC Centre for Innovation and Clean Energy
Ged McLean	BC Centre for Innovation and Clean Energy
Dr. Guy Gensey	BC Ministry of Energy, Mines and Low Carbon Innovation
Gavin Dirom	Geoscience BC
Chief Justin Napoleon	Saulteau First Nations

Project Advisory Committee

Ron Stefik	BC Oil and Gas Commission
Warren Walsh	BC Ministry of Energy, Mines and Low Carbon Innovation
Sara McPhail	BC Ministry of Energy, Mines and Low Carbon Innovation
Dr. Sonya Dehler	Natural Resources Canada
Ron Hill	Tourmaline Oil Corp
Santiago Arribas Picon	Enbridge Inc
Tim Shaw	NorthRiver Midstream

Canadian Discovery Ltd. would like to thank the following contributors to this Atlas:

Natalie Sweet MSc, P. Geo	Project Manager, Senior Geologist
Allison Gibbs, P. Geol	Senior Hydrodynamicist
John Xie, P. Eng	Reservoir Engineer
Meridee Fockler, P.Geol, B.App.GIS	GIS Analyst
Tessa Wilson, MSc, P. Geol	Geologist
W. Steven Donaldson PhD, P. Geol	Senior Geologist
Jeff Horton, P. Eng	Reservoir Engineer
Candace Keeler, BAH	GIS Analysist and Cartographer
Lina Hage	Graphic Designer/Production Manager
Paul Patton	Senior Graphic Designer

Carbon Capture and Storage (CCS) Basics

Introduction

Carbon capture and storage (CCS) refers to a set of technologies developed with the goal of reducing carbon dioxide (CO_2) emissions and levels of CO_2 in the atmosphere. CCS technologies are proven to capture large-scale CO_2 emissions from major stationary sources and store it deep underground in geologic rock formations (PCOR Atlas, 2021). CCS can provide a safe, effective and efficient means of managing CO_2 emissions. It can be used alongside existing infrastructure to produce hydrogen which can be used to generate electricity, as a base fuel itself, and for other industrial processes.

Carbon Capture

Types of Carbon Capture

Carbon can either be captured from the atmosphere in a process known as Direct Air Capture (DAC), or captured from stationary carbon-emitting sources. Non-stationary sources are not suitable for carbon capture due to the large scale required to make carbon capture cost-effective. Each of these processes have unique characteristics with advantages and disadvantages, but they all share a common goal of producing a concentrated stream of CO_2 that can be transported to a storage site or put to use in other ways. Carbon capture typically involves the separation of CO_2 from other gases through the use of solvents, sorbents, permeable membranes, or separation via cooling. The following text provides a generalized overview of common carbon capture technologies, with the note that details will vary in specific applications.

Direct Air Capture (DAC)

DAC involves the extraction of carbon dioxide from the atmosphere. The Earth's air is largely nitrogen (78%) and oxygen (21%), with a minor component of carbon dioxide (0.04%). Carbon dioxide is extracted from air using chemical or physical sorbents — solids or liquids that trap the carbon dioxide via a chemical reaction (in the case of chemical sorbents) or physically trap the carbon on the surface of the sorbent (i.e. adsorption) or inside the sorbent material (i.e. absorption). After the sorbent is saturated with carbon dioxide, the chemical or physical process must be reversed, producing a concentrated stream of carbon dioxide while regenerating the sorbent. Sorbent regeneration requires energy, and any carbon emissions associated with energy used in this step must be accounted for when evaluating projects.

An important advantage of DAC is that the location of the plant is not limited by the location of carbon-emitting sources. The plant can be installed near areas with appropriate geologic storage to reduce transportation costs, or near areas with low-emission energy sources (i.e. hydroelectric power) to power the plant. DAC provides a method to reduce the total carbon in the atmosphere, rather than simply mitigating future emissions as in the case of capture from emitting sources. Once captured, the CO_2 can either be stored or combined with hydrogen to create synthetic fuel.

The primary disadvantage is the lower efficiency of DAC compared to capture from carbon-emitting sources. Given the low concentration of carbon dioxide in Earth's air, a large volume of air must be circulated over the sorbent material, requiring more energy. Wide-spread adoption of this technology will be vital for reducing costs and improving the economics. BC-based Carbon Engineering has a DAC pilot plant that captures one tonne of CO_2 per day, and is working on designs for full-scale 1 Mt/year commercial plants (Keith et al., 2018) *(figure 2.1)*.

2.1 | Direct Air Capture Plant

Source: https://www.forbes.com/sites/jamesconca/2019/10/08/carbon-engineering-taking-co_2-right-out-of-the-air-to-make-gasoline/?sh=643d97ec13cc

 Figure 2.1

Post-Combustion Capture

Post-combustion capture involves the separation of CO_2 from exhaust gases emitted during the combustion of fuels such as natural gas or coal *(Figure 2.2)*. This technology has significant near-term potential to reduce CO_2 emissions as it can be used on existing hydrocarbon-powered plants and other industrial emitters (NPC, 2019a).

Exhaust gas, often referred to as flue gas, comprises mostly nitrogen (N_2), CO_2, carbon monoxide (CO), sulphur oxides and nitrogen oxides. Solvents with amine, a derivative of ammonia (NH_3), are typically used to extract CO_2 from flue gas. The gas is brought into contact with the solvent and a chemical reaction between CO_2 in the air and amine in the solvent traps the carbon inside the solvent. The solvent is then transferred to a regenerator where heat is used to reverse the chemical reaction and release the CO_2 for transportation and storage. The regenerated solvent can then be used in another cycle of carbon capture.

The CO_2 concentration in flue gas is significantly higher than Earth's atmosphere and ranges from 5 to 15% depending on the hydrocarbon source (FECM, 2022), which makes post-combustion capture more efficient and less expensive than DAC. Carbon extraction with amine-based solvents has been used for decades and the technology is well understood. Current research focuses on developing alternate solvents that are more energy efficient.

2.2 Post-Combustion Capture

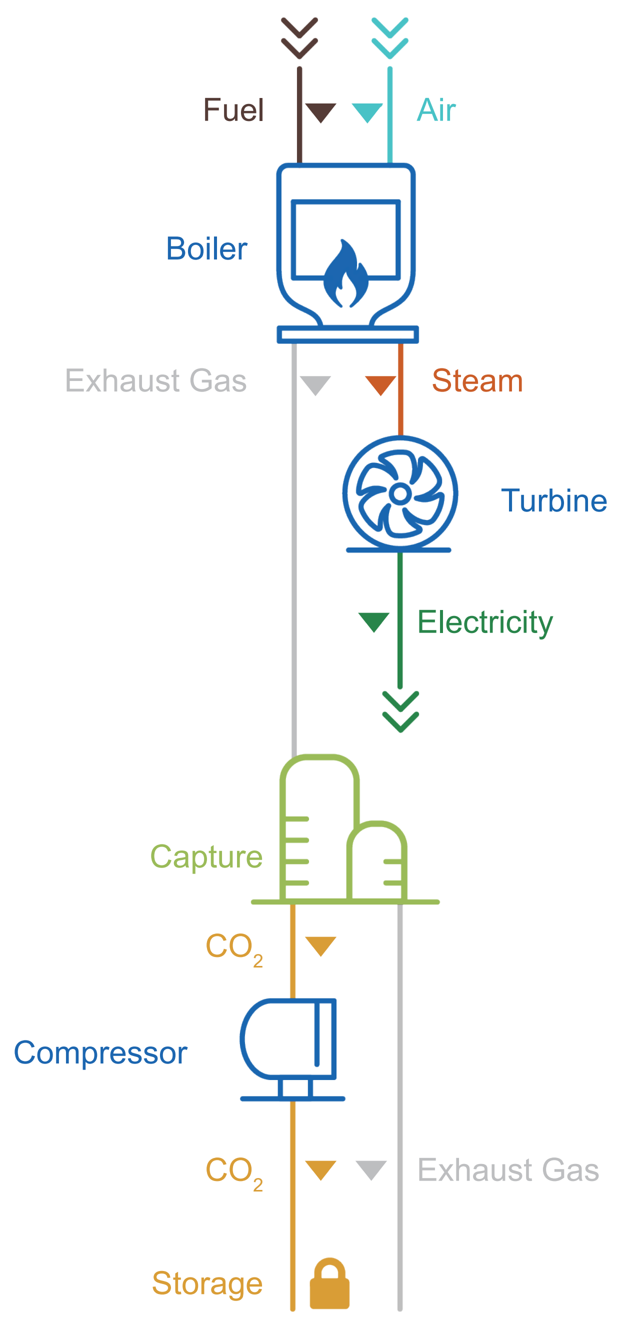

© Canadian Discovery Ltd. *Figure 2.2*

Pre-Combustion Capture

In pre-combustion capture, a series of chemical reactions are used to convert hydrocarbons, typically coal or methane, into hydrogen (H_2) and CO_2. The carbon dioxide is extracted from the mixture and transported for storage. The hydrogen can be burned to generate electricity without producing carbon emissions.

The process occurs in three steps. First, the hydrocarbons are converted into hydrogen and carbon monoxide (CO), a mixture known as synthesis gas, or syngas. This first step is known as gasification when coal is used as the hydrocarbon, and methane reforming in the case of natural gas. Next, the CO reacts with water in the presence of a catalyst to produce CO_2 and more hydrogen. Third, the CO_2 is separated from the hydrogen using physical absorption (NPC, 2019a).

There are several advantages to the pre-combustion process over post-combustion capture. The CO_2 concentration of the syngas can range from 15 to 50%, compared to 5 to 15% for flue gas (FECM, 2022). The higher concentration makes the absorption process more efficient. Additionally, the CO_2 and hydrogen mixture is produced at a high pressure, which provides a driving force to help facilitate the absorption of CO_2. (In post-combustion capture, the exhaust gases are at atmospheric pressure.)

The primary drawback of pre-combustion capture is the higher complexity of the process and higher capital costs required for the gasification process compared to traditional coal power plants. Implementing pre-combustion capture in existing plants is more complicated compared to post-combustion capture.

Capture During Combustion

The extraction of CO_2 from exhaust gases can be simplified by burning hydrocarbons in the presence of pure oxygen, rather than air. This process, known as oxy-combustion, produces a mixture of water vapour and CO_2. The mixture is easily separated when cooled as the water vapour condenses to liquid water while the carbon dioxide remains a gas, leaving concentrated CO_2 without the nitrogen side-products associated with combustion in air (IPCC, Chapter 3, 2005). Power generation during oxy-combustion is more efficient than combustion with air as energy is not wasted heating up nitrogen. The main disadvantage is that energy is required initially to isolate the oxygen from air.

Transportation

Pipelines provide an efficient method for transporting large volumes of CO_2 for storage *(figure 2.3)*. Prior to transportation, water must be removed to prevent corrosion (CO_2 is acidic when mixed with water). After the water is removed, the CO_2 is compressed to a supercritical state at pressures of approximately 8,000–15,000 kPa (1,200–2,200 psi) (NPC, 2019b). At this pressure, the CO_2 will be in either a liquid or supercritical state (see *Chapter 3* for more information) depending on the temperature of the fluid in the pipeline. The higher density of the liquid or supercritical fluid allows the pipeline to carry significantly more CO_2 than if it were transported as a gas. Compared to natural gas pipelines, CO_2 pipelines require thicker walls to withstand the higher pressures used in CO_2 transportation.

2.3 | CO_2 Transportation via Pipeline

Source: https://www.globalccsinstitute.com/wp-content/uploads/2018/11/7_CO_2-Transport-Onshore-1.jpg

Figure 2.3

Geological Storage Overview

Types of Storage

There are several types of geological reservoirs under consideration for CCS *(figure 2.4)* (NETL, 2021):

1. Depleted oil and natural gas reservoirs are porous rock formations (usually sandstones or carbonates) containing oil and gas that have been physically trapped. These are good geologic storage sites because they have trapped hydrocarbons for thousands to millions of years and should therefore have conditions suitable for CO_2 storage.
2. CO_2 can be injected into mature oil fields (fields that have been producing for many years) to increase oil recovery (enhanced oil recovery or EOR). This is a process that has been successfully carried out for more than 40 years. Although some CO_2 is co-produced with the oil (and is ultimately re-injected), a large portion, up to 90% in many cases remains sequestered within the reservoir (Vox, 2019).
3. Deep saline formations are layers of porous and permeable sedimentary rock filled with salty water called brine. These formations are known to be widespread in NEBC and have potential for CO_2 storage. It is important that a regionally extensive confining zone (often called a caprock or seal) overlies the porous rock layer. Saline formations represent an enormous potential for CO_2 storage and results from this study indicate that they can be used as reliable, long-term storage sites.
4. Unmineable coal seams that are too thin, too deep, or too discontinuous to be mined using current technology have the potential for CO_2 storage. Coal preferentially holds CO_2 over methane (natural gas), which is found naturally in coal seams, at a ratio of 2–13 times.
5. Injection of CO_2 into a coal seam for storage will potentially displace and liberate coal bed methane. Although the recovery and sale of the produced methane gas can help to offset the cost of CO_2 storage, methane itself is a potent GHG, meaning that this process alone is not a net carbon sink.
6. Basalt (solidified lava) formations are another potential CO_2 storage option. Although these rock types have been simulated in laboratory conditions to potentially convert injected CO_2 to a solid mineral form, innate challenges in how volcanic rocks are deposited create challenges identifying areas with large reservoirs with connected pores. More research is needed to better understand the time frame and chemical inputs and outputs of this process, and is not the focus of this Atlas, as the study are of NEBC does not contain any basaltic rocks at depths that are economic to drill.

Another potential storage type are in organic-rich shales formed from silicate minerals, which are weathered into clay particles that accumulate over millions of years. Some shales that are rich in organic matter have the potential for CO_2 storage. Similar to coal, injected CO_2 will stick to mineral surfaces, displacing methane, while locking the CO_2 in place. Recent advances in horizontal drilling and hydraulic fracturing technology have increased interest in the energy sector for natural gas production from organic-rich shales. With these technologies, operators create flow pathways within the shale, allowing CO_2 to be injected to enhance natural gas recovery, similar to the process described for coal, above. Although the recovery and sale of the produced methane gas can help to offset the cost of CO_2 storage, methane itself is a potent GHG, meaning that this process on its own is not a net carbon sink.

2.4 Options for Storing CO_2

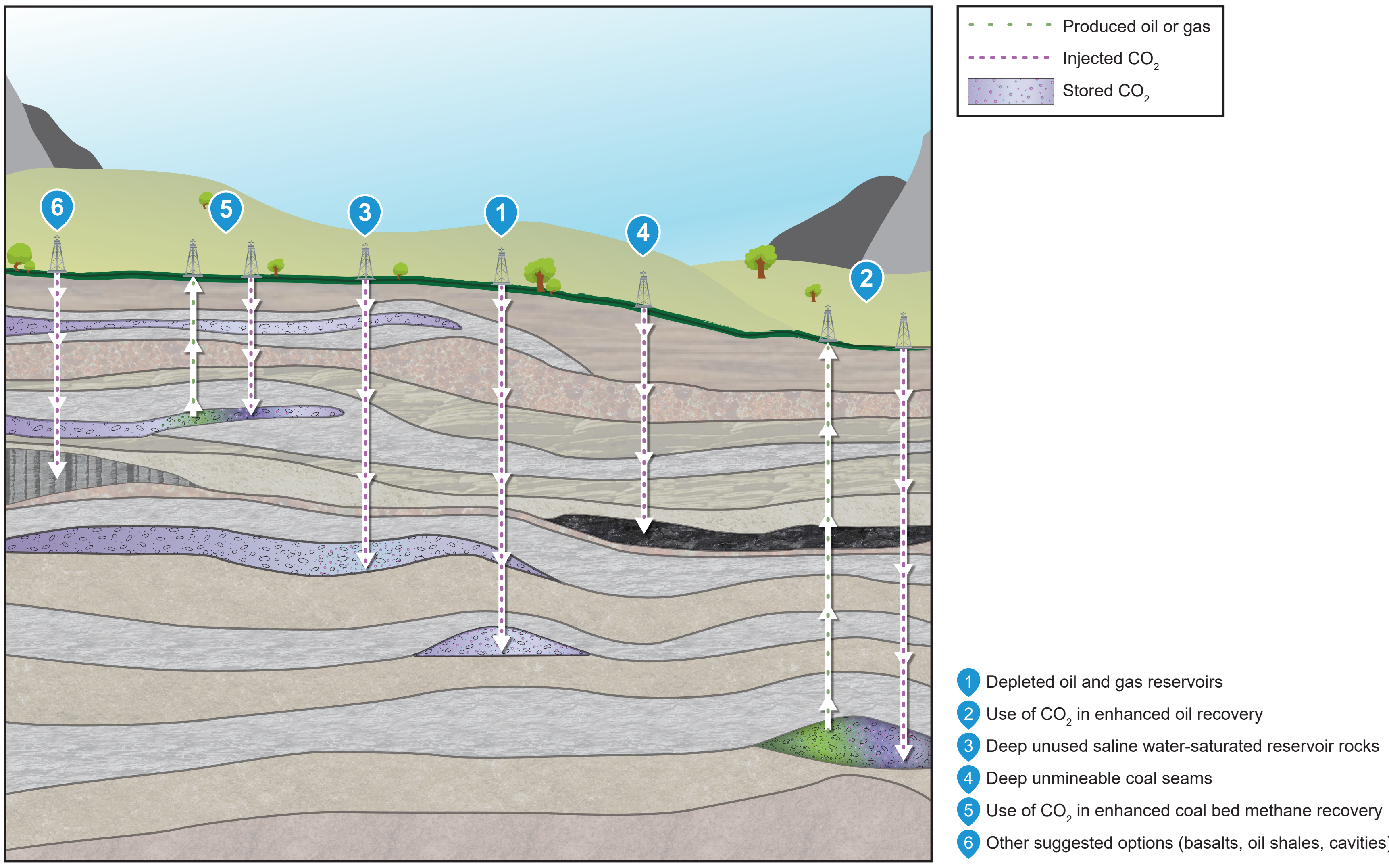

Modified from IPCC, 2018, Fig 5.3

Figure 2.4

CO_2 Trapping Mechanisms

Four main mechanisms exist for trapping CO_2 within depleted oil and gas reservoirs and deep saline formations:

Structural Trapping

Structural trapping is the physical trapping of CO_2 and is the mechanism that traps the largest volume (NETL, 2021). Rock layers and sealing faults within and above the storage formation where the CO_2 is injected can act as seals, preventing the CO_2 from escaping *(figure 2.5a)*. Once injected, supercritical CO_2 is usually more buoyant than other liquids present in the surrounding pore space (usually a salty brine), depending on the density of the in-situ brines. As a result, the CO_2 may migrate upwards through the porous rocks until it reaches a sealing layer consisting of relatively impermeable rock such as shale or salt, which prevents upward migration out of the reservoir. This primary trapping mechanism has held naturally-occurring subsurface accumulations of CO_2 for millions of years (PCOR Atlas, 2021).

Residual Trapping

Residual trapping refers to the CO_2 that remains trapped in the pore spaces between the rock grains as an injected CO_2 plume flows through the rock *(figure 2.5b)*. When supercritical CO_2 is injected into a storage formation, it displaces existing fluid as it flows through the porous rock (NETL, 2021). As the CO_2 continues to move through the reservoir, small droplets may become detached and remain trapped within the centre of pore spaces, typically surrounded by brine. These residual droplets are effectively immobilized (PCOR Atlas, 2021).

Solubility (Dissolution) Trapping

With solubility trapping, a portion of the injected CO_2 dissolves into formation water within the reservoir rock pore space *(figure 2.5c)* (NETL, 2021). At the CO_2-formation water interface, some of the CO_2 will dissolve into brine in the pore spaces, just like sugar dissolves in water. Brine with dissolved CO_2 becomes denser than the surrounding brine and will sink to the bottom of the reservoir, minimizing the possibility of further migration (PCOR Atlas, 2021).

Mineral Trapping

Mineral trapping refers to a chemical reaction that can occur when the CO_2 dissolved in the rock's saline water reacts with the minerals in the rock *(figure 2.5d)* (NETL, 2021). This chemical reaction between the dissolved CO_2 in the formation fluids and the minerals in the target formation and cap rock forms new solid minerals such as carbonates, effectively locking the CO_2 in place. Mineral trapping may occur over longer timescales and is difficult to predict with accuracy (PCOR Atlas, 2021) although newer research (Gunnarsson et al, 2018) suggest that mineral trapping in basalts can occur in a matter of years.

Figure 2.6 shows how the relative importance of each of these four trapping methods changes over time once CO_2 injection stops within a reservoir.

2.5 Subsurface CO_2 Trapping Mechanisms

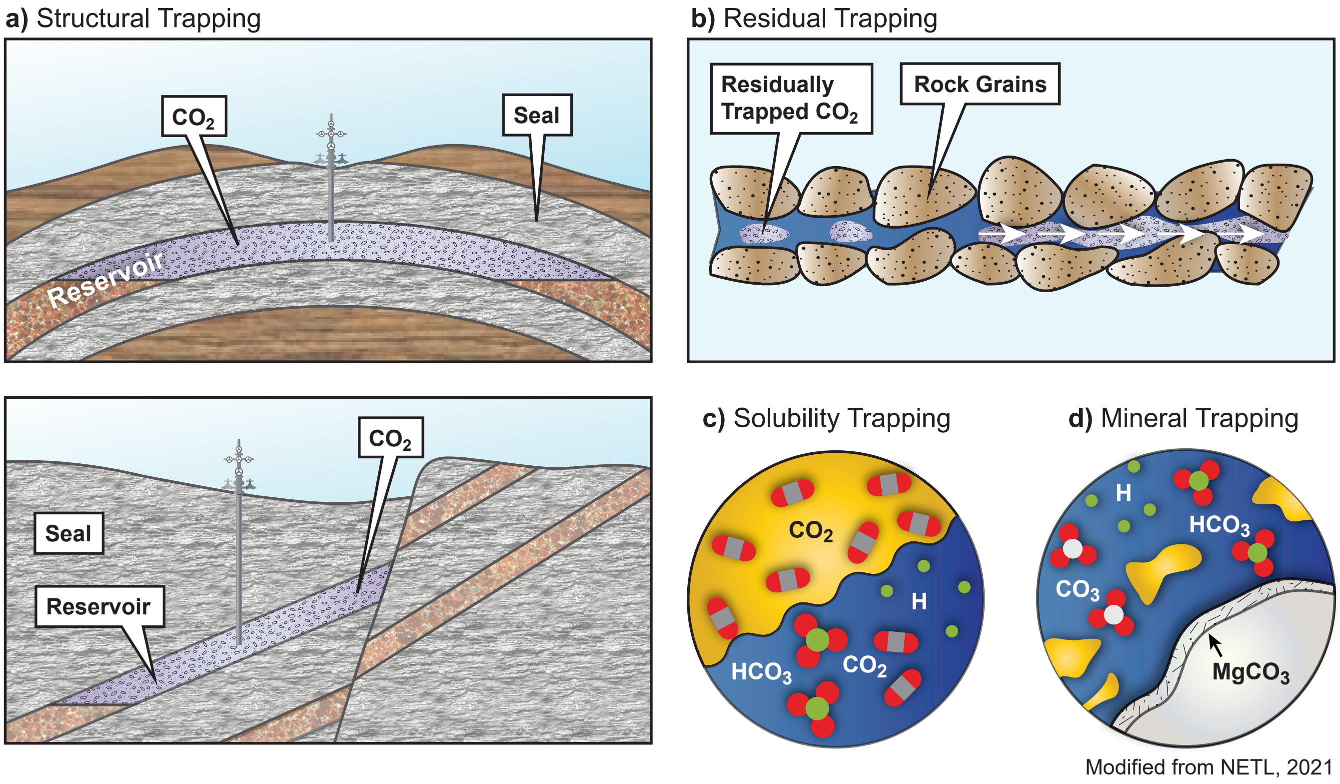

© Canadian Discovery Ltd. *Figure 2.5*

2.6 CO_2 Trapping Over Time in Saline Formations and Depleted Oil and Gas Reservoirs

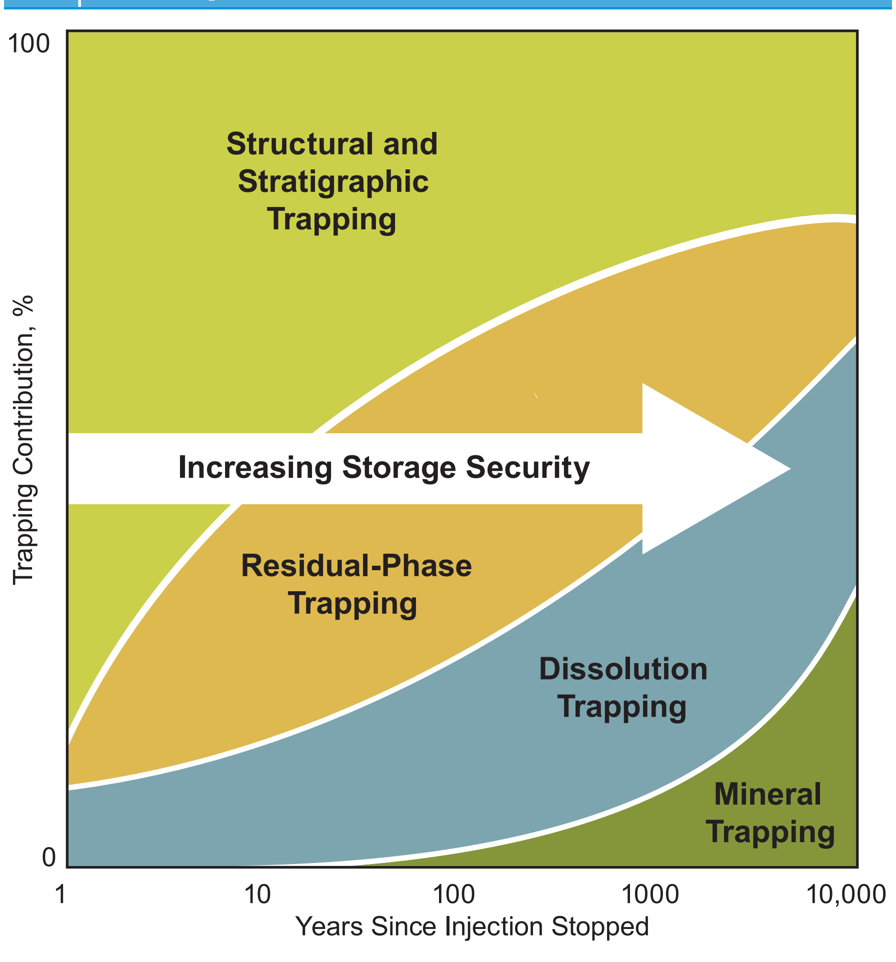

© Canadian Discovery Ltd. *Figure 2.6*

Current Carbon Storage Projects in Canada

Permanent Geological Storage can be in both depleted oil and gas pools as well as deep saline aquifers and both storage types are available in NEBC and is discussed in detail in this Atlas. CO_2, in the form of acid gas disposal, has been successfully stored in BC (BCOGC, 2019) and elsewhere for decades. Examples of large scale CO_2 storage projects in Canada are discussed below.

CO_2 has been successfully captured and stored within two saline aquifers in Canada: the Shell Quest facility in Alberta and the Aquistore facility in Saskatchewan.

Shell Quest Facility

The Quest CCS facility is operated by Shell Canada at the date of this publication. This facility at its current capacity captures and stores about one-third of the CO_2 emissions from the Scotford upgrader near Fort Saskatchewan, AB, which turns oil sands bitumen into synthetic crude that can be refined into fuel and other products. After capture, the CO_2 is transported 65 km north via pipeline *(figure 2.7)* and injected more than 2 km underground below multiple layers of impermeable rock, into a deep saline aquifer. *Figure 2.7* shows the project area outlined in red which is approximately 100km^2 in size. Injection wells and monitoring wells are shown as well as seismic that has been planned or acquired. The milestone of 4 Mt of CO_2 storage was achieved on May 23, 2019.

In its first 16 months of operation, CO_2 injectivity at Quest has been up to 150 tonnes/hour. Shell forecasts that no further project well development will be needed to support injection and storage potential over the 25-year life of the project. Two of the three injection wells drilled specifically for the project have been used as of December 2016. The third unused injection well might be safely abandoned as it would probably not be required before 2040 to sustain operation of the storage site (International Energy Association Greenhouse Gas R&D Programme (IEAGHG), 2019.).

Boundary Dam and Aquistore Projects

The Boundary Dam Carbon Capture Project is the world's first commercial-scale, fully integrated CCS project at a coal-fired power station, with post-combustion capture of CO_2 from the rebuilt Unit 3. The capital cost of $C1.2 billion was supported by funding from the provincial Government of Saskatchewan and the federal Government of Canada. Operated by the government-owned utility SaskPower, the project is designed to capture up to 1 Mt of CO_2 per year; between the commencement of operations in October 2014 and May 2021, SaskPower reports that 4.14 Mt of CO_2 has been captured.

Unit 3 provides 115 MW of power. In addition to reducing CO_2 emissions from Unit 3 by up to 90%, the capture process removes 100% of polluting SO_2 (sulphur dioxide) emissions, which are converted to sulphuric acid for industrial use.

The main destination for captured CO_2 is the Weyburn oil field in SE Saskatchewan, with Whitecap Resources transporting the purchased CO_2 via a 66-km pipeline. At Weyburn the CO_2 is used for enhanced oil recovery (EOR). A branch of the pipeline in close proximity to the Boundary Dam power station feeds the Aquistore Project, which is designed to provide dedicated storage for unsold CO_2 *(figure 2.8)*.

Aquistore is a dual-purpose project. From a commercial perspective, Aquistore provides a dedicated storage option for unsold CO_2 from Boundary Dam — in effect providing buffer storage so as to prevent any need for SaskPower to vent CO_2 from capture operations. Injection operations commenced in April 2015, making Aquistore the first dedicated storage project to be operating in Canada. As of April 2021, over 370,000 tonnes of CO_2 have been injected.

Monitoring of the Aquistore site is managed by Petroleum Technology Research Centre (PTRC), which installed the injection well plus an observation well and other monitoring infrastructure through funding by federal and provincial government agencies and private industry. In addition to providing monitoring data for the regulator in accordance with permitting of the storage site, Aquistore is run as a collaborative PTRC research project that aims to demonstrate that dedicated storage in a deep saline formation is a safe and workable solution to reduce GHG emissions.

2.7 Shell Quest Project Area

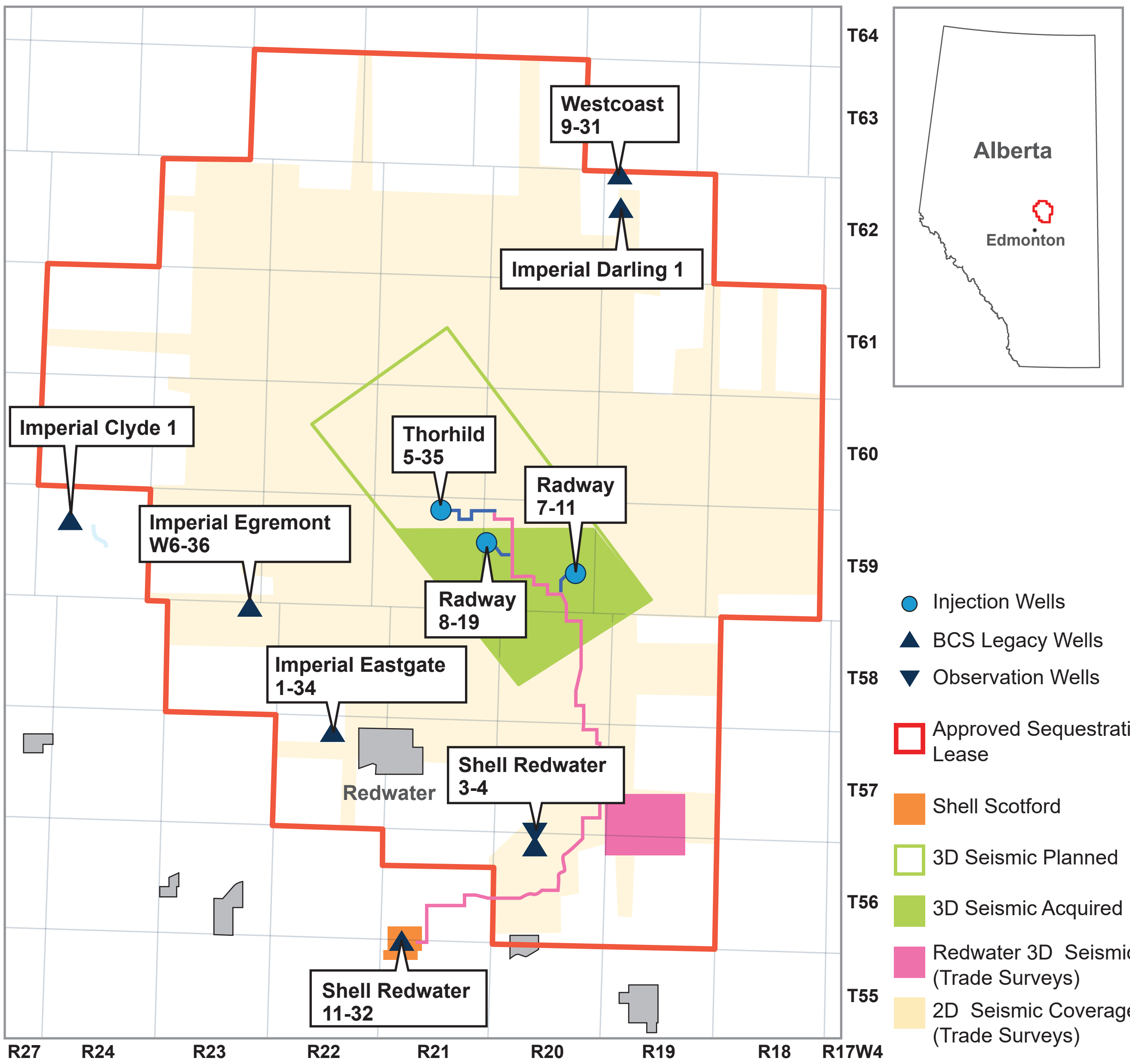

Donaldson, 2020, CDL Digest article: Shell's Quest for the Holy Grail of Carbon Capture and Storage, Fig 1.
Modified from IEAGHG, 2019, Fig 18

Figure 2.7

2.8 Aquistore Location Map

Modified from PCOR Partnership Atlas, 6th Edition; Photo provided by and is property of SaskPower.

Figure 2.8

CARBON STORAGE PROJECT CONSIDERATIONS

Geological Carbon Storage Suitability Criteria

As discussed in *Chapter 2*, subsurface geological carbon storage is the process of injecting CO_2 into rock formations deep underground for permanent storage. The geological formation requires sufficient pore space and pore connectivity (permeability), with a caprock (overlying seal) to ensure CO_2 remains securely underground. To ensure that geological carbon storage is done successfully, identifying possible risks and having a plan to minimize and/or mitigate these risks is necessary.

There are a number of criteria that are important to consider ensuring that a depleted natural gas pool or deep saline aquifer is suitable to safely store CO_2 in the subsurface.

These include:

- Identifying reservoirs with seals to help ensure containment
- Low to moderate faults and fracturing
- Sufficient pore volume available for storage — ideally greater than approximately 5–10m reservoir thickness at greater than 6% porosity, with good continuity over the injection area
- Suitable reservoir conditions that affect CO_2 density and phase — how "compact" the CO_2 is will determine the potential amount that can be stored in the formation
- Sufficient permeability to maintain the required CO_2 injection rates for a project. Permeability allows gases and fluids to migrate more easily through pores away from injection wells — this is needed for a reservoir to be able to accept the CO_2 at the rates required for a project like a storage hub.

Understanding the overall dynamics and relationships between the oil, gas and brine in the system is also important for determining factors like storage containment and the ranges in storage potential estimates.

Pressure, Temperature and Depth Requirements

CO_2 gas can be stored underground as a supercritical fluid. Supercritical conditions for CO_2 comprise a temperature in excess of 31.1°C and a pressure greater than 72.9 atmospheres (about 7,500 kilopascals (kPa)); this temperature and pressure define the critical point for CO_2. At these conditions, the CO_2 is dense like a liquid, but has low viscosity like a gas, which is ideal for injecting and storing larger quantities of CO_2. Viscosity is defined as a measure of a fluid's (liquid or gas) resistance to flow. A high viscosity fluid resists motion (flows slowly) because its molecular makeup gives it a lot of internal friction. A low viscosity fluid flows easily because its molecular makeup results in very little friction when it is in motion (Princeton University, 2022).

For most places on Earth, at depths below about 800m, natural temperatures and pressures exceed the critical point of CO_2. This means that CO_2 injected at this depth or deeper will remain at a supercritical state. The main advantage of storing CO_2 in a supercritical condition is that the storage volume needed is less than if the CO_2 were at surface conditions *(figure 3.1)* (NETL, 2021).

Potential CCS Risks and Risk Mitigation

Proper subsurface site selection (e.g. contained storage zone, low seismicity), rigorous evaluation of the selected site, and if necessary, the implementation of a monitoring program to verify secure containment and conformance is paramount in reducing CO_2 leakage and emission risk. Understanding the storage formation and surrounding geology to assess leakage pathways is required to properly mitigate risks, whether in depleted pools or saline aquifers.

Depleted oil and gas pools present a storage option that provides less uncertainty in terms of storage potential and injectivity, however risk lies in the presence of legacy wellbores, where there is potential for leakage of CO_2 to surface via the wellbore. Low well density is one of the main benefits of targeting deep saline aquifers for storage, however risk lies in the lack of well control in the aquifer to determine the reservoir characteristics. Also, both types of storage (depleted oil & gas pools, and deep saline aquifers) need to be assessed as to the risk of reactivation along existing faults and potential for faults to breach the caprocks (seals).

Focused geological and engineering studies will be required before a suitable CCS site is selected and a risk mitigation plan created. High level potential CCS risks are discussed below.

Legacy Wellbores

Leakage of CO_2 to surface through legacy (pre-existing) wellbores can occur as the wellbores can be pathways for CO_2 to travel vertically into overlying reservoirs, and potentially all the way to the surface. Any well that penetrates the storage formation should be assessed for wellbore integrity.

Faults and Seals

Areas of existing natural faulting need to be understood and assessed as to the risk of reactivation along the fault and potential for the fault to breach the caprocks (seals). *Figure 3.2* illustrates some of the major faults and structural elements that exist in the project area. NEBC has had a complex history of faulting and a detailed local assessment of faulting is required to characterize the risk of storing CO_2. Faults can also be sealing in nature and would limit lateral continuity and could decrease storage potential.

3.1 Pressure Effects on CO_2

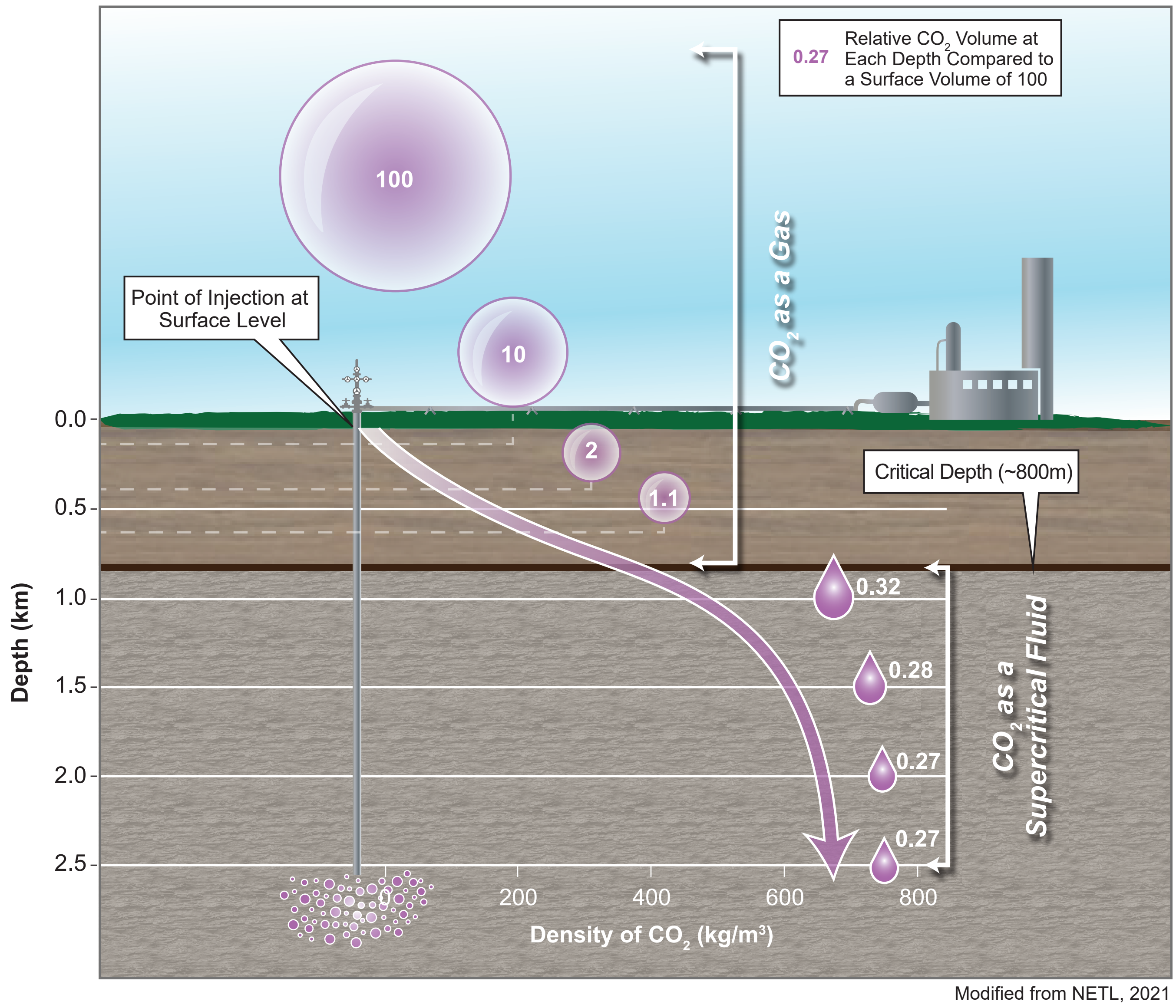

© Canadian Discovery Ltd.

Figure 3.1

Seals (caprocks) occur both locally and regionally and at several levels through the subsurface. The seals overlying the potential storage reservoir need to provide containment and be geomechanically stable. In addition to caprocks that immediately overlie depleted oil and gas pools (these caprocks prevented oil and gas from migrating upward), the Shaftesbury Formation is a thick regional shale that extends throughout the study area and is situated below the deepest groundwater level. This zone is an additional containment layer to prevent CO_2 migration to surface.

Measurement, Monitoring and Verification

Once a suitable storage site is determined, a Measurement, Monitoring and Verification (MMV) plan must be established. Measurement and ongoing monitoring may include:

- Geosphere
  - Observation wells: downhole pressure and temperature monitoring within the storage reservoir
  - Microseismicity
- Hydrosphere
  - Groundwater monitoring
- Biosphere
  - Remote sensing, brine and CO_2 trace monitoring
- Atmosphere
  - Measurement of baseline CO_2 and ongoing monitoring to identify emissions at site

Tracking of injected volumes as a result of measurement and monitoring allows for proper verification to occur and the amount of carbon stored to be calculated.

Hub Storage and Local Storage

CO_2 storage project requirements — whether greater or less than 1 Mt/yr— will dictate the size of the storage complex and the injection rates needed to make the project a success. This Atlas includes areas and zones that are suitable for smaller and local scale storage, as well as identifying and assessing areas of largest storage potential, where a CCS hub model may be feasible. Low carbon intensity hydrogen projects will also require CCS storage. This Atlas can help guide site selection for CO_2 sequestration for any of these projects.

CCS Hub

A CCS hub, as well as cluster networks, allows for multiple CO_2 emitters to share infrastructure and capture facilities while reducing associated risks and costs. Storing into a shared prime geological site also allows for smaller emitters to have access for their CCS requirements. The CCS hub model is a viable means of decarbonizing industrial processes while supporting cleaner energy and low-carbon industries.

Local Scale Storage

CO_2 storage can be done on a local scale at or near emission sites if there is a suitable geological storage formation available to safely sequester the CO_2. This method would be suitable for geographically isolated emission sources emitters requiring a CCS solution.

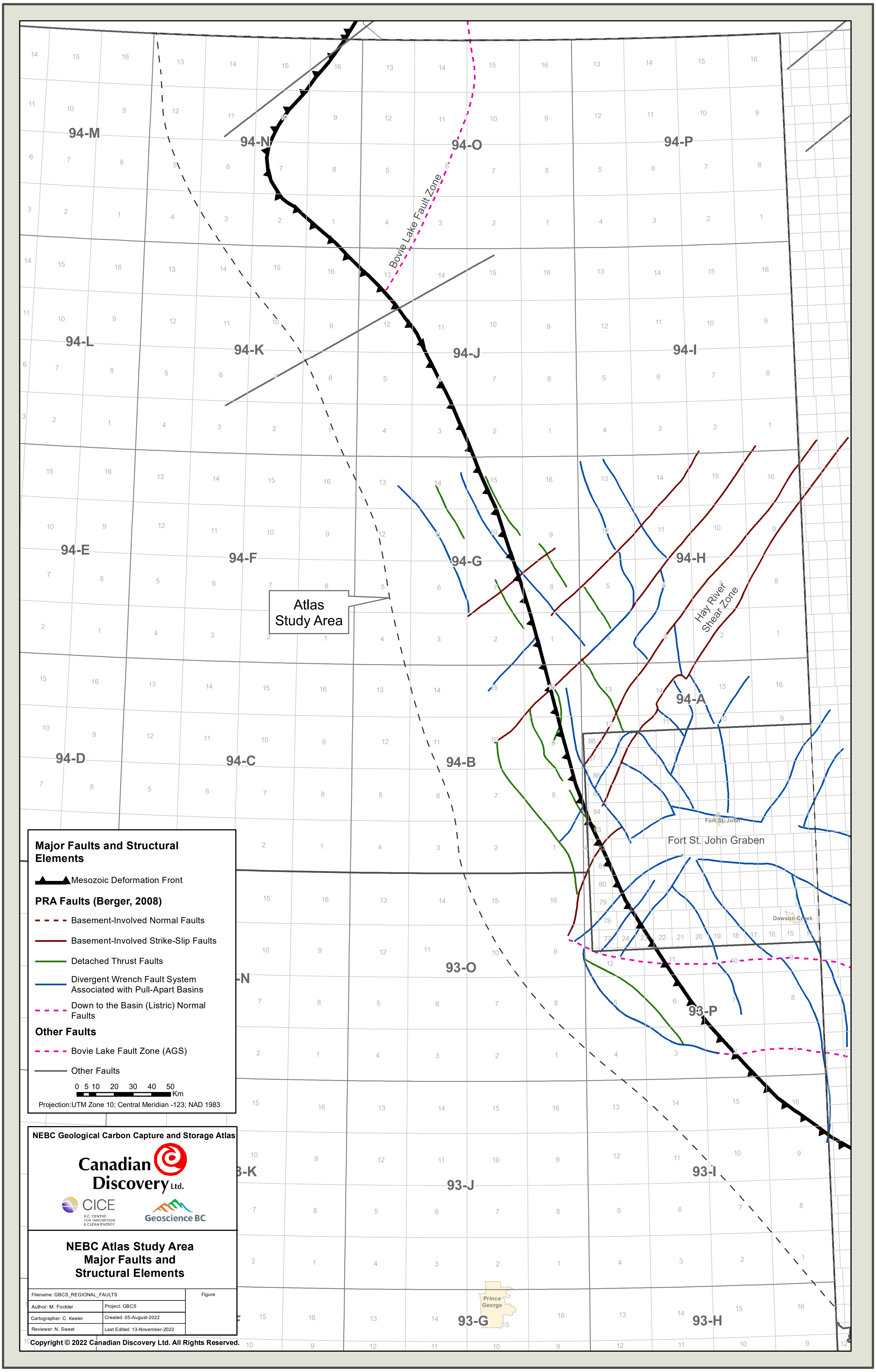

© Canadian Discovery Ltd.

Figure 3.2

Northeast BC Geological Carbon Capture and Storage Atlas

ATLAS OVERVIEW

Introduction to the Atlas

The Northeast BC Geological Carbon Capture and Storage Atlas is intended to be used as a guide to provide high level, regional identification and assessment of two types of carbon storage opportunities, namely depleted and nearly depleted gas reservoirs and saline aquifers. This first phase of the Atlas will focus on preliminary reconnaissance mapping to identify prospective zones, provide a high level look at the geology, reservoir quality and conditions, and hydrodynamics of depleted pools and saline aquifers as well as a preliminary estimate of their CO_2 storage potential. The previous chapter focused on an overview of storage project considerations, while this chapter will focus on the components provided in this Atlas to help address these considerations, as well as some important information regarding how these components were mapped and compiled.

Chapter Organization

Starting in *Chapter 5*, storage reservoirs are presented within a geological formation — or group of related formations — that represent a "storage complex", which encompasses the main storage reservoir(s), as well as the sealing units above and below. Each chapter has key maps and graphs that are required for early subsurface carbon storage target scoping, including infrastructure and emitter proximity.

The stratigraphic/hydrostratigraphic chart *(figure 4.1)* outlines the formations that exist in the subsurface of the study area. The starred formations host depleted pools that meet basic selection criteria for carbon storage, while the red circles indicate formations with aquifers that could potentially store carbon. The hydrostratigraphy refers to whether a formation is considered an aquifer, a seal or both. An aquifer is an underground layer of water-bearing permeable rock that allows for the flow of water (saline or fresh), and in this study it could also be considered a potential carbon storage reservoir. An aquitard is a lower permeability underground layer that limits the flow of water from one aquifer to another and acts as a barrier to flow. It is also referred to as a seal, and has previously trapped hydrocarbons in depleted pools, or is capable of trapping injected CO_2 in an aquifer. Some formations are considered "mixed" as they can locally act as a reservoir or seal depending on the geology and hydrodynamics.

Formation Selection and Exclusion Criteria

Formations are reviewed as viable carbon storage candidates if they host depleted pools and/or aquifers. Once meeting basic criteria, estimates are made regarding how much CO_2 the depleted pools or aquifers could potentially hold. For depleted pools, these estimates were based on previous fluid production. For aquifers, the estimates were based on a percentage of the aquifer pore volume, which requires net reservoir thickness maps and porosity estimates. Previous studies provided several of the net reservoir thickness maps, with net reservoir cutoffs from 6% to 12% porosity. For additional aquifer mapping, log porosities of 6% and greater were considered to have sufficient reservoir quality for carbon storage. Core data and water recoveries from DST analyses were used to support these cutoffs.

Some formations did not meet the selection criteria above and have been excluded from consideration as potential carbon storage targets. Other formations that were too variable and difficult to assess were also excluded from discussion in this phase of the Atlas. Excluded formations are the Cardium, Dunvegan, Chinkeh, Belcourt-Taylor Flat, Mattson-Kiskatinaw and Wabamun.

4.1 Hydrostratigraphic Chart

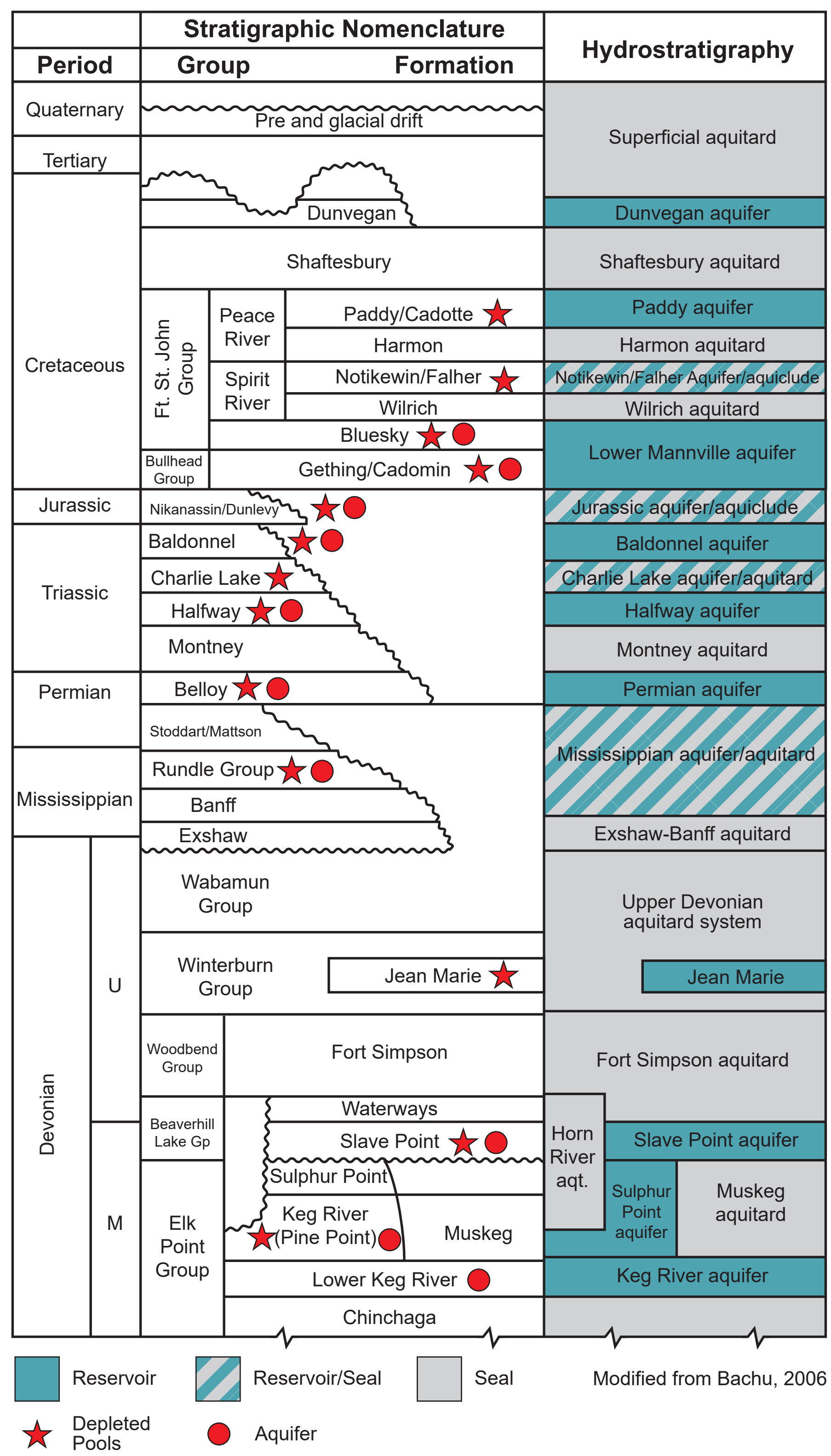

 Figure 4.1

Depleted and Nearly Depleted Pools Selection and Exclusion Criteria

The BC Oil and Gas Commission (BC OGC) defines depleted pools as ones that have no remaining reserves or production. The BC OGC also recognizes that there are nearly depleted pools that could become CO_2 storage candidates in the (relatively) near future. The nearly depleted CO_2 storage candidates include pools where 90+% of the reserves have been recovered, or no production has occurred in over five years.

The BC OGC excludes depleted pools as candidates for CO_2 storage when:

- The zones are deemed unconventional (DPR Schedule 2), such as the Heritage Montney, Northern Montney, Deep Basin Cadomin and Horn River Muskwa Evie Otter pools
- All the wells have been decommissioned with surface reclamation completed
- The true vertical depth (TVD) is less than 600m

Canadian Discovery (CDL) has further refined the depleted and nearly depleted pool candidates by excluding:

- Pools shallower than 800m TVD. As mentioned previously, at depths below about 800m, natural temperature and pressures tend to exceed the critical point of CO_2. In areas where this transition is deeper than 800m, pressure and temperature transitions have been indicated on the maps.
- Hydrocarbon pools that produced greater than or equal to 20% oil. These pools were categorized as candidates for future evaluation for carbon capture and utilization (CCUS) studies and enhanced oil recovery. In these scenarios, the CO_2 may need to be produced and re-injected, rather than injected for permanent, dedicated storage.
- Pools that are west of the Mesozoic deformation front, as that area hosts considerable faulting and potential risk. Some exceptions were made for depleted pools in the southern part of the study area that were proximal to emitting areas where few other options for storage are currently available.

Aquifer Selection and Exclusion Criteria

For saline aquifers, data regarding reservoirs and seals, depth, net reservoir thickness, and pressure and temperature conditions were collected from previous studies (Geoscience BC, Canadian Discovery, other industry). Water recoveries from drillstem test (DST) data were also considered. Additional mapping was completed by CDL where required to identify prospective aquifers. Aquifers shallower than 800m, thinner than about 5-10m and exhibiting porosity below 6% were excluded from analysis.

Atlas Components

In each chapter, a brief *geological write-up and schematic* is provided to give general geological depositional information and stratigraphy of the formation(s), including both the reservoirs and the seals, which together make up the storage complex. As this Atlas is a high level regional study, the formation deposition and descriptions are generalized to encompass a broad area.

A *structure map* shows the topography of the mapped zone in the subsurface. Since the displacement of a CO_2 plume is governed by gravity and buoyancy, the plume tends to migrate up-structure (towards the surface) during its injection period. As a result, it is important to be aware of the structural trends of the storage reservoir. This map also contains key true vertical depth, pressure and temperature contours that highlight where CO_2 is expected to be in supercritical state. As discussed earlier in the introduction, supercritical CO_2 is dense like a liquid and requires less volume for storage, but has low viscosity like a gas. Supercritical conditions for CO_2 comprise a temperature in excess of 31.1°C and a pressure greater than 7,500 kPa, so a 7,500 kPa and 31°C contour are included on the map. A total vertical depth (TVD) cutoff of 800m is shown on the maps to indicate the approximate depth limit for the evaluation for each zone.

Net reservoir maps are provided for the depleted pools and for the saline aquifers (where mapped). These maps can help indicate the most favourable areas for CO_2 injection within storage reservoirs — i.e. where the reservoir rock has the highest quality, often the highest porosity and permeability. The net reservoir contours within the pools were provided by the BC OGC. The net reservoir contours within the saline aquifers were sourced from several existing studies. CDL has merged these datasets and provided geological support to fill in any gaps between previously existing datasets and the Atlas study area.

Core data were obtained from geoLOGIC and filtered for better quality reservoir that is more conducive to carbon storage. Establishing detailed *porosity trends* requires examination of log suites and petrophysical models, which is beyond the scope of this phase of the Atlas. However, available core data can be used to provide a high level estimate of porosity trends, particularly within the aquifers, where this information is needed for storage potential estimates. The core data were aggregated to estimate porosity trends in the aquifers, which is necessary information for storage calculations, and to do a preliminary analysis of porosity-permeability trends observed in various areas and rock types. While permeability is not directly part of a storage potential calculation, it has an impact on accessibility of the porosity to the injected CO_2 and on maintaining the required injection rate for the project lifespan. Higher permeability rock allows fluids to migrate more easily through better connected pores away from the injection well, which subsequently magnifies the potential and efficiency of the aquifer to store CO_2. The kh (permeability x thickness) is proportional to the injectivity. Injectivity is defined as the ratio of the injection rate to the pressure change between the well and storage zone.

To delineate the extent of the aquifers and understand the relationship between the aquifers and the depleted pools, an analysis is done on the *hydrodynamics* (interaction of fluids in the subsurface). Hydrofax drillstem test (DST) data from within the aquifers, and the initial pressure and datum depth of each depleted pool from the BC OGC reserves databases were used to create a pressure vs elevation (P/E) graph. A P/E graph can provide information such as the structural extent and flow of an aquifer; or for a depleted pool, whether it has structural closure underlain by a conventional aquifer (open system); or whether it is an isolated sweet spot within tighter reservoir (closed system). Determining the type of system can have important implications on the storage potential of the reservoir, and is a factor that needs to be considered in the subsequent steps of modelling the storage reservoir.

Carbon Storage Calculations

Using the components discussed above, estimates are made regarding how much CO_2 the depleted pools or aquifers can potentially hold. For depleted pools, these estimates are based on previous fluid production. For aquifers, the estimates are based on a percentage of the aquifer pore volume, which requires net reservoir thickness maps and porosity estimates. More detail is provided on the carbon storage calculations for both depleted pools and aquifers in *Appendix B*, and data are provided for all depleted pools included in this study in *Appendix C*.

Depleted and Nearly Depleted Pools

The *theoretical* CO_2 storage potential represents the mass of CO_2 that can be stored in the hydrocarbon reservoirs assuming that the volume occupied previously by the produced gas will be occupied entirely by the injected CO_2. These calculations have been provided by the BC OGC and are based on historical pool production.

For depleted pools, the estimated *effective* CO_2 storage potential represents the mass of CO_2 that can be stored in hydrocarbon reservoirs after taking into account intrinsic reservoir characteristics and flow processes, such as heterogeneity (how much variability there is in the rock), aquifer support, sweep efficiency, gravity override, and CO_2 mobility (Bachu, 2006). The estimated effective CO_2 storage potential is calculated by CDL and reduces the theoretical storage potential by as little as 13% and as much as 75%.

The depleted and nearly depleted pools that are deemed to be CO_2 storage candidates by CDL are coloured by their effective storage potential mass on the summary maps.

Aquifers

For aquifers, a *theoretical* CO_2 storage potential can be calculated using the mapped pore volume of the reservoir and CO_2 density, and assumes that the pore volume will be occupied entirely by the injected CO_2. We know this is not the case however, since the pore space is already occupied by water and the water will need to be displaced during the sequestration process. As a result, a *storage efficiency* factor is introduced into storage potential calculations that accounts for the presence of both water and CO_2 in the aquifer. The storage efficiency factor is a function of reservoir and fluid properties and dynamics, including the geometry of the trap, gravity segregation, heterogeneity, permeability distribution and pressure, and may reduce the theoretical storage potential by anywhere from 95% to 99%.

Aquifers considered favourable targets for CO_2 storage are indicated on the summary map and labelled with their estimated P10, P50 and P90 effective storage potential in Mt.

PEACE RIVER (PADDY/CADOTTE) FORMATION

Peace River Overview

Storage potential in the Peace River Formation *(figure 5.1)* occurs predominantly to the south of Fort St. John in the Peace River area. Favourability attributes are summarized in *table 5.1* with green and yellow circles indicating whether an attribute is considered generally favourable (green), or has risk and/or requires additional work (yellow). Both depleted pool reservoirs and saline aquifers are candidates and offer minor storage opportunities. The top 10 depleted pools are shown in *figure 5.2*. *Figure 5.3* displays the effective storage potential of the Peace River, as well as emitters and infrastructure in the NEBC study area.

Peace River Favourability Attributes

Top 10 Depleted Pool Total Potential	13 Mt	yellow
Aquifer Storage (P50)	12 Mt	yellow
Regional Seal Potential	High	green
Lithology	Sandstone	green
Porosity	8-22%	green
Permeability	10-300 mD	green
Depth (TVD)	800-2,400m	green
Net Reservoir Thickness	2-20m	green

Table 5.1

5.1 Hydrostratigraphic Chart

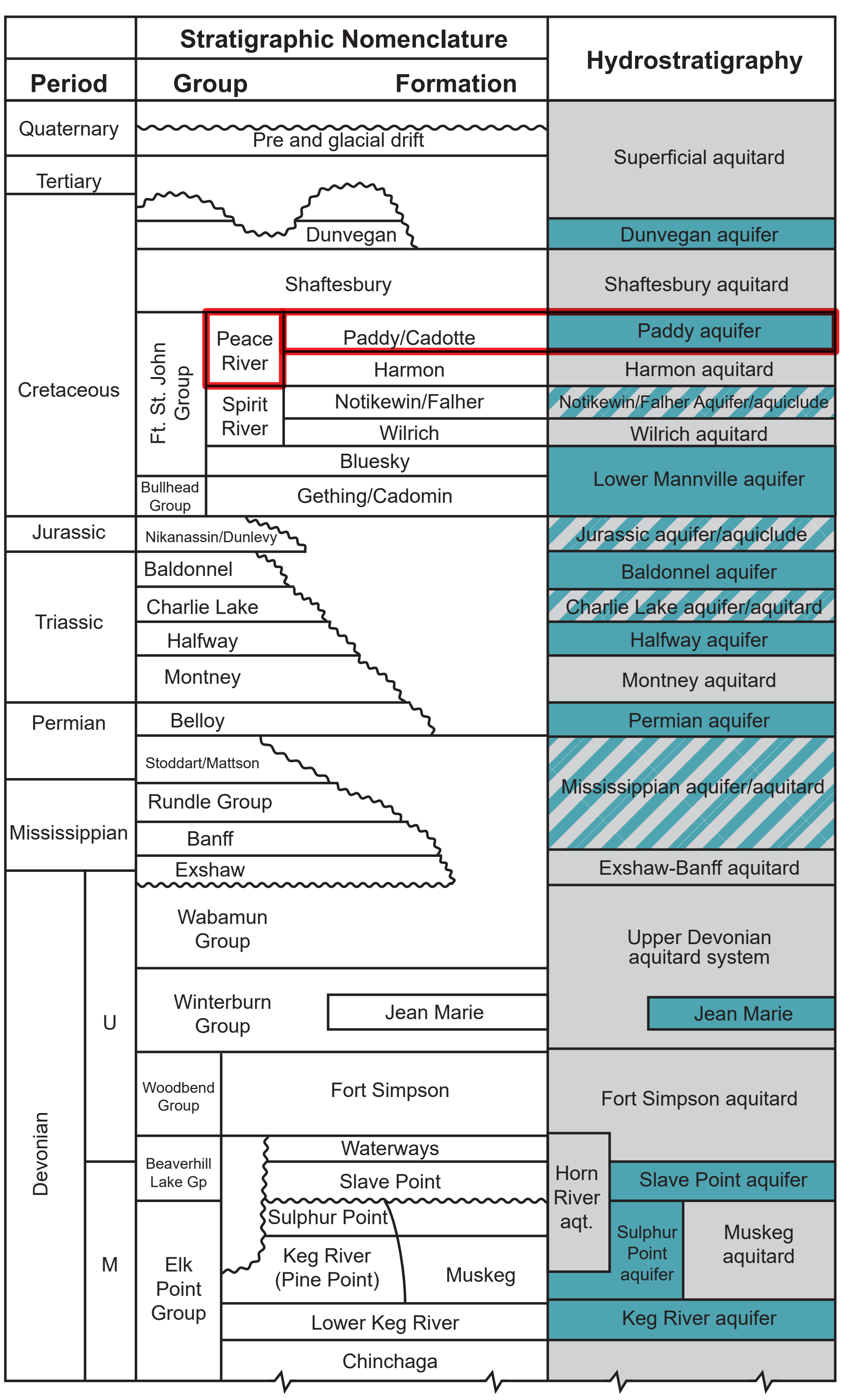

Modified from Bachu, 2006

 Figure 5.1

5.2 Top 10 Depleted Peace River Pools

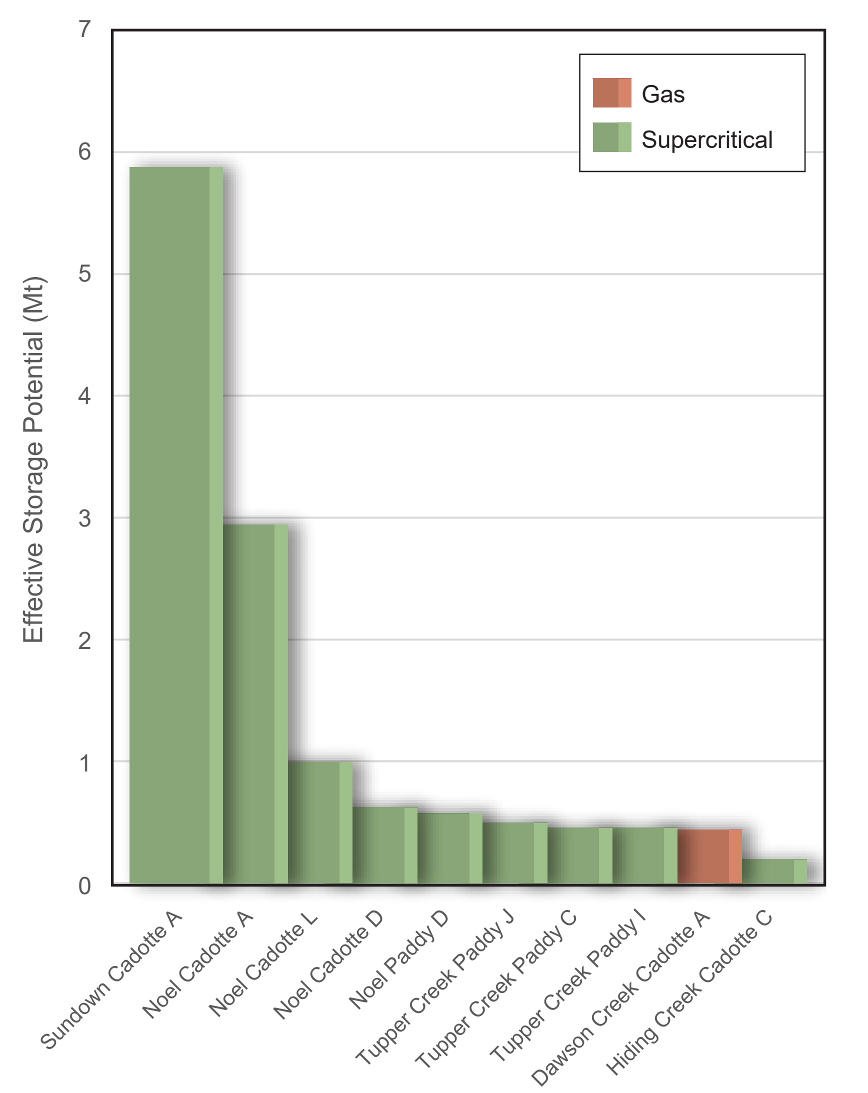

 Figure 5.2

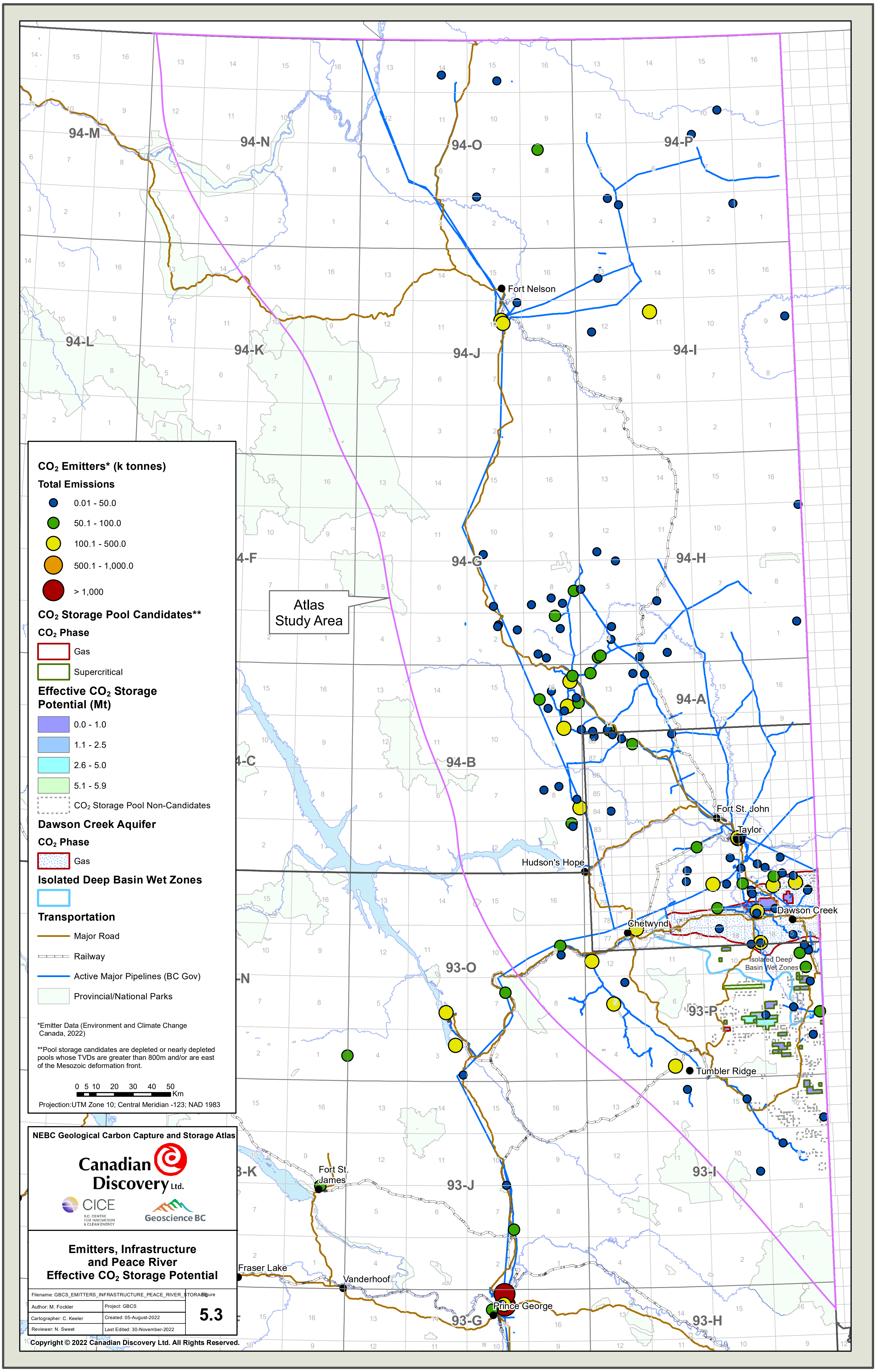

© Canadian Discovery Ltd.

Figure 5.3

5.4 Peace River Play Schematic

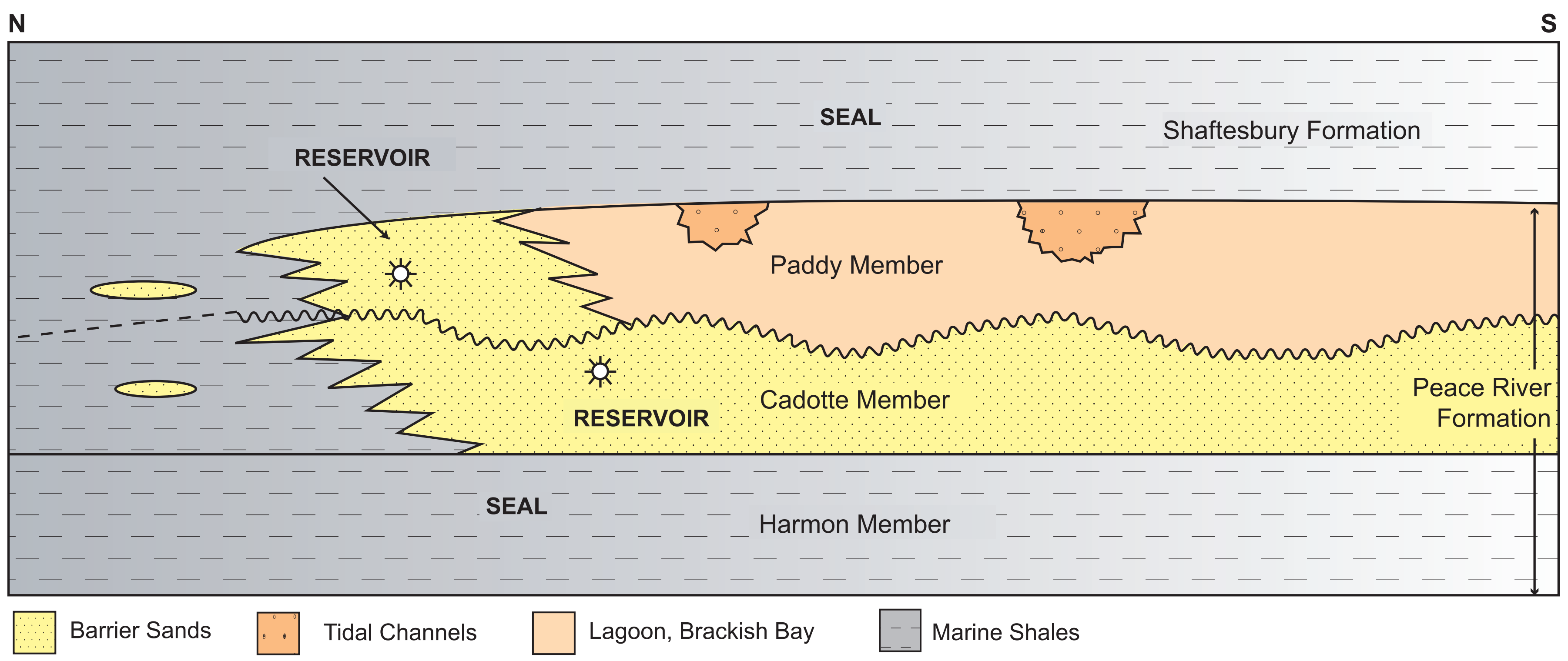

Figure 5.4

Storage Complex

The early Cretaceous-age Peace River Formation (Paddy, Cadotte and Harmon members) trend is located in the Peace River area; it is confined to the west by the deformation front and to the north by non-deposition of reservoir-quality sands *(figure 5.4)*. The Paddy Member in northeastern BC is equivalent to the Viking Formation and was deposited in the upper Albian, when the Peace River Arch was a negative feature. The Paddy lies unconformably over the Cadotte and Harmon members. The Cadotte is a significant reservoir in the area and was deposited as a barrier bar on a high-energy, prograding shoreline that initially trended northwest-southeast and then shifted to a more easterly direction as a result of progradation (Reinson et al, 1994). A fall in relative sea level caused valley incision and erosion of the Cadotte. As sea level rose, Paddy sediments were deposited in the valleys and then in a tide-dominated brackish bay or estuarine environment separated from open marine conditions by a northeasterly-trending barrier bar (Smith et al. 1984). Gas was trapped structurally in the Paddy and Cadotte barriers on the Peace River Arch and now present depleted pool opportunities.

The reservoir is sealed above by the thick and regionally extensive shales of the Shaftesbury Formation. The basal seal is formed from the shales of the Harmon Member, and the shale equivalents of the Paddy/Cadotte sands provide updip lateral seals. This storage complex is well contained and will act as a suitable trap for CO_2.

The Peace River subsea structure map *(figure 5.5)* shows the topography of the top of the Peace River in the subsurface. Since the displacement of a CO_2 plume is governed by gravity and buoyancy, the plume tends to migrate up-structure during its injection period. This map shows the 800m true vertical depth contour, which indicates the approximate depth limit for this evaluation. As supercritical conditions for CO_2 comprise a temperature in excess of 31.1°C and a pressure greater than 7,500 kPa, the Peace River 7,500 kPa and 31°C contours indicate where CO_2 injection is expected to be in the supercritical phase.

Figure 5.6 is a net reservoir map for the Dawson Creek saline aquifer. The net reservoir contours within the saline aquifer were sourced primarily from Geoscience BC Report 2021-14 (PRCL, 2021). Also indicated on the map is an area where isolated wet conglomerates may provide attractive local aquifer targets with more detailed mapping.

Net reservoir contours within the depleted pools were provided by the BC Oil and Gas Commission *(figure 5.7)*. These maps can help indicate the most favourable areas for CO_2 injection within storage reservoirs; i.e. where the reservoir rock is the thickest, and sometimes the highest porosity and/or permeability.

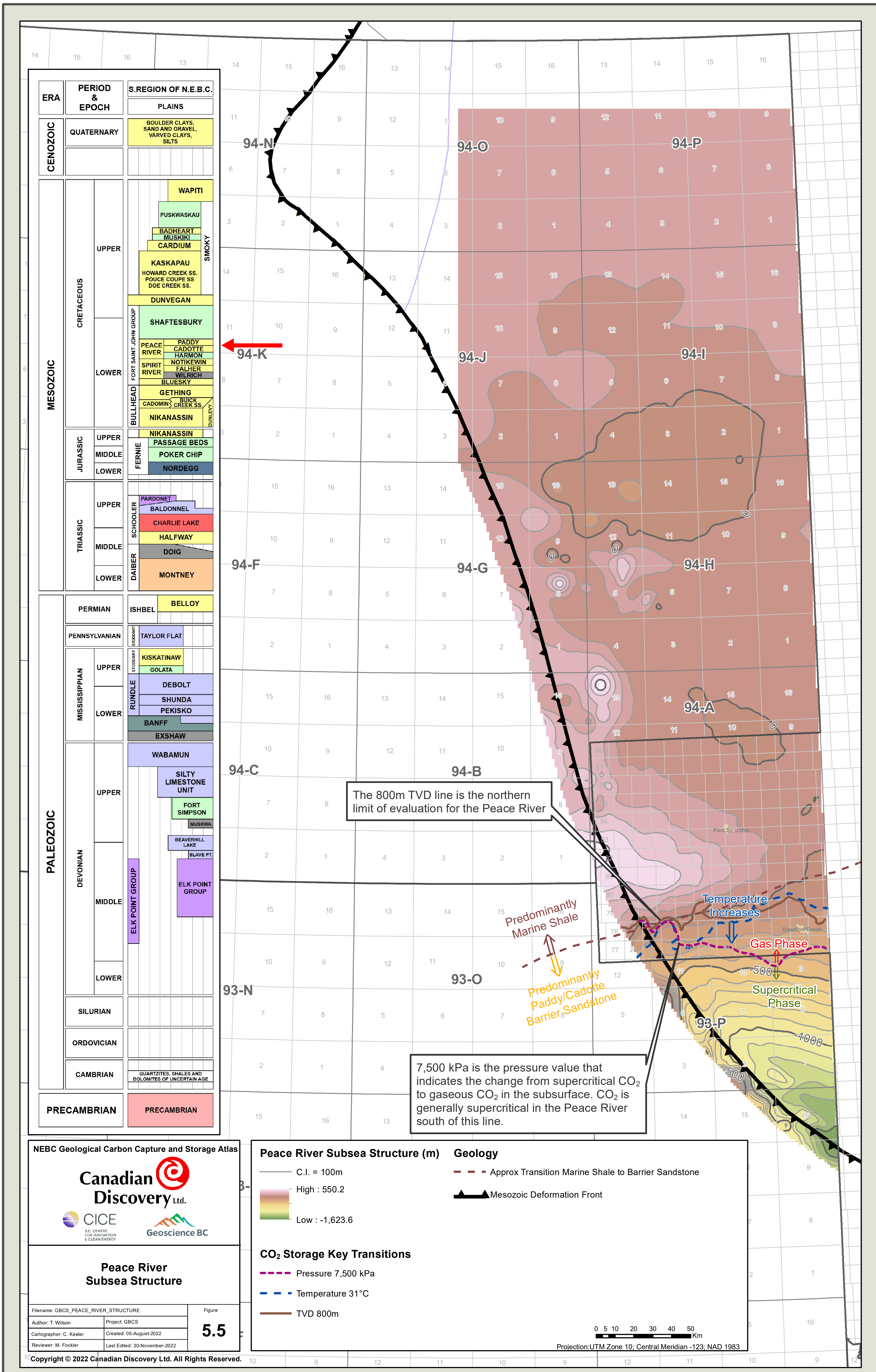

© Canadian Discovery Ltd. *Figure 5.5*

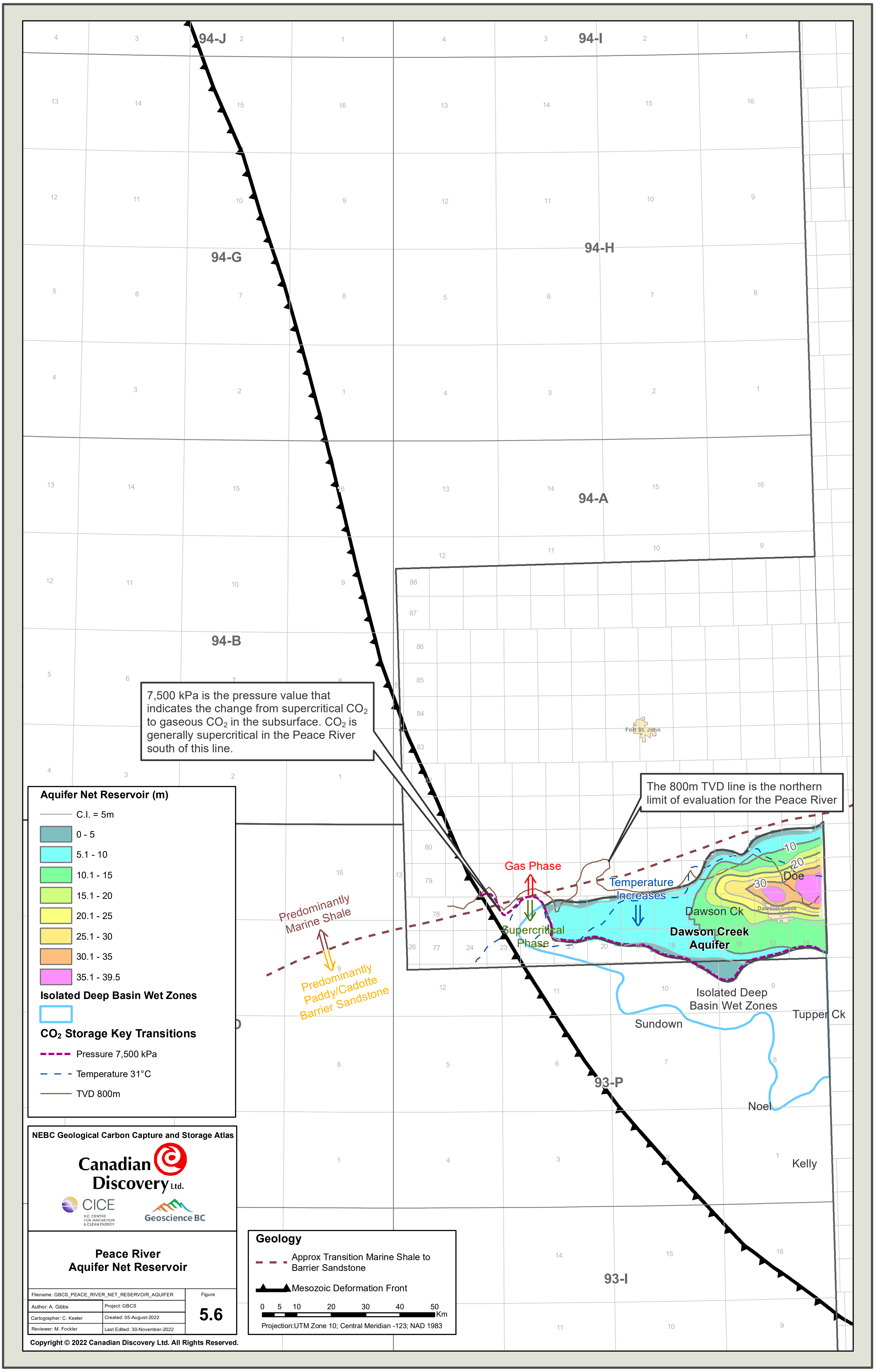

94-J
94-I
94-G
94-H
94-A
94-B
93-P
93-I
Fort St. John
7,500 kPa is the pressure value that indicates the change from supercritical CO_2 to gaseous CO_2 in the subsurface. CO_2 is generally supercritical in the Peace River south of this line.
The 800m TVD line is the northern limit of evaluation for the Peace River
Gas Phase
Supercritical Phase
Temperature Increases
Predominantly Marine Shale
Predominantly Paddy/Cadotte Barrier Sandstone
Dawson Ck
Dawson Creek Aquifer
Doe
Isolated Deep Basin Wet Zones
Sundown
Tupper Ck
Noel
Kelly
Aquifer Net Reservoir (m)
C.I. = 5m
0 - 5
5.1 - 10
10.1 - 15
15.1 - 20
20.1 - 25
25.1 - 30
30.1 - 35
35.1 - 39.5
Isolated Deep Basin Wet Zones
CO_2 Storage Key Transitions
Pressure 7,500 kPa
Temperature 31°C
TVD 800m
NEBC Geological Carbon Capture and Storage Atlas
Canadian Discovery Ltd.
CICE
Geoscience BC
Peace River
Aquifer Net Reservoir
Filename: GBCS_PEACE_RIVER_NET_RESERVOIR_AQUIFER
Figure
5.6
Author: A. Gibbs
Project: GBCS
Cartographer: C. Keeler
Created: 05-August-2022
Reviewer: M. Fockler
Last Edited: 30-November-2022
Copyright © 2022 Canadian Discovery Ltd. All Rights Reserved.
Geology
Approx Transition Marine Shale to Barrier Sandstone
Mesozoic Deformation Front
0 5 10 20 30 40 50 Km
Projection:UTM Zone 10; Central Meridian -123; NAD 1983

Figure 5.6

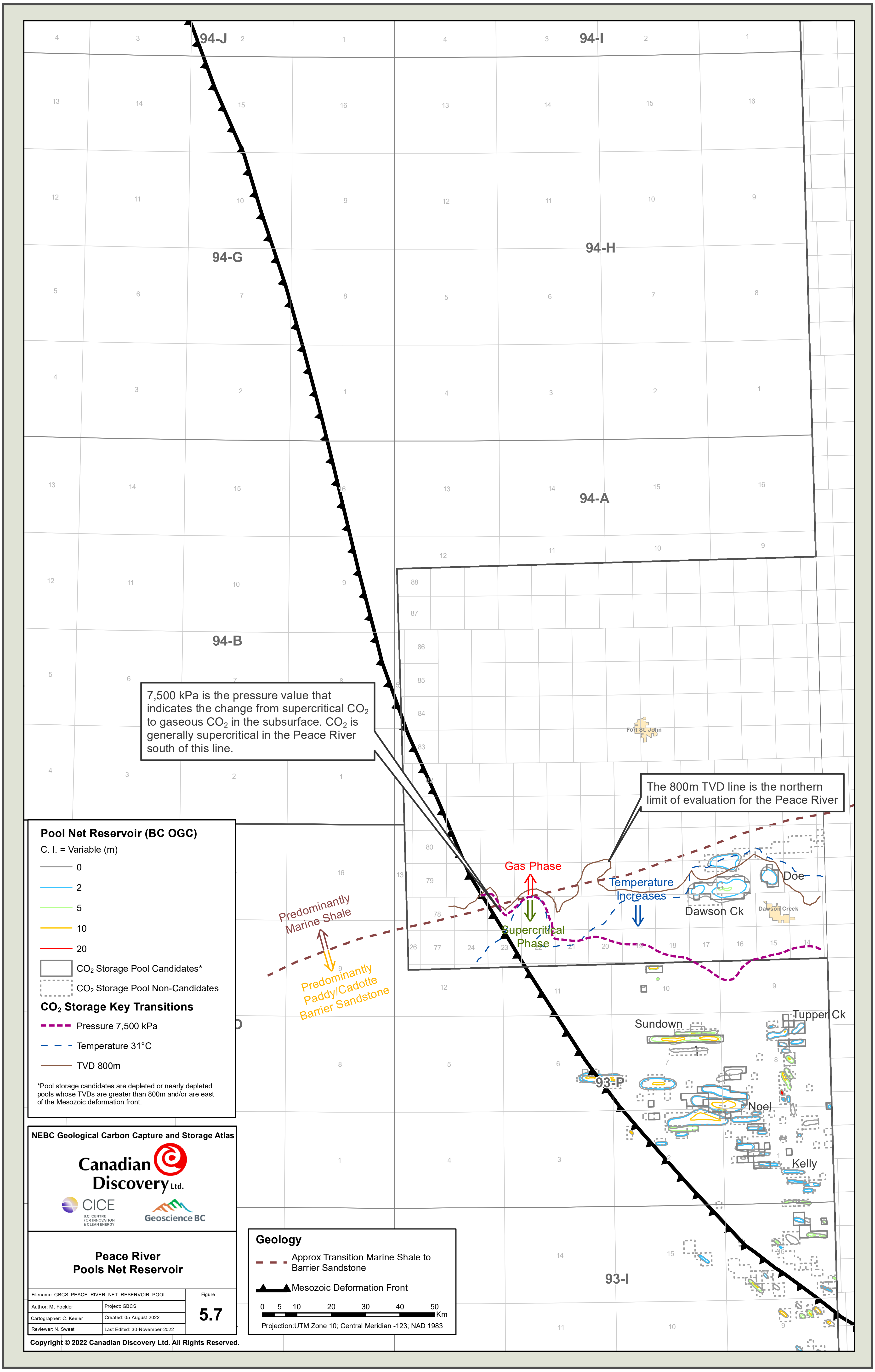

© Canadian Discovery Ltd.

Figure 5.7

Porosity-Permeability Correlations

Core data for the Peace River were obtained from geoLOGIC and filtered for better quality reservoir that is more conducive to carbon storage (greater than 8% porosity and 10 mD permeability) within the study area. These data were used to estimate porosity trends in the aquifers for storage calculations and to do a preliminary analysis of the multiple porosity-permeability trends that are observed in the Peace River *(figure 5.8)*.

In the area of the Dawson Creek aquifer (Twp 78-79), Paddy and Cadotte barrier shoreface and estuarine sandstones stack atop one another. Porosity is quite high ranging from 16 to 28%, particularly in less-compacted strata in the east. Permeability is moderate in the 50–150 mD range.

In the south, narrow east-west-trending Cadotte sand and conglomerate reservoirs have porosities ranging from 12 to 20%, which may exhibit permeability in the range of 100s of mD, and host either water or gas (PRCL, 2021). Transition to a Deep Basin system gas-charged system begins south of Twp 77, and this area contains isolated wet conglomerates that may provide attractive local aquifer targets with more detailed mapping. Further south, Deep Basin depleted gas pools at Tupper Creek, Sundown, Noel and Kelly provide lower porosity (9–14%) reservoirs with very high permeabilities (up to 1 Darcy).

5.8 Peace River Porosity-Permeability Plot

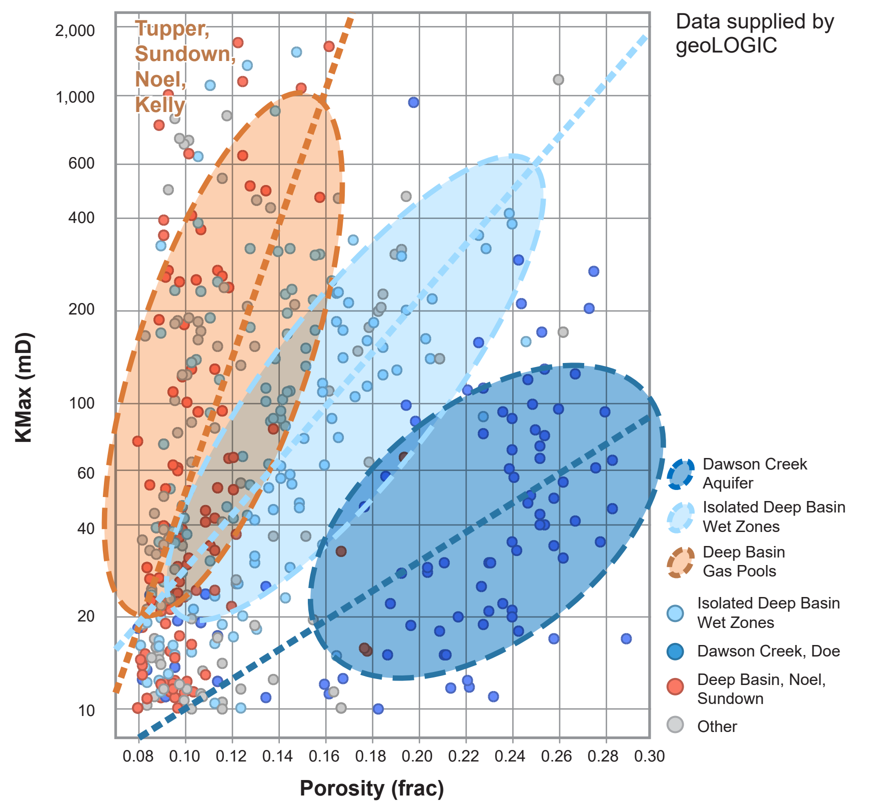

© Canadian Discovery Ltd. *Figure 5.8*

Hydrodynamics

To delineate the extent of the aquifers and understand the relationship between the aquifers and the depleted pools, a high-level analysis was done on Peace River hydrodynamics *(figure 5.9)* using Hydrofax drillstem test (DST) data from within the aquifers and the initial pressure and datum depth of each depleted pool from the BC OGC reserves databases.

In the Dawson Creek area, where Paddy and Cadotte barrier shoreface and estuarine sandstones stack atop one another, the conventionally trapped pools at Dawson Creek, Doe and Sunrise sit above an aquifer system. The Pressure vs Elevation (P/E) graph *(figure 5.9)* shows that the entire system is below supercritical pressure for CO_2 (7,500 kPa) and is therefore not ideal for CO_2 storage.

To the south, isolated sweet spots of good quality reservoir support a transition to an underpressured Deep Basin. This area contains isolated wet conglomerates that may provide attractive local CO_2 storage targets with more detailed mapping. Depleted gas pools at Tupper Creek, Sundown, Noel and Kelly provide lower porosity, but very high permeability potential CO_2 storage candidates. Reservoirs within the Deep Basin exhibit good containment, but their limited regional extent may also limit storage potential.

5.9 Peace River Pressure vs Elevation Plot

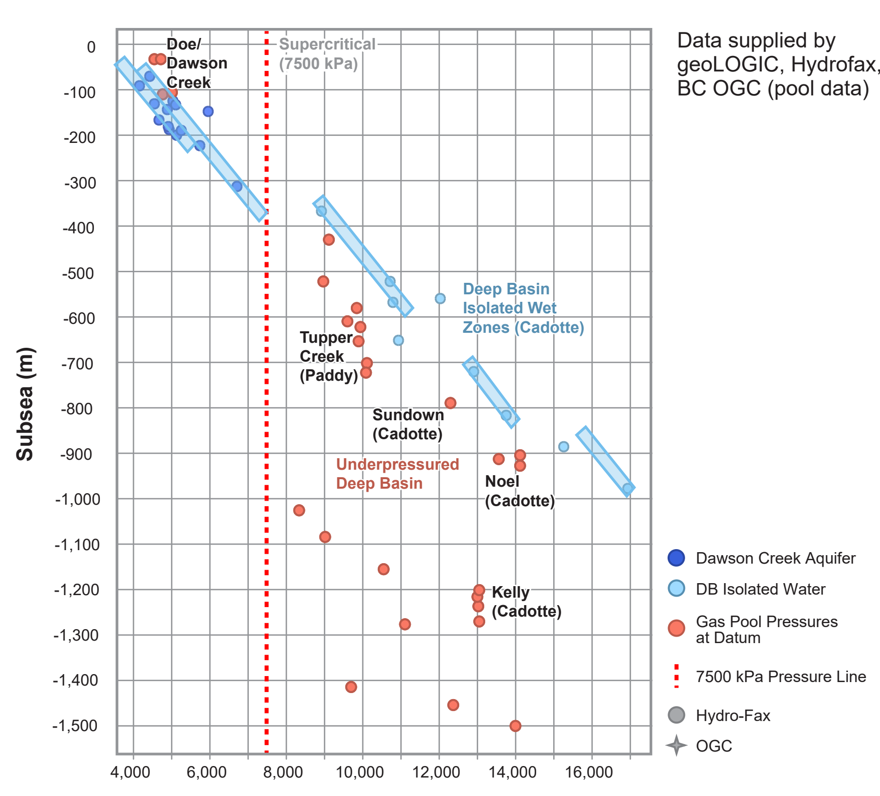

© Canadian Discovery Ltd. *Figure 5.9*

Carbon Storage Calculations

Depleted and Nearly Depleted Pools

The depleted pool candidates for carbon storage potential within the Peace River Formation are shown in *Table 5.2*.

The BC OGC defines depleted pools as ones that have no remaining reserves or production. The BC OGC also recognizes that there are nearly depleted pools that could become CO_2 storage candidates in the (relatively) near future. The nearly depleted CO_2 storage candidates include pools where 90%+ of the reserves have been recovered, or no production has occurred in over five years. Furthermore, CDL has excluded pools that are shallower than 800m TVD, or are west of the Mesozoic deformation front. See Depleted Pools Selection Criteria in *Chapter 4* for a more thorough discussion.

The theoretical CO_2 storage potential represents the mass of CO_2 that can be stored in the hydrocarbon reservoirs assuming that the volume occupied previously by the produced gas will be occupied entirely by the injected CO_2. These calculations have been provided by the BC OGC and are based on historical pool production.

The effective CO_2 storage potential represents the mass of CO_2 that can be stored in hydrocarbon reservoirs after taking into account intrinsic reservoir characteristics and flow processes, such as heterogeneity (how much variability there is in the rock), aquifer support, sweep efficiency, gravity override, and CO_2 mobility (Bachu, 2006). The effective CO_2 storage potential is calculated by CDL and reduces the theoretical storage potential by as little as 13% and as much as 75%. More detail is provided on the carbon storage calculations for depleted pools in *Appendix B*, and data are provided for all depleted pools included in this study in *Appendix C*.

The depleted and nearly depleted pools that are deemed to be CO_2 storage candidates by CDL are coloured by their effective storage potential mass on the summary map *(figure 5.10)*.

Aquifers

The Peace River aquifer parameters are summarized in *Table 5.3*. Theoretical CO_2 storage potential can be calculated using the mapped pore volume of the reservoir and CO_2 density, and assumes that the pore volume will be occupied entirely by the injected CO_2. We know this is not the case however, since the pore space is already occupied by water and the water will need to be displaced in the process. As a result, a storage efficiency factor is introduced into storage potential calculations that accounts for the presence of both water and CO_2 in the aquifer. The storage efficiency factor is a function of reservoir and fluid properties and dynamics, including the geometry of the trap, gravity segregation, heterogeneity, permeability distribution and pressure, and may reduce the theoretical storage potential by 95 to 99%.

Aquifers considered favourable targets for CO_2 storage are indicated on the summary map *(figure 5.10)* and labelled with their estimated P10, P50 and P90 effective storage potential in Mt. More detail is provided on the aquifer carbon storage calculations in *Appendix B*.

Depleted Peace River Pools

Pool Name	Pool Type	Well Count	Initial Pressure (kPa)	Temperature (˚C)	Average Porosity (%)	CO_2 Phase	Theoretical Storage Potential (Mt)	Effective Storage Potential (Mt)
Sundown Cadotte A	Gas	6	12,304	62	6.9	Supercritical	6.7	5.9
Noel Cadotte A	Gas	13	9,027	71	8.4	Supercritical	3.4	3.0
Noel Cadotte L	Gas	7	8,359	72	8.9	Supercritical	1.2	1.0
Noel Cadotte D	Gas	3	13,050	74	8.2	Supercritical	0.7	0.6
Noel Paddy D	Gas	1	22,437	68	7.6	Supercritical	0.7	0.6
Tupper Creek Paddy J	Gas	2	10,134	59	13.0	Supercritical	0.6	0.5
Tupper Creek Paddy C	Gas	1	9,946	55	10.7	Supercritical	0.6	0.5
Tupper Creek Paddy I	Gas	4	9,910	55	13.9	Supercritical	0.6	0.5
Dawson Creek Cadotte A	Gas	5	4,778	37	16.0	Gas	0.5	0.5
Hiding Creek Cadotte C	Gas	3	14,012	81	8.6	Supercritical	0.3	0.2
Brassey Cadotte B	Gas	2	9,130	64	8.1	Supercritical	0.2	0.2
Tupper Creek Paddy G	Gas	2	10,100	60	14.7	Supercritical	0.2	0.2
Sunrise Cadotte A	Gas	12	5,033	37	23.4	Gas	0.2	0.1
Noel Cadotte N	Gas	2	14,132	69	8.5	Supercritical	0.1	0.1
Tupper Creek Paddy E	Gas	1	9,608	58	12.0	Supercritical	0.1	0.1
Tupper Creek Paddy D	Gas	1	9,851	55	17.0	Supercritical	0.1	0.1
Kelly Cadotte E	Gas	1	13,006	71	6.2	Supercritical	0.1	0.1
Noel Cadotte G	Gas	3	10,557	74	8.5	Supercritical	0.1	0.1
Kelly Cadotte F	Gas	1	13,054	74	8.2	Supercritical	0.1	0.1
Hiding Creek Cadotte J	Gas	2	12,388	82	11.0	Supercritical	0.1	0.1
Noel Cadotte J	Gas	1	13,064	77	7.1	Supercritical	0.1	0.1
Jackpine Cadotte E	Gas	1	3,959	67	5.9	Gas	0.1	0.1

© Canadian Discovery Ltd. Data supplied by BC OGC and Canadian Discovery Ltd.

Table 5.2

Peace River Aquifers Properties and Storage Potential

Aquifer Name	Type	Thickness Range (m)	Pressure Range (MPa)	Temperature Range (˚C)	Porosity Range (%)	CO_2 Phase	P10 Effective Storage Potential at 0.5% (Mt)	P50 Effective Storage Potential at 2% (Mt)	P90 Effective Storage Potential at 5.4% (Mt)
Dawson Creek Hydraulic System	Aquifer	5-40	3.9-7.5	27-48	16-28%	Gas	3.0	12.2	32.8

© Canadian Discovery Ltd.

Table 5.3

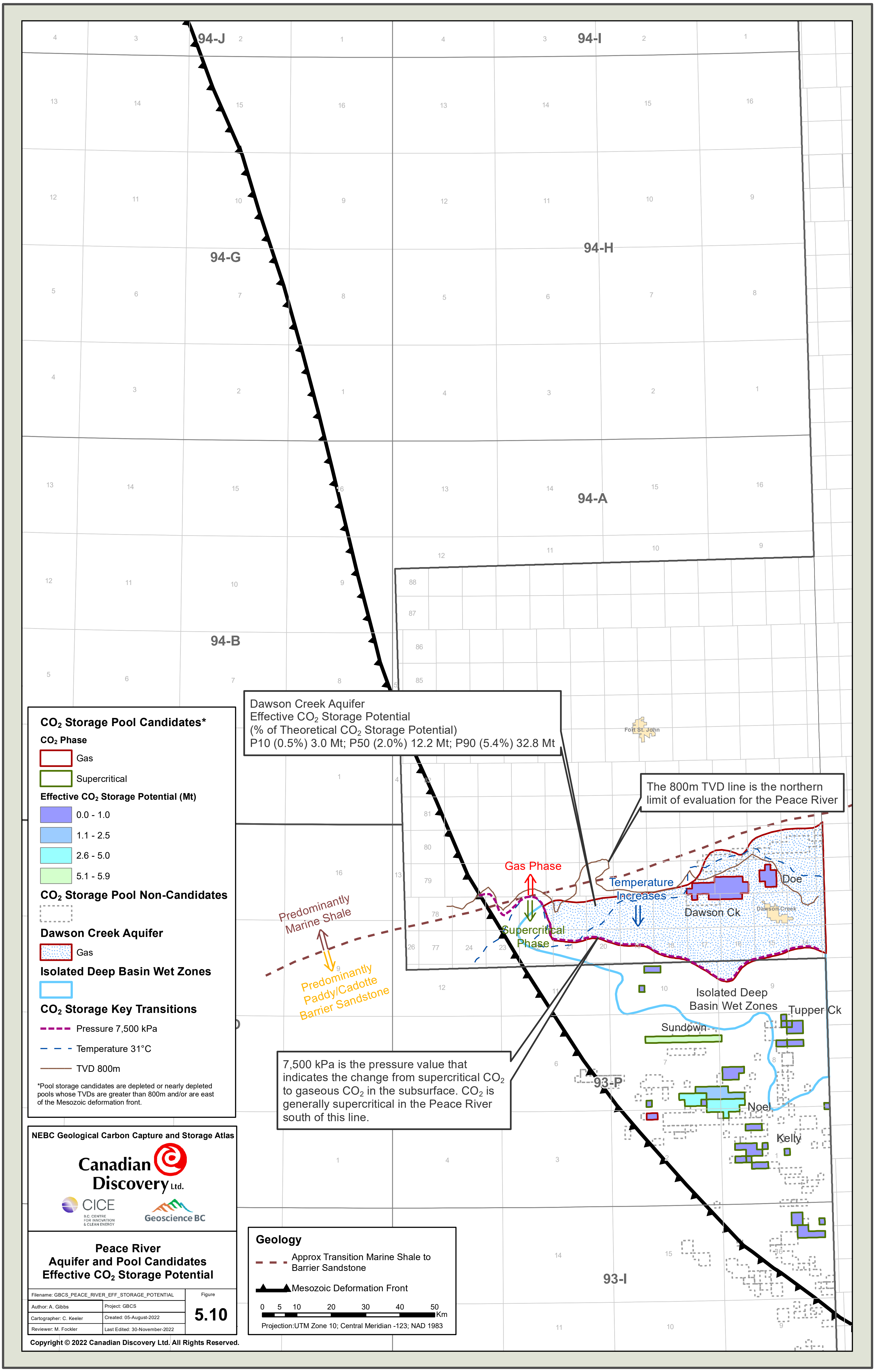

© Canadian Discovery Ltd.

Figure 5.10

Spirit River (Notikewin, Falher) Formation

Spirit River Overview

Storage potential in the Spirit River *(figure 6.1)* occurs north (mostly Notikewin) and south (mainly Falher, with some Notikewin) of the Peace River area in the southern portion of the study area. Favourability attributes are summarized in *table 6.1* with green and yellow circles indicating whether an attribute is considered generally favourable (green) or has risk and requires additional work (yellow). Due to geological complexity, the aquifer potential of the Spirit River members is difficult to map and assess, and is therefore not included for this phase of the Atlas. Depleted pools have limited carbon storage potential. The top 10 depleted pools are shown in *figure 6.2*. *Figure 6.3* displays the effective storage potential of the Spirit River depleted pools, as well as the emitters and infrastructure in the NEBC study area.

Spirit River Favourability Attributes		
Top 10 Depleted Pool Total Potential	11 Mt	yellow
Aquifer Storage (P50)	n/a	
Regional Seal Potential	High	green
Lithology	Sandstone	green
Porosity	6-15%	green
Permeability	10-100 mD	green
Depth (TVD)	800-2,650m	green
Net Reservoir Thickness	4-12m	green

Table 6.1

6.1 Hydrostratigraphic Chart

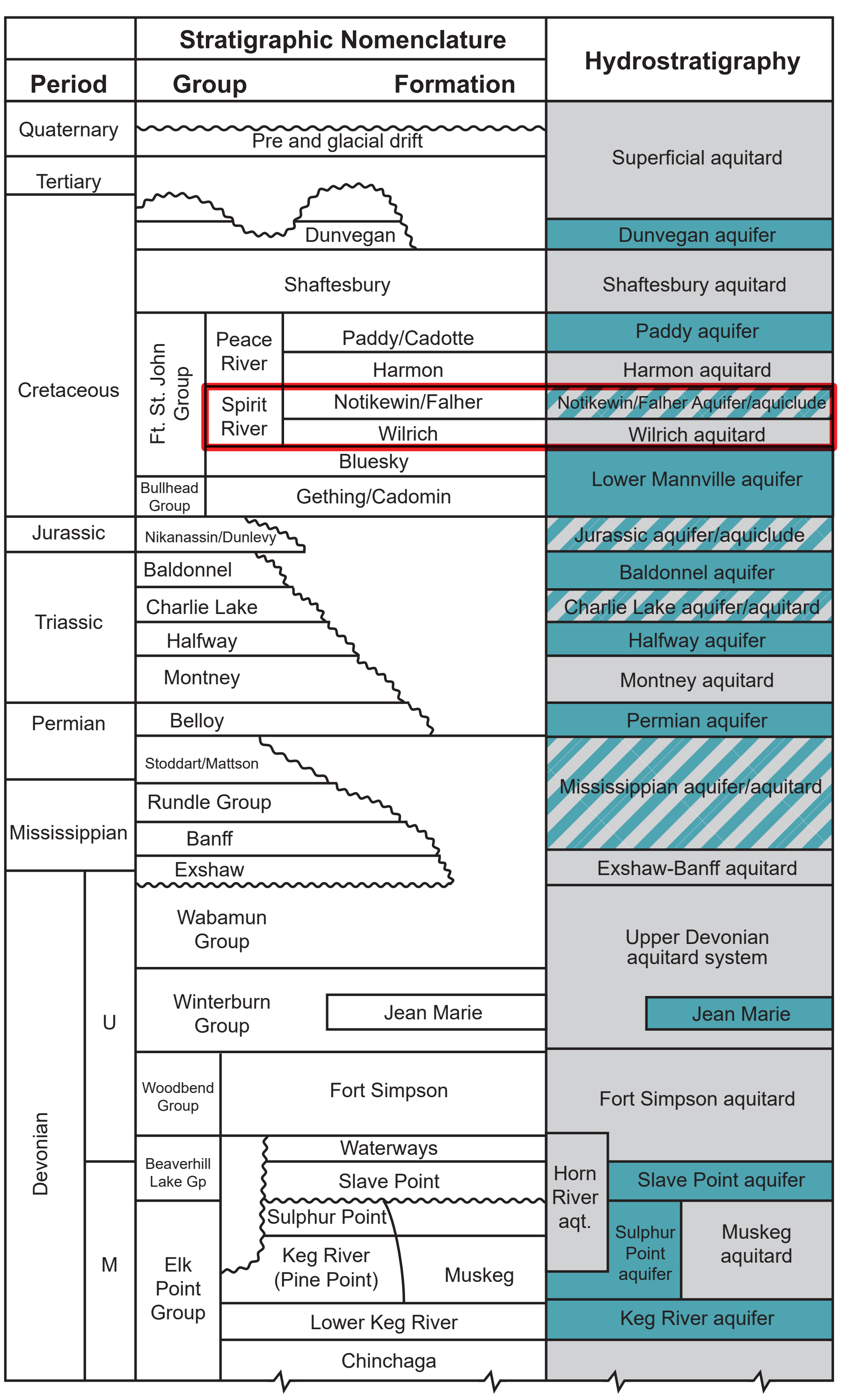

Modified from Bachu, 2006

© Canadian Discovery Ltd. *Figure 6.1*

6.2 Top 10 Depleted Spirit River Pools

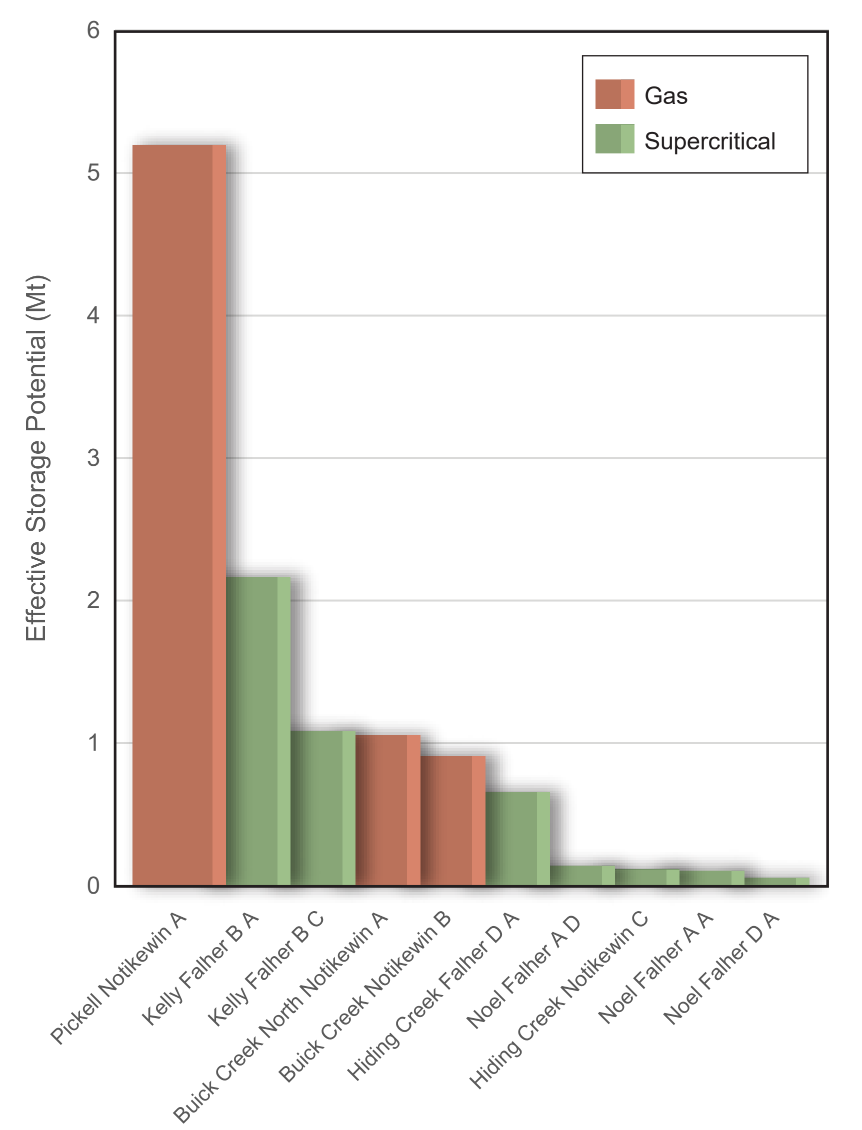

© Canadian Discovery Ltd. *Figure 6.2*

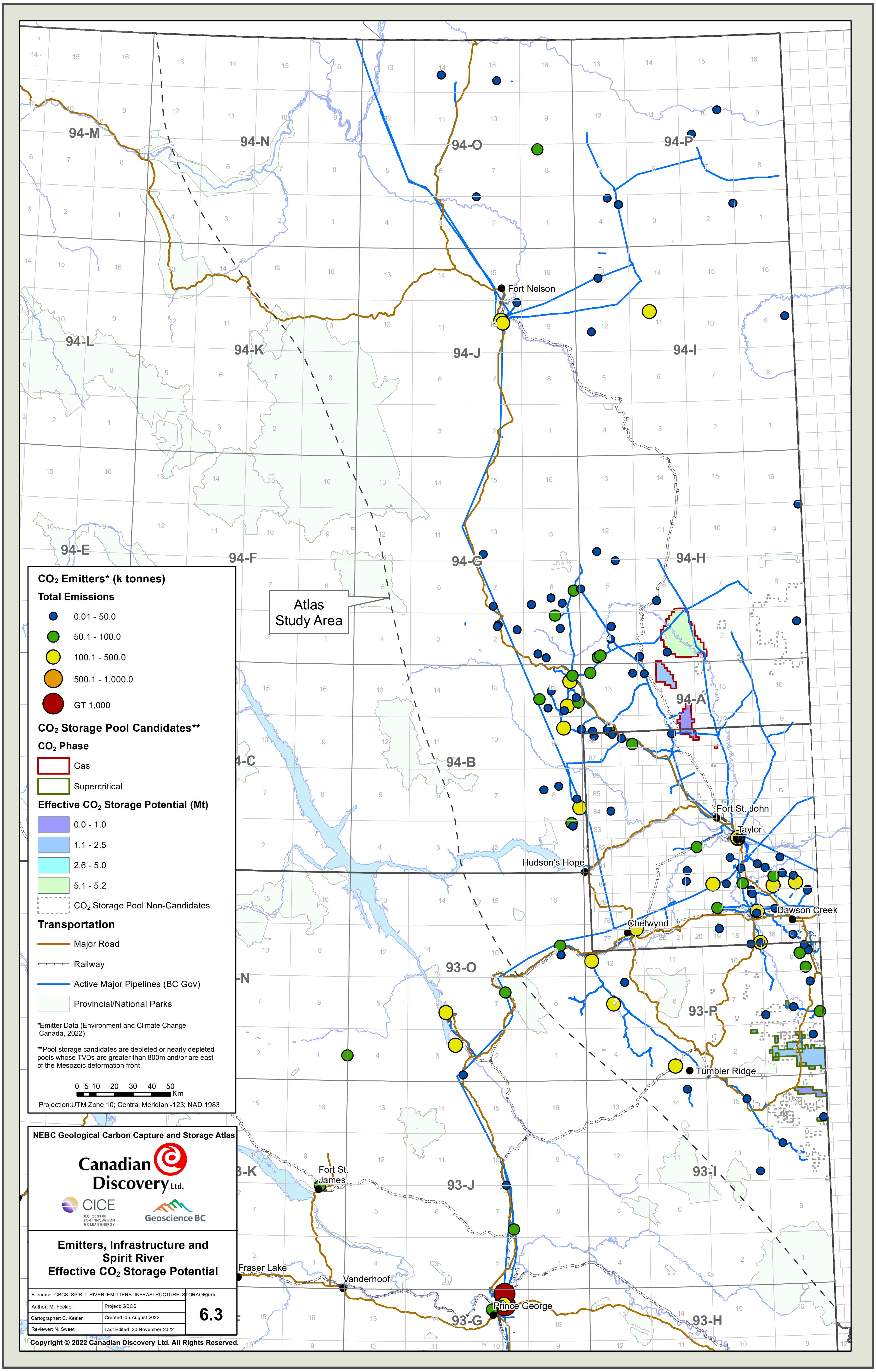

© Canadian Discovery Ltd.

Figure 6.3

6.4 Spirit River Play Schematic

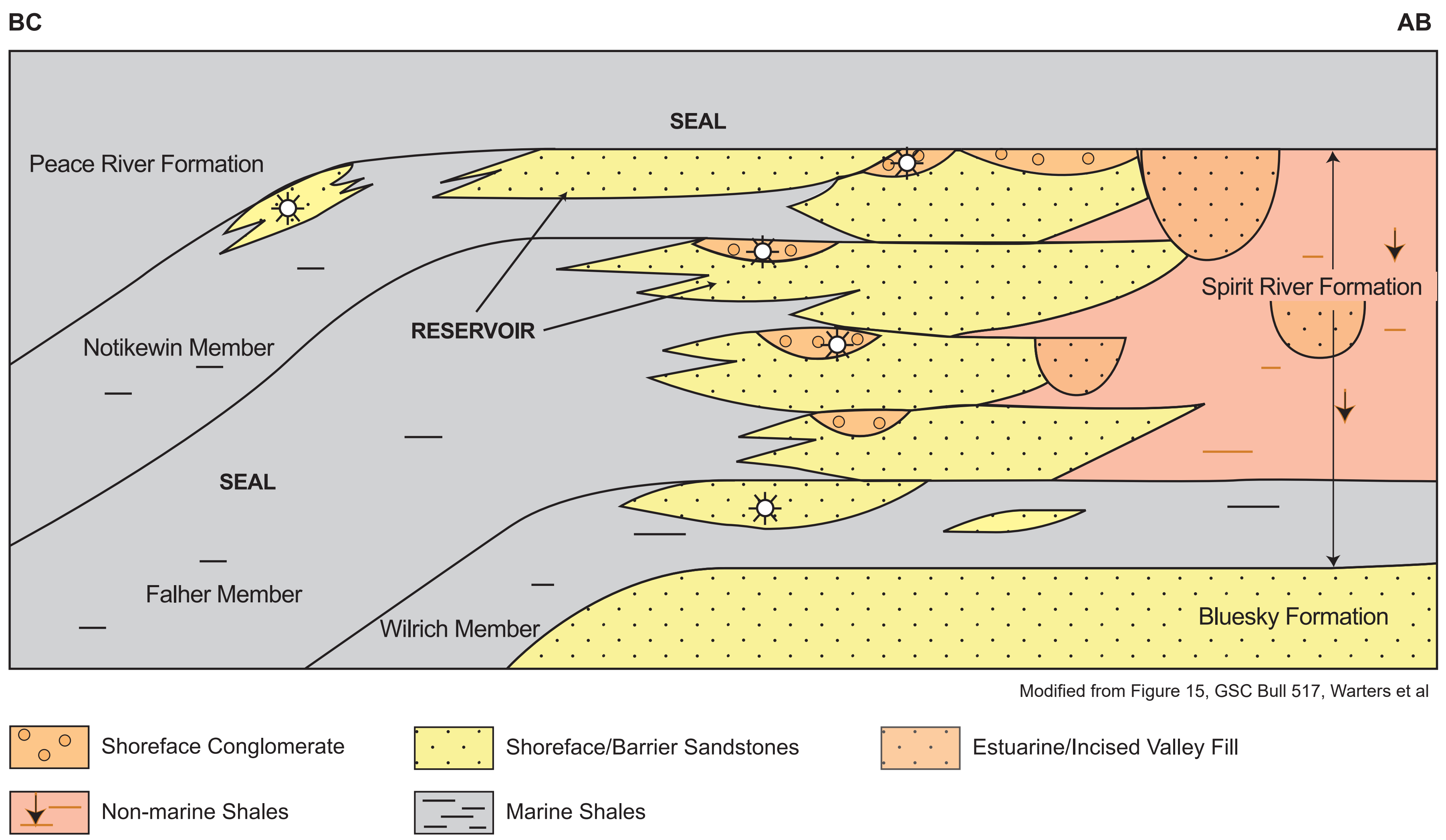

Figure 6.4

Storage Complex

The Spirit River Formation *(figure 6.4)* is the product of a basin-wide progradational episode (sea level rise) during mid-Albian time. In the BC Deep Basin, it comprises six major stacked shoreface successions, termed (from the top down) Notikewin, Falher A, B, C, D, and F. An individual cycle typically consists of a coarsening-upward succession, passing from very fine-grained sandstone to coarse sandstone or conglomerate, capped by continental mudstone and coal. There are complex internal stratigraphic relationships that can be important at a field development scale (BC OGC, 2006).

In the Peace River Block and northwards, Spirit River shoreface sandstone grades to finer-grained, more distal facies. Individual Notikewin and Falher sub-members lose their identity, as capping conglomerate and coal pinch out seaward (Warters et al, 1997). Only the uppermost sandstone remains north of about Twp. 87, overlying a succession of shelfal siltstone and shale.

Spirit River sandstone grades up from underlying Wilrich Member marine shale, and are capped by transgressive marine shale of the Harmon Member (of the Peace River Formation), which provide an effective seal.

Net reservoir maps are provided for the depleted pools *(figure 6.5)*. These maps can help indicate the most favourable areas for CO_2 injection within storage reservoirs; i.e. where the reservoir rock has the highest quality and most often the highest porosity and permeability. The net reservoir contours within the pools were provided by the BC Oil and Gas Commission (BC OGC). The Spirt River in NEBC is gas-prone and the depleted pools are all gas pools.

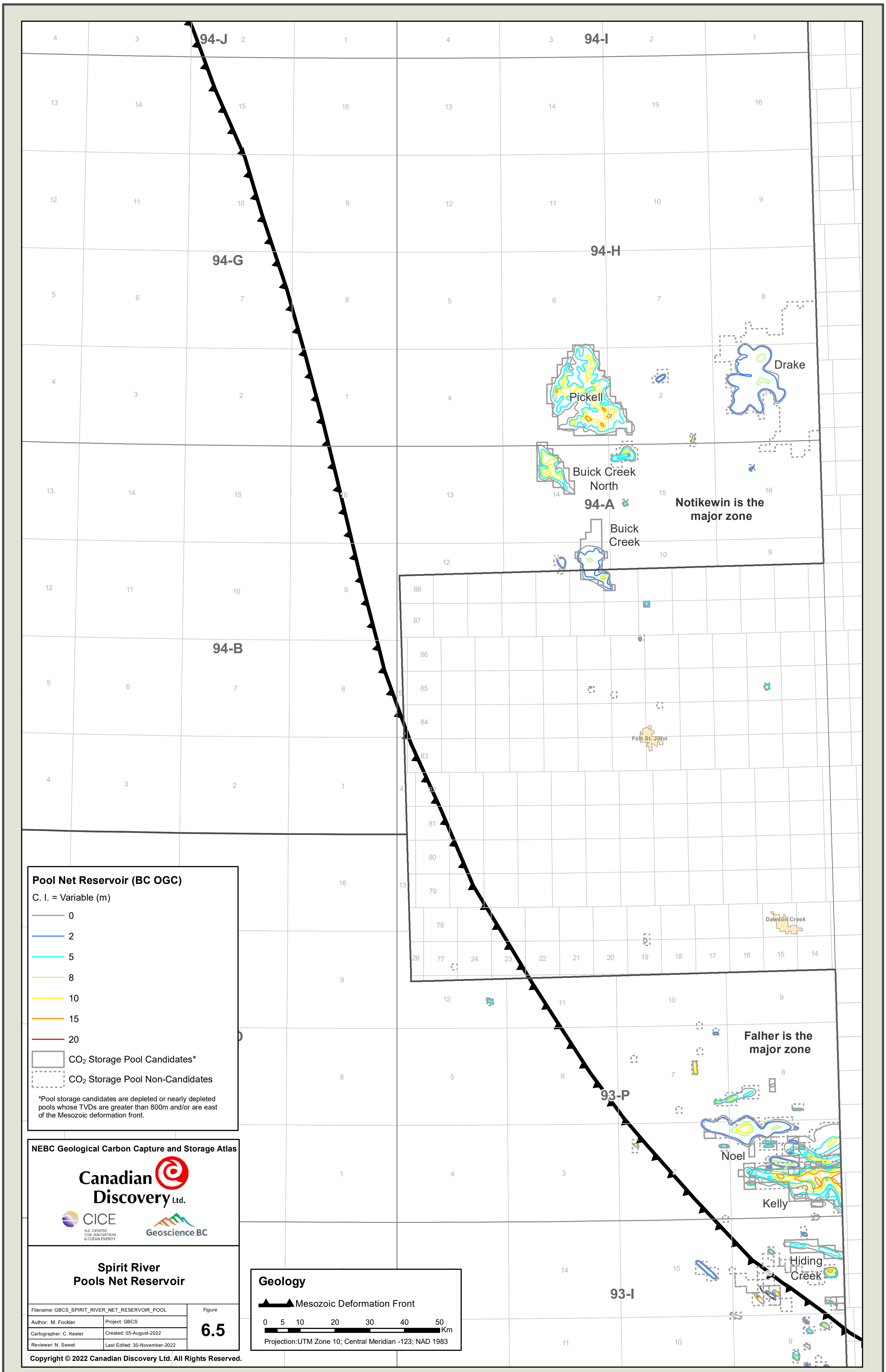

© Canadian Discovery Ltd.

Figure 6.5

Carbon Storage Calculations

Depleted and Nearly Depleted Pools

The pool candidates (all gas) for carbon storage potential within the Spirit River are shown in *table 6.2*.

The BC OGC defines depleted pools as ones that have no remaining reserves or production. The BC OGC also recognizes that there are nearly depleted pools that could become CO_2 storage candidates in the (relatively) near future. The nearly depleted CO_2 storage candidates include pools where 90%+ of the reserves have been recovered, or no production has occurred in over five years. Furthermore, CDL has excluded pools that are shallower than 800m TVD, or are west of the Mesozoic deformation front. See Depleted Pools Selection Criteria in *Chapter 4* for a more thorough discussion.

The theoretical CO_2 storage potential represents the mass of CO_2 that can be stored in the hydrocarbon reservoirs assuming that the volume occupied previously by the produced gas will be occupied entirely by the injected CO_2. These calculations have been provided by the BC OGC and are based on historical pool production.

The effective CO_2 storage potential represents the mass of CO_2 that can be stored in hydrocarbon reservoirs after taking into account intrinsic reservoir characteristics and flow processes, such as heterogeneity (how much variability there is in the rock), aquifer support, sweep efficiency, gravity override, and CO_2 mobility (Bachu, 2006). The effective CO_2 storage potential is calculated by CDL and reduces the theoretical storage potential by as little as 13% and as much as 75%. More detail is provided on the carbon storage calculations for depleted pools in *Appendix B*, and data are provided for all depleted pools included in this study in *Appendix C*.

The depleted and nearly depleted pools that are deemed to be CO_2 storage candidates by CDL are coloured by their effective storage potential mass on the summary map *(figure 6.6)*.

The northern Notikewin pools are at shallow depths, which put them outside the supercritical conditions for CO_2, although the Pickell Notikewin A Pool is the top Spirit River pool with respect to carbon storage potential.

Aquifers

Due to geological complexity, the aquifer potential of the Spirit River is difficult to map and assess, and is therefore not included for this phase of the Atlas.

Depleted Spirit River Pools

Pool Name	Pool Type	Well Count	Initial Pressure (kPa)	Temperature (°C)	Average Porosity (%)	CO_2 Phase	Theoretical Storage Potential (Mt)	Effective Storage Potential (Mt)
Pickell Notikewin A	Gas	224	4,612	42	14.9	Gas	8.3	5.2
Kelly Falher B A	Gas	24	15,180	80	6.4	Supercritical	2.5	2.2
Kelly Falher B C	Gas	4	15,035	78	6.3	Supercritical	1.2	1.1
Buick Creek North Notikewin A	Gas	55	4,842	40	15.4	Gas	1.2	1.1
Buick Creek Notikewin B	Gas	49	4,401	40	13.0	Gas	1.0	0.9
Hiding Creek Falher D A	Gas	7	21,039	90	7.5	Supercritical	0.8	0.7
Noel Falher A D	Gas	1	18,322	75	7.7	Supercritical	0.2	0.1
Hiding Creek Notikewin C	Gas	1	18,562	91	8.6	Supercritical	0.1	0.1
Noel Falher A A	Gas	1	15,228	76	4.3	Supercritical	0.1	0.1
Noel Falher D A	Gas	1	17,789	80	6.8	Supercritical	0.1	0.1

© Canadian Discovery Ltd. Data supplied by BC OGC and Canadian Discovery Ltd. *Table 6.2*

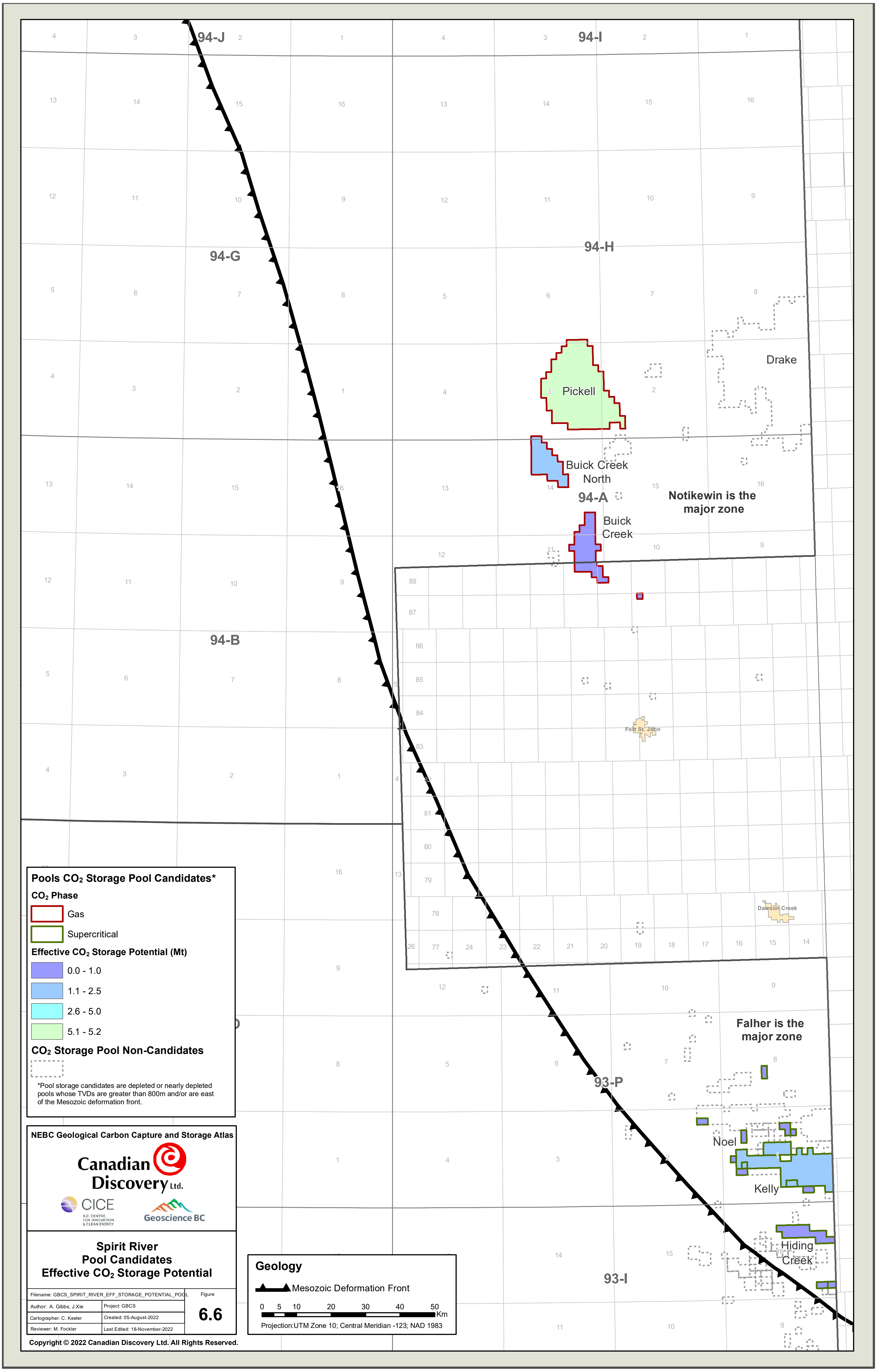

94-J
94-I
94-G
94-H
94-A
94-B
93-P
93-I
Pickell
Drake
Buick Creek North
Buick Creek
Notikewin is the major zone
Fort St. John
Dawson Creek
Falher is the major zone
Noel
Kelly
Hiding Creek
Pools CO2 Storage Pool Candidates*
CO2 Phase
Gas
Supercritical
Effective CO2 Storage Potential (Mt)
0.0 - 1.0
1.1 - 2.5
2.6 - 5.0
5.1 - 5.2
CO2 Storage Pool Non-Candidates
*Pool storage candidates are depleted or nearly depleted pools whose TVDs are greater than 800m and/or are east of the Mesozoic deformation front.
NEBC Geological Carbon Capture and Storage Atlas
Canadian Discovery Ltd.
CICE
Geoscience BC
Spirit River
Pool Candidates
Effective CO2 Storage Potential
Filename: GBCS_SPIRIT_RIVER_EFF_STORAGE_POTENTIAL_POOL
Figure
6.6
Author: A. Gibbs, J.Xie
Project: GBCS
Cartographer: C. Keeler
Created: 05-August-2022
Reviewer: M. Fockler
Last Edited: 18-November-2022
Copyright © 2022 Canadian Discovery Ltd. All Rights Reserved.
Geology
Mesozoic Deformation Front
0 5 10 20 30 40 50 Km
Projection:UTM Zone 10; Central Meridian -123; NAD 1983

Figure 6.6

Bluesky Formation

Bluesky Overview

Storage potential in the Bluesky *(figure 7.1)* occurs in the southern portion of the study area near Fort St. John and is proximal to emitters and infrastructure. Favourability attributes are summarized in *table 7.1* with green and yellow circles indicating whether an attribute is considered generally favourable (green) or has risk and requires additional work (yellow). Both depleted pool reservoirs and saline aquifers are candidates and offer a range of storage opportunities. The top 10 depleted pools are shown in *figure 7.2*. *Figure 7.3* displays the effective storage potential of the Bluesky, as well as the emitters and infrastructure in the NEBC study area.

Bluesky Favourability Attributes		
Top 10 Depleted Pool Total Potential	59 Mt	●
Aquifer Storage (P50)	42 Mt	●
Regional Seal Potential	High	●
Lithology	Sandstone	●
Porosity	6-26%	●
Permeability	10-600 mD	●
Depth (TVD)	800-2,725m	●
Net Reservoir Thickness	2-35m	●

Table 7.1

7.1 Hydrostratigraphic Chart

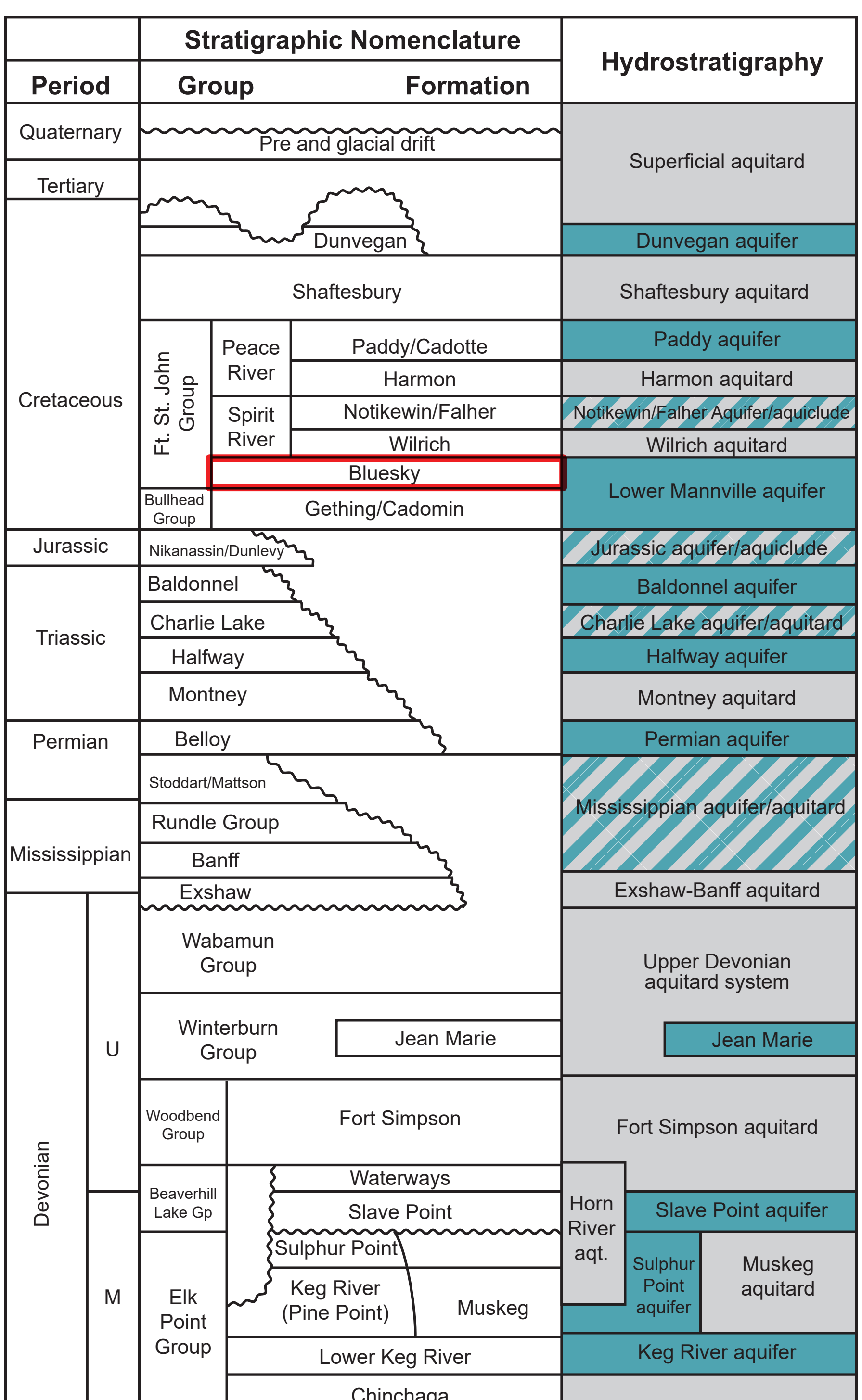

 Figure 7.1

7.2 Top 10 Depleted Bluesky Pools

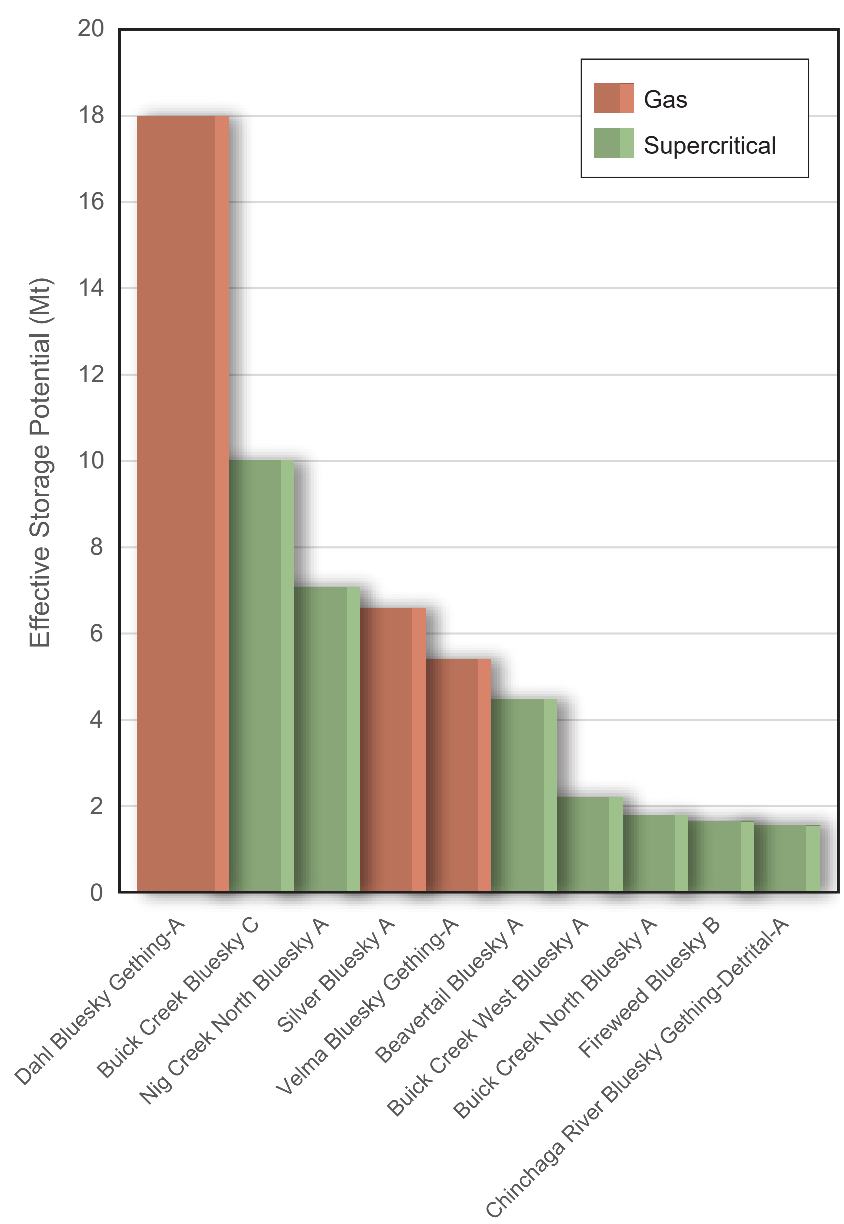

 Figure 7.2

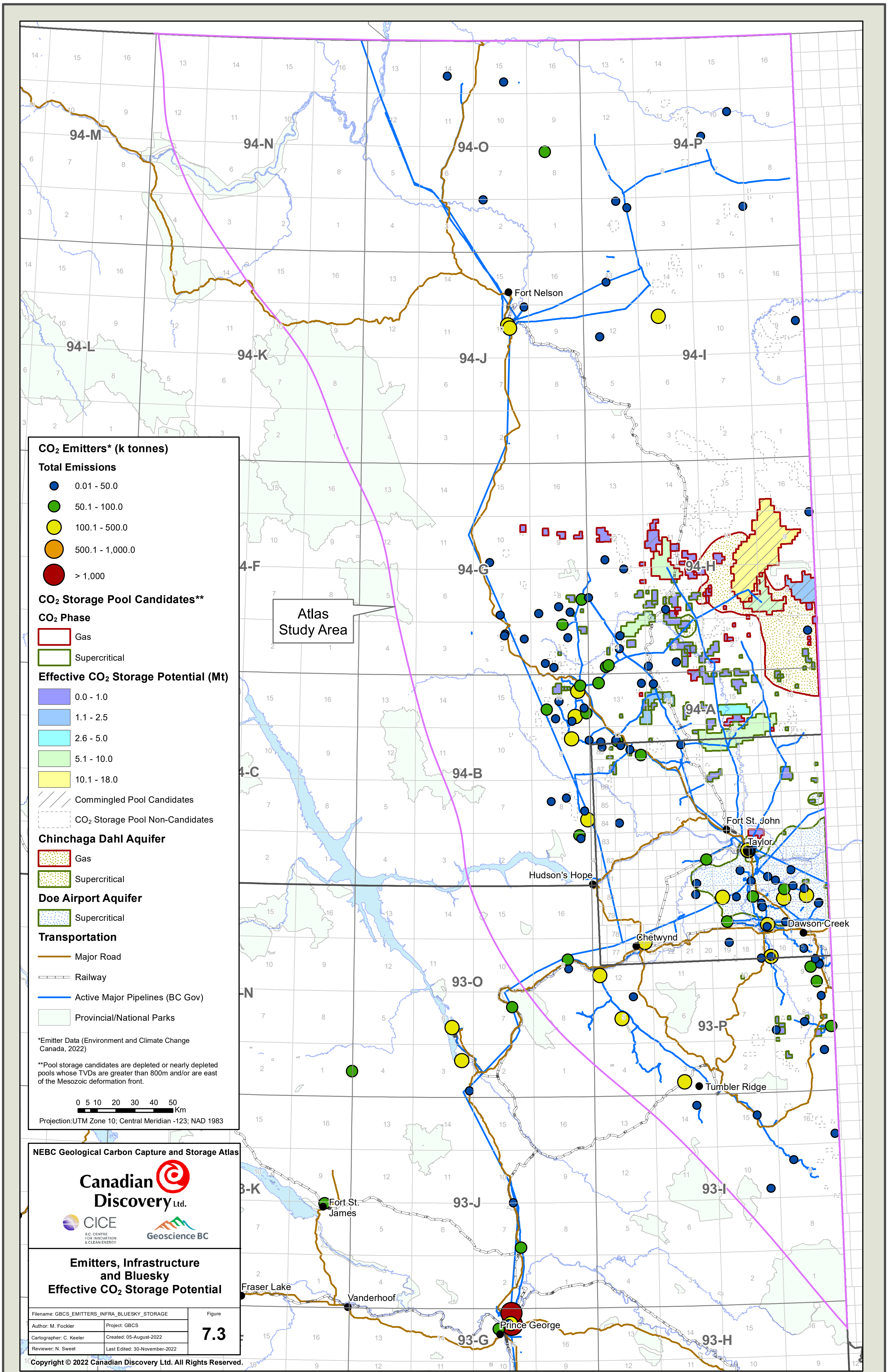

© Canadian Discovery Ltd.

Figure 7.3

7.4 | Bluesky Play Schematic

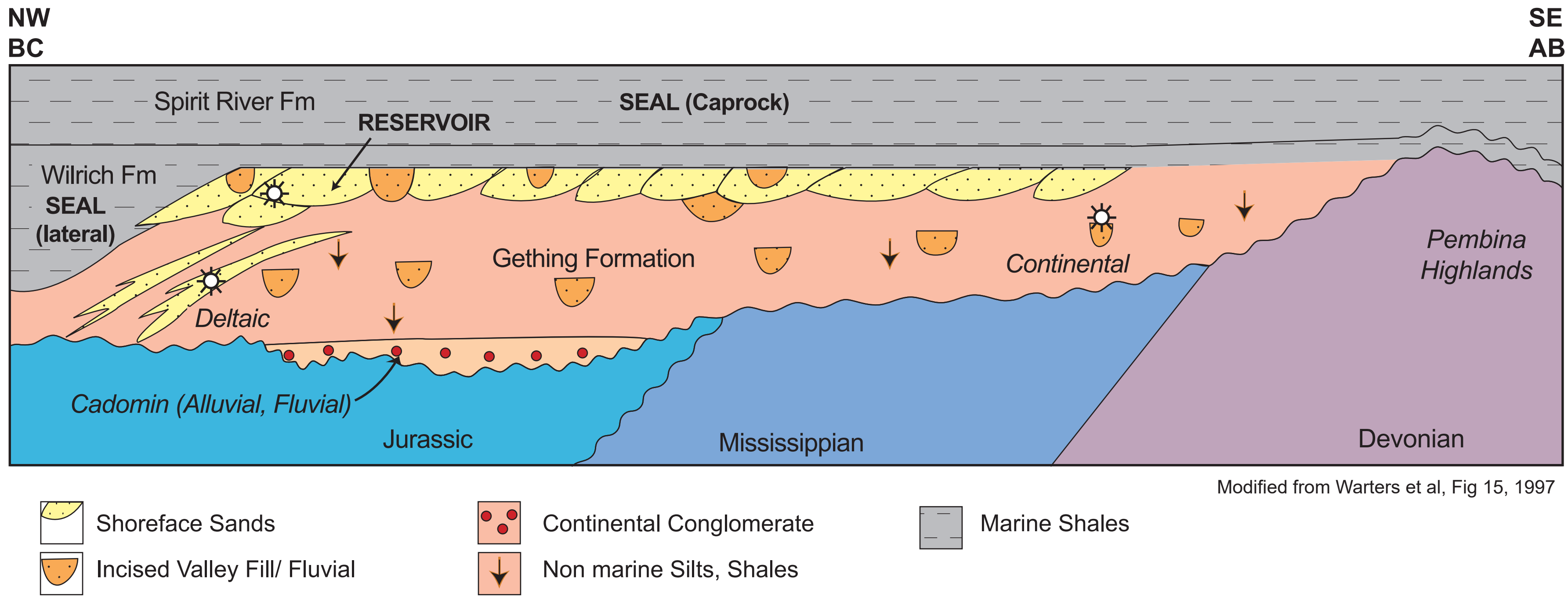

Figure 7.4

Storage Complex

The Early Cretaceous-age Bluesky Formation encompasses a wide variety of reservoir sandstone bodies associated with sea level rises and falls across the Western Canada Sedimentary Basin (WCSB). Deposition occurred primarily adjacent to southwesterly source areas, and on the southern flank of the Keg River Highlands in the north. Marine shoreface, deltaic, and estuarine reservoirs occur in discrete areas across northeastern British Columbia *(figure 7.4)*. Excellent reservoir quality occurs in thin, well-sorted, coarse-grained, areally limited shoreface sandstone and conglomerate, whereas widespread deltaic and finer-grained shoreface sandstone generally exhibits poorer reservoir quality (NEBC Play Atlas, 2006). Overlying shale of the Wilrich and Spirit River formations act as containment seals (caprock) preventing migration of gas or fluids upwards. The underlying Gething Formation is composed primarily of siltstone, shale, coal and isolated sand bodies that act both as a limited reservoir (sand) and a seal/baffle (discussed further in the Gething-Cadomin chapter).

In the northern portion of the study area, the Bluesky has limited storage potential as reservoir sandstone is localized, fine-grained and too shallow to meet the storage criteria. In the southern portion of the study area, the Bluesky has storage potential in depleted pools as well as two aquifers and is discussed in detail below.

The Bluesky structure map *(figure 7.5)* shows the topography of the top of the Bluesky in the subsurface. Since the displacement of a CO_2 plume is governed by gravity and buoyancy, the plume tends to migrate up-structure during its injection period. This map shows the 800m true vertical depth contour, which indicates the approximate depth limit for this evaluation — above this depth, injected CO_2 is likely to be in a gaseous phase. As supercritical conditions for CO_2 comprise a temperature in excess of 31.1°C and a pressure greater than 7,500 kPa, the Bluesky 7,500 kPa and 31°C contours indicate where CO_2 injection is expected to be in the supercritical phase.

Net reservoir maps are provided for the saline aquifers *(figure 7.6)* and depleted pools *(figure 7.7)*. These maps can help to indicate the most favourable areas for CO_2 injection within storage reservoirs; i.e. where the reservoir rock has the highest quality and most often the highest porosity and permeability. The net reservoir contours within the pools were provided by the BC Oil and Gas Commission (BC OGC). The net reservoir contours within the saline aquifers were sourced primarily from Geoscience BC Report 2021-14 (PRCL, 2021), with CDL providing geological support to fill in any gaps between previously existing datasets.

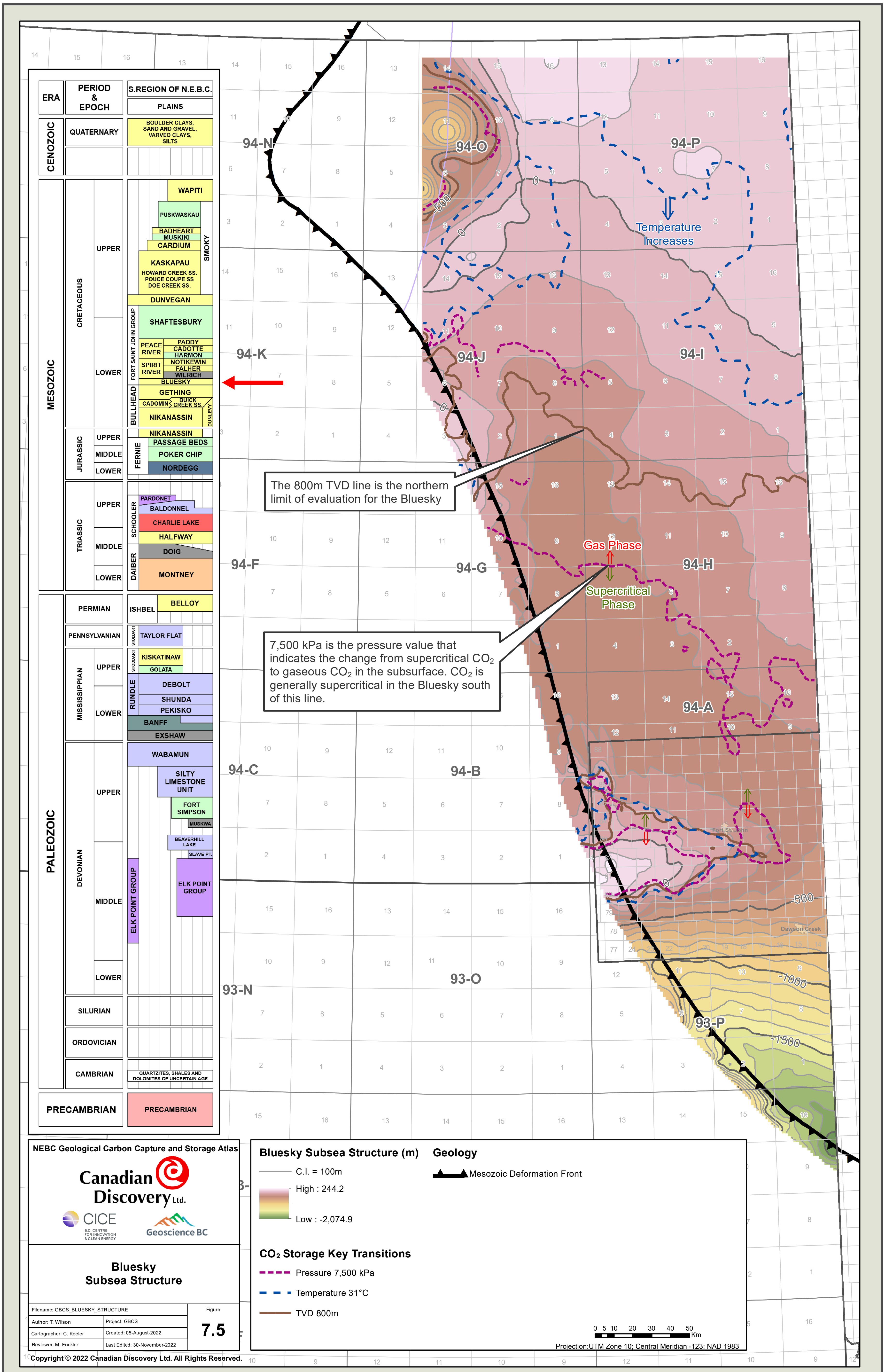

© Canadian Discovery Ltd.

Figure 7.5

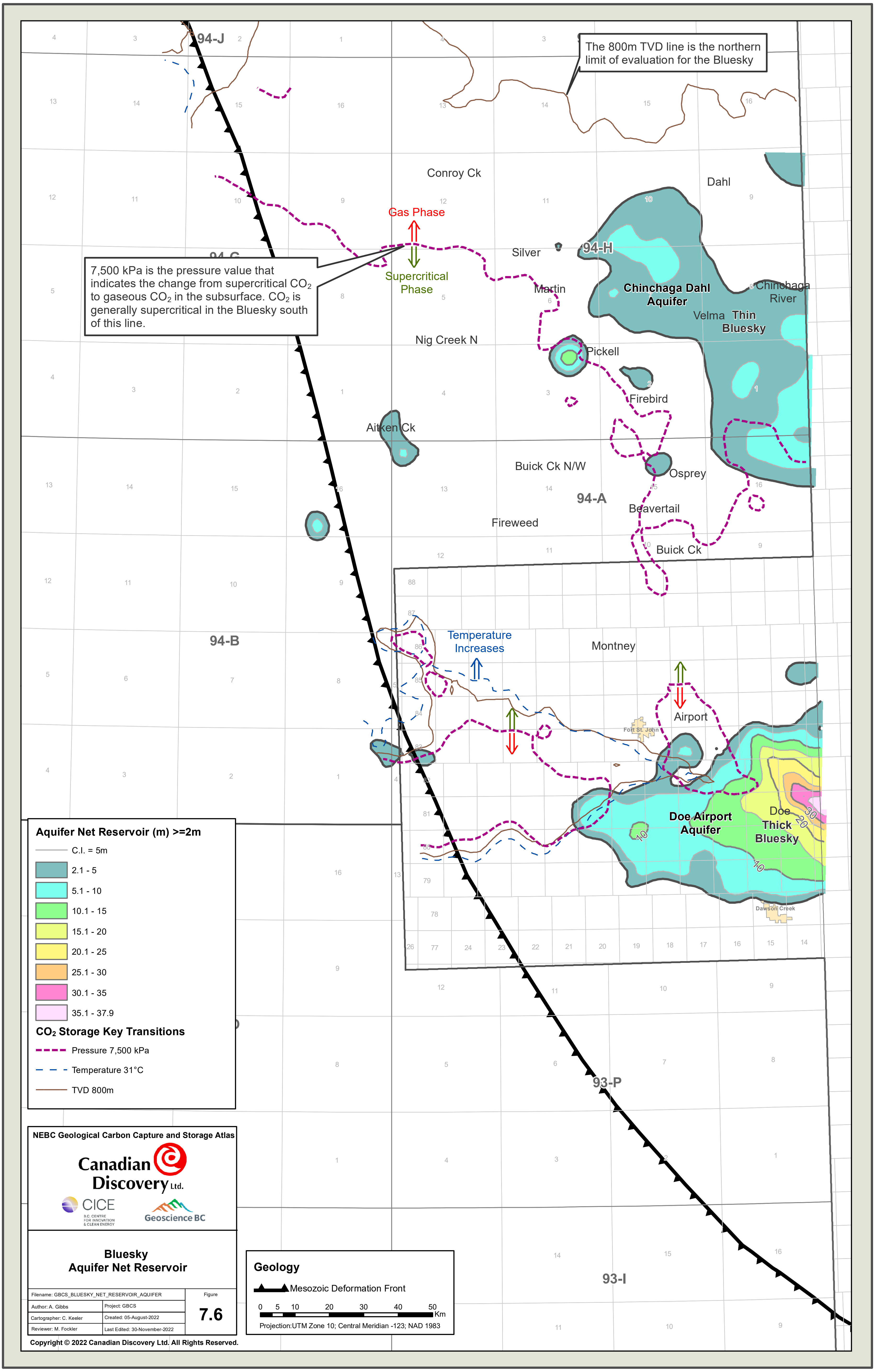

94-J
94-H
94-G
94-A
94-B
93-P
93-I
The 800m TVD line is the northern limit of evaluation for the Bluesky
7,500 kPa is the pressure value that indicates the change from supercritical CO_2 to gaseous CO_2 in the subsurface. CO_2 is generally supercritical in the Bluesky south of this line.
Gas Phase
Supercritical Phase
Temperature Increases
Conroy Ck
Dahl
Silver
Martin
Chinchaga Dahl Aquifer
Chinchaga River
Velma
Thin Bluesky
Nig Creek N
Pickell
Firebird
Aitken Ck
Buick Ck N/W
Osprey
Beavertail
Fireweed
Buick Ck
Montney
Airport
Fort St. John
Doe Airport Aquifer
Doe
Thick Bluesky
Dawson Creek
Aquifer Net Reservoir (m) >=2m
C.I. = 5m
2.1 - 5
5.1 - 10
10.1 - 15
15.1 - 20
20.1 - 25
25.1 - 30
30.1 - 35
35.1 - 37.9
CO_2 Storage Key Transitions
Pressure 7,500 kPa
Temperature 31°C
TVD 800m
NEBC Geological Carbon Capture and Storage Atlas
Canadian Discovery Ltd.
CICE
Geoscience BC
Bluesky
Aquifer Net Reservoir
Filename: GBCS_BLUESKY_NET_RESERVOIR_AQUIFER
Figure
7.6
Author: A. Gibbs
Project: GBCS
Cartographer: C. Keeler
Created: 05-August-2022
Reviewer: M. Fockler
Last Edited: 30-November-2022
Copyright © 2022 Canadian Discovery Ltd. All Rights Reserved.
Geology
Mesozoic Deformation Front
0 5 10 20 30 40 50 Km
Projection:UTM Zone 10; Central Meridian -123; NAD 1983

Figure 7.6

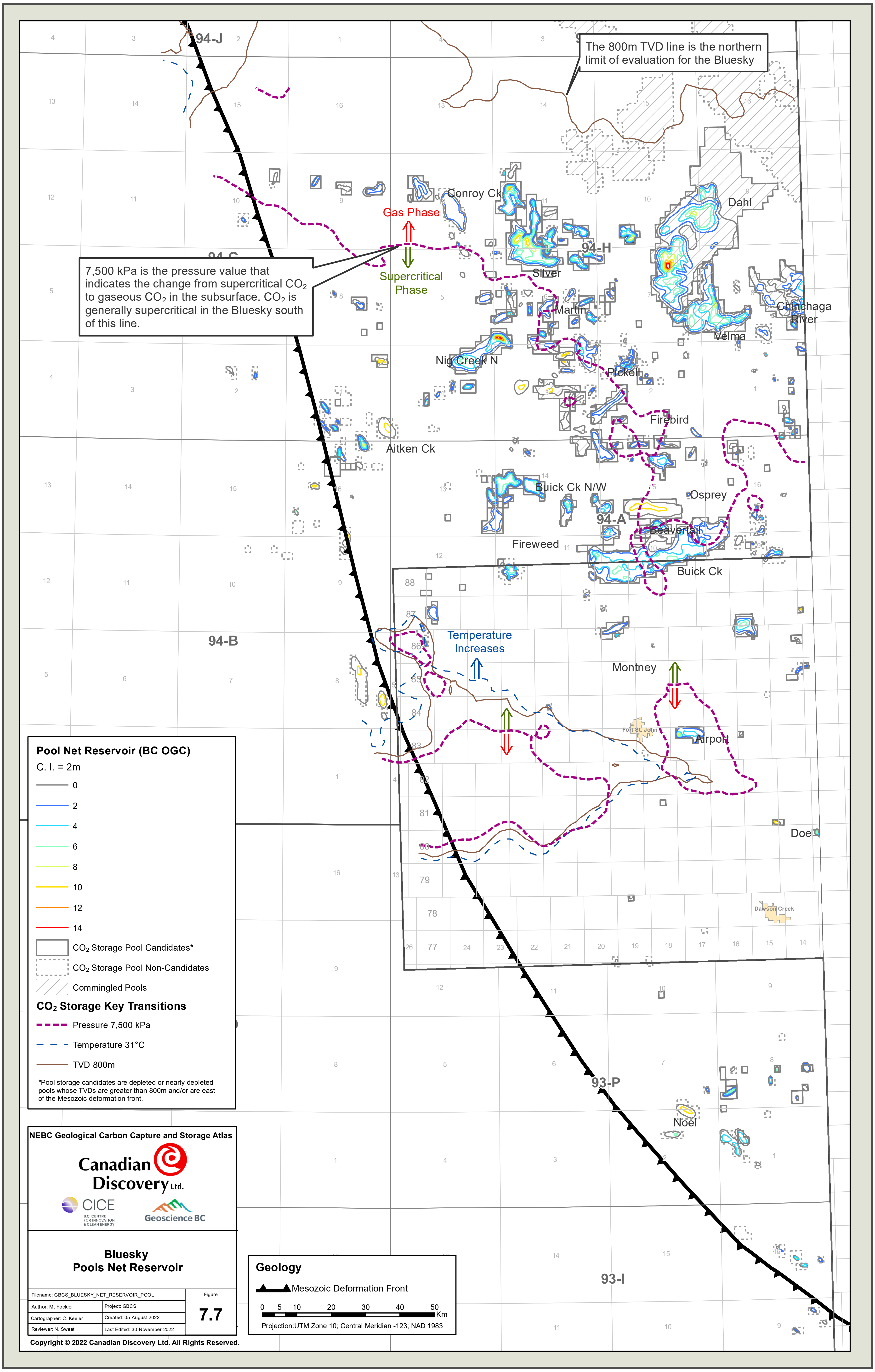

© Canadian Discovery Ltd.

Figure 7.7

Porosity-Permeability Correlations

Core data for the Bluesky were obtained from geoLOGIC and filtered for better quality reservoir that is more conducive to carbon storage (greater than 10% porosity and 10 mD permeability) within the study area. These data were used to estimate porosity trends in the aquifers for storage calculations and to do a preliminary analysis of the multiple porosity-permeability trends that have been observed in the Bluesky in past studies *(figure 7.8)*. The Chinchaga River, Dahl, Velma, and Beatton River areas tend to display very good permeability, but more modest porosity values, and may be dominated by coarser-grained sandstones and conglomerates (as discussed in Petrel Robertson, 2021). Finer-grained shoreface sandstones at Silver and into the Peace River block at Doe tend to display much higher porosities and good permeability (Petrel Robertson, 2021). Porosity-permeability trends observed in this phase of the Atlas will be better established in future Atlas phases using petrophysical models and more detailed mapping.

Note that a cluster of high permeability Bluesky reservoir is present in the Aitken Creek Bluesky A and B pools, however these pools are used for underground natural gas storage and have been removed as CO_2 storage candidates for this Atlas.

7.8 Bluesky Porosity-Permeability Plots

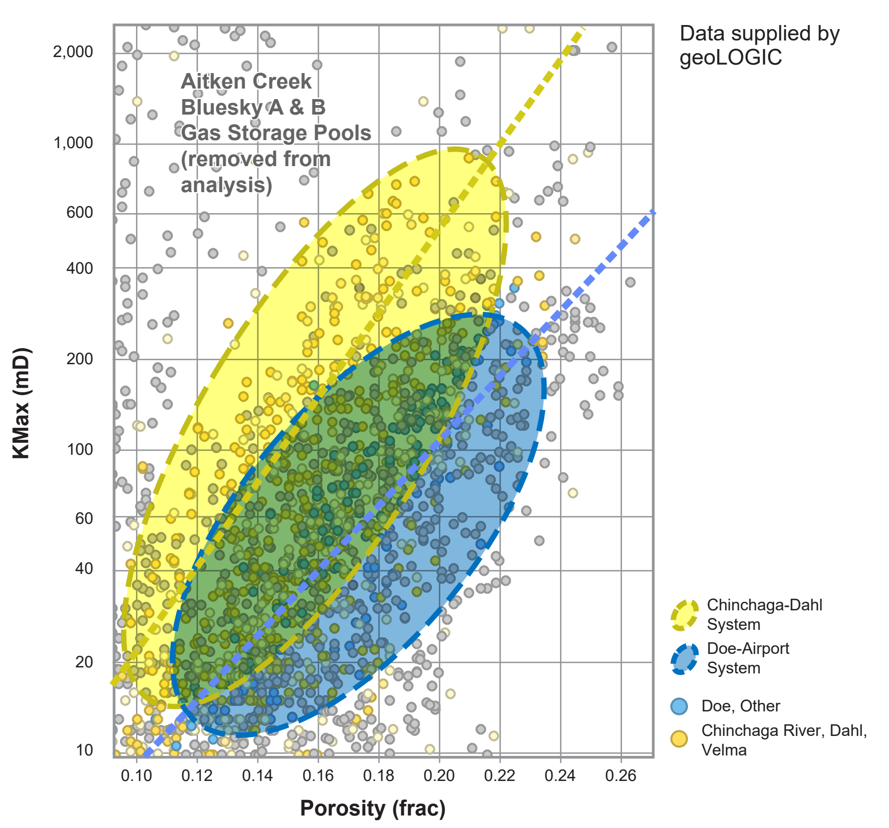

© Canadian Discovery Ltd. *Figure 7.8*

Hydrodynamics

To delineate the extent of the aquifers and understand the relationship between the aquifers and the depleted pools, an analysis was done on Bluesky hydrodynamics. Hydrofax drillstem test (DST) data from within the aquifers and the initial pressure and datum depth of each depleted pool from the BC OGC reserves databases were used to create a pressure vs elevation (P/E) graph *(figure 7.9)*.

In the Bluesky, there are two main aquifers: one in the north (shown in yellow) that underlies large northern gas pools such as Chinchaga River, Dahl and Velma; and one in the south (shown in blue) that underlies very small gas pools such as Doe and Airport. Depleted pools that are underlain by an aquifer may have a larger margin of error on CO_2 storage potential due to possible pressure support from the aquifer and/or additional potential that could be provided due to connection with the aquifer.

The northern Chinchaga–Dahl aquifer lies primarily outside and north of the supercritical window for CO_2, and is therefore less favourable for carbon storage than the Doe–Airport aquifer to the south. Several pools to the west of the northern aquifer (e.g. Silver, Black Creek, and Conroy Creek) are also located north of the 7,500 kPa line and outside the window for supercritical CO_2. These pools are annotated by the area of low pressure-depth (P/D) ratio on the pressure versus elevation (P/E) graph *(figure 7.9)*. They may be in hydraulic communication with other lower pressured zones, rendering them less favourable for carbon storage. Pools falling to the south and west of this contour (e.g. Nig Creek North, Buick Creek North and West, Fireweed, and Cache Creek) are likely isolated sweet spots within tighter reservoir and may therefore provide more secure containment opportunities for carbon storage. These are annotated on the P/E graph by the area of higher P/D ratio.

7.9 Bluesky Pressure vs Elevation Plot

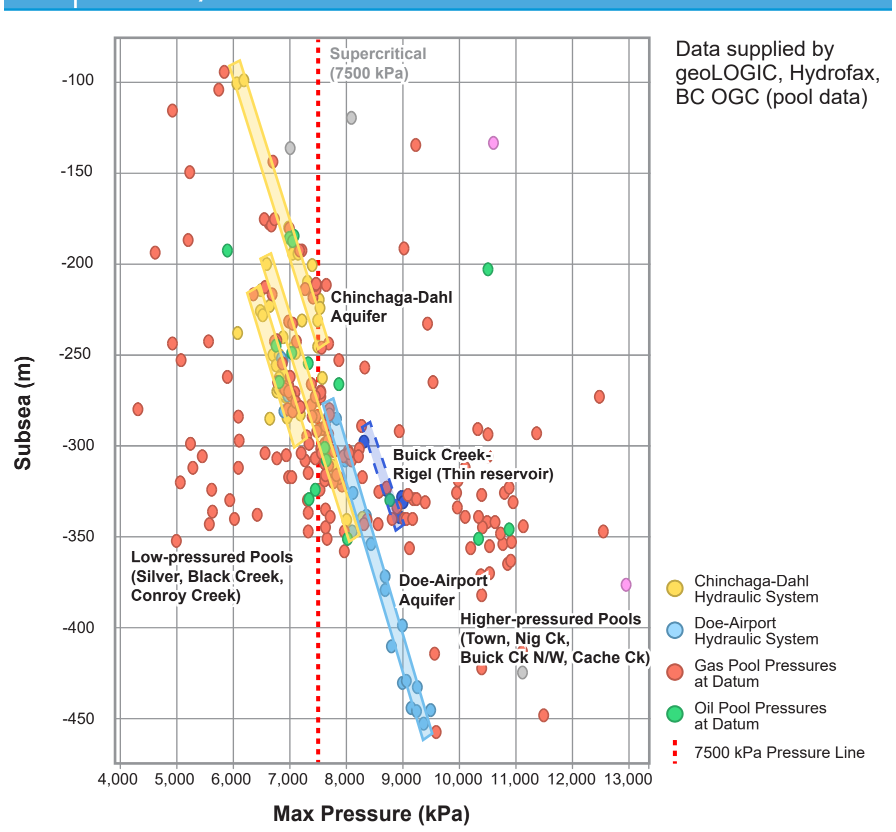

© Canadian Discovery Ltd. *Figure 7.9*

Carbon Storage Calculations

Depleted and Nearly Depleted Pools

The top 25 depleted and nearly depleted pool candidates for carbon storage potential within the Bluesky Formation are shown in *table 7.2*.

The BC OGC defines depleted pools as ones that have no remaining reserves or production. The BC OGC also recognizes that there are nearly depleted pools that could become CO_2 storage candidates in the (relatively) near future. The nearly depleted CO_2 storage candidates include pools where 90%+ of the reserves have been recovered, or no production has occurred in over five years. Furthermore, CDL has excluded pools that are shallower than 800m TVD, or are west of the Mesozoic deformation front. See Depleted Pools Selection Criteria in *Chapter 4* for a more thorough discussion.

In the table, the theoretical CO_2 storage potential represents the mass of CO_2 that can be stored in the hydrocarbon reservoirs assuming that the volume occupied previously by the produced gas will be occupied entirely by the injected CO_2. These calculations have been provided by the BC OGC and are based on historical pool production.

The effective CO_2 storage potential represents the mass of CO_2 that can be stored in hydrocarbon reservoirs after taking into account intrinsic reservoir characteristics and flow processes, such as heterogeneity (how much variability there is in the rock), aquifer support, sweep efficiency, gravity override, and CO_2 mobility (Bachu, 2006). The effective CO_2 storage potential is calculated by CDL and reduces the theoretical storage potential by as little as 13% and as much as 75%. More detail is provided on the carbon storage calculations for depleted pools in *Appendix B*, and data are provided for all depleted pools included in this study in *Appendix C*.

The depleted and nearly depleted pools that are deemed to be CO_2 storage candidates by CDL are coloured by their effective storage potential mass on the summary map *(figure 7.10)*.

Aquifers

The Bluesky aquifers parameters are summarized in *table 7.3*. Theoretical CO_2 storage potential can be calculated using the mapped pore volume of the reservoir and CO_2 density, and assumes that the pore volume will be occupied entirely by the injected CO_2. We know this is not the case however, since the pore space is already occupied by water, and the water will need to be displaced in the process. As a result, a storage efficiency factor is introduced into storage potential calculations that accounts for the presence of both water and CO_2 in the aquifer. The storage efficiency factor is a function of reservoir and fluid properties and dynamics, including the geometry of the trap, gravity segregation, heterogeneity, permeability distribution, and pressure, and may reduce the theoretical storage potential by 95 to 99%.

Aquifers considered favourable targets for CO_2 storage are indicated on the summary map included as *figure 7.10* and labelled with their estimated P10, P50 and P90 effective storage potential in Mt. More detail is provided on the aquifer carbon storage calculations in *Appendix B*.

Top 25 Depleted Bluesky Pools

Pool Name	Pool Type	Well Count	Initial Pressure (kPa)	Temperature (˚C)	Average Porosity (%)	CO_2 Phase	Theoretical Storage Potential (Mt)	Effective Storage Potential (Mt)
Dahl Bluesky Gething-A	Gas	198	6,564	51	15.0	Gas	20.6	18.0
Buick Creek Bluesky C	Gas	130	7,714	48	14.0	Supercritical	11.4	10.0
Nig Creek North Bluesky A	Gas	38	10,332	58	13.7	Supercritical	8.1	7.1
Silver Bluesky A	Gas	37	6,971	59	14.4	Gas	7.6	6.6
Velma Bluesky Gething-A	Gas	41	6,692	53	15.6	Gas	6.1	5.4
Beavertail Bluesky A	Gas	16	7,770	48	12.0	Supercritical	5.1	4.5
Buick Creek West Bluesky A	Gas	12	9,388	54	9.0	Supercritical	2.5	2.1
Buick Creek North Bluesky A	Gas	10	9,080	51	8.9	Supercritical	2.0	1.7
Fireweed Bluesky B	Gas	11	9,062	53	13.5	Supercritical	1.9	1.6
Chinchaga River Bluesky Gething-Detrital-A	Gas	116	6,549	48	17.3	Gas	2.4	1.5
Osprey Bluesky A	Gas	10	7,475	49	12.8	Supercritical	1.1	0.9
Pickell Bluesky Gething-A	Gas	16	7,957	51	11.2	Supercritical	1.0	0.8
Montney Bluesky A	Gas	7	8,715	49	13.7	Supercritical	0.9	0.8
Conroy Creek Bluesky A	Gas	11	5,626	60	15.2	Gas	0.9	0.8
Noel Basal Bluesky B	Gas	2	24,155	77	6.5	Supercritical	0.9	0.8
Fireweed Bluesky A	Gas	4	9,168	53	10.4	Supercritical	0.9	0.8
Tommy Lakes Bluesky A	Gas	6	5,575	56	13.5	Gas	0.8	0.7
Firebird Bluesky A	Gas	13	7,699	53	14.7	Supercritical	1.0	0.6
Martin Bluesky A	Gas	7	8,215	60	16.6	Supercritical	0.7	0.6
Siphon East Bluesky A	Gas	11	8,025	49	14.6	Supercritical	2.3	0.6
Ladyfern Bluesky M	Gas	3	7,449	43	19.4	Supercritical	0.8	0.5
Buick Creek Bluesky A	Gas	6	7,660	48	10.8	Supercritical	0.5	0.5
Noel Basal Bluesky J	Gas	2	28,268	86	8.1	Supercritical	0.5	0.5
Nig Creek Bluesky C	Gas	6	10,199	61	11.4	Supercritical	0.7	0.4
Town Bluesky D	Gas	9	10,392	60	13.0	Supercritical	0.5	0.4

Table 7.2

Bluesky Aquifer Properties and Storage Potential

Aquifer Name	Type	Thickness Range (m)	Pressure Range (MPa)	Temperature Range (°C)	Porosity Range (%)	CO_2 Phase	P10 Effective Storage Potential at 0.5% (Mt)	P50 Effective Storage Potential at 2% (Mt)	P90 Effective Storage Potential at 5.4% (Mt)
Chinchaga-Dahl Regional System	Aquifer	2-10	5.7-7.9	43-60	9-21%	Mostly Gas	1.5	6.1	16.5
Doe-Airport Regional System	Aquifer	2-35	6.6-11.1	27-56	8-22%	Mostly Supecritical	9.1	36.2	97.8

Table 7.3

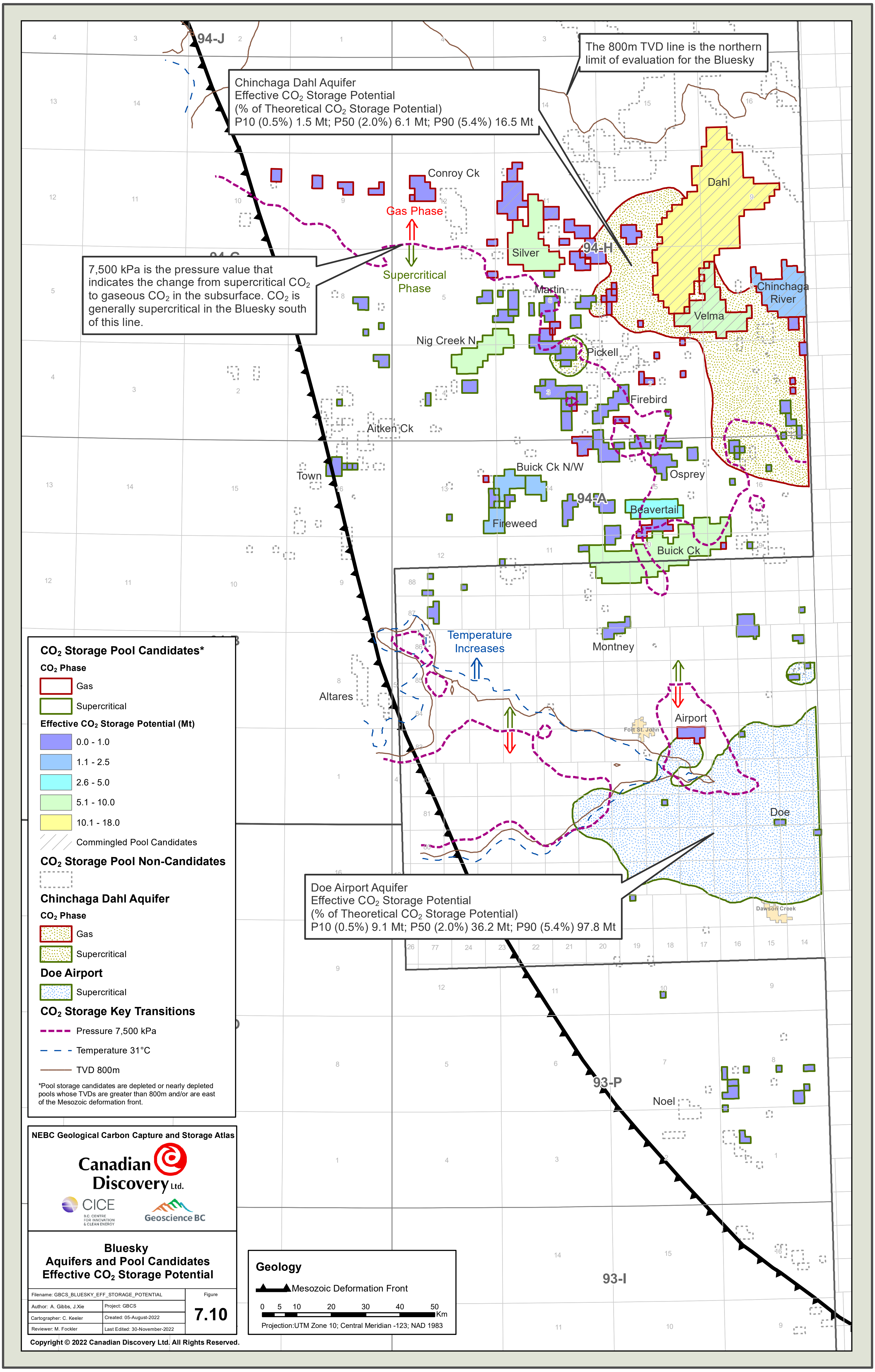

The 800m TVD line is the northern limit of evaluation for the Bluesky
Chinchaga Dahl Aquifer
Effective CO2 Storage Potential
(% of Theoretical CO2 Storage Potential)
P10 (0.5%) 1.5 Mt; P50 (2.0%) 6.1 Mt; P90 (5.4%) 16.5 Mt
7,500 kPa is the pressure value that indicates the change from supercritical CO2 to gaseous CO2 in the subsurface. CO2 is generally supercritical in the Bluesky south of this line.
Gas Phase
Supercritical Phase
Temperature Increases
Doe Airport Aquifer
Effective CO2 Storage Potential
(% of Theoretical CO2 Storage Potential)
P10 (0.5%) 9.1 Mt; P50 (2.0%) 36.2 Mt; P90 (5.4%) 97.8 Mt
94-J
94-H
94-A
93-P
93-I
Conroy Ck
Silver
Dahl
Martin
Chinchaga River
Velma
Nig Creek N
Pickell
Firebird
Aitken Ck
Town
Buick Ck N/W
Osprey
Fireweed
Beavertail
Buick Ck
Montney
Altares
Airport
Fort St. John
Doe
Dawson Creek
Noel
CO2 Storage Pool Candidates*
CO2 Phase
Gas
Supercritical
Effective CO2 Storage Potential (Mt)
0.0 - 1.0
1.1 - 2.5
2.6 - 5.0
5.1 - 10.0
10.1 - 18.0
Commingled Pool Candidates
CO2 Storage Pool Non-Candidates
Chinchaga Dahl Aquifer
CO2 Phase
Gas
Supercritical
Doe Airport
Supercritical
CO2 Storage Key Transitions
Pressure 7,500 kPa
Temperature 31°C
TVD 800m
*Pool storage candidates are depleted or nearly depleted pools whose TVDs are greater than 800m and/or are east of the Mesozoic deformation front.
NEBC Geological Carbon Capture and Storage Atlas
Canadian Discovery Ltd.
CICE B.C. Centre for Innovation & Clean Energy
Geoscience BC
Bluesky
Aquifers and Pool Candidates
Effective CO2 Storage Potential
Filename: GBCS_BLUESKY_EFF_STORAGE_POTENTIAL
Author: A. Gibbs, J.Xie
Project: GBCS
Cartographer: C. Keeler
Created: 05-August-2022
Reviewer: M. Fockler
Last Edited: 30-November-2022
Figure
7.10
Copyright © 2022 Canadian Discovery Ltd. All Rights Reserved.
Geology
Mesozoic Deformation Front
0 5 10 20 30 40 50 Km
Projection:UTM Zone 10; Central Meridian -123; NAD 1983

Figure 7.10

CADOMIN-GETHING FORMATION

Cadomin-Gething Overview

The Cadomin and Gething formations *(figure 8.1)* are discussed in one chapter as they are stratigraphically and hydrodynamically associated. Storage potential in the Cadomin and Gething occurs in the southern portion of the study area near Fort St. John and is proximal to emitters and infrastructure. The Cadomin has primarily aquifer storage candidates, whereas the Gething is limited to depleted pools. Favourability attributes are summarized in *table 8.1* with green and yellow circles indicating whether an attribute is considered generally favourable (green) or has risk and requires additional work (yellow). The top 10 depleted pools are shown in *figure 8.2*. *Figure 8.3* displays effective storage potential of the Cadomin and Gething, as well as emitters and infrastructure in the NEBC study area.

Cadomin-Gething Favourability Attributes		
Top 10 Depleted Pool Total Potential	11 Mt	yellow
Aquifer Storage (P50)	213 Mt	green
Regional Seal Potential	High	green
Lithology	Sandstone	green
Porosity	6-20%	green
Permeability	10-700 mD	green
Depth (TVD)	800-2,750m	green
Net Reservoir Thickness	5-45m	green

Table 8.1

8.1 Hydrostratigraphic Chart

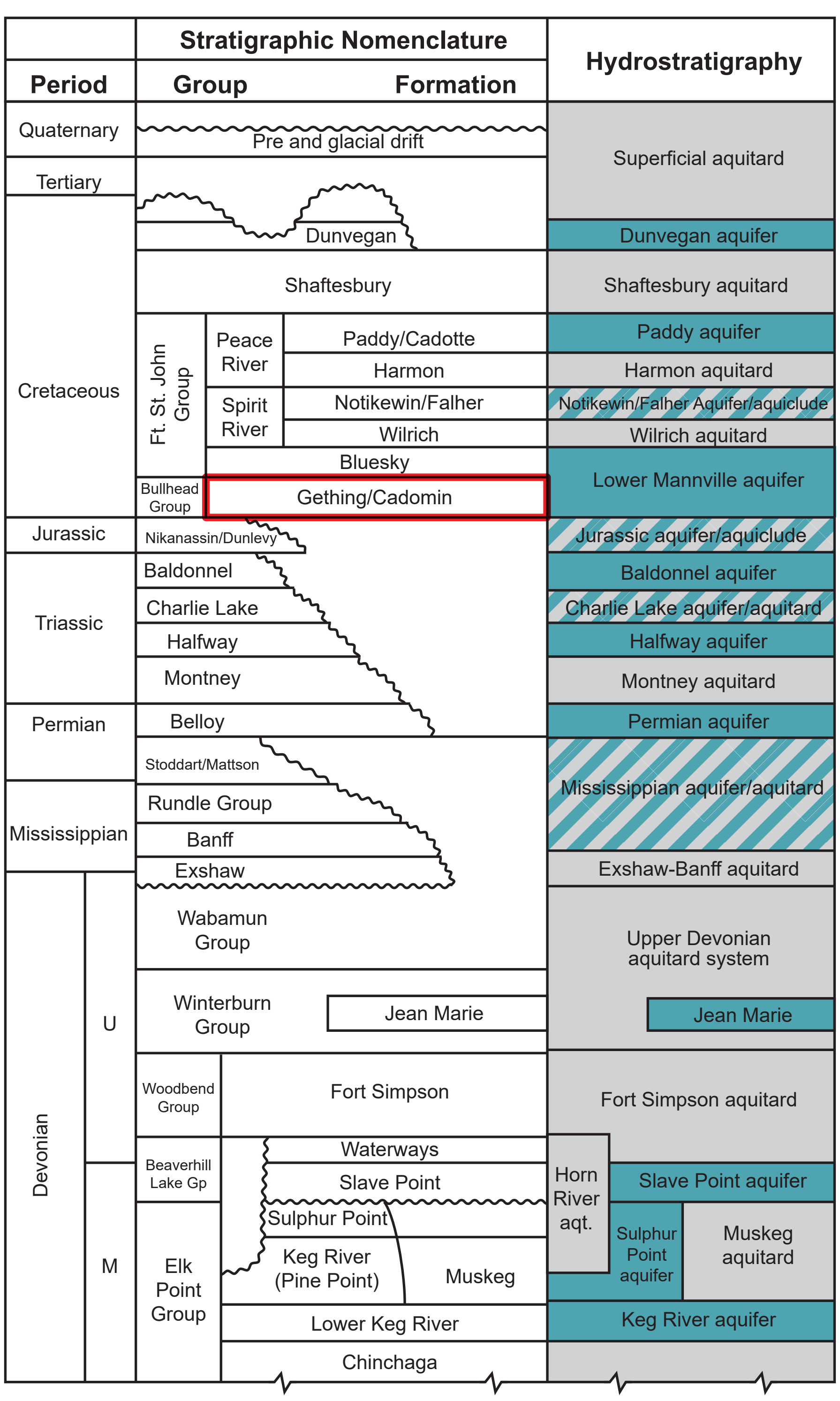

© Canadian Discovery Ltd. *Figure 8.1*

8.2 Top 10 Depleted Cadomin-Gething Pools

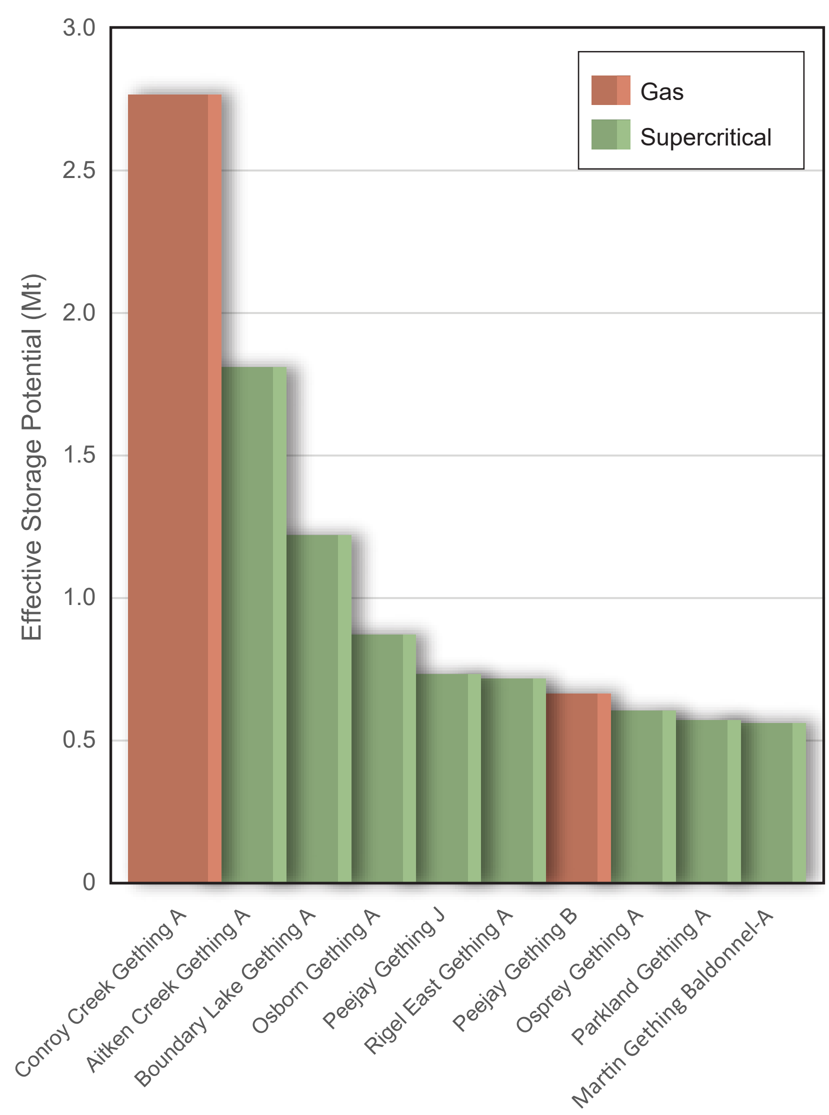

© Canadian Discovery Ltd. *Figure 8.2*

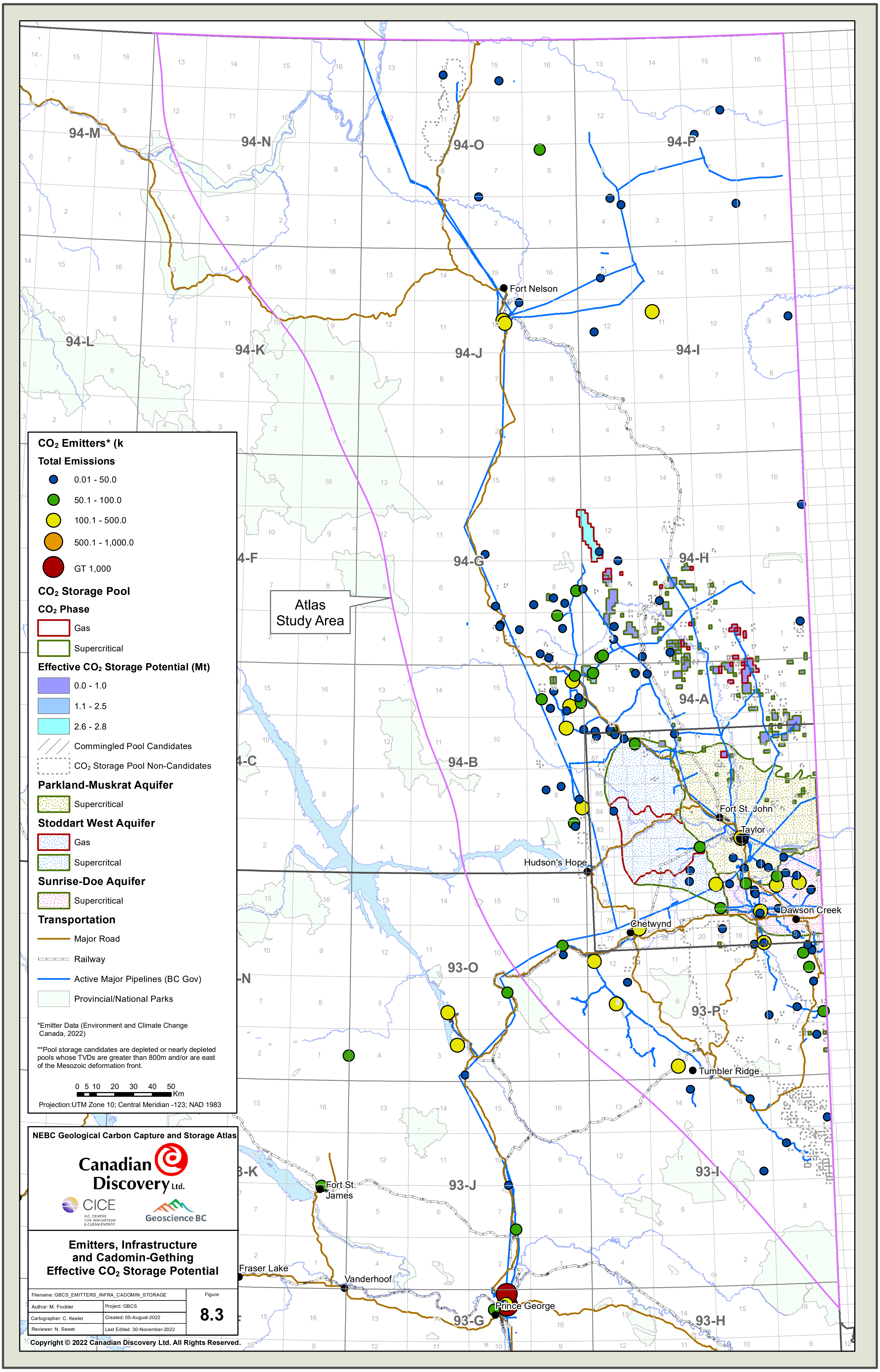

© Canadian Discovery Ltd.

Figure 8.3

8.4 Cadomin-Gething Play Schematic

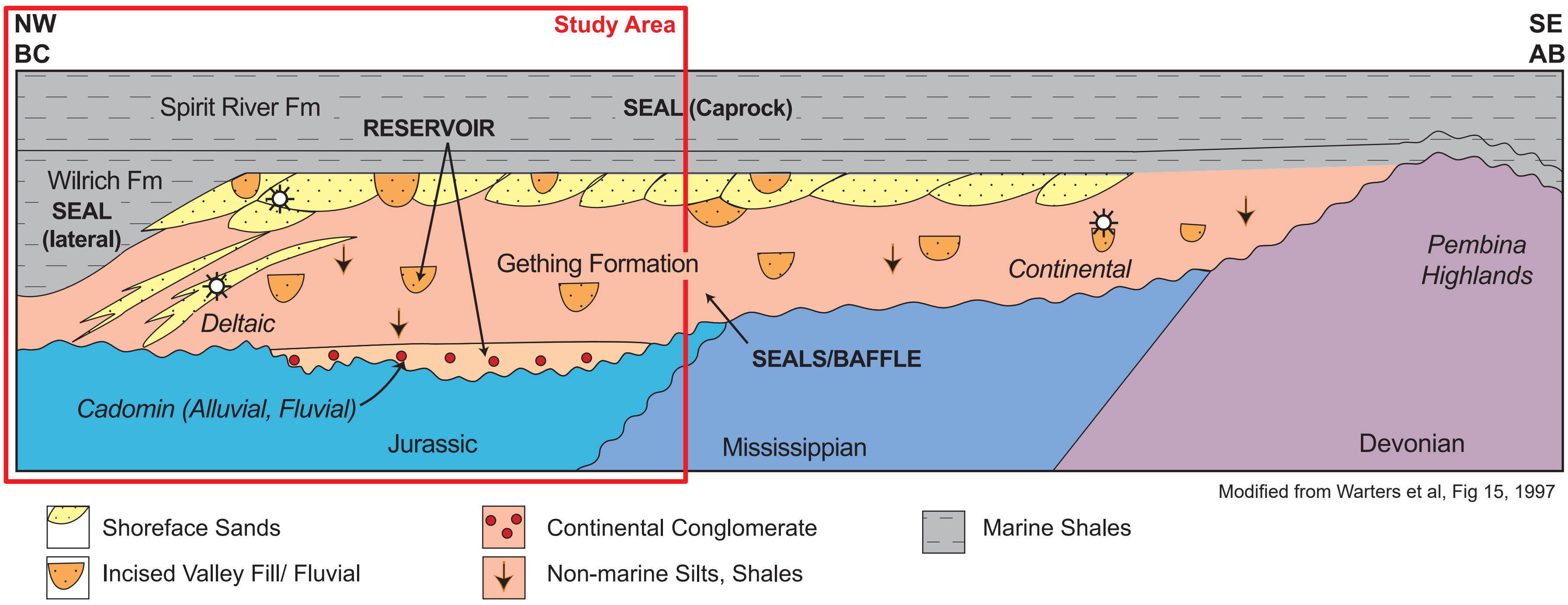

Figure 8.4

Storage Complex

The Cadomin-Gething-Bluesky Succession

The Early Cretaceous Cadomin and Gething formations are the non-marine section of the Cadomin-Gething-Bluesky transgressive succession *(figure 8.4)*, and are therefore grouped together in this chapter. The marine Bluesky Formation is discussed in another chapter. The Gething Formation is composed primarily of siltstone, shale, coal, and isolated sand bodies that act both as a limited reservoir (sandstone) and a seal/baffle above the Cadomin unit, but hydraulic continuity can exist between the three formations in some areas. The overlying shale of the Wilrich Member of the Spirit River Formation acts as the uppermost containment seal (caprock) preventing migration of gas or fluids upwards from the Cadomin, Gething or Bluesky.

Cadomin

As described in PRCL (2021), the Cadomin lies sharply on the pre-Mannville unconformity in the Spirit River Valley, west and southwest of the erosional scarp edge of the Fox Creek escarpment. Where the Cadomin overlies Fernie or older strata, the basal contact is easily picked based on lithological contrast. Cadomin strata were deposited as an outwash of alluvial fan to alluvial plain sedimentation in Early Cretaceous time, following renewed uplift of the Columbian orogenic highlands to the west (Hayes et al, 1994). Poorly sorted fine- to coarse-grained sandstone and chert pebble conglomerates characterize the Cadomin, with sediment reaching a northern depositional limit in northern 94-A and B. The reservoir quality is variable, ranging from poor in the south — particularly in the gas-saturated Deep Basin south of the Peace River Block — to very good in the north, where it is coarser-grained, less cemented, and water-bearing. The Deep Basin Cadomin A Pool is considered to be an unconventional reservoir by the BC OGC and is therefore excluded as a carbon storage candidate.

The Cadomin structure map *(figure 8.5)* shows the topography of the top of the Cadomin in the subsurface. Since the displacement of a CO_2 plume is governed by gravity and buoyancy, the plume tends to migrate up-structure during its injection period. This map shows the 800m true vertical depth contour, which indicates the approximate depth limit for this evaluation; above this depth, injected CO_2 is likely to be in a gaseous phase. As supercritical conditions for CO_2 comprise a temperature in excess of 31.1°C and a pressure greater than 7,500 kPa, the contours for these conditions indicate where CO_2 injection is expected to be in the supercritical phase. Supercritical conditions are reached over most of the study area, except for a small portion of the Peace River block.

Geoscience BC Report 2021-14 (PRCL, 2021) mapped the net reservoir within the Cadomin aquifers using a 10% porosity cutoff *(figure 8.6)*. The net reservoir maps can help indicate the most favourable areas for CO_2 injection within the aquifer; i.e. where the reservoir rock has the highest quality, and often the highest porosity and permeability.

Gething

Gething deposition took place in response to a rise in sea level and abundant sediment supply from the Columbian Orogen rising in the west. In the south, fine-grained clastics and coal were deposited in alluvial plain and coal-swamp settings, cut locally by fine- to medium-grained fluvial (river) channel sandstone. To the north, the lower Gething comprises sandy fluvial facies deposited in well-defined valleys, while the upper Gething includes deltaic to alluvial plain facies deposited over broader areas (Hayes et al, 1994). Gething deposition was terminated with the first major Cretaceous transgression of the Boreal (northerly) sea that triggered the onset of marine Bluesky deposition.

Gething reservoirs primarily comprise fluvial channels within tighter siltstone and are overlain by the Bluesky. The shale and siltstone act as a baffle between the underlying Cadomin reservoirs and the overlying Bluesky reservoirs.

Unlike the Cadomin, the Gething is primarily hydrocarbon-bearing, and therefore the majority of carbon storage opportunities within the Gething are within depleted pools *(figure 8.7)*. The net reservoir contours within the pools were provided by the BC Oil and Gas Commission (BC OGC), and can help indicate the most favourable areas for CO_2 injection within storage reservoirs.

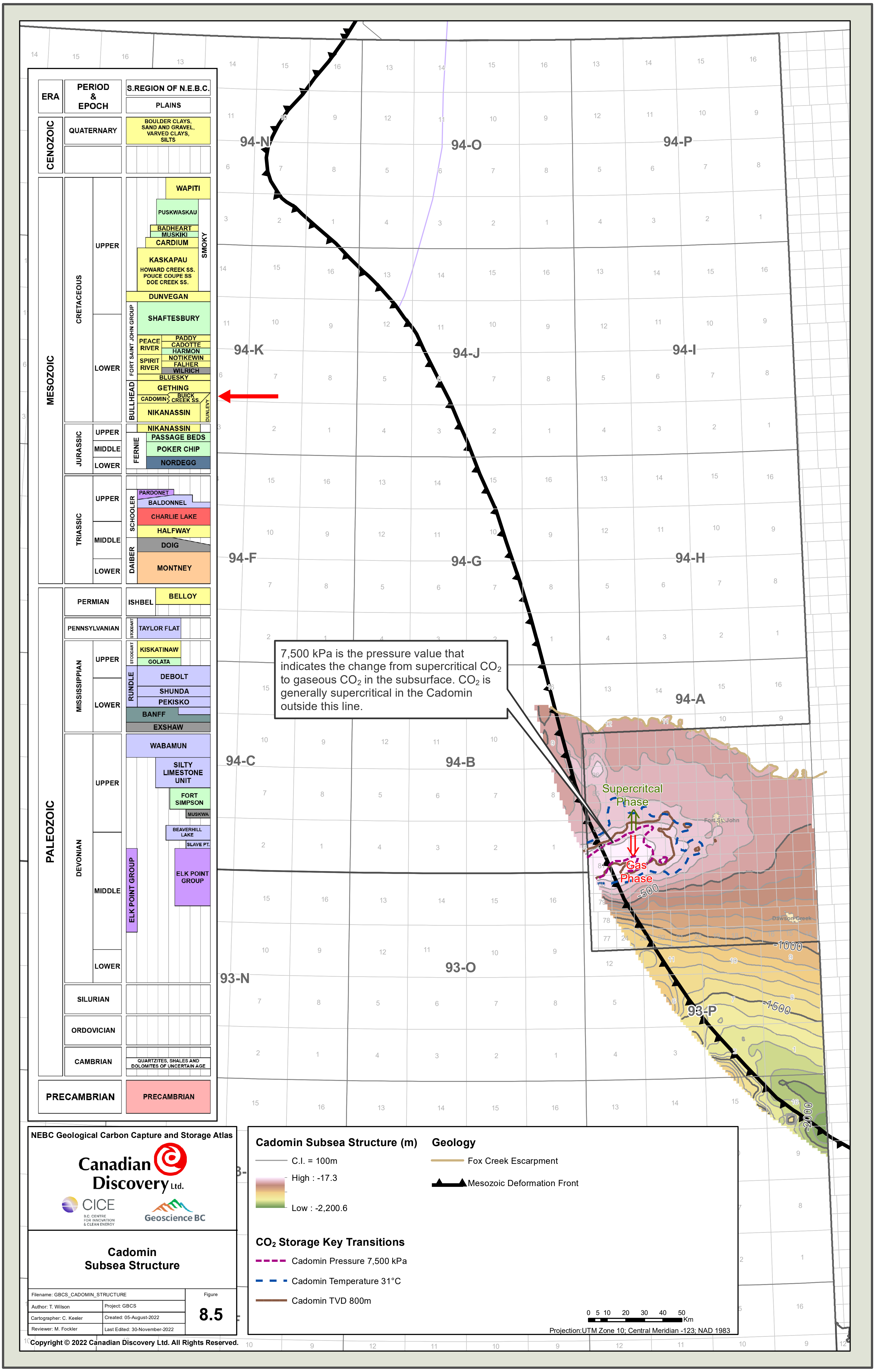

© Canadian Discovery Ltd.

Figure 8.5

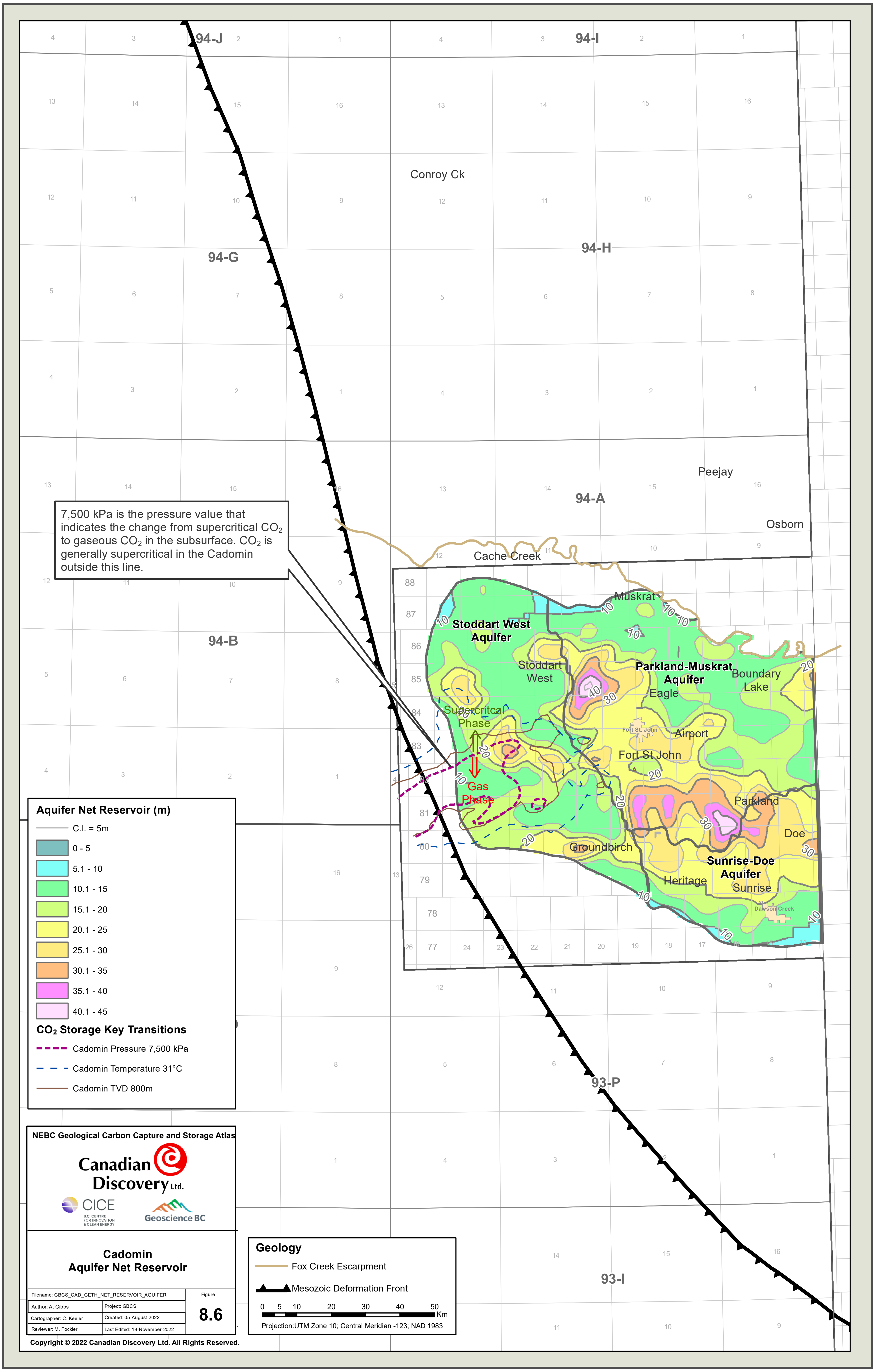
94-J
94-I
94-G
94-H
94-A
94-B
93-P
93-I
Conroy Ck
Peejay
Osborn
Cache Creek
Muskrat
Stoddart West Aquifer
Stoddart West
Parkland-Muskrat Aquifer
Boundary Lake
Eagle
Supercritical Phase
Gas Phase
Airport
Fort St John
Parkland
Doe
Groundbirch
Sunrise-Doe Aquifer
Heritage
Sunrise
7,500 kPa is the pressure value that indicates the change from supercritical CO_2 to gaseous CO_2 in the subsurface. CO_2 is generally supercritical in the Cadomin outside this line.
Aquifer Net Reservoir (m)
C.I. = 5m
0 - 5
5.1 - 10
10.1 - 15
15.1 - 20
20.1 - 25
25.1 - 30
30.1 - 35
35.1 - 40
40.1 - 45
CO_2 Storage Key Transitions
Cadomin Pressure 7,500 kPa
Cadomin Temperature 31°C
Cadomin TVD 800m
NEBC Geological Carbon Capture and Storage Atlas
Canadian Discovery Ltd.
CICE
Geoscience BC
Cadomin
Aquifer Net Reservoir
Filename: GBCS_CAD_GETH_NET_RESERVOIR_AQUIFER
Author: A. Gibbs
Project: GBCS
Cartographer: C. Keeler
Created: 05-August-2022
Reviewer: M. Fockler
Last Edited: 18-November-2022
Figure
8.6
Copyright © 2022 Canadian Discovery Ltd. All Rights Reserved.
Geology
Fox Creek Escarpment
Mesozoic Deformation Front
0 5 10 20 30 40 50 Km
Projection:UTM Zone 10; Central Meridian -123; NAD 1983

 Figure 8.6

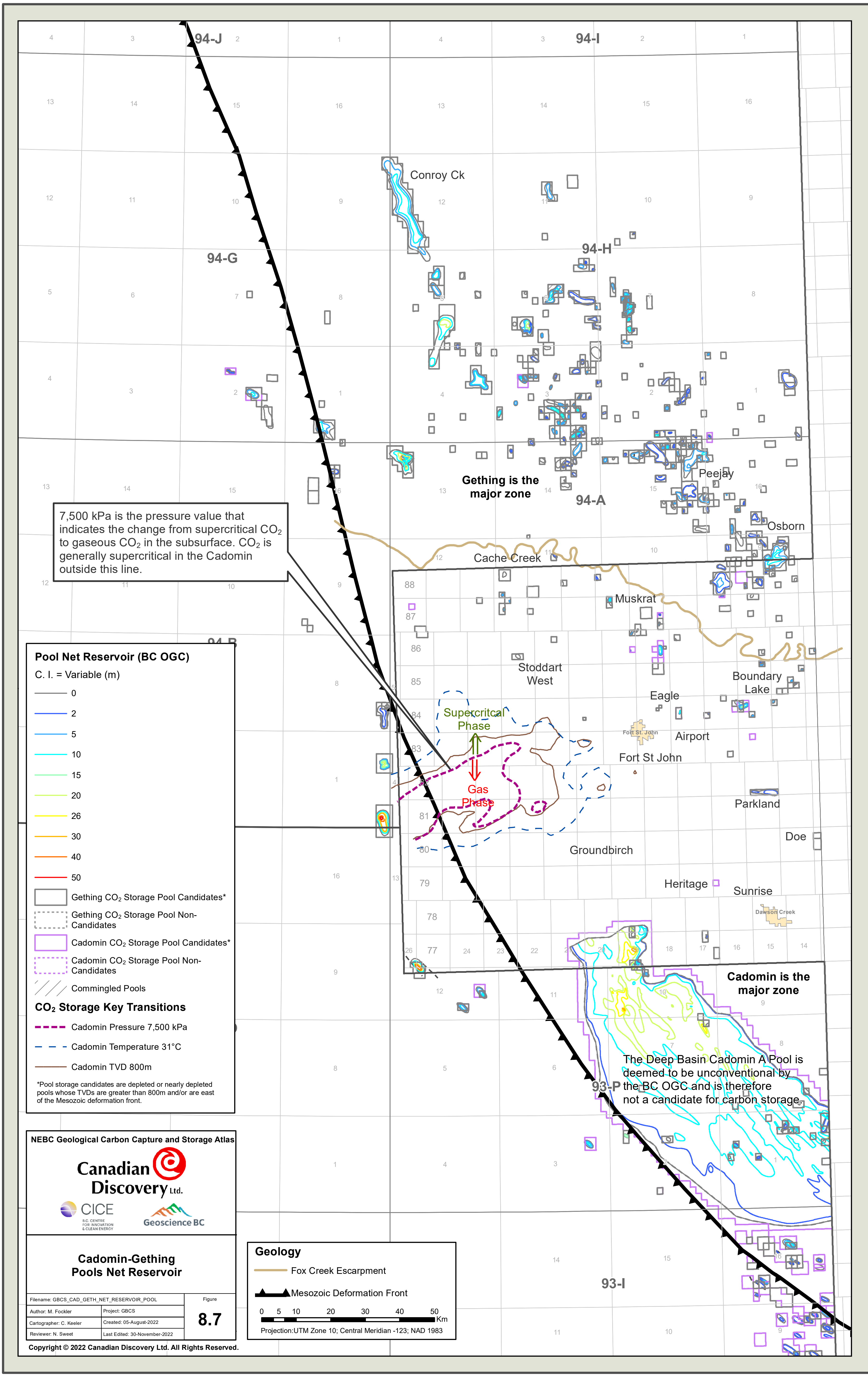

© Canadian Discovery Ltd.

Figure 8.7

Porosity-Permeability Correlations

Establishing detailed porosity trends requires examination of log suites and petrophysical models, which is beyond the scope of this phase of the Atlas. However, available core data can be used to provide a high level estimate of porosity trends, particularly within the aquifers, where this information is needed for storage potential estimates. Core data for the Cadomin were obtained from geoLOGIC and filtered for better quality reservoir that is more conducive to carbon storage within the study area. Core data was not analyzed for the Gething, as carbon storage estimates in the Gething are based on fluid production from depleted pools (see Carbon Storage Calculations).

The Cadomin core data were used to estimate porosity trends in the aquifers for storage calculations and to conduct a preliminary analysis of porosity-permeability trends *(figure 8.8)*. The best reservoir quality is found in the Parkland-Muskrat system (shown in yellow) and can reach up to 18–20% porosity and hundreds of millidarcies of permeability. As the reservoir quality decreases to the west and south, the porosity-permeability correlation does not change significantly, however the range of porosity observed decreases to closer to 10–16% and the permeability to less than 200 mD.

8.8 Cadomin-Gething Porosity-Permeability Plot

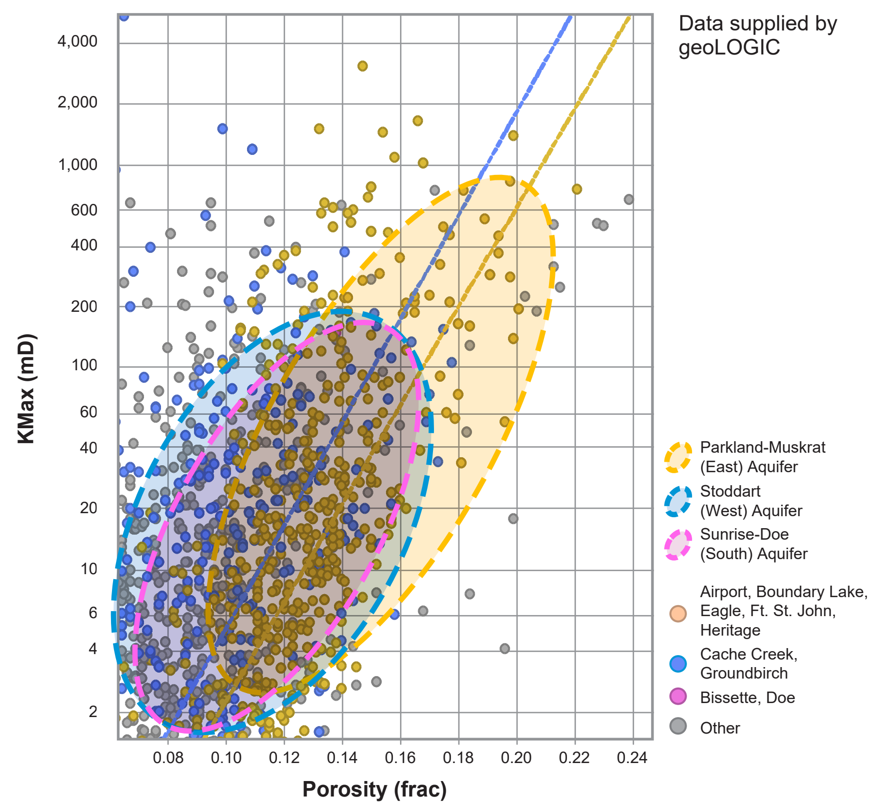

© Canadian Discovery Ltd. *Figure 8.8*

Hydrodynamics

To delineate the extent of the aquifers and understand the relationship between the aquifers and the depleted pools, a high-level analysis was done on Cadomin and Gething hydrodynamics. Hydrofax drillstem test (DST) data from within the Cadomin aquifers and initial pressure and datum depth from depleted Gething pools from the BC OGC reserves databases are shown on the Pressure vs Elevation graph *(figure 8.9)*.

While the majority of Cadomin aquifers fall primarily within the supercritical range for CO_2, there is one shallow area within the Stoddart aquifer (shown in blue) that is significantly uplifted and storage conditions are not as favourable. The majority of the Gething pools tend to be underpressured with respect to the Cadomin aquifers, which is likely a result of pressure equilibration and possible interconnectivity between the Gething pools and the lower-pressured Bluesky aquifers. The gradients for the Bluesky aquifers are included on the P/E graph for reference. While this entire complex is capped by overlying Wilrich shales, further work should be done when planning any storage project within these zones to better understand any potential interconnectivity between the Cadomin, Gething and Bluesky.

8.9 Cadomin-Gething Pressure vs Elevation Plot

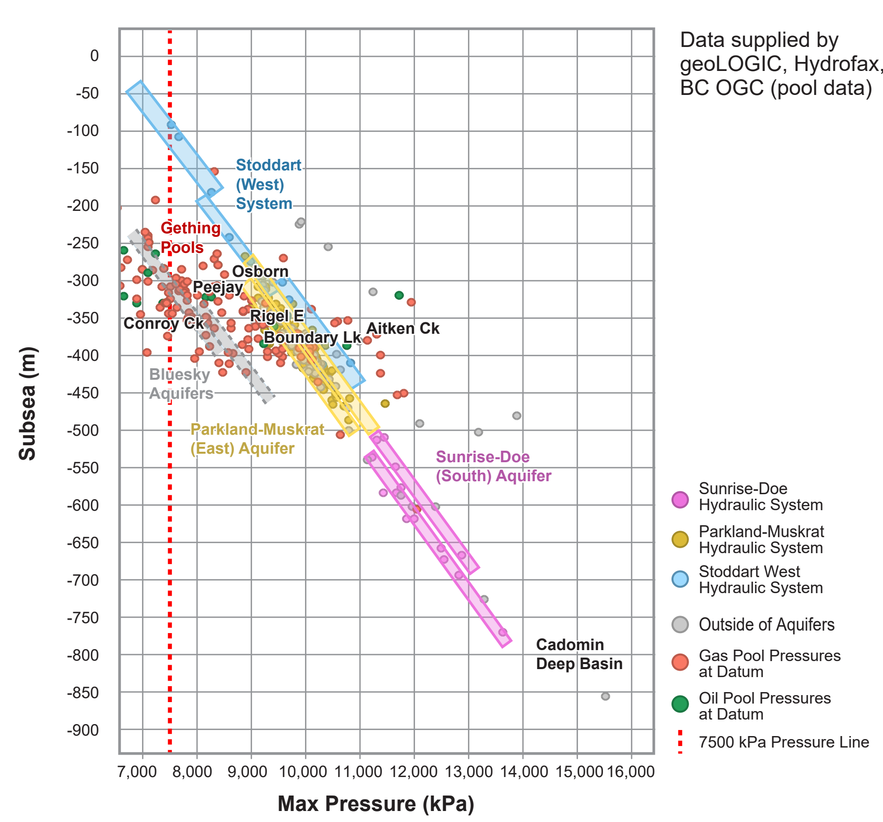

© Canadian Discovery Ltd. *Figure 8.9*

Carbon Storage Calculations

Depleted and Nearly Depleted Pools

The top 25 depleted and nearly depleted candidates for carbon storage potential within the Gething Formation are shown in *Table 8.2*.

The BC OGC defines depleted pools as ones that have no remaining reserves or production. The BC OGC also recognizes that there are nearly depleted pools that could become CO_2 storage candidates in the (relatively) near future. The nearly depleted CO_2 storage candidates include pools where 90%+ of the reserves have been recovered, or no production has occurred in over five years. Furthermore, CDL has excluded pools that are shallower than 800m TVD, or are west of the Mesozoic deformation front. See Depleted Pools Selection Criteria in *Chapter 4* for a more thorough discussion.

In the table, the theoretical CO_2 storage potential represents the mass of CO_2 that can be stored in the hydrocarbon reservoirs assuming that the volume occupied previously by the produced gas will be occupied entirely by the injected CO_2. These calculations have been provided by the BC OGC and are based on historical pool production.

The effective CO_2 storage potential represents the mass of CO_2 that can be stored in hydrocarbon reservoirs after taking into account intrinsic reservoir characteristics and flow processes, such as heterogeneity (how much variability there is in the rock), aquifer support, sweep efficiency, gravity override, and CO_2 mobility (Bachu, 2006). The effective CO_2 storage potential is calculated by CDL and reduces the theoretical storage potential by as little as 13% and as much as 75%. More detail is provided on the carbon storage calculations for depleted pools in *Appendix B*, and data are provided for all depleted pools included in this study in *Appendix C*.

The depleted and nearly depleted pools that are deemed to be CO_2 storage candidates by CDL are coloured by their effective storage potential mass on the summary map *(figure 8.10)*.

Aquifers

The Cadomin aquifer parameters are summarized in *table 8.3*. Theoretical CO_2 storage potential can be calculated using the mapped pore volume of the reservoir and CO_2 density, and assumes that the pore volume will be occupied entirely by the injected CO_2. We know this is not the case however, since the pore space is already occupied by water and the water will need to be displaced in the process. As a result, a storage efficiency factor is introduced into storage potential calculations that accounts for the presence of both water and CO_2 in the aquifer. The storage efficiency factor is a function of reservoir and fluid properties and dynamics, including the geometry of the trap, gravity segregation, heterogeneity, permeability distribution, and pressure, and may reduce the theoretical storage potential by 95 to 99%.

Aquifers considered favourable targets for CO_2 storage are indicated on the summary map *(figure 8.10)* and are labelled with their estimated P10, P50 and P90 effective storage potential in Mt. More detail is provided on the aquifer carbon storage calculations in *Appendix B*.

Top 25 Depleted Cadomin-Gething Pools

Pool Name	Pool Type	Well Count	Initial Pressure (kPa)	Temperature (˚C)	Average Porosity (%)	CO_2 Phase	Theoretical Storage Potential (Mt)	Effective Storage Potential (Mt)
Conroy Creek Gething A	Gas	89	5,409	60	12.2	Gas	3.2	2.8
Aitken Creek Gething A	Gas	19	10,760	60	11.9	Supercritical	3.7	1.8
Boundary Lake Gething A	Gas	3	9,533	46	16.6	Supercritical	1.4	1.2
Osborn Gething A	Gas	20	8,874	49	15.1	Supercritical	1.4	0.9
Peejay Gething J	Gas	11	7,779	53	13.3	Supercritical	0.8	0.7
Rigel East Gething A	Gas	7	9,218	55	15.6	Supercritical	2.9	0.7
Peejay Gething B	Gas	21	7,364	50	14.0	Gas	1.1	0.7
Osprey Gething A	Gas	7	8,396	53	12.8	Supercritical	0.7	0.6
Parkland Gething A	Gas	5	10,640	49	13.2	Supercritical	0.7	0.6
Martin Gething Baldonnel-A	Gas	5	8,598	57	12.3	Supercritical	0.6	0.6
Peejay Gething A	Gas	1	7,396	49	16.5	Supercritical	0.5	0.4
Currant Gething B	Gas	5	7,448	52	15.5	Supercritical	0.5	0.4
Martin Gething D	Gas	6	7,512	56	14.0	Supercritical	0.4	0.4
Nig Creek Gething A	Gas	7	11,137	60	12.9	Supercritical	0.4	0.3
Pickell Gething B	Gas	1	7,832	69	14.5	Supercritical	0.4	0.3
Rigel East Cadomin A	Gas	1	9,073	52	14.0	Supercritical	0.3	0.3
Prespatou Basal Gething A	Gas	4	9,298	54	13.2	Supercritical	0.3	0.3
Oak Cadomin A	Gas	1	10,070	51	12.0	Supercritical	0.3	0.3
Peejay Gething F	Gas	1	7,781	49	19.4	Supercritical	0.3	0.2
Rigel East Gething G	Gas	1	7,912	52	13.2	Supercritical	0.3	0.2
Boundary Lake Gething I	Gas	1	10,074	44	17.0	Supercritical	0.3	0.2
Boundary Lake Gething E	Gas	1	9,850	44	17.0	Supercritical	0.2	0.2
Osborn Gething D	Gas	3	7,487	54	12.6	Supercritical	0.2	0.2
Doe Gething B	Gas	1	12,058	42	18.5	Supercritical	0.3	0.2
Boundary Lake Gething B	Gas	1	9,926	45	15.0	Supercritical	0.2	0.1

Table 8.2

Cadomin Aquifer Properties and Storage Potential

Aquifer Name	Type	Thickness Range (m)	Pressure Range (MPa)	Temperature Range (°C)	Porosity Range (%)	CO_2 Phase	P10 Effective Storage Potential at 0.5% (Mt)	P50 Effective Storage Potential at 2% (Mt)	P90 Effective Storage Potential at 5.4% (Mt)
Parkland-Muskrat Regional System	Aquifer	10-50	8.0-11.1	29-54	6-17%	Supercritical	26.2	104.8	283.0
Stoddart West Regional System	Aquifer	10-37	6.4-13.0	22-54	7-13%	Mostly Supercritical	16.2	65.0	175.4
Sunrise-Doe Regional System	Aquifer	10-40	10.8-15.1	41-67	7-14%	Supercritical	10.7	42.7	115.3

Table 8.3

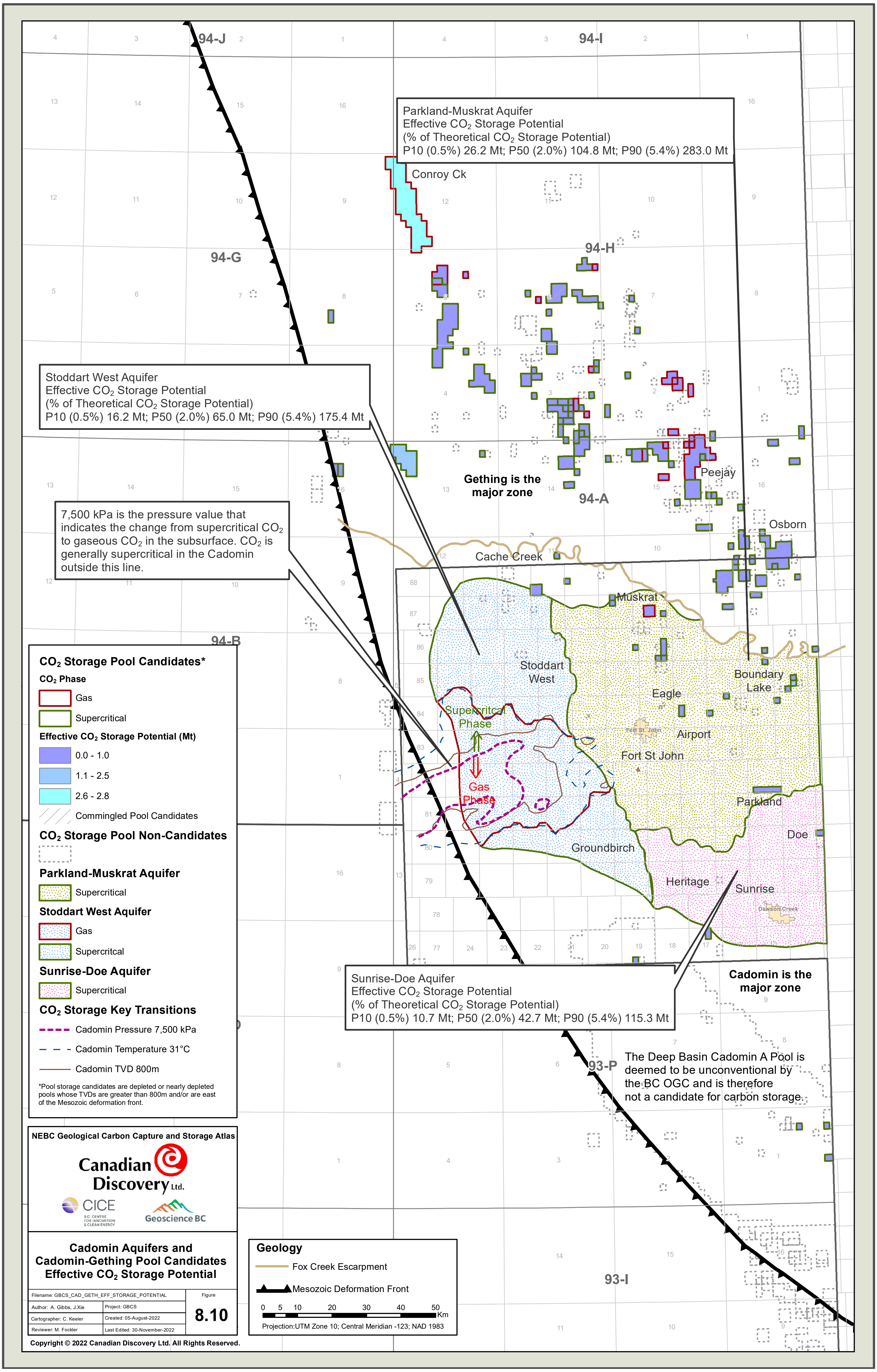

Parkland-Muskrat Aquifer
Effective CO_2 Storage Potential
(% of Theoretical CO_2 Storage Potential)
P10 (0.5%) 26.2 Mt; P50 (2.0%) 104.8 Mt; P90 (5.4%) 283.0 Mt
Stoddart West Aquifer
Effective CO_2 Storage Potential
(% of Theoretical CO_2 Storage Potential)
P10 (0.5%) 16.2 Mt; P50 (2.0%) 65.0 Mt; P90 (5.4%) 175.4 Mt
7,500 kPa is the pressure value that indicates the change from supercritical CO_2 to gaseous CO_2 in the subsurface. CO_2 is generally supercritical in the Cadomin outside this line.
Sunrise-Doe Aquifer
Effective CO_2 Storage Potential
(% of Theoretical CO_2 Storage Potential)
P10 (0.5%) 10.7 Mt; P50 (2.0%) 42.7 Mt; P90 (5.4%) 115.3 Mt
Gething is the major zone
Cadomin is the major zone
The Deep Basin Cadomin A Pool is deemed to be unconventional by the BC OGC and is therefore not a candidate for carbon storage.
94-J
94-I
94-G
94-H
94-A
94-B
93-P
93-I
Conroy Ck
Peejay
Osborn
Cache Creek
Muskrat
Stoddart West
Boundary Lake
Eagle
Airport
Fort St John
Parkland
Doe
Groundbirch
Heritage
Sunrise
Supercritical Phase
Gas Phase
CO₂ Storage Pool Candidates*
CO₂ Phase
Gas
Supercritical
Effective CO₂ Storage Potential (Mt)
0.0 - 1.0
1.1 - 2.5
2.6 - 2.8
Commingled Pool Candidates
CO₂ Storage Pool Non-Candidates
Parkland-Muskrat Aquifer
Supercritical
Stoddart West Aquifer
Gas
Supercritcal
Sunrise-Doe Aquifer
Supercritical
CO₂ Storage Key Transitions
Cadomin Pressure 7,500 kPa
Cadomin Temperature 31°C
Cadomin TVD 800m
*Pool storage candidates are depleted or nearly depleted pools whose TVDs are greater than 800m and/or are east of the Mesozoic deformation front.
NEBC Geological Carbon Capture and Storage Atlas
Canadian Discovery Ltd.
CICE
Geoscience BC
Cadomin Aquifers and Cadomin-Gething Pool Candidates Effective CO₂ Storage Potential
Filename: GBCS_CAD_GETH_EFF_STORAGE_POTENTIAL
Author: A. Gibbs, J.Xie
Project: GBCS
Cartographer: C. Keeler
Created: 05-August-2022
Reviewer: M. Fockler
Last Edited: 30-November-2022
Figure 8.10
Copyright © 2022 Canadian Discovery Ltd. All Rights Reserved.
Geology
Fox Creek Escarpment
Mesozoic Deformation Front
0 5 10 20 30 40 50 Km
Projection:UTM Zone 10; Central Meridian -123; NAD 1983

Figure 8.10

Nikanassin-Dunlevy Formation

Nikanassin-Dunlevy Overview

Storage potential in the Nikanassin and its stratigraphic equivalent, the Dunlevy *(figure 9.1)*, occurs in the southern portion of the study area near Fort St. John and is proximal to emitters and infrastructure. Favourability attributes are summarized in *table 9.1*, with green and yellow circles indicating whether an attribute is considered generally favourable (green), or has risk and requires additional work (yellow). Both depleted pool reservoirs and saline aquifers are candidates and offer a range of storage opportunities. The top 10 depleted pools are shown in *figure 9.2*. *Figure 9.3* displays the effective storage potential of the Nikanassin and Dunlevy, as well as the emitters and infrastructure in the NEBC study area.

Nikanassin-Dunlevy Favourability Attributes		
Top 10 Depleted Pool Total Potential	66 Mt	●
Aquifer Storage (P50)	560 Mt	●
Regional Seal Potential	High	●
Lithology	Sandstone	●
Porosity	6-18%	●
Permeability	10-600 mD	●
Depth (TVD)	800-2,900m	●
Net Reservoir Thickness	5-95m	●

Table 9.1

9.1 Hydrostratigraphic Chart

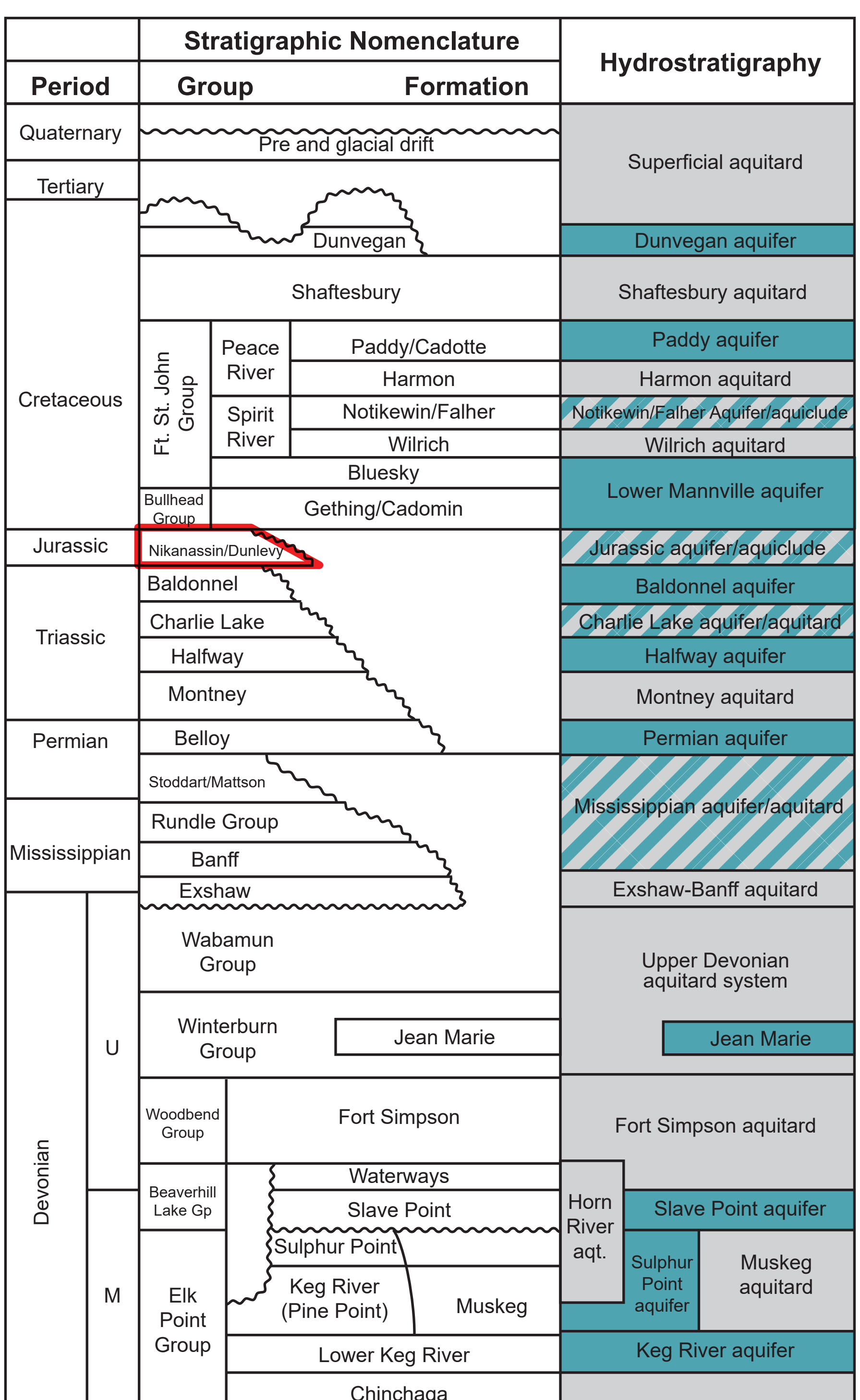

© Canadian Discovery Ltd. *Figure 9.1*

9.2 Top 10 Depleted Nikanassin-Dunlevy Pools

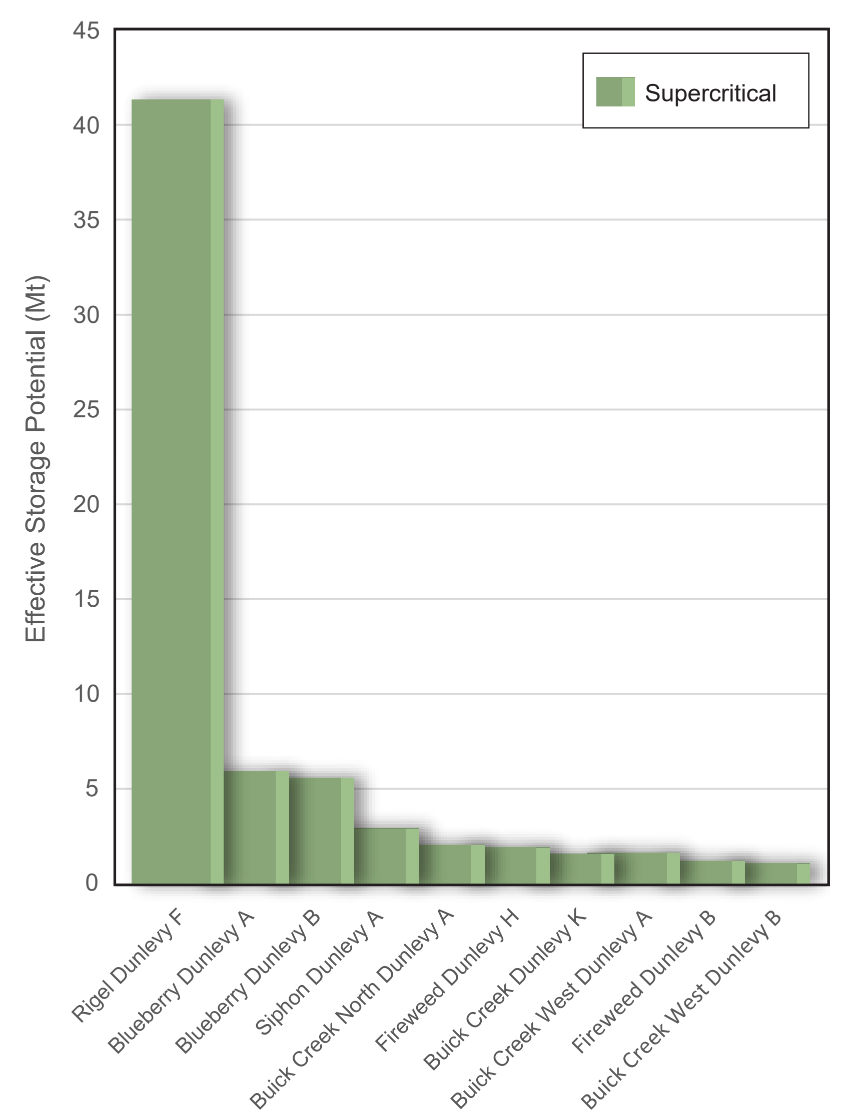

© Canadian Discovery Ltd. *Figure 9.2*

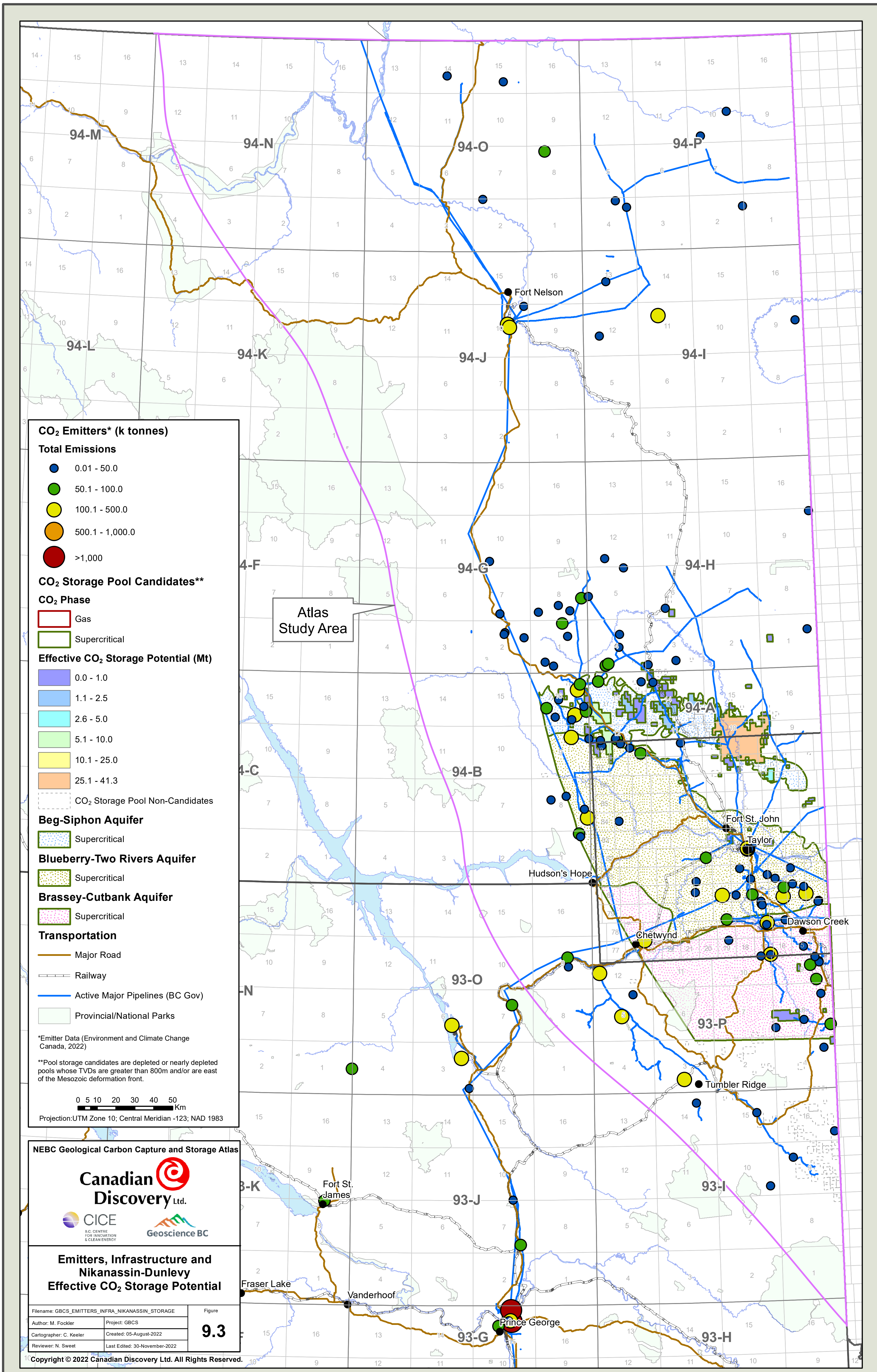

© Canadian Discovery Ltd.

Figure 9.3

9.4 Nikanassin-Dunlevy Play Schematic

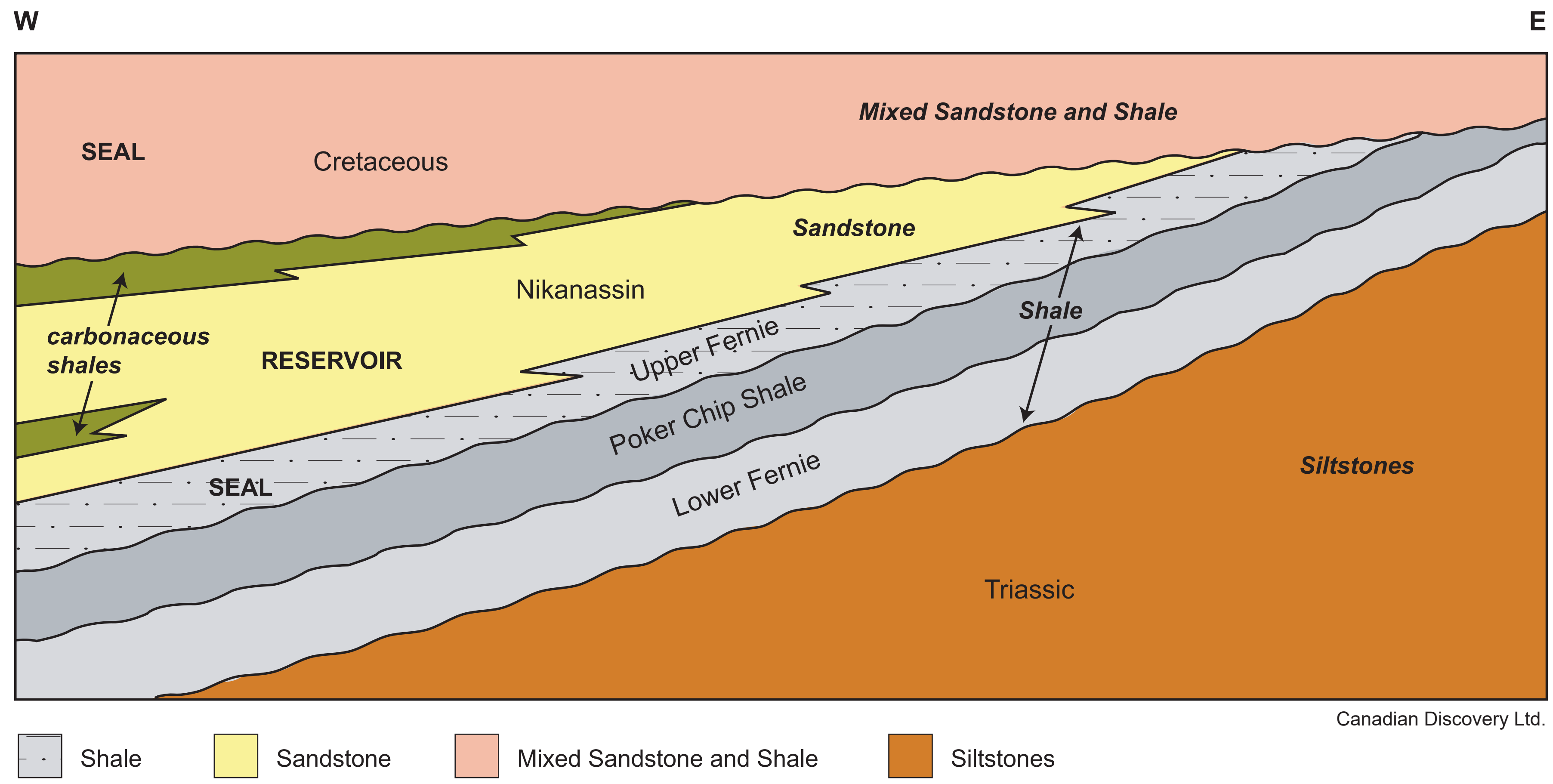

© Canadian Discovery Ltd.

Figure 9.4

Storage Complex

Nikanassin and equivalent strata comprise a thick, easterly-thinning wedge of clastics, deposited during latest Jurassic and earliest Cretaceous time *(figure 9.4)*. During Nikanassin time, the Jurassic Fernie Sea retreated northward from the WCSB in response to sea level fall and immense volumes of sediment being shed from the rising Columbian Orogen (mountains) to the west (NEBC Play Atlas, 2006). With further marine retreat and orogenic uplift, deposition was terminated and uppermost Nikanassin strata were eroded.

Nikanassin strata grade up from marine Fernie shale at the base, and are capped by the basin-scale pre-Mannville unconformity. Blocky to fining-upward sandstone bodies are interbedded with siltstone, shale, and minor coal. Deposition took place in marginal marine to continental settings, resulting in an absence of regional stratigraphic markers and mappable depositional trends.

As discussed in the Conventional Natural Gas Play Atlas of NEBC (NEBC Play Atlas, 2006), Nikanassin-equivalent strata on the northern flank of the Peace River block comprise highly quartzose sandstone, shale, and coal, deposited in a southwesterly-prograding deltaic setting. Pre-Gething valleys incise the Nikanassin to the north and south, leaving it almost an erosional outlier. In this area, the terms "Buick Creek" and "Dunlevy" have often been applied to Nikanassin, Cadomin, and Gething strata, causing considerable confusion in correlations and pool assignments. As will be discussed in the hydrodynamics section, these systems appear to be interconnected from a hydrodynamics perspective, and the geology within the area of 94-A-13 to 16 should be examined in detail before pursuing a carbon storage project in this region.

The Nikanassin structure map *(figure 9.5)* shows the topography of the top of the Nikanassin in the subsurface. Since the displacement of a CO_2 plume is governed by gravity and buoyancy, the plume tends to migrate up-structure during its injection period. This map shows the 800m true vertical depth contour; above this depth, injected CO_2 is likely to be in a gaseous phase. As supercritical conditions for CO_2 comprise a temperature in excess of 31.1°C and a pressure greater than 7,500 kPa, the contours for these conditions indicate where CO_2 injection is expected to be in the supercritical phase. Supercritical conditions are reached over most of the study area, except for a small portion of the Peace River block.

Net reservoir maps are provided for the saline aquifers *(figure 9.6)* and depleted pools *(figure 9.7)*. These maps can indicate the most favourable areas for CO_2 injection within storage reservoirs; i.e. where the reservoir rock has the highest quality and most often the highest porosity and permeability. The net reservoir contours within the pools were provided by the BC Oil and Gas Commission (BC OGC). Geoscience BC Report 2021-14 (PRCL, 2021) mapped the net reservoir within the Nikanassin aquifers using a 12% porosity cut-off *(figure 9.6)*.

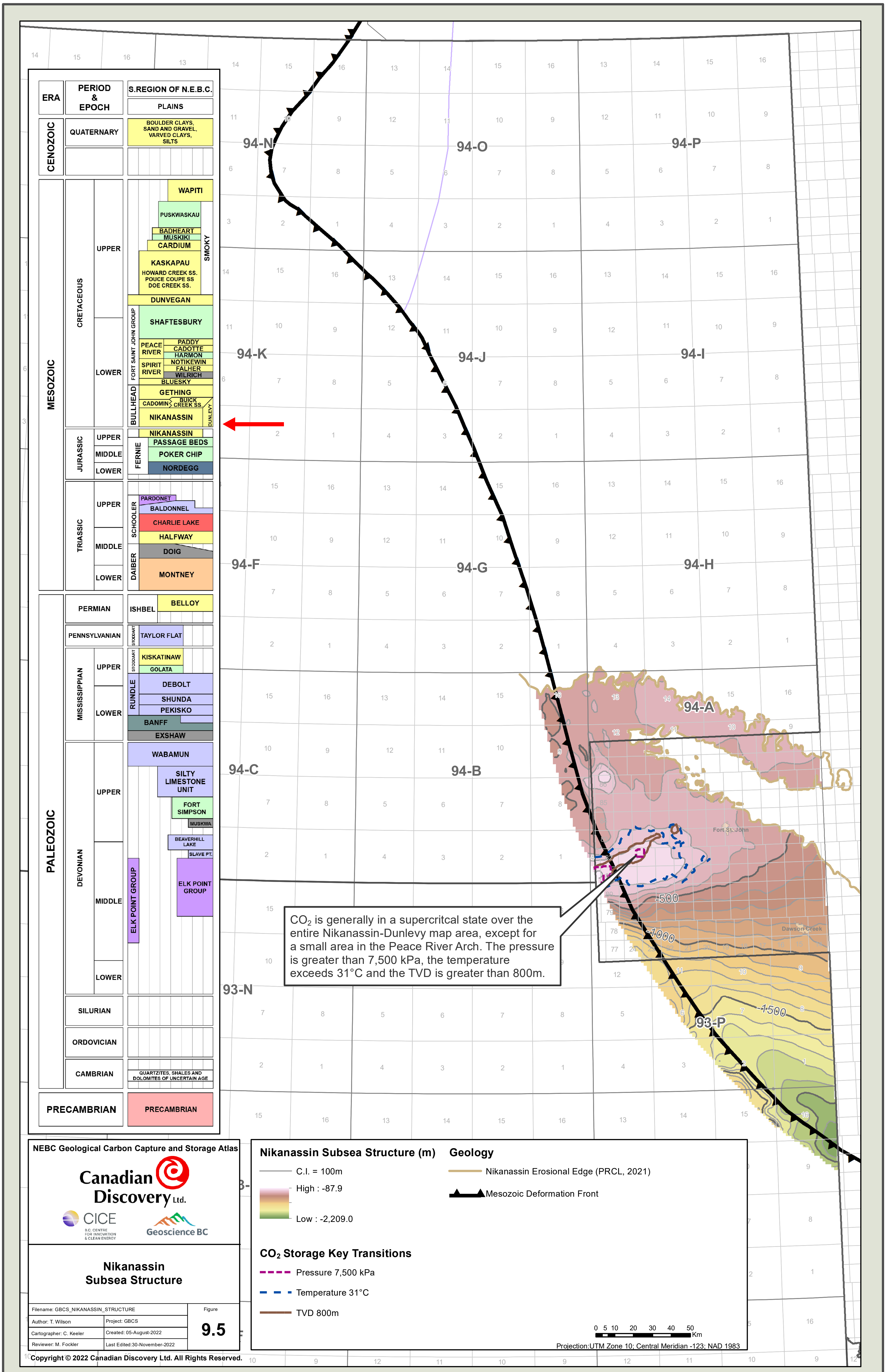

© Canadian Discovery Ltd.

Figure 9.5

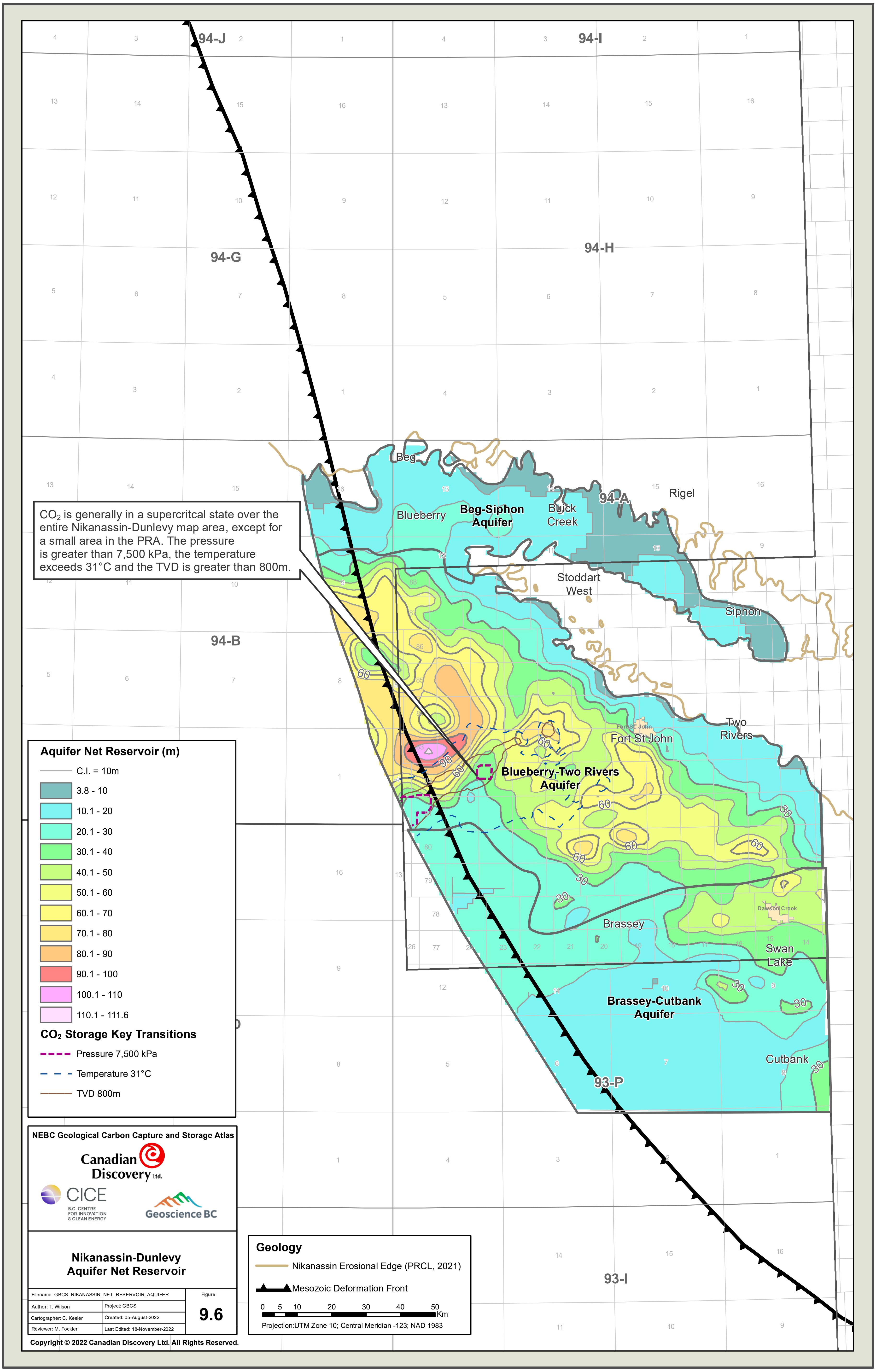

94-J
94-I
94-G
94-H
94-A
94-B
93-P
93-I
Beg
Blueberry
Beg-Siphon Aquifer
Buick Creek
Rigel
Stoddart West
Siphon
Two Rivers
Fort St John
Blueberry-Two Rivers Aquifer
Brassey
Dawson Creek
Swan Lake
Brassey-Cutbank Aquifer
Cutbank
CO2 is generally in a supercritcal state over the entire Nikanassin-Dunlevy map area, except for a small area in the PRA. The pressure is greater than 7,500 kPa, the temperature exceeds 31°C and the TVD is greater than 800m.
Aquifer Net Reservoir (m)
C.I. = 10m
3.8 - 10
10.1 - 20
20.1 - 30
30.1 - 40
40.1 - 50
50.1 - 60
60.1 - 70
70.1 - 80
80.1 - 90
90.1 - 100
100.1 - 110
110.1 - 111.6
CO2 Storage Key Transitions
Pressure 7,500 kPa
Temperature 31°C
TVD 800m
NEBC Geological Carbon Capture and Storage Atlas
Canadian Discovery Ltd.
CICE
B.C. CENTRE FOR INNOVATION & CLEAN ENERGY
Geoscience BC
Nikanassin-Dunlevy Aquifer Net Reservoir
Filename: GBCS_NIKANASSIN_NET_RESERVOIR_AQUIFER
Figure
9.6
Author: T. Wilson
Project: GBCS
Cartographer: C. Keeler
Created: 05-August-2022
Reviewer: M. Fockler
Last Edited: 18-November-2022
Copyright © 2022 Canadian Discovery Ltd. All Rights Reserved.
Geology
Nikanassin Erosional Edge (PRCL, 2021)
Mesozoic Deformation Front
0 5 10 20 30 40 50 Km
Projection:UTM Zone 10; Central Meridian -123; NAD 1983

Figure 9.6

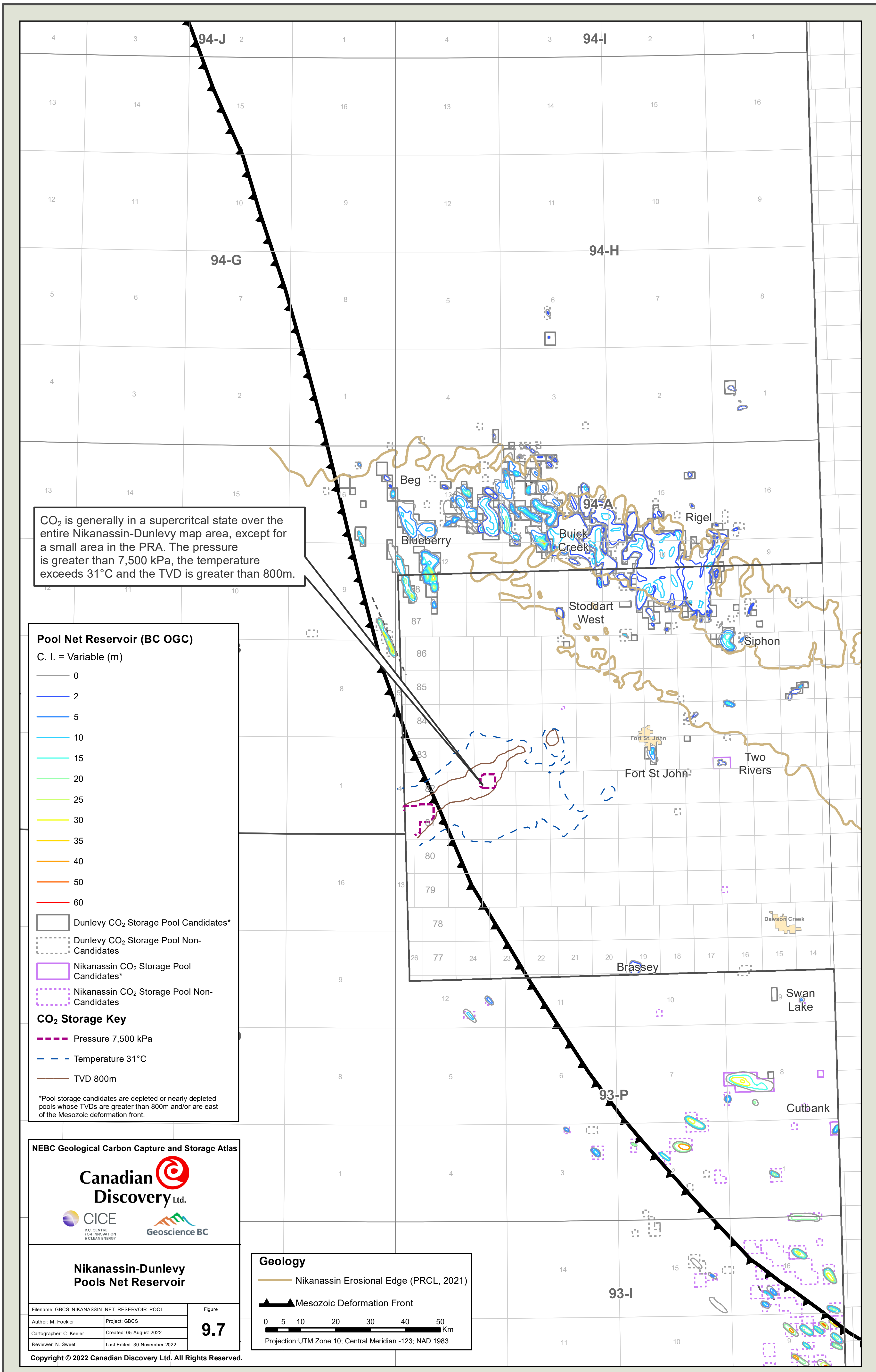

© Canadian Discovery Ltd.

Figure 9.7

Porosity-Permeability Correlations

Establishing detailed porosity trends requires examination of log suites and petrophysical models, which is beyond the scope of this phase of the Atlas. However, available core data can be used to provide a high level estimate of porosity trends, particularly within the aquifers, where this information is needed for storage potential estimates. Core data for the Nikanassin were obtained from geoLOGIC and filtered for better quality reservoir that is more conducive to carbon storage within the study area.

The Nikanassin core data were used to estimate porosity trends in the aquifers for storage calculations and to do a preliminary analysis of porosity-permeability trends *(figure 9.8)*. Porosity in the Nikanassin is generally less than 16%, however very thick Nikanassin through the Peace River can provide high pore volumes available for carbon storage. The highest permeability is found in the Beg-Siphon aquifer, where Nikanassin equivalent strata on the northern flank of the Peace River block comprise highly quartzose sandstone, shale, and coal, and where porosity in the sandstone can reach 16–18% and permeability can reach up to 600 mD. Although the thickest reservoirs are located further south in the Peace River block, the stacked channelized bodies tend to be fine- to medium-grained siliceous litharenites with permeability up to 100 mD. The poorest quality reservoir is found to the south in the Brassey–Cutbank area, where the Nikanassin transitions to a Deep Basin style play, and in many areas the permeability barely reaches the 20 mD permeability cutoff required for a low injection rate carbon storage project.

9.8 | Nikanassin-Dunlevy Porosity-Permeability Plot

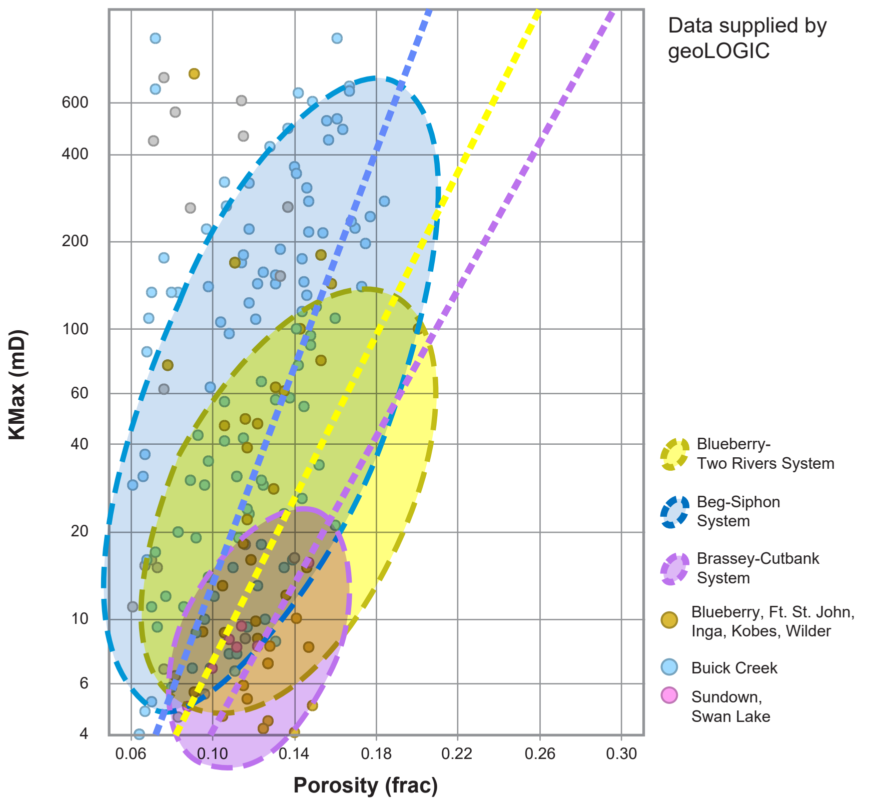

© Canadian Discovery Ltd. *Figure 9.8*

Hydrodynamics

To delineate the extent of the aquifers and understand the relationship between the aquifers and the depleted pools, a high-level analysis was done on Nikanassin hydrodynamics. Hydrofax drillstem test (DST) data from within the Nikanassin aquifers, and initial pressure and datum depth from depleted Nikanassin and Dunlevy pools from the BC OGC reserves databases are shown on the Pressure vs Elevation (P/E) graph *(figure 9.9)*.

The Nikanassin aquifers fall primarily within the supercritical range for CO_2. The aquifers are relatively continuous throughout the study area, although several areas can be differentiated by variations in reservoir quality and pressure. The Nikanassin is separated into three distinct aquifers that can be distinguished as separate systems on the P/E graph *(figure 9.9)*.

The Blueberry–Two River region has the best overall carbon storage potential within the aquifer due to thick, high quality reservoir within stacked channel bodies and moderate pressures (generally 7-15 MPa) and permeability (up to 100 mD). There are also some good depleted pool opportunities in the Blueberry area. It must be noted however, that a significant amount of faulting exists within the Fort St. John graben; efforts should be made to avoid faulting, or the risk of reactivating any nearby faults through injection should be investigated prior to pursuing any carbon storage project in this area.

The Brassey–Cutbank system, although exhibiting moderate storage potential, tends to have lowest permeability and is likely suitable for only low injection rate carbon storage projects.

Although exhibiting lower net reservoir and overall aquifer storage potential, both the highest permeabilities and the best opportunities for depleted pools (Rigel, Siphon and Buick Creek) are found in the Beg–Siphon system. As mentioned previously, the terms "Buick Creek" and "Dunlevy" have been often been applied to Nikanassin, Cadomin, and Gething strata in this area, causing considerable confusion in correlations and pool assignments. The aquifer also shows a very similar pressure trend to the Parkland–Muskrat aquifer in the Cadomin, and the pools in this area tend to be underpressured with respect to the Beg–Siphon aquifer, similar to the relationship observed between the Cadomin aquifers and Gething pools. As discussed in the previous chapter, these lower pressures are likely a result of pressure equilibration and possible interconnectivity between the Gething and Nikanassin pools and the lower-pressured Bluesky aquifers above. While this entire complex is capped by overlying Wilrich (Spirit River) shale, further work should be done when planning any storage project within these zones to better understand any potential interconnectivity between the Nikanassin, Cadomin, Gething, and Bluesky.

9.9 Nikanassin-Dunlevy Pressure vs Elevation Plot

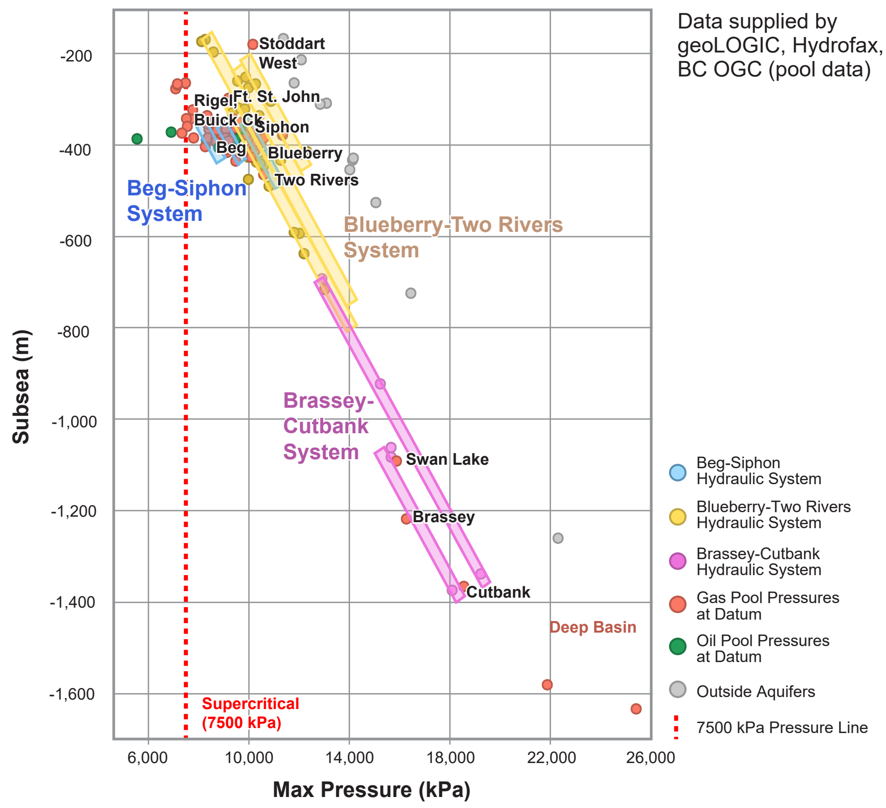

 Figure 9.9

Carbon Storage Calculations

Depleted and Nearly Depleted Pools

The top 25 depleted natural gas pool candidates for carbon storage potential within the Nikanassin-Dunlevy are shown in *Table 9.2*.

The BC OGC defines depleted pools as ones that have no remaining reserves or production. The BC OGC also recognizes that there are nearly depleted pools that could become CO_2 storage candidates in the (relatively) near future. The nearly depleted CO_2 storage candidates include pools where 90%+ of the reserves have been recovered, or no production has occurred in over five years. Furthermore, CDL has excluded pools that are shallower than 800m TVD, or are west of the Mesozoic deformation front. See Depleted Pools Selection Criteria in *Chapter 4* for a more thorough discussion.

In the table, the theoretical CO_2 storage potential represents the mass of CO_2 that can be stored in the hydrocarbon reservoirs assuming that the volume occupied previously by the produced gas will be occupied entirely by the injected CO_2. These calculations have been provided by the BC OGC and are based on historical pool production.

The effective CO_2 storage potential represents the mass of CO_2 that can be stored in hydrocarbon reservoirs after taking into account intrinsic reservoir characteristics and flow processes, such as heterogeneity (how much variability there is in the rock), aquifer support, sweep efficiency, gravity override, and CO_2 mobility (Bachu, 2006). The effective CO_2 storage potential is calculated by CDL and reduces the theoretical storage potential by as little as 13% and as much as 75%. More detail is provided on the carbon storage calculations for depleted pools in *Appendix B*, and data are provided for all depleted pools included in this study in *Appendix C*.

The depleted and nearly depleted pools that are deemed to be CO_2 storage candidates by CDL are coloured by their effective storage potential mass on the summary map *(figure 9.10)*.

Aquifers

The Nikanassin aquifer parameters are summarized in *Table 9.3*. Theoretical CO_2 storage potential can be calculated using the mapped pore volume of the reservoir and CO_2 density, and assumes that the pore volume will be occupied entirely by the injected CO_2. We know this is not the case however, since the pore space is already occupied by water, and the water will need to be displaced in the process. As a result, a storage efficiency factor is introduced into storage potential calculations that accounts for the presence of both water and CO_2 in the aquifer. The storage efficiency factor is a function of reservoir and fluid properties and dynamics, including the geometry of the trap, gravity segregation, heterogeneity, permeability distribution, and pressure, and may reduce the theoretical storage potential by 95 to 99%.

Aquifers considered favourable targets for CO_2 storage are indicated on the summary map *(figure 9.10)* and labelled with their estimated P10, P50 and P90 effective storage potential in Mt. More detail is provided on the aquifer carbon storage calculations in *Appendix B*.

Top 25 Depleted Nikanassin-Dunlevy Pools

Pool Name	Pool Type	Well Count	Initial Pressure (kPa)	Temperature (˚C)	Average Porosity (%)	CO_2 Phase	Theoretical Storage Potential (Mt)	Effective Storage Potential (Mt)
Rigel Dunlevy F	Gas	156	8,880	48	14.1	Supercritical	47.3	41.3
Blueberry Dunlevy A	Gas	32	9,356	52	8.4	Supercritical	7.0	6.1
Blueberry Dunlevy B	Gas	24	9,494	52	10.6	Supercritical	6.5	5.7
Siphon Dunlevy A	Gas	9	9,846	51	15.5	Supercritical	4.8	3.0
Buick Creek North Dunlevy A	Gas	10	9,108	53	11.2	Supercritical	2.5	2.2
Fireweed Dunlevy H	Gas	13	9,484	56	9.2	Supercritical	2.3	2.0
Buick Creek Dunlevy K	Gas	7	9,094	50	13.4	Supercritical	2.0	1.7
Buick Creek West Dunlevy A	Gas	12	9,129	52	11.3	Supercritical	6.7	1.7
Fireweed Dunlevy B	Gas	2	9,115	55	10.1	Supercritical	1.5	1.3
Buick Creek West Dunlevy B	Gas	9	9,129	52	11.2	Supercritical	5.0	1.2
Gundy Creek West Dunlevy A	Gas	5	10,204	56	8.8	Supercritical	1.3	1.2
Buick Creek Dunlevy H	Gas	7	8,768	50	13.8	Supercritical	1.2	1.1
Fireweed Dunlevy A	Gas	17	9,225	56	8.0	Supercritical	3.9	1.0
Inga Dunlevy D	Gas	3	9,532	55	9.5	Supercritical	1.1	0.9
Fireweed Dunlevy C	Gas	1	9,280	56	11.8	Supercritical	0.9	0.8
Beg Dunlevy C	Gas	3	8,896	59	10.3	Supercritical	0.9	0.8
Bernadet Dunlevy A	Gas	2	9,429	55	12.5	Supercritical	1.1	0.7
Blueberry West Dunlevy A	Gas	24	10,627	52	11.6	Supercritical	1.1	0.7
Beg Dunlevy A	Gas	2	9,391	58	8.0	Supercritical	0.7	0.6
Buick Creek North Dunlevy P	Gas	6	9,023	38	12.6	Supercritical	0.9	0.6
Stoddart West Dunlevy B	Gas	4	10,208	52	11.8	Supercritical	0.6	0.5
Buick Creek West Dunlevy J	Gas	13	9,126	58	12.1	Supercritical	0.5	0.4
Cutbank Nikanassin A	Gas	1	18,564	81	10.5	Supercritical	0.4	0.4
Kelly Nikanassin A	Gas	5	21,898	85	7.0	Supercritical	0.4	0.3
Muskrat Dunlevy A	Gas	4	8,691	52	13.5	Supercritical	0.4	0.3

© Canadian Discovery Ltd. Data supplied by BC OGC and Canadian Discovery Ltd.

Table 9.2

Nikanassin-Dunlevy Aquifer Properties and Storage Potential

Aquifer Name	Type	Thickness Range (m)	Pressure Range (MPa)	Temperature Range (°C)	Porosity Range (%)	CO_2 Phase	P10 Effective Storage Potential at 0.5% (Mt)	P50 Effective Storage Potential at 2% (Mt)	P90 Effective Storage Potential at 5.4% (Mt)
Beg-Siphon Regional System	Aquifer	10-30	8.4-13.7	45-66	7-12%	Supercritical	5.9	23.7	64.1
Blueberry - Two Rivers Regional System	Aquifer	10-110	7-15	26-60	7-14%	Mostly Supercritical	110.2	440.6	1,189.6
Brassey-Cutbank Regional System	Aquifer	10-60	11.5-25.0	48-100	7-14%	Supercritical	23.9	95.7	258.4

Table 9.3

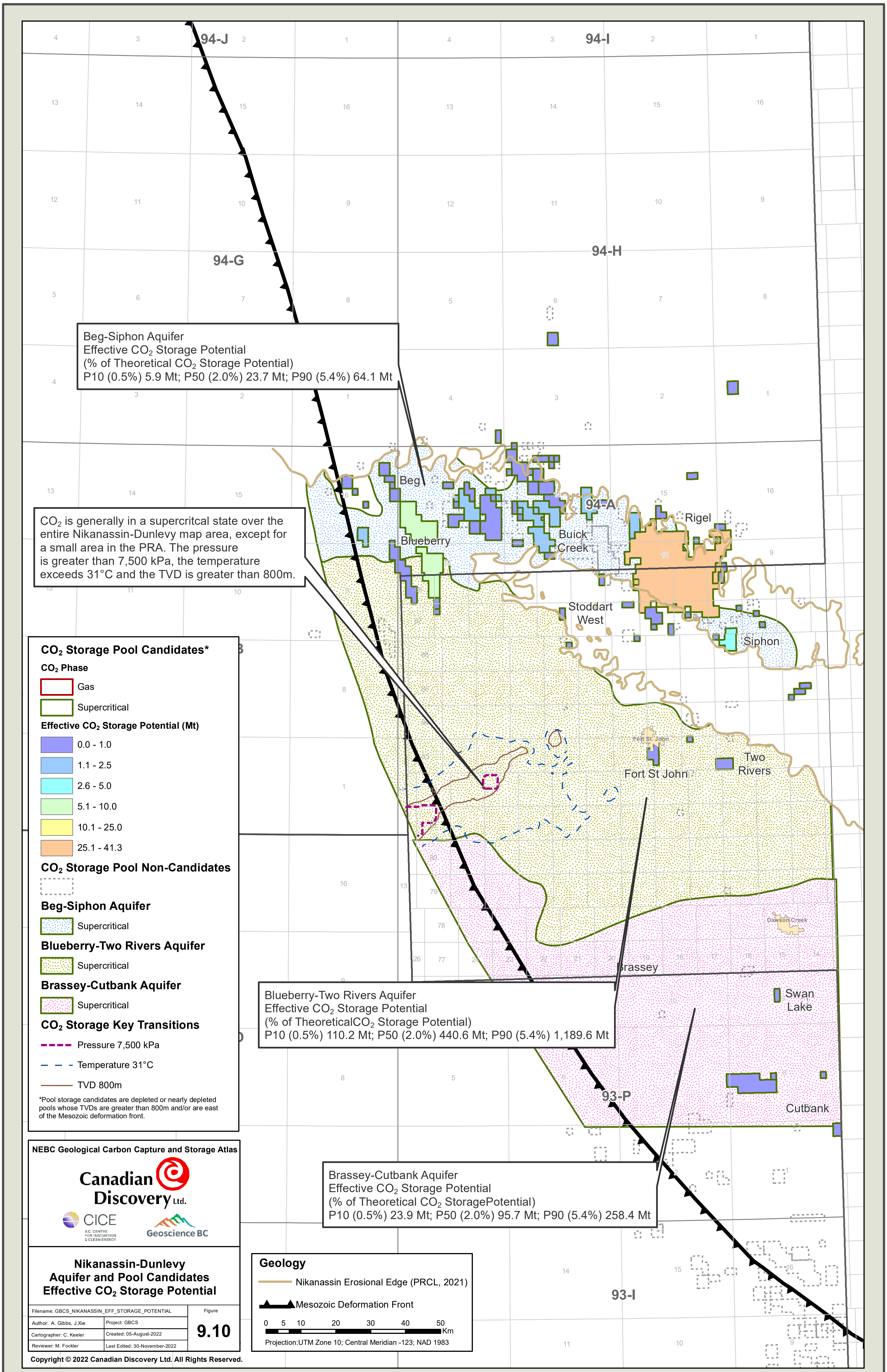

94-J
94-I
94-G
94-H
94-A
93-P
93-I
Beg-Siphon Aquifer
Effective CO2 Storage Potential
(% of Theoretical CO2 Storage Potential)
P10 (0.5%) 5.9 Mt; P50 (2.0%) 23.7 Mt; P90 (5.4%) 64.1 Mt
CO2 is generally in a supercritcal state over the entire Nikanassin-Dunlevy map area, except for a small area in the PRA. The pressure is greater than 7,500 kPa, the temperature exceeds 31°C and the TVD is greater than 800m.
Beg
Blueberry
Buick Creek
Rigel
Stoddart West
Siphon
Fort St John
Two Rivers
Brassey
Swan Lake
Cutbank
Blueberry-Two Rivers Aquifer
Effective CO2 Storage Potential
(% of TheoreticalCO2 Storage Potential)
P10 (0.5%) 110.2 Mt; P50 (2.0%) 440.6 Mt; P90 (5.4%) 1,189.6 Mt
Brassey-Cutbank Aquifer
Effective CO2 Storage Potential
(% of Theoretical CO2 StoragePotential)
P10 (0.5%) 23.9 Mt; P50 (2.0%) 95.7 Mt; P90 (5.4%) 258.4 Mt
CO2 Storage Pool Candidates*
CO2 Phase
Gas
Supercritical
Effective CO2 Storage Potential (Mt)
0.0 - 1.0
1.1 - 2.5
2.6 - 5.0
5.1 - 10.0
10.1 - 25.0
25.1 - 41.3
CO2 Storage Pool Non-Candidates
Beg-Siphon Aquifer
Supercritical
Blueberry-Two Rivers Aquifer
Supercritical
Brassey-Cutbank Aquifer
Supercritical
CO2 Storage Key Transitions
Pressure 7,500 kPa
Temperature 31°C
TVD 800m
*Pool storage candidates are depleted or nearly depleted pools whose TVDs are greater than 800m and/or are east of the Mesozoic deformation front.
NEBC Geological Carbon Capture and Storage Atlas
Nikanassin-Dunlevy Aquifer and Pool Candidates Effective CO2 Storage Potential
Filename: GBCS_NIKANASSIN_EFF_STORAGE_POTENTIAL
Figure
9.10
Author: A. Gibbs, J.Xie
Project: GBCS
Cartographer: C. Keeler
Created: 05-August-2022
Reviewer: M. Fockler
Last Edited: 30-November-2022
Copyright © 2022 Canadian Discovery Ltd. All Rights Reserved.
Geology
Nikanassin Erosional Edge (PRCL, 2021)
Mesozoic Deformation Front
0 5 10 20 30 40 50 Km
Projection:UTM Zone 10; Central Meridian -123; NAD 1983

Figure 9.10

Northeast BC Geological Carbon Capture and Storage Atlas

BALDONNEL-PARDONET FORMATION

Baldonnel-Pardonet Overview

Storage potential in the Baldonnel (and Pardonet, with which the Baldonnel is often commingled) *(figure 10.1)* occurs in the southern portion of the study area near Fort St. John and is proximal to many emitters and infrastructure. Favourability attributes are summarized in *table 10.1* with green and yellow circles indicating whether an attribute is considered generally favourable (green) or has risk and requires additional work (yellow). Both depleted pool reservoirs and saline aquifers are candidates and offer a range of storage opportunities. The top 10 depleted pools are shown in *figure 10.2*. *Figure 10.3* displays effective storage potential of the Baldonnel-Pardonet, as well as emitters and infrastructure in the NEBC study area.

Baldonnel-Pardonet Favourability Attributes		
Top 10 Depleted Pool Total Potential	156 Mt	● (green)
Aquifer Storage (P50)	184 Mt	● (green)
Regional Seal Potential	variable	● (yellow)
Lithology	Mixed carbonates	● (green)
Porosity	6-22%	● (green)
Permeability	10-1,000 mD	● (green)
Depth (TVD)	940-3,500m	● (green)
Net Reservoir Thickness	2-18m	● (green)

Table 10.1

10.1 Hydrostratigraphic Chart

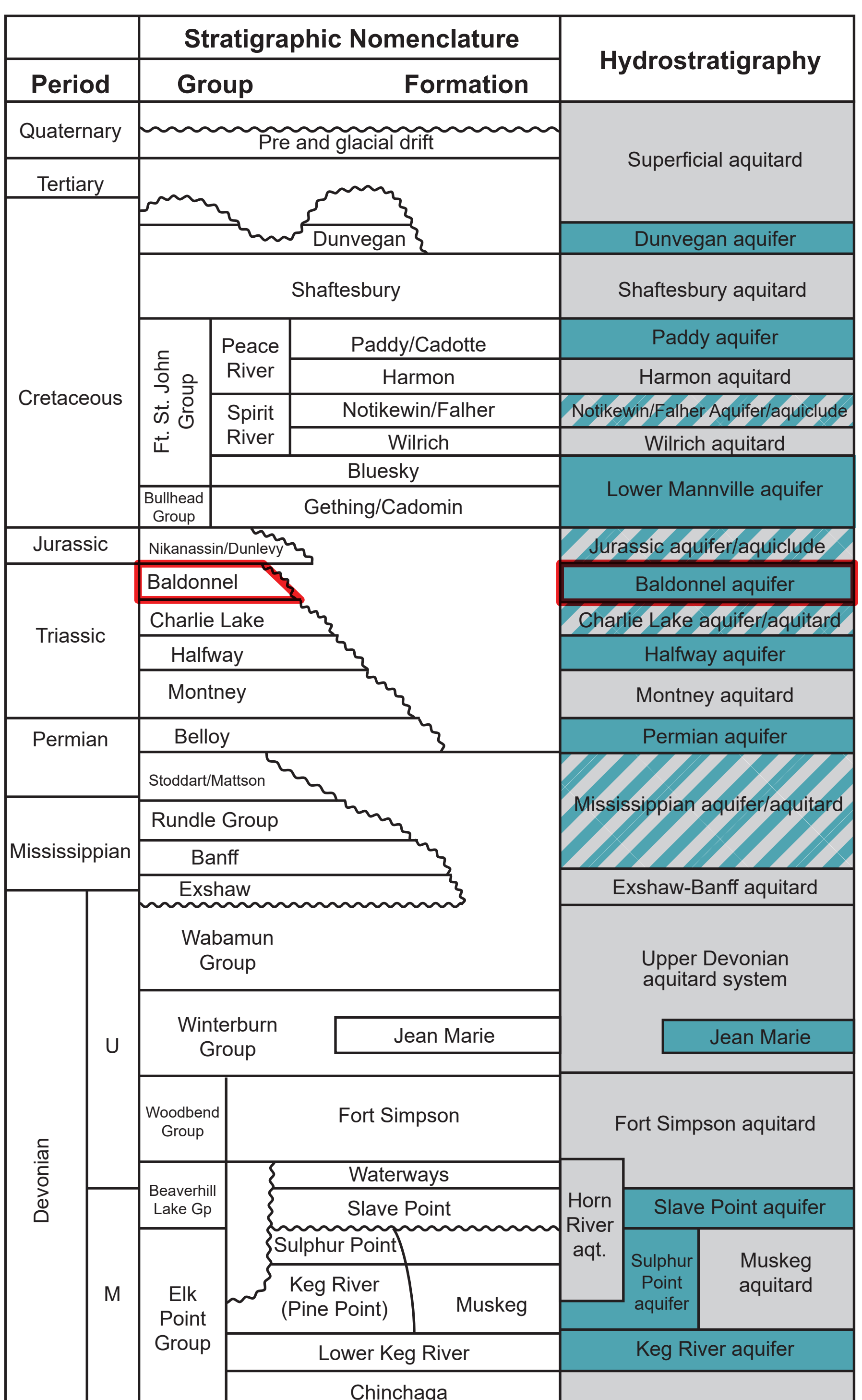

Modified from Bachu, 2006

 Figure 10.1

10.2 Top 10 Depleted Baldonnel-Pardonet Pools

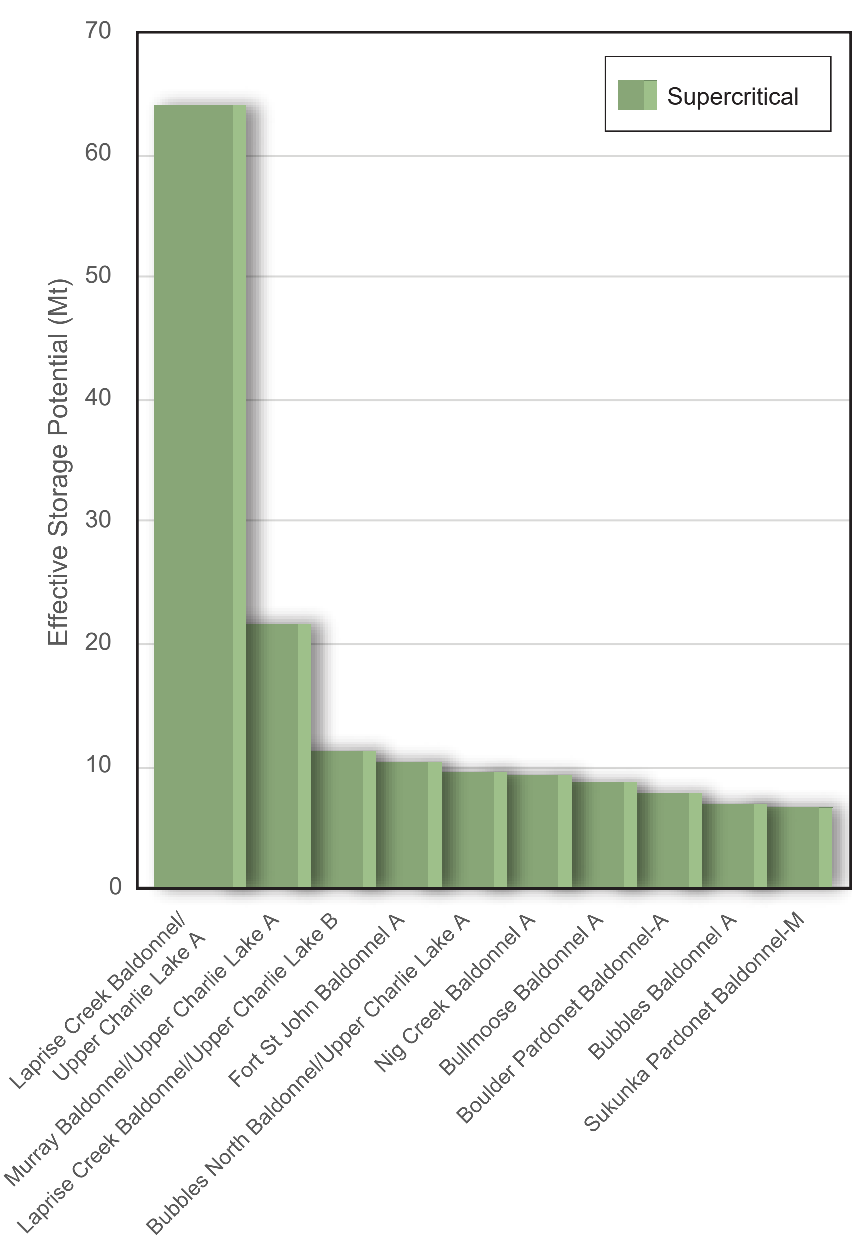

 Figure 10.2

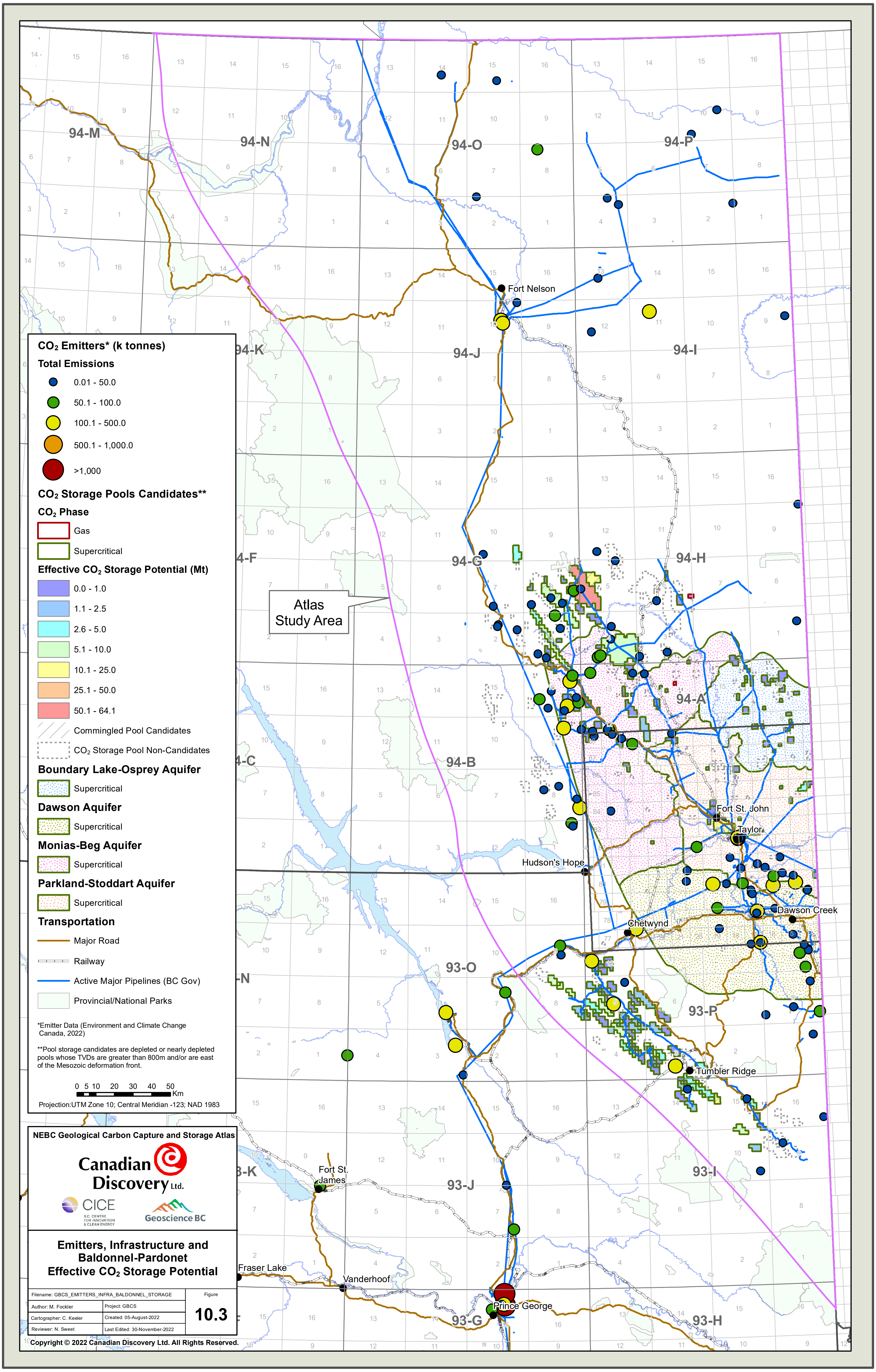

© Canadian Discovery Ltd.

Figure 10.3

10.4 Baldonnel-Pardonet Schematic Section

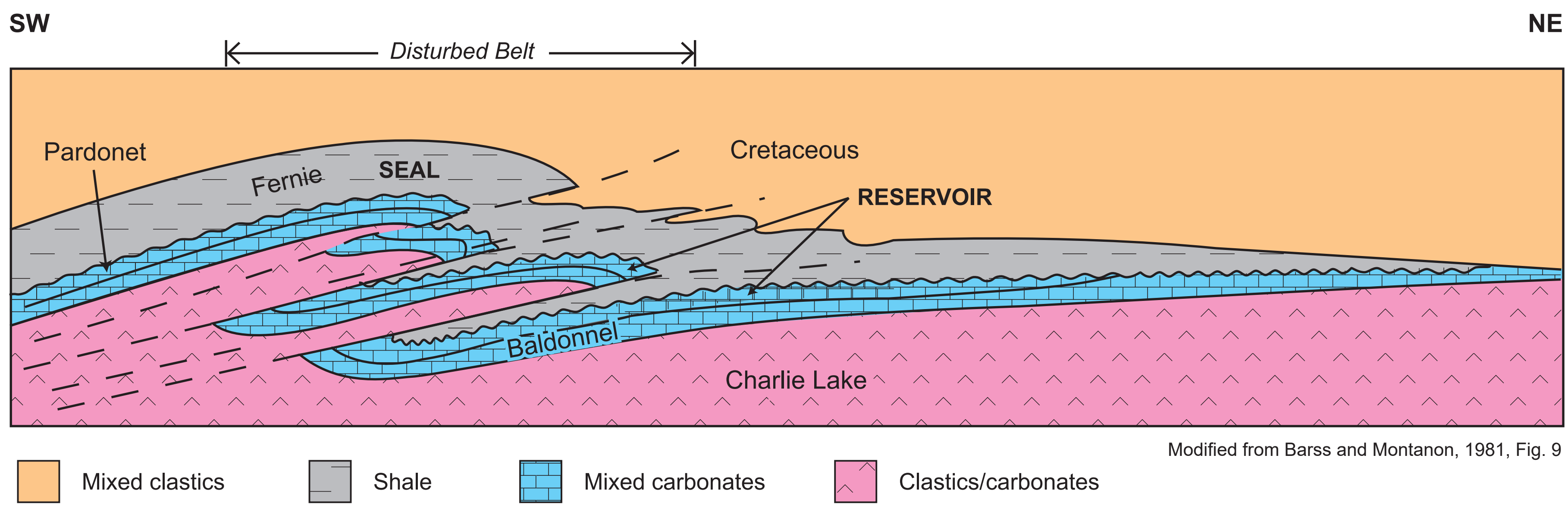

Figure 10.4

Storage Complex

The entire Upper Triassic storage complex comprises mixed lithologies that were deposited in an arid, shallow shelf environment. Baldonnel strata *(figure 10.4)* are widespread shallow marine to shelfal carbonates, deposited during a regional late Triassic transgression that drowned Charlie Lake arid coastline environments (Davies, 1997a). As described in the NEBC Play Atlas (2006), reservoir rocks are primarily dolomitized skeletal calcarenites, with considerable variation in reservoir quality arising from the interplay of depositional facies, diagenesis and structural overprint. The Baldonnel can be mapped continuously from the southern Deep Basin to a northern subcrop edge in 94G and 94H. The Pardonet is a deeper water limestone with localized porous reservoir and overlies the Baldonnel. The Baldonnel lies, more or less, conformably on the Charlie Lake, and the Pardonet (and Baldonnel east of the Pardonet subcrop edge) is unconformably overlain by Jurassic marine shale of the Nordegg and/or Fernie formations.

Unlike other formations, the Baldonnel-Pardonet evaluation extends southwest into the disturbed belt. As explained later in this chapter, pools in this area remain in the evaluation due to their proximity to Prince George, and some may provide carbon storage opportunities provided that additional mapping and risk assessment are done.

The Baldonnel structure map *(figure 10.5)* shows the topography of the top of the Baldonnel in the subsurface. Since the displacement of a CO_2 plume is governed by gravity and buoyancy, the plume tends to migrate up-structure during its injection period. The entire Baldonnel area is within supercritical conditions for CO_2 injection as the temperature and pressure exceed 31.1°C and 7,500 kPa, respectively.

Net reservoir maps are provided for the saline aquifers *(figure 10.6)* and depleted pools *(figure 10.7)*. These maps can help indicate the most favourable areas for CO_2 injection within storage reservoirs; i.e. where the reservoir rock has the highest quality and most often the highest porosity and permeability. The net reservoir contours within the pools were provided by the BC Oil and Gas Commission (BC OGC). Baldonnel net reservoir contours for the saline aquifers were not available from previous studies, therefore CDL did some very preliminary regional mapping for the aquifers in this zone using a 6% net reservoir cutoff using a limited number of wells (56) containing wet drillstem tests (DSTs). These maps should be considered to be very high level estimates and should be supported with more detailed mapping in future studies.

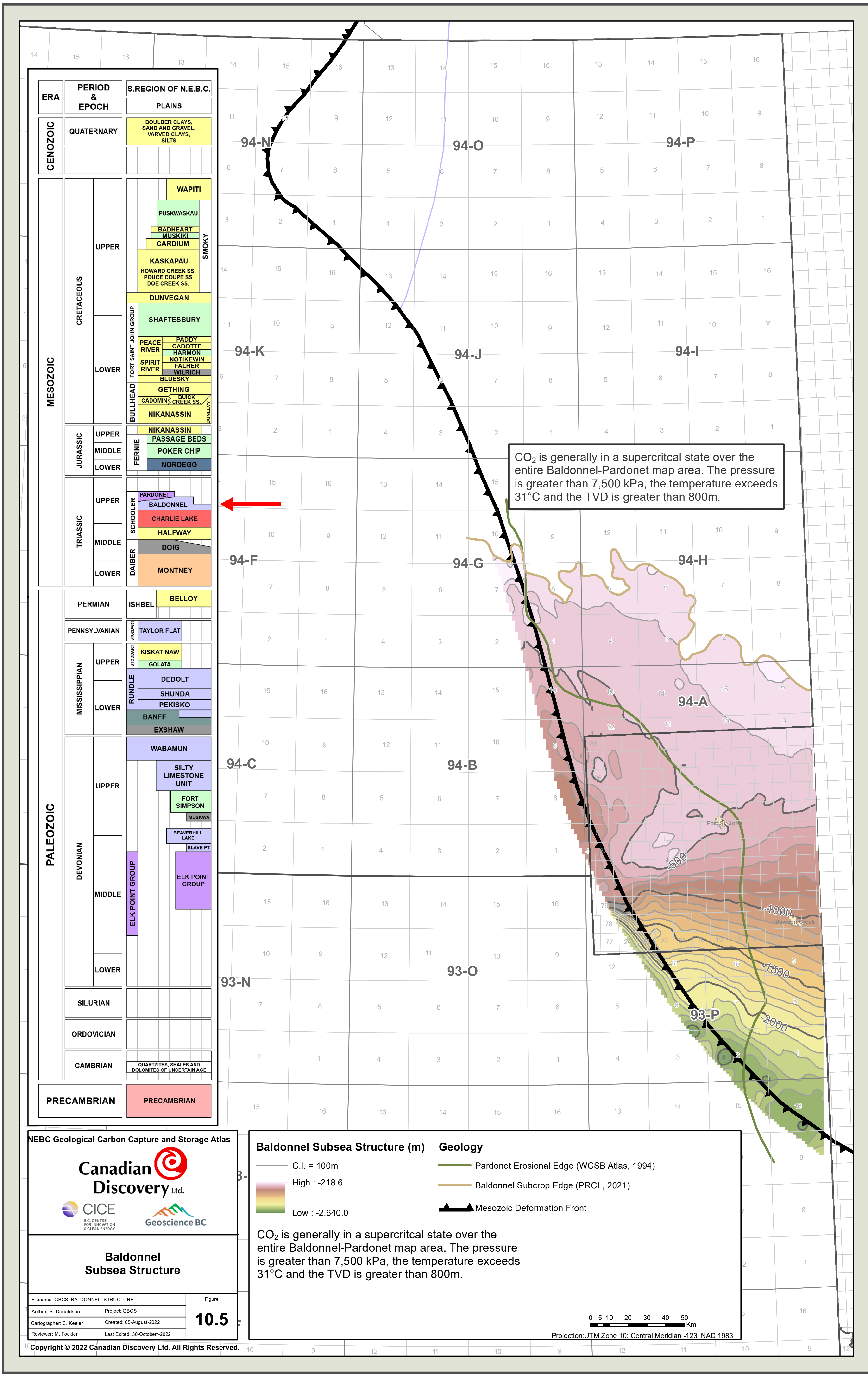

© Canadian Discovery Ltd. Figure 10.5

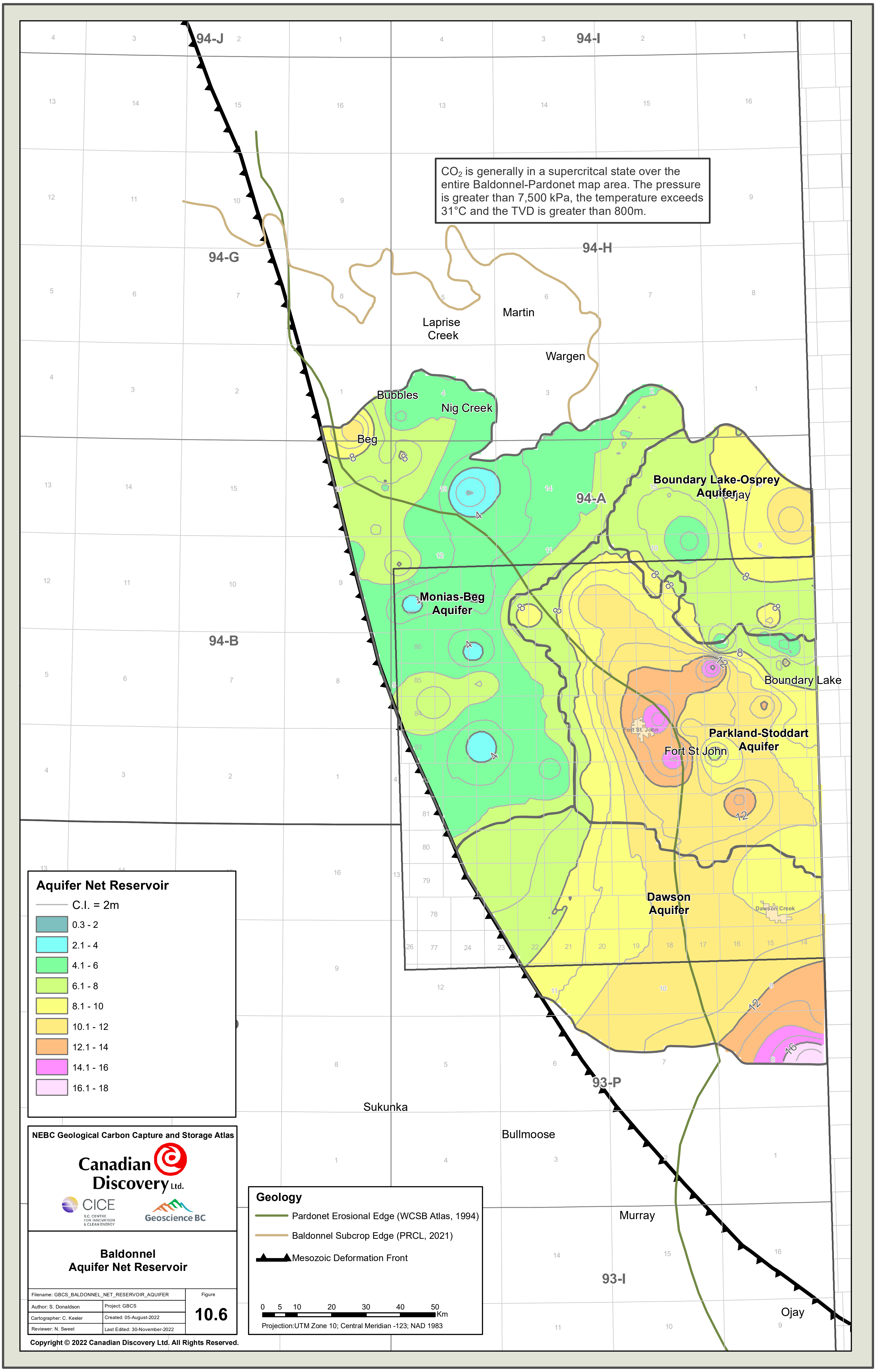

CO2 is generally in a supercritcal state over the entire Baldonnel-Pardonet map area. The pressure is greater than 7,500 kPa, the temperature exceeds 31°C and the TVD is greater than 800m.
94-J
94-I
94-G
94-H
94-A
94-B
93-P
93-I
Laprise Creek
Martin
Wargen
Bubbles
Nig Creek
Beg
Boundary Lake-Osprey Aquifer
Ojay
Monias-Beg Aquifer
Boundary Lake
Parkland-Stoddart Aquifer
Fort St John
Dawson Aquifer
Dawson Creek
Sukunka
Bullmoose
Murray
Aquifer Net Reservoir
C.I. = 2m
0.3 - 2
2.1 - 4
4.1 - 6
6.1 - 8
8.1 - 10
10.1 - 12
12.1 - 14
14.1 - 16
16.1 - 18
NEBC Geological Carbon Capture and Storage Atlas
Canadian Discovery Ltd.
CICE
Geoscience BC
Baldonnel Aquifer Net Reservoir
Filename: GBCS_BALDONNEL_NET_RESERVOIR_AQUIFER
Figure
Author: S. Donaldson
Project: GBCS
Cartographer: C. Keeler
Created: 05-August-2022
Reviewer: N. Sweet
Last Edited: 30-November-2022
10.6
Copyright © 2022 Canadian Discovery Ltd. All Rights Reserved.
Geology
Pardonet Erosional Edge (WCSB Atlas, 1994)
Baldonnel Subcrop Edge (PRCL, 2021)
Mesozoic Deformation Front
0 5 10 20 30 40 50 Km
Projection:UTM Zone 10; Central Meridian -123; NAD 1983

 Figure 10.6

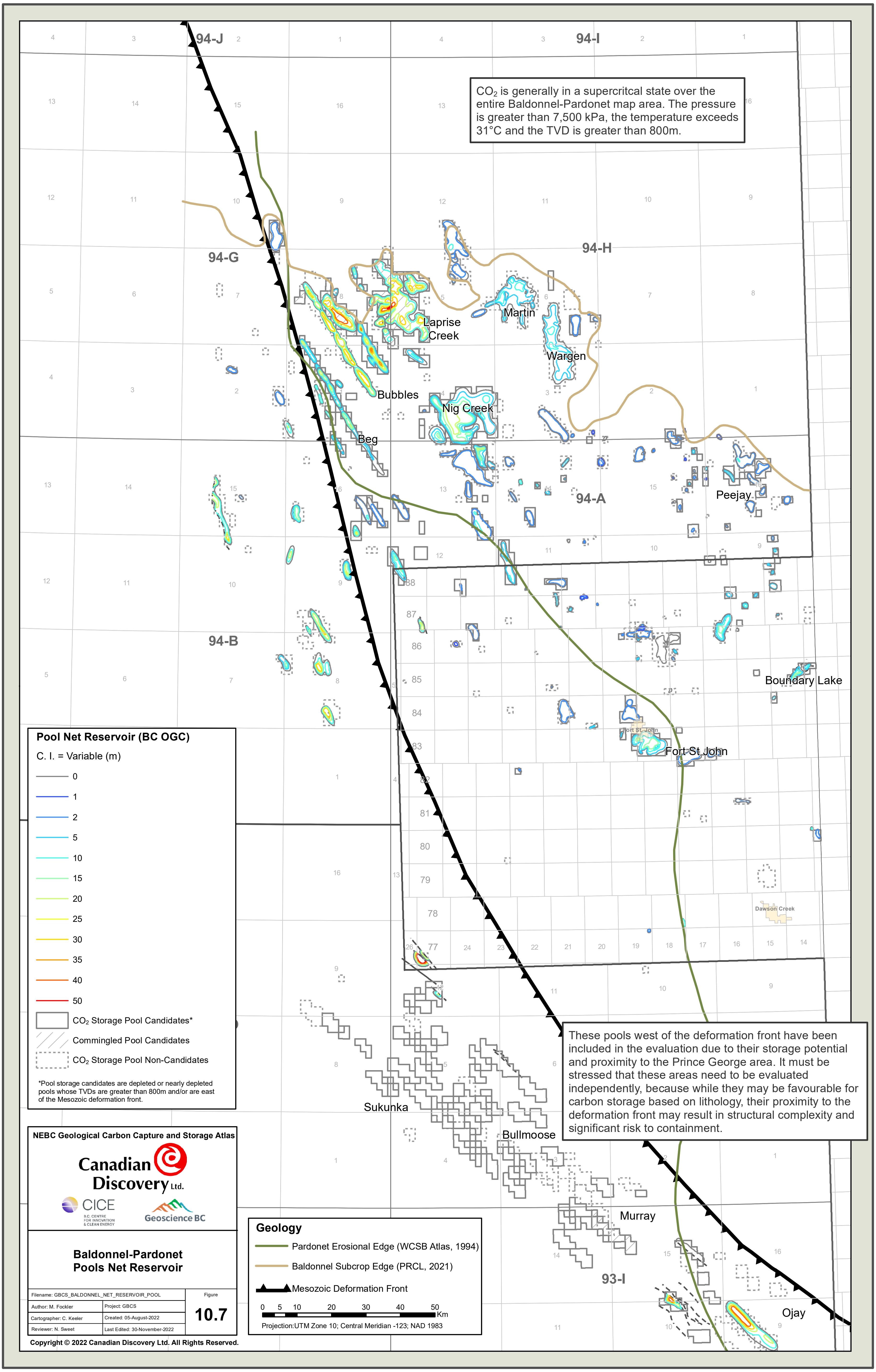

94-J
94-I
94-G
94-H
94-A
94-B
93-I
CO_2 is generally in a supercritcal state over the entire Baldonnel-Pardonet map area. The pressure is greater than 7,500 kPa, the temperature exceeds 31°C and the TVD is greater than 800m.
Laprise Creek
Martin
Wargen
Bubbles
Nig Creek
Beg
Peejay
Boundary Lake
Fort St John
Dawson Creek
Sukunka
Bullmoose
Murray
Ojay
These pools west of the deformation front have been included in the evaluation due to their storage potential and proximity to the Prince George area. It must be stressed that these areas need to be evaluated independently, because while they may be favourable for carbon storage based on lithology, their proximity to the deformation front may result in structural complexity and significant risk to containment.
Pool Net Reservoir (BC OGC)
C. I. = Variable (m)
0
1
2
5
10
15
20
25
30
35
40
50
CO_2 Storage Pool Candidates*
Commingled Pool Candidates
CO_2 Storage Pool Non-Candidates
*Pool storage candidates are depleted or nearly depleted pools whose TVDs are greater than 800m and/or are east of the Mesozoic deformation front.
NEBC Geological Carbon Capture and Storage Atlas
Canadian Discovery Ltd.
CICE
B.C. CENTRE FOR INNOVATION & CLEAN ENERGY
Geoscience BC
Baldonnel-Pardonet Pools Net Reservoir
Filename: GBCS_BALDONNEL_NET_RESERVOIR_POOL
Figure
10.7
Author: M. Fockler
Project: GBCS
Cartographer: C. Keeler
Created: 05-August-2022
Reviewer: N. Sweet
Last Edited: 30-November-2022
Copyright © 2022 Canadian Discovery Ltd. All Rights Reserved.
Geology
Pardonet Erosional Edge (WCSB Atlas, 1994)
Baldonnel Subcrop Edge (PRCL, 2021)
Mesozoic Deformation Front
0 5 10 20 30 40 50
Km
Projection:UTM Zone 10; Central Meridian -123; NAD 1983

Figure 10.7

Porosity-Permeability Correlations

Establishing detailed porosity trends requires examination of log suites and petrophysical models, which is beyond the scope of this phase of the Atlas. However, available core data can be used to provide a high level estimate of porosity trends, particularly within the aquifers, where this information is needed for storage potential estimates. Core data for the Baldonnel were obtained from geoLOGIC and filtered for better quality reservoir that is more conducive to carbon storage (greater than 6% porosity and 5 mD permeability) within the study area. These data were used to estimate porosity trends in the aquifers for storage calculations and to do a preliminary analysis of the multiple porosity-permeability trends that have been observed in the Baldonnel in past studies *(figure 10.8)*.

The carbonate nature of the Baldonnel results in a poor correlation between porosity and permeability as demonstrated by the cloud of data in *figure 10.8*. Overall, the best reservoir quality is found within the Parkland–Stoddart system (shown in yellow) with porosity and permeability averaging 13% and approximately 20 mD, respectively. However, there is a lot of scatter in the data, and values can reach greater than 20% porosity and over 1 darcy of permeability. Core data are sparse within the southern Dawson system, but in general, reservoir quality is better in the east (Parkland–Stoddart, Boundary Lake–Osprey and Dawson systems) than in the west (Monias–Beg system). The Baldonnel is shallower to the east so perhaps there has been less porosity destruction due to burial and compaction.

The Monias–Beg system exhibits the lowest porosities (often <10%) and thinnest reservoir, however some of the highest permeabilities are observed with several data points reaching 1000s of millidarcies of permeability. This may be due to preferential dolomitization or potential faulting and fracturing.

10.8 | Baldonnel-Pardonet Porosity-Permeability Plot

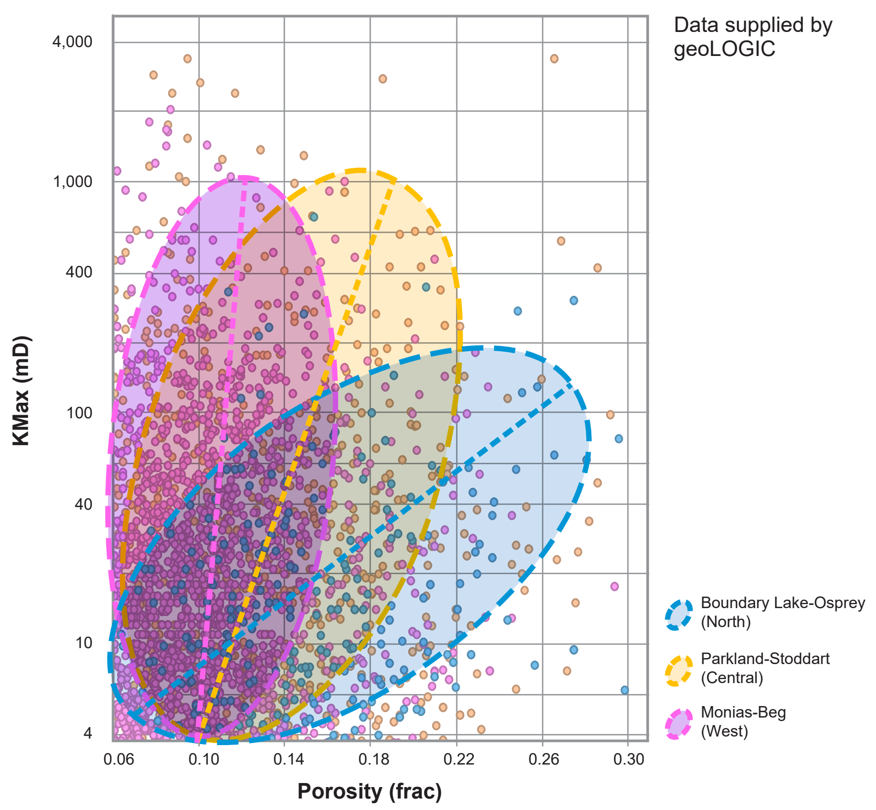

© Canadian Discovery Ltd. *Figure 10.8*

Hydrodynamics

To delineate the extent of the aquifers and understand the relationship between the aquifers and the depleted pools, a high-level analysis was done on Baldonnel hydrodynamics *(figure 10.9)* using Hydrofax drillstem test (DST) data from within the aquifers and the initial pressure and datum depth of each depleted pool from the BC OGC reserves databases.

Baldonnel aquifers are relatively continuous throughout the study area, however several areas can be differentiated by variations in reservoir quality and pressure. The Baldonnel was separated into four distinct aquifers, one in the west and three in the east. Reservoir quality (thickness and porosity) was the main criterion used to separate the east and west systems, and absolute pressure cutoffs were used to separate the north, central and southern aquifer systems in the east. The four aquifers can also be distinguished as separate systems on the pressure vs elevation graph *(figure 10.9)*. All four aquifers fall within the supercritical range for CO_2.

The western Monias–Beg system is the most areally extensive aquifer. It is characterized by thinner net aquifer reservoir (4–8m) that extends from Monias in the south to the Baldonnel subcrop edge in the north, where several large depleted pools occur in dominantly stratigraphic traps. The porosity in the aquifer averages 8–12% porosity, but due to the variability in reservoir quality, the permeability can range from 10s to 100s of millidarcies. Sweet spots occurring in tighter, higher-pressured reservoir in the west, such as Laprise Creek, Beg and Bubbles, and larger pools with slightly more connection to the aquifer such as Nig Creek should have relatively good containment from above, provided that distance is maintained from observed faulting. Pools at the northeastern edge of the Baldonnel near 94-H-05/06 — such as Martin, Wargen and Peejay — have lower pressures, which may indicate potential connectivity with the overlying Cretaceous.

The northeastern Boundary Lake–Osprey aquifer is the lowest pressured aquifer (8-10 MPa), likely due to its proximity to the Baldonnel subcrop edge and potential connection with Cretaceous units above. This connection may result in significant containment risk, and should be examined more thoroughly before pursuing a project in this area. Reservoir quality is generally good (porosity averages 14%), and there are a few small conventional pools that may offer potential for combined pool-aquifer storage opportunities.

The east-central Parkland–Stoddart aquifer has the best overall carbon storage potential with thick, high quality reservoir and moderate pressures (generally 10-14.5 MPa). There are several depleted pools within the region, including the Fort St. John pool, which may increase the overall storage potential of this system as a whole. However, the Fort St. John Graben is also present within this area, and the presence of faulting increases the risk of both potential leakage for carbon storage projects and potential for compartmentalization within the aquifer. These risks should be more closely evaluated before pursuing a project in this area.

10.9 Baldonnel-Pardonet Pressure vs Elevation Plot

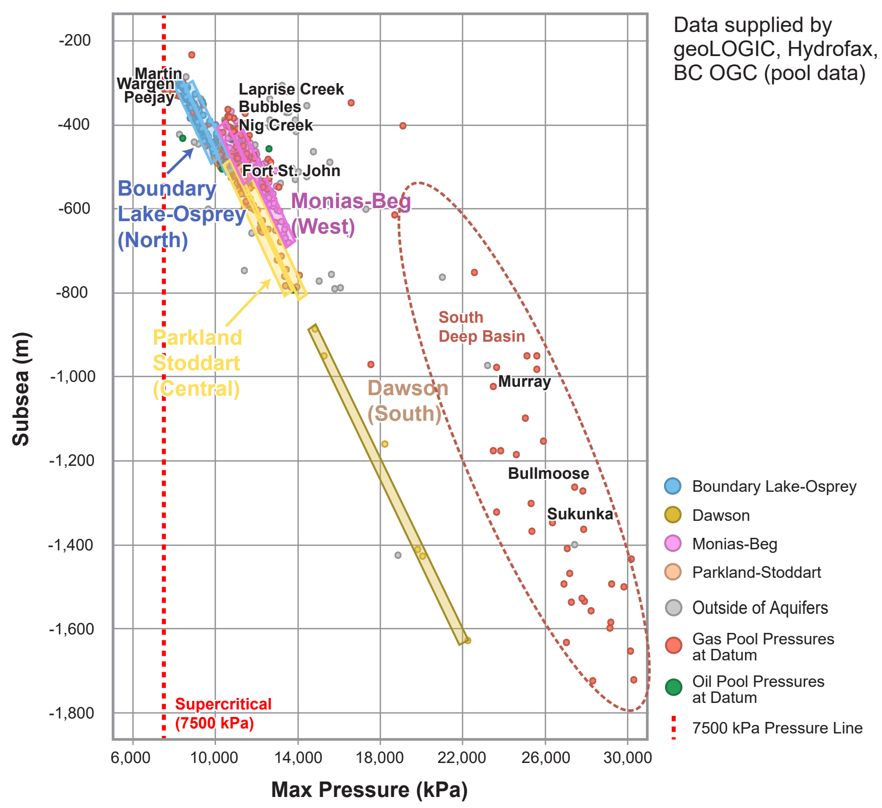

 Figure 10.9

Pressures drastically increase to the south into the Dawson (south) system, with pressures over 25 MPa in some areas. The high pressure and locally thick net reservoir in this system have led to the largest estimated carbon storage volumes of the four Baldonnel aquifer systems. However, there is a significant amount of uncertainty in estimates in this region as reservoir quality is very poorly defined due to a lack of core control. More work should be done in this area in future phases to better quantify its true potential.

There is also a population of higher-pressured Deep Basin pools south of the Baldonnel aquifers at Murray, Sukunka, and Bullmoose, to name a few. They have been included in the evaluation due to their storage potential and proximity to the Prince George area. It must be stressed that these areas need to be evaluated independently, as while they may be favourable for carbon storage based on lithology, their proximity to the deformation front may result in structural complexity and significant risk to containment.

In general, the Baldonnel is a high-quality target for carbon storage, particularly from an aquifer perspective, but additional mapping and more detailed analysis of reservoir quality should be completed to ensure containment and to locate reservoir sweet spots associated with preferential dolomitization.

Carbon Storage Calculations

Depleted and Nearly Depleted Pools

The top 25 depleted and nearly depleted pool candidates for carbon storage potential within the Baldonnel-Pardonet formations are shown in *Table 10.2*. Note that commingled Baldonnel-Charlie Lake pools were included in this Baldonnel evaluation; for the most part in these pools, the Baldonnel is much thicker than the Charlie Lake and hosts most of the perforations, and therefore production.

The BC OGC defines depleted pools as ones that have no remaining reserves or production. The BC OGC also recognizes that there are nearly depleted pools that could become CO_2 storage candidates in the (relatively) near future. The nearly depleted CO_2 storage candidates include pools where 90%+ of the reserves have been recovered, or no production has occurred in over five years. Furthermore, CDL has excluded pools that are shallower than 800m TVD. See Depleted Pools Selection Criteria in *Chapter 4* for a more thorough discussion.

In the table, the theoretical CO_2 storage potential represents the mass of CO_2 that can be stored in the hydrocarbon reservoirs assuming that the volume occupied previously by the produced gas will be occupied entirely by the injected CO_2. These calculations have been provided by the BC OGC and are based on historical pool production.

The effective CO_2 storage potential represents the mass of CO_2 that can be stored in hydrocarbon reservoirs after taking into account intrinsic reservoir characteristics and flow processes, such as heterogeneity (how much variability there is in the rock), aquifer support, sweep efficiency, gravity override, and CO_2 mobility (Bachu, 2006). The effective CO_2 storage potential is calculated by CDL and reduces the theoretical storage potential by as little as 13% and as much as 75%. More detail is provided on the carbon storage calculations for depleted pools in *Appendix B* and data are provided for all depleted pools included in this study in *Appendix C*.

The depleted and nearly depleted pools that are deemed to be CO_2 storage candidates by CDL are coloured by their effective storage potential mass on the summary map *(figure 10.10)*.

Note that there is a population of higher-pressured, Deep Basin pools to the east and south of the Baldonnel aquifers. These areas need to be evaluated independently, as while lithologically these pools may be favourable for carbon storage, their proximity to the deformation front may result in structural complexity and significant risk to containment. These pools remain in this evaluation as some of them are within trucking distance of Prince George and may provide carbon storage opportunities, provided more mapping and risk assessment is done.

Aquifers

The Baldonnel aquifer parameters are summarized in *Table 10.3*. Theoretical CO_2 storage potential can be calculated using the mapped pore volume of the reservoir and CO_2 density, and assumes that the pore volume will be occupied entirely by the injected CO_2. We know this is not the case however, since the pore space is already occupied by water and the water will need to be displaced in the process. As a result, a storage efficiency factor is introduced into storage potential calculations that accounts for the presence of both water and CO_2 in the aquifer. The storage efficiency factor is a function of reservoir and fluid properties and dynamics, including the geometry of the trap, gravity segregation, heterogeneity, permeability distribution and pressure, and may reduce the theoretical storage potential by 95 to 99%.

Aquifers considered favourable targets for CO_2 storage are indicated on the summary map *(figure 10.10)* and labelled with their estimated P10, P50 and P90 effective storage potential in Mt. More detail is provided on the aquifer carbon storage calculations in *Appendix B*.

Top 25 Depleted Baldonnel-Pardonet Pools

Pool Name	Pool Type	Well Count	Initial Pressure (kPa)	Temperature (˚C)	Average Porosity (%)	CO_2 Phase	Theoretical Storage Potential (Mt)	Effective Storage Potential (Mt)
Laprise Creek Baldonnel/ Upper Charlie Lake A	Gas	104	10,632	61	10.0	Supercritical	73.4	64.1
Murray Baldonnel/ Upper Charlie Lake A	Gas	4	22,567	59	4.6	Supercritical	24.9	21.7
Laprise Creek Baldonnel/ Upper Charlie Lake B	Gas	11	10,620	62	11.0	Supercritical	12.9	11.3
Fort St John Baldonnel A	Gas	16	11,149	49	12.0	Supercritical	11.9	10.4
Bubbles North Baldonnel/ Upper Charlie Lake A	Gas	27	10,903	65	8.1	Supercritical	10.8	9.5
Nig Creek Baldonnel A	Gas	58	11,252	61	10.5	Supercritical	36.5	9.1
Bullmoose Baldonnel A	Gas	2	27,434	62	5.2	Supercritical	9.8	8.6
Boulder Pardonet Baldonnel-A	Gas	1	25,126	71	6.2	Supercritical	8.9	7.8
Bubbles Baldonnel A	Gas	22	11,121	65	11.2	Supercritical	10.8	6.8
Sukunka Pardonet Baldonnel-M	Gas	2	25,370	69	5.7	Supercritical	7.6	6.7
Bullmoose West Pardonet Baldonnel-C	Gas	1	25,616	68	n/a	Supercritical	7.6	6.6
Boulder Pardonet Baldonnel-B	Gas	2	25,595	56	5.9	Supercritical	7.1	6.2
Grizzly South Baldonnel B	Gas	1	18,372	46	6.8	Supercritical	6.6	5.8
Beg Baldonnel A	Gas	31	11,583	59	7.6	Supercritical	9.2	5.8
Sukunka Pardonet Baldonnel-L	Gas	2	35,665	90	3.1	Supercritical	6.5	5.7
Brazion Pardonet Baldonnel-B	Gas	5	25,930	60	3.3	Supercritical	5.9	5.2
Bullmoose West Pardonet Baldonnel-D	Gas	4	25,050	65	4.6	Supercritical	5.6	4.9
Murray Baldonnel A	Gas	3	23,650	83	5.3	Supercritical	5.2	4.5
Boundary Lake Baldonnel B	Gas	12	10,046	47	11.4	Supercritical	4.2	3.6
Bullmoose Baldonnel C	Gas	2	27,888	78	3.7	Supercritical	4.1	3.6
Wolverine Pardonet Baldonnel-B	Gas	4	31,764	91	4.2	Supercritical	4.1	3.6
Murray Baldonnel B	Gas	2	23,650	83	5.6	Supercritical	3.9	3.4
Green Creek Baldonnel B	Gas	11	8,862	47	7.7	Supercritical	3.6	3.1
Fort St John Southeast Baldonnel A	Gas	8	11,363	48	18.0	Supercritical	3.2	2.8
Brazion Pardonet Baldonnel-A	Gas	3	29,829	80	4.6	Supercritical	4.3	2.7

© Canadian Discovery Ltd. Data supplied by BC OGC and Canadian Discovery Ltd. *Table 10.2*

Baldonnel-Pardonet Aquifer Properties and Storage Potential

Aquifer Name	Type	Thickness Range (m)	Pressure Range (MPa)	Temperature Range (°C)	Porosity Range (%)	CO_2 Phase	P10 Effective Storage Potential at 0.5% (Mt)	P50 Effective Storage Potential at 2% (Mt)	P90 Effective Storage Potential at 5.4% (Mt)
Boundary Lake - Osprey Regional System	Aquifer	5-12	8.1-10.0	46-60	8-15%	Supercritical	3.4	13.6	36.8
Dawson Regional System	Aquifer	6-18	11.8-28.9	40-103	8-14%	Supercritical	17.9	71.6	193.4
Monias-Beg Regional System	Aquifer	2-11	7.9-15.4	33-68	6-14%	Supercritical	9.2	36.7	99.0
Parkland-Stoddart Regional System	Aquifer	5-16	9.5-15.0	36-63	7-17%	Supercritical	15.6	62.3	168.2

Table 10.3

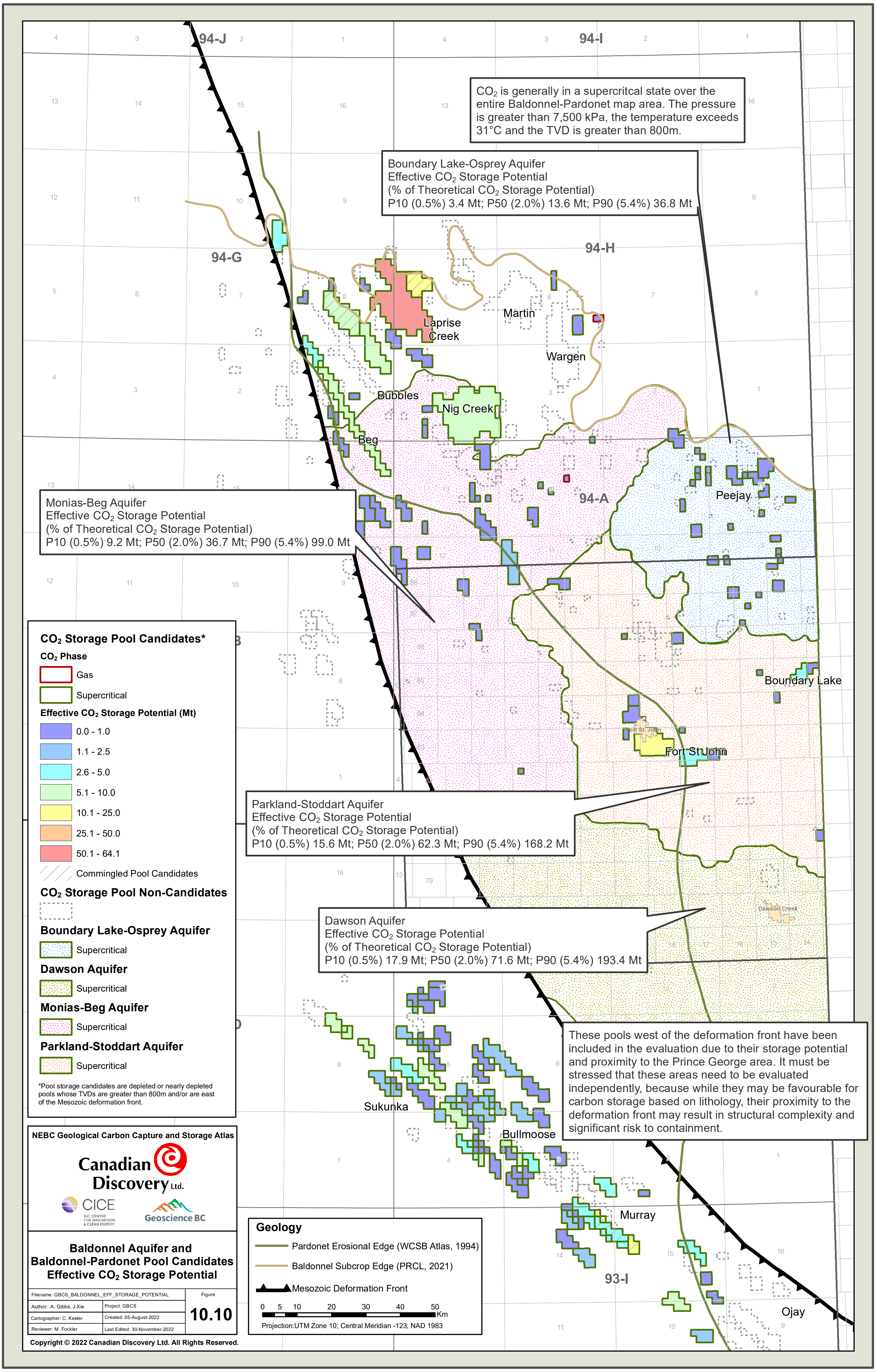

94-J
94-I
94-G
94-H
94-A
93-I
CO_2 is generally in a supercritcal state over the entire Baldonnel-Pardonet map area. The pressure is greater than 7,500 kPa, the temperature exceeds 31°C and the TVD is greater than 800m.
Boundary Lake-Osprey Aquifer
Effective CO_2 Storage Potential
(% of Theoretical CO_2 Storage Potential)
P10 (0.5%) 3.4 Mt; P50 (2.0%) 13.6 Mt; P90 (5.4%) 36.8 Mt
Laprise Creek
Martin
Wargen
Bubbles
Nig Creek
Beg
Peejay
Monias-Beg Aquifer
Effective CO_2 Storage Potential
(% of Theoretical CO_2 Storage Potential)
P10 (0.5%) 9.2 Mt; P50 (2.0%) 36.7 Mt; P90 (5.4%) 99.0 Mt
Boundary Lake
Fort St John
Parkland-Stoddart Aquifer
Effective CO_2 Storage Potential
(% of Theoretical CO_2 Storage Potential)
P10 (0.5%) 15.6 Mt; P50 (2.0%) 62.3 Mt; P90 (5.4%) 168.2 Mt
Dawson Aquifer
Effective CO_2 Storage Potential
(% of Theoretical CO_2 Storage Potential)
P10 (0.5%) 17.9 Mt; P50 (2.0%) 71.6 Mt; P90 (5.4%) 193.4 Mt
These pools west of the deformation front have been included in the evaluation due to their storage potential and proximity to the Prince George area. It must be stressed that these areas need to be evaluated independently, because while they may be favourable for carbon storage based on lithology, their proximity to the deformation front may result in structural complexity and significant risk to containment.
Sukunka
Bullmoose
Murray
Ojay
CO_2 Storage Pool Candidates*
CO_2 Phase
Gas
Supercritical
Effective CO_2 Storage Potential (Mt)
0.0 - 1.0
1.1 - 2.5
2.6 - 5.0
5.1 - 10.0
10.1 - 25.0
25.1 - 50.0
50.1 - 64.1
Commingled Pool Candidates
CO_2 Storage Pool Non-Candidates
Boundary Lake-Osprey Aquifer
Supercritical
Dawson Aquifer
Supercritical
Monias-Beg Aquifer
Supercritical
Parkland-Stoddart Aquifer
Supercritical
*Pool storage candidates are depleted or nearly depleted pools whose TVDs are greater than 800m and/or are east of the Mesozoic deformation front.
NEBC Geological Carbon Capture and Storage Atlas
Canadian Discovery Ltd.
CICE
Geoscience BC
Baldonnel Aquifer and Baldonnel-Pardonet Pool Candidates Effective CO_2 Storage Potential
Filename: GBCS_BALDONNEL_EFF_STORAGE_POTENTIAL
Figure
10.10
Author: A. Gibbs, J.Xie
Project: GBCS
Cartographer: C. Keeler
Created: 05-August-2022
Reviewer: M. Fockler
Last Edited: 30-November-2022
Copyright © 2022 Canadian Discovery Ltd. All Rights Reserved.
Geology
Pardonet Erosional Edge (WCSB Atlas, 1994)
Baldonnel Subcrop Edge (PRCL, 2021)
Mesozoic Deformation Front
0 5 10 20 30 40 50 Km
Projection:UTM Zone 10; Central Meridian -123; NAD 1983

Figure 10.10

Charlie Lake Formation

Charlie Lake Overview

Storage potential in the Charlie Lake *(figure 11.1)* occurs mainly in the Peace River area in the southern portion of the study area. Favourability attributes are summarized in *table 11.1* with green and yellow circles indicating whether an attribute is considered generally favourable (green) or has risk and requires additional work (yellow). Due to geological complexity, the aquifer potential of the Charlie Lake is difficult to map and assess, and is therefore not included for this phase of the Atlas. Depleted pools, while numerous, individually have limited storage opportunities, mostly due to the thinness of the reservoir. The top 10 depleted pools are shown in *figure 11.2*. *Figure 11.3* displays the effective storage potential of the Charlie Lake, as well as the emitters and infrastructure in the NEBC study area.

Charlie Lake Favourability Attributes

Top 10 Depleted Pool Total Potential	12 Mt	●
Aquifer Storage (P50)	n/a	
Regional Seal Potential	Variable	●
Lithology	Mixed	●
Porosity	8-20%	●
Permeability	n/a	
Depth (TVD)	1,050-2,600m	●
Net Reservoir Thickness	2-15m	●

Table 11.1

11.1 Hydrostratigraphic Chart

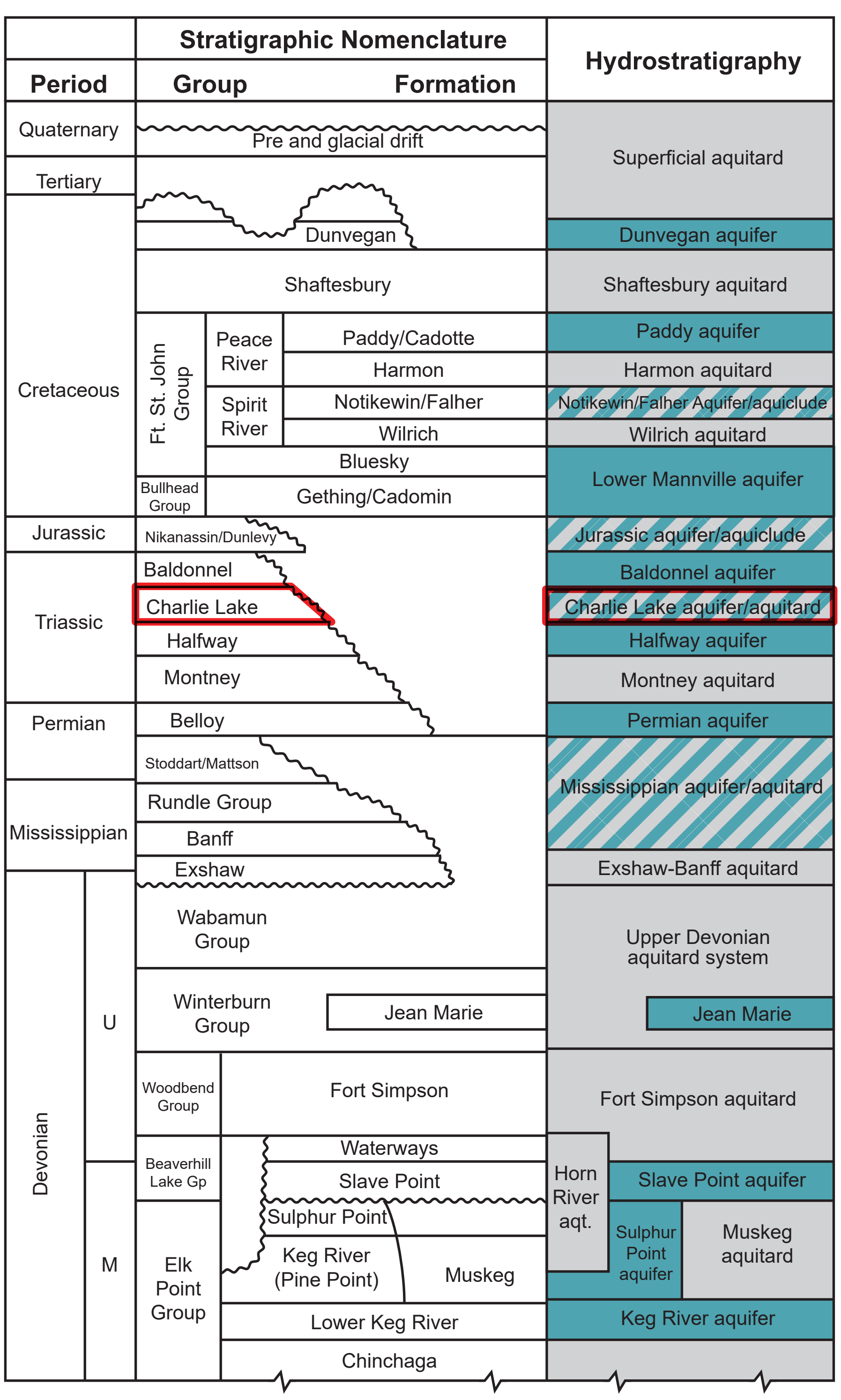

Figure 11.1

11.2 Top 10 Depleted Charlie Lake Pools

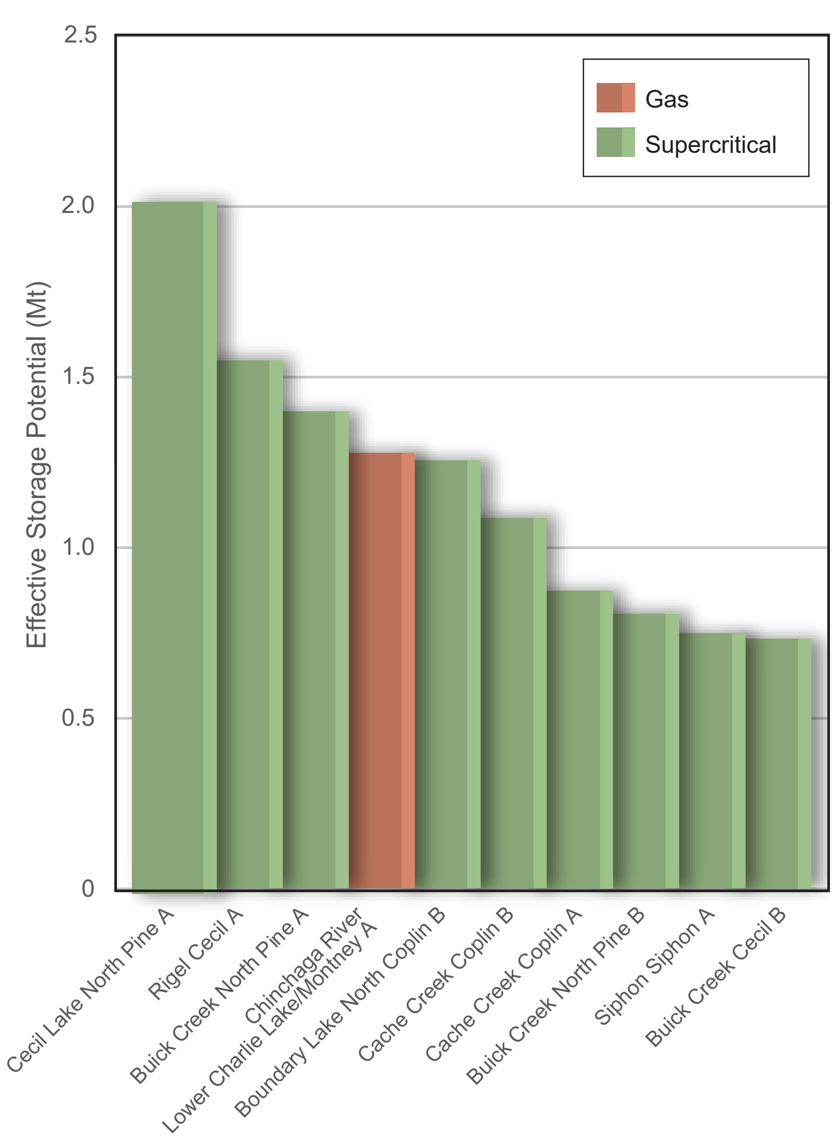

Figure 11.2

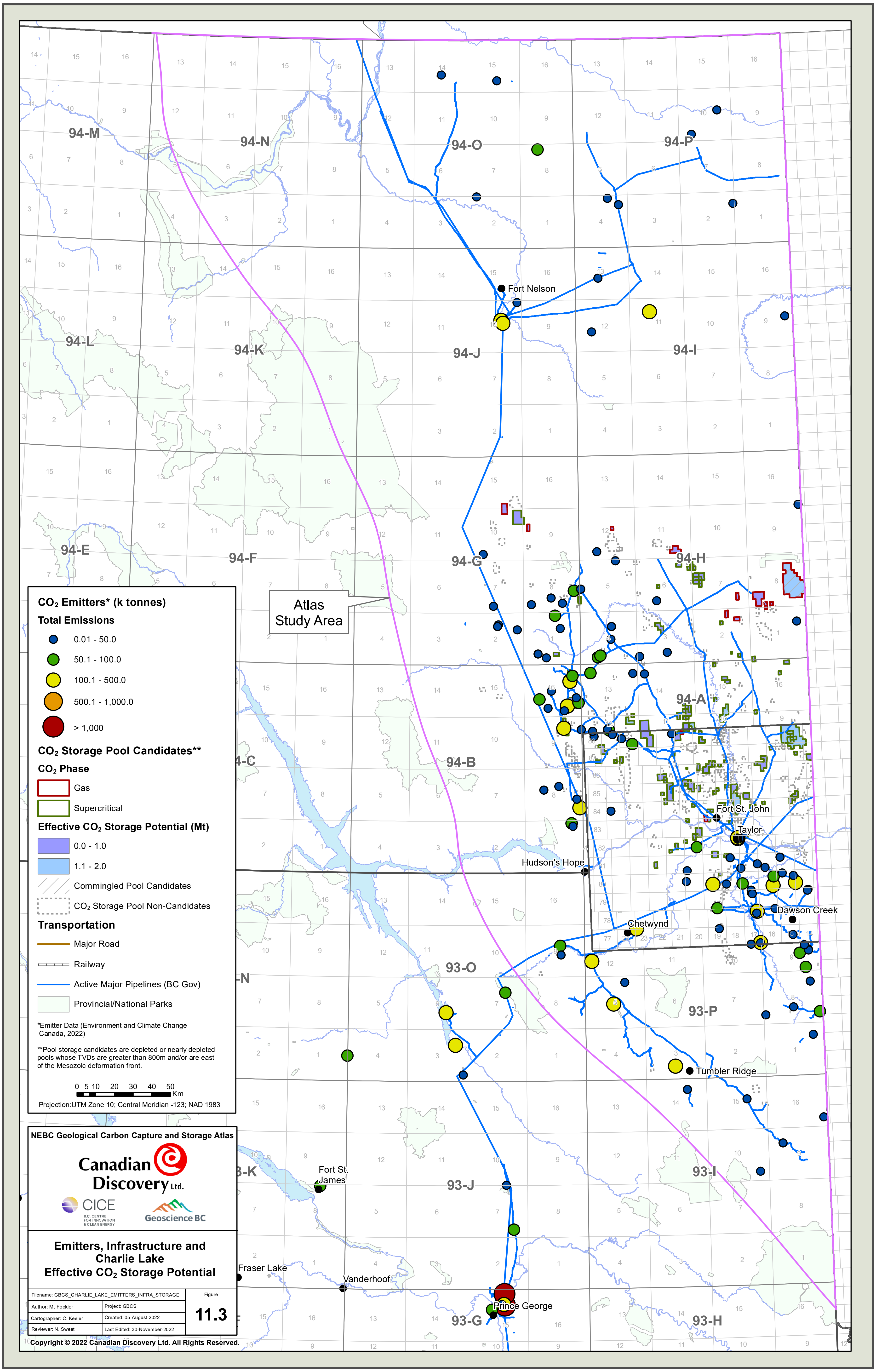

© Canadian Discovery Ltd.

Figure 11.3

11.4 Charlie Lake Play Schematic

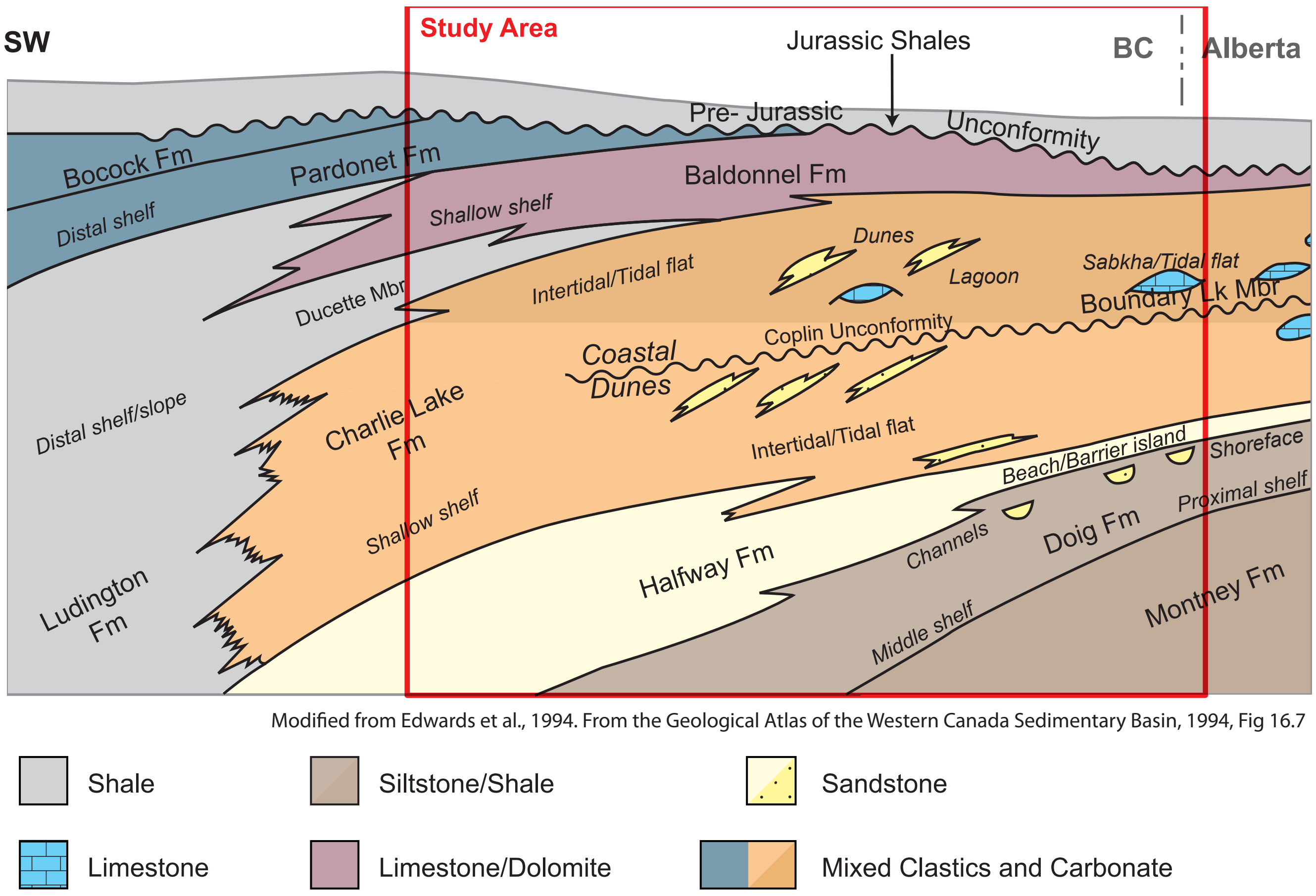

Modified from Edwards et al., 1994. From the Geological Atlas of the Western Canada Sedimentary Basin, 1994, Fig 16.7

Figure 11.4

Storage Complex

The Charlie Lake comprises a thick succession of interbedded siliciclastic, carbonate and evaporitic rocks that were deposited at the culmination of a major transgressive-regressive (sea level rise and fall) cycle encompassing the Doig, Halfway and Charlie Lake *(figure 11.4)*. Reservoir units include very fine- to medium-grained sandstone, deposited in arid coastline to shallow marine settings, and crystalline to skeletal limestone and dolostone, primarily of shallow marine origin (Edwards, 1994). Stratigraphic markers can be correlated regionally in the Charlie Lake, reflecting very widespread, low-relief deposition, although reservoir units tend to be thin and discontinuous. Several internal unconformity surfaces can also be traced throughout NEBC and one of these, the Coplin unconformity, serves as the boundary between the Lower and Upper Charlie Lake. It progressively truncates all Lower Charlie Lake members, as well as the Halfway, Doig, and Montney, in a northeasterly direction and thus records a major Late Triassic tectonic and erosional event (Davies, 1997b). The Charlie Lake is overlain by the Baldonnel Formation. The contact is locally disconformable, but can be difficult to identify consistently on logs because of lithological similarities between the two units.

Lower Charlie Lake sandstone and carbonate reservoirs occur below the Coplin unconformity. Like the Upper Charlie Lake, they consist of thin arid coastline to shallow marine sandstone and shallow to restricted marine carbonates, occurring in highly-correlative stratigraphic successions. The Lower Charlie Lake contact with the underlying Halfway Formation is generally sharp in the east, but assumes a more interfingering nature to the west as the Lower Charlie Lake succession becomes sandier, and grades to more homogeneous marine facies (NEBC Play Atlas, 2006).

Net reservoir maps are provided for the depleted pools *(figure 11.5)*. These maps can help indicate the most favourable areas for CO_2 injection within storage reservoirs; i.e. where the reservoir rock has the highest quality and most often the highest porosity and permeability. The net reservoir contours within the pools were provided by the BC Oil and Gas Commission (BC OGC). Charlie Lake reservoirs host both oil and gas in NEBC, and those with greater than 20% oil production have been removed from this analysis. Individual Charlie Lake pools tend to be thin (generally less than 7m, except at Tommy Lakes on the northwest edge of the play) and areally small, reflecting low-relief environments of deposition and truncation by unconformities. Tight evaporitic facies provide effective seals throughout the formation.

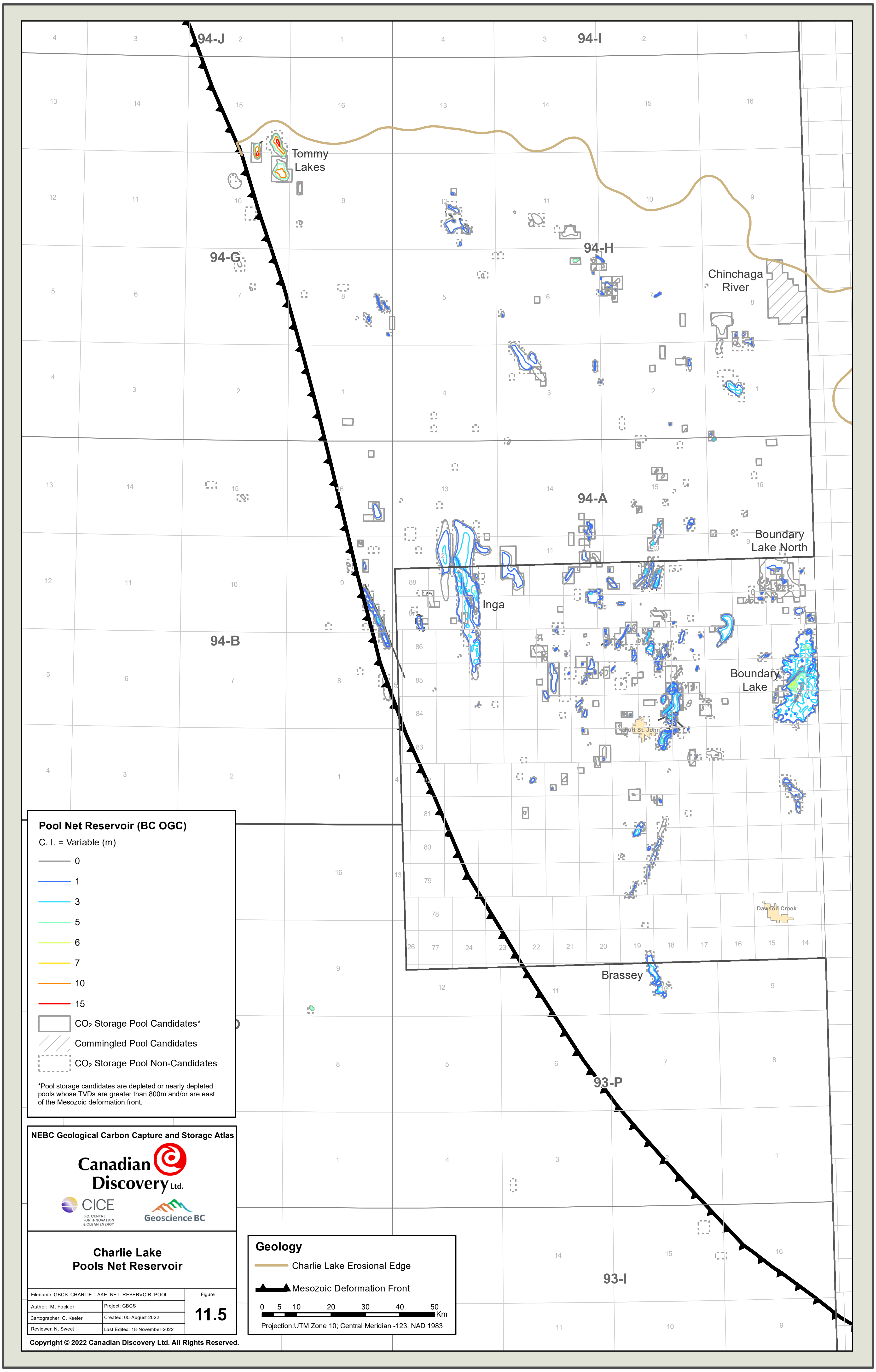

94-J
94-I
94-G
94-H
94-A
94-B
93-P
93-I
Tommy Lakes
Chinchaga River
Boundary Lake North
Inga
Boundary Lake
Fort St. John
Dawson Creek
Brassey
Pool Net Reservoir (BC OGC)
C. I. = Variable (m)
0
1
3
5
6
7
10
15
CO_2 Storage Pool Candidates*
Commingled Pool Candidates
CO_2 Storage Pool Non-Candidates
*Pool storage candidates are depleted or nearly depleted pools whose TVDs are greater than 800m and/or are east of the Mesozoic deformation front.
NEBC Geological Carbon Capture and Storage Atlas
Canadian Discovery Ltd.
CICE
B.C. CENTRE FOR INNOVATION & CLEAN ENERGY
Geoscience BC
Charlie Lake
Pools Net Reservoir
Filename: GBCS_CHARLIE_LAKE_NET_RESERVOIR_POOL
Figure
11.5
Author: M. Fockler
Project: GBCS
Cartographer: C. Keeler
Created: 05-August-2022
Reviewer: N. Sweet
Last Edited: 18-November-2022
Copyright © 2022 Canadian Discovery Ltd. All Rights Reserved.
Geology
Charlie Lake Erosional Edge
Mesozoic Deformation Front
0 5 10 20 30 40 50 Km
Projection:UTM Zone 10; Central Meridian -123; NAD 1983

Figure 11.5

Carbon Storage Calculations

Depleted and Nearly Depleted Pools

The top 25 depleted and nearly depleted pool candidates for carbon storage potential within the Charlie Lake Formation are shown in *table 11.2*.

The BC OGC defines depleted pools as ones that have no remaining reserves or production. The BC OGC also recognizes that there are nearly depleted pools that could become CO_2 storage candidates in the (relatively) near future. The nearly depleted CO_2 storage candidates include pools where 90%+ of the reserves have been recovered, or no production has occurred in over five years. Furthermore, CDL has excluded pools that are shallower than 800m TVD, or are west of the Mesozoic deformation front. See Depleted Pools Selection Criteria in *Chapter 4* for a more thorough discussion.

The theoretical CO_2 storage potential represents the mass of CO_2 that can be stored in the hydrocarbon reservoirs assuming that the volume occupied previously by the produced gas will be occupied entirely by the injected CO_2. These calculations have been provided by the BC OGC and are based on historical pool production.

The effective CO_2 storage potential represents the mass of CO_2 that can be stored in hydrocarbon reservoirs after taking into account intrinsic reservoir characteristics and flow processes, such as heterogeneity (how much variability there is in the rock), aquifer support, sweep efficiency, gravity override, and CO_2 mobility (Bachu, 2006). The effective CO_2 storage potential is calculated by CDL and reduces the theoretical storage potential by as little as 13% and as much as 75%. More detail is provided on the carbon storage calculations for depleted pools in *Appendix B*, and data are provided for all depleted pools included in this study in *Appendix C*.

The depleted and nearly depleted pools that are deemed to be CO_2 storage candidates by CDL are coloured by their effective storage potential mass on the summary map *(figure 11.6)*.

Aquifers

Due to geological complexity, the aquifer potential of the Charlie Lake is difficult to map and assess, and is therefore not included for this phase of the Atlas.

Top 25 Depleted Charlie Lake Pools

Pool Name	Pool Type	Well Count	Initial Pressure (kPa)	Temperature (˚C)	Average Porosity (%)	CO_2 Phase	Theoretical Storage Potential (Mt)	Effective Storage Potential (Mt)
Cecil Lake North Pine A	Gas	16	13,381	54	13.1	Supercritical	4.2	2.0
Rigel Cecil A	Gas	9	11,332	59	12.6	Supercritical	1.8	1.6
Buick Creek North Pine A	Gas	3	12,701	53	10.7	Supercritical	1.6	1.4
Chinchaga River Lower Charlie Lake/Montney A	Gas	169	6,602	49	15.6	Gas	5.1	1.3
Boundary Lake North Coplin B	Gas	37	9,880	57	10.3	Supercritical	1.4	1.3
Cache Creek Coplin B	Gas	2	15,886	57	7.8	Supercritical	1.3	1.1
Cache Creek Coplin A	Gas	17	15,842	57	19.1	Supercritical	3.5	0.9
Buick Creek North Pine B	Gas	2	12,701	53	13.3	Supercritical	0.9	0.8
Siphon Siphon A	Gas	7	10,678	54	12.4	Supercritical	1.2	0.7
Buick Creek Cecil B	Gas	5	10,684	54	14.6	Supercritical	0.8	0.7
Red Creek Bear Flat A	Gas	5	12,169	53	9.9	Supercritical	0.8	0.7
Montney North Pine A	Gas	4	12,792	57	14.7	Supercritical	0.8	0.7
North Pine North Pine B	Gas	3	13,355	56	10.2	Supercritical	1.2	0.6
Fort St John Southeast Siphon A	Gas	5	11,873	49	13.2	Supercritical	0.6	0.5
Boundary Lake Coplin A	Gas	4	10,257	54	11.5	Supercritical	0.6	0.5
Flatrock Siphon A	Gas	2	11,445	53	11.4	Supercritical	0.5	0.4
Velma A Marker/Base Of Lime A	Gas	4	6,860	54	17.5	Gas	0.4	0.4
Stoddart West Bear Flat B	Gas	2	13,547	62	n/a	Supercritical	0.4	0.3
Tommy Lakes Artex/Halfway A	Gas	14	7,524	53	9.9	Supercritical	0.4	0.3
Halfway Coplin A	Gas	3	14,153	54	13.6	Supercritical	0.3	0.3
Boundary Lake Basal Boundary A	Gas	2	11,825	48	20.0	Supercritical	0.3	0.3
Other Areas North Pine 11-26-084-20-W6M	Gas	1	14,090	55	7.8	Supercritical	0.3	0.2
Buick Creek Cecil A	Gas	3	10,818	54	13.0	Supercritical	0.3	0.2
Stoddart West North Pine C	Gas	1	12,715	53	11.2	Supercritical	0.3	0.2
Eagle West Cecil A	Gas	1	12,700	52	10.2	Supercritical	0.2	0.2

Table 11.2

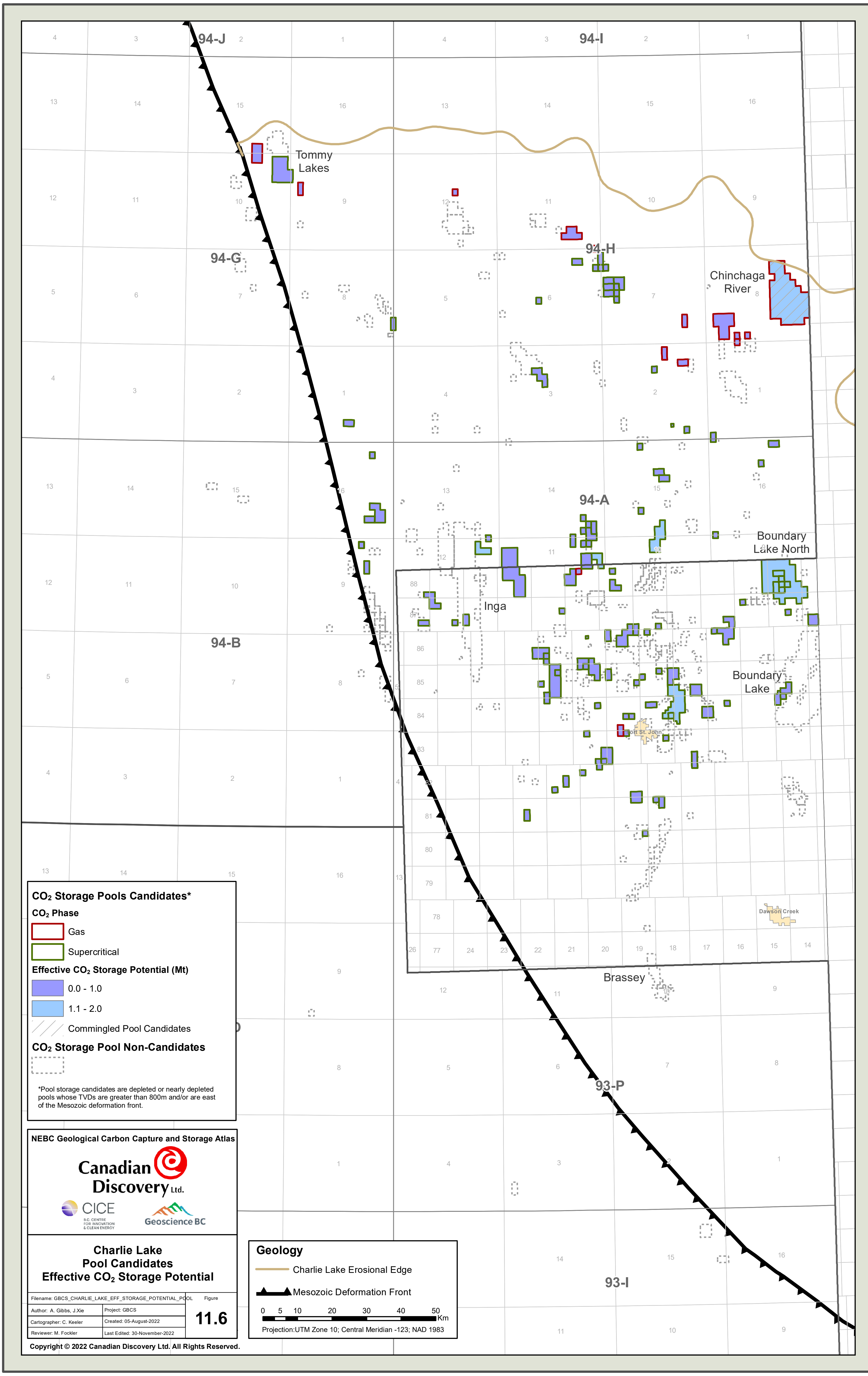

© Canadian Discovery Ltd.

Figure 11.6

HALFWAY FORMATION

Halfway Overview

Storage potential in the Halfway *(figure 12.1)* occurs in the southern portion of the study area near Fort St John and is proximal to many emitters and infrastructure. Favourability attributes are summarized in *table 12.1* with green and yellow circles indicating whether an attribute is considered generally favourable (green) or has risk and requires additional work (yellow). Both depleted pool reservoirs and saline aquifers are candidates and offer a range of storage opportunities. The top 10 depleted pools are shown in *figure 12.2*. *Figure 12.3* displays the effective storage potential of the Halfway, as well as emitters and infrastructure in the NEBC study area.

Halfway Favourability Attributes		
Top 10 Depleted Pool Total Potential	131 Mt	● (green)
Aquifer Storage (P50)	99 Mt	● (green)
Regional Seal Potential	Variable	● (yellow)
Lithology	Sandstone	● (green)
Porosity	8-30%	● (green)
Permeability	10-2,000 mD	● (green)
Depth (TVD)	900-3,600m	● (green)
Net Reservoir Thickness	2-50m	● (green)

Table 12.1

12.1 Hydrostratigraphic Chart

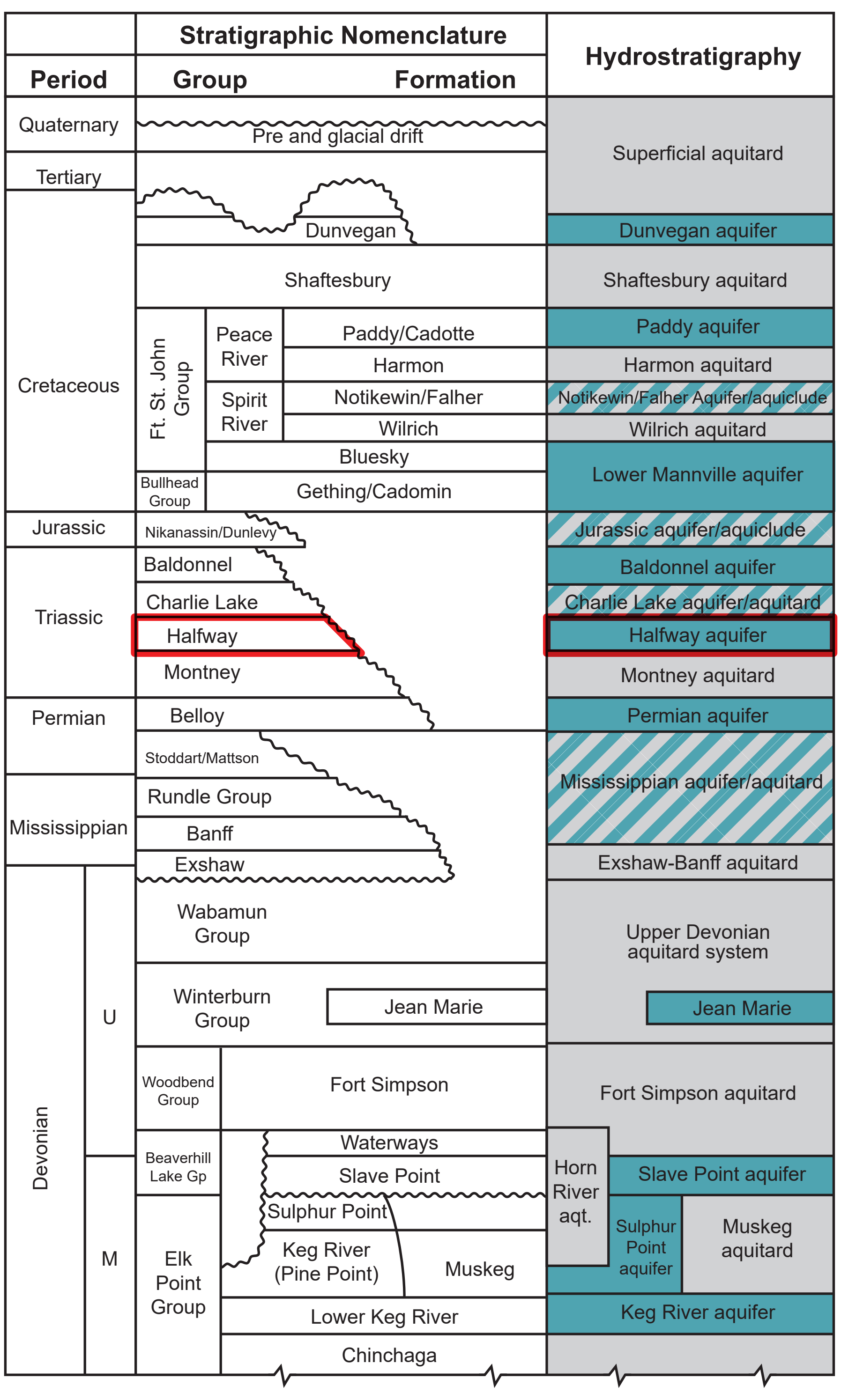

 Figure 12.1

12.2 Top 10 Depleted Halfway Pools

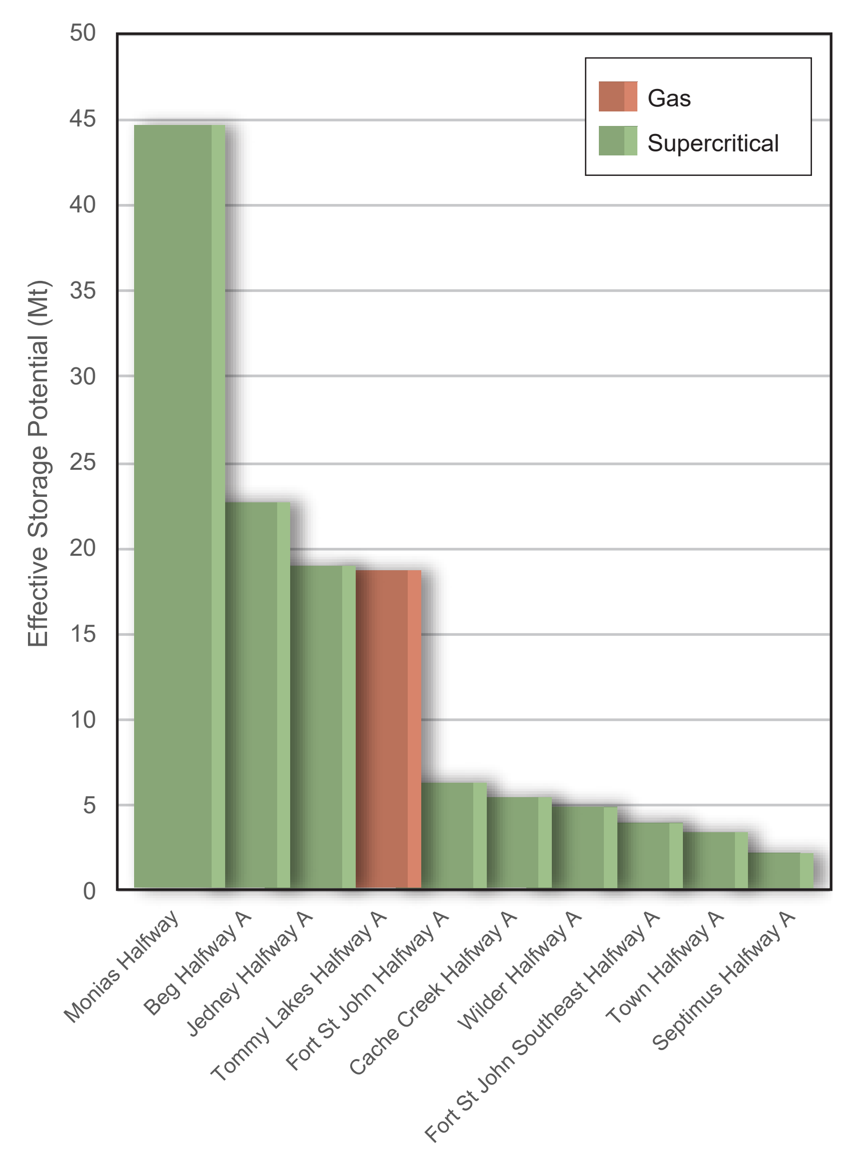

 Figure 12.2

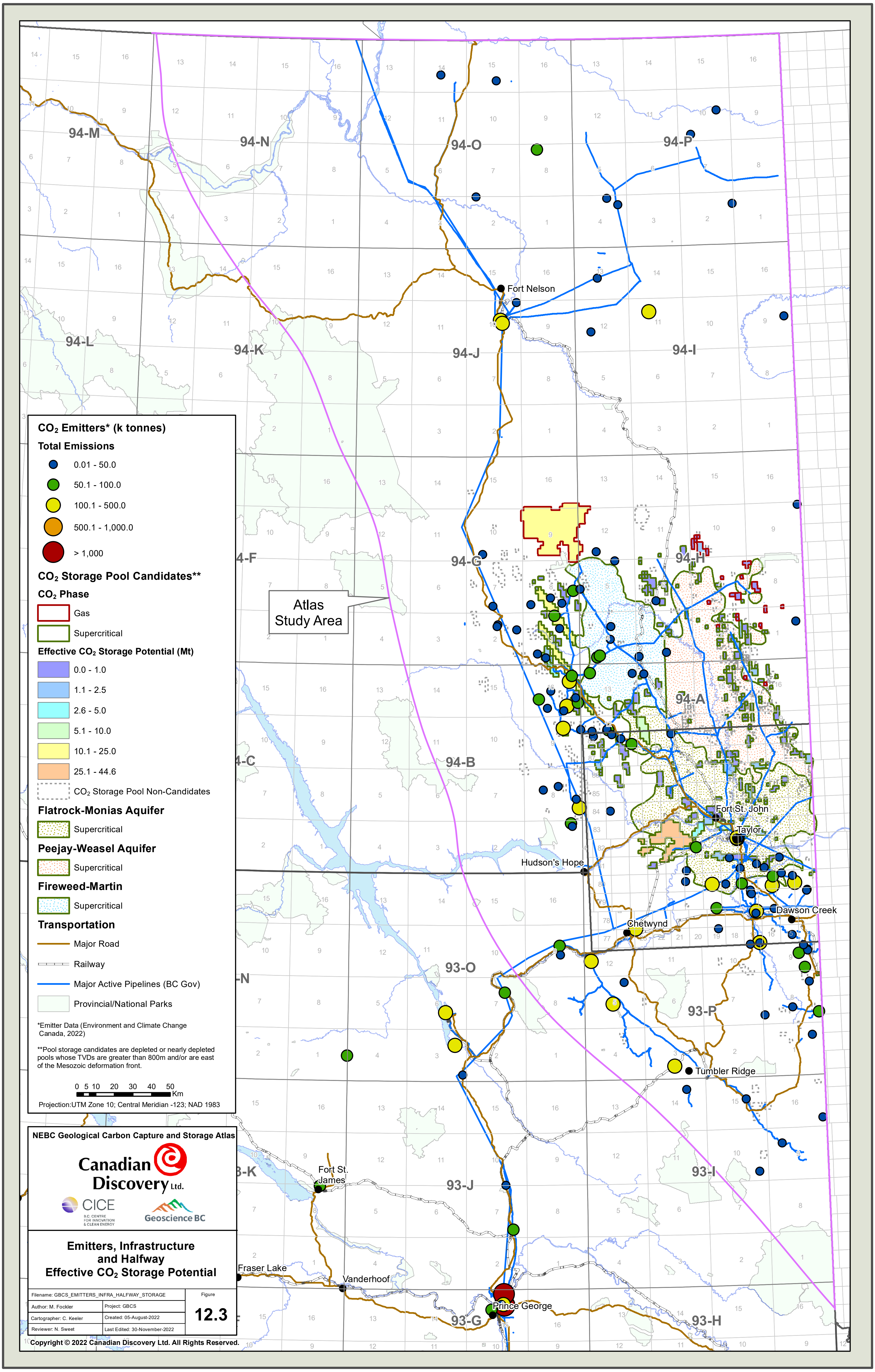

© Canadian Discovery Ltd.

Figure 12.3

12.4 Halfway Play Schematic

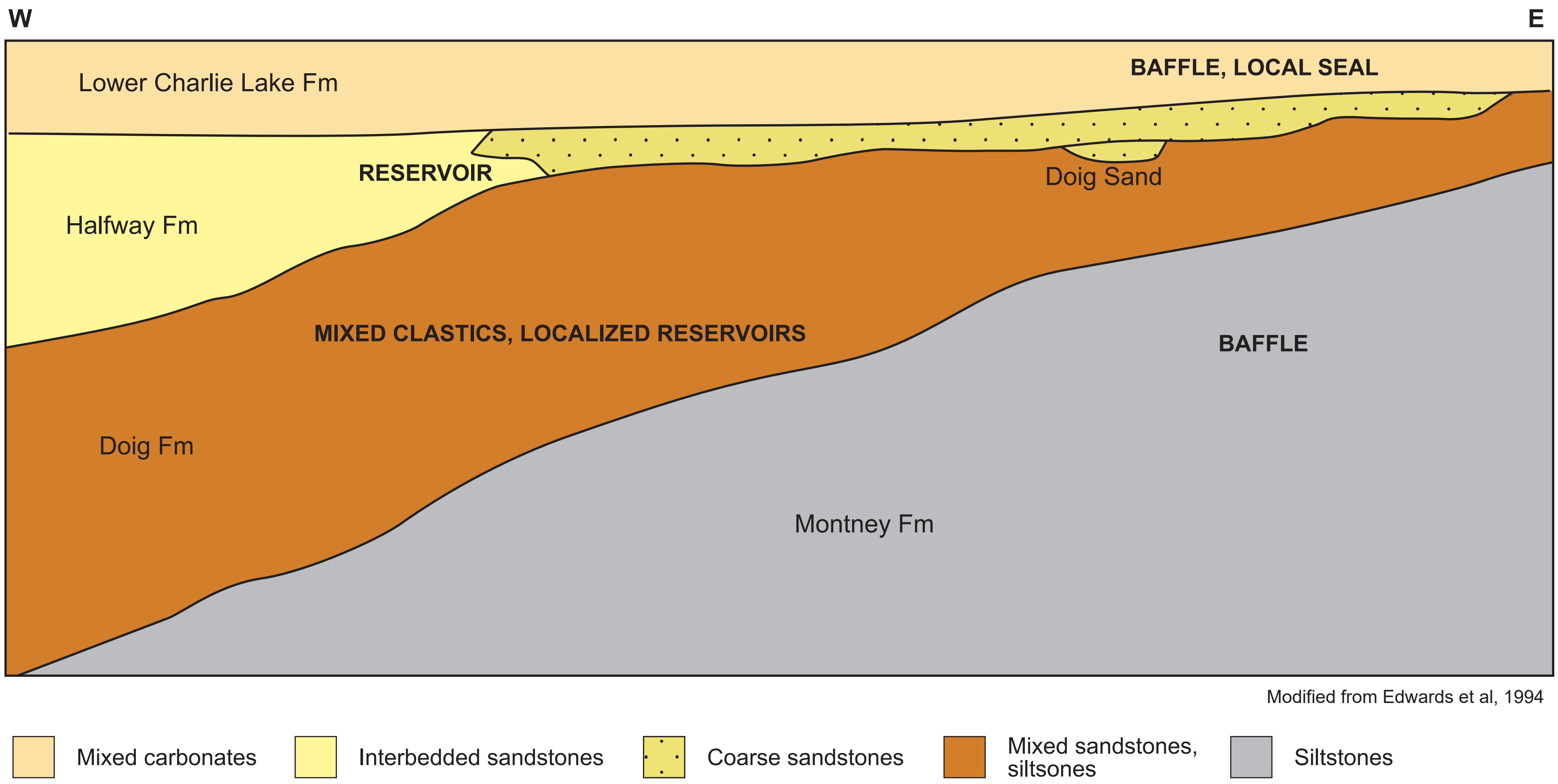

Figure 12.4

Storage Complex

The middle Triassic-age Halfway encompasses shallow marine sandstone deposited along the western margin of the North American craton in barrier island, shoreface and tidal inlet channel environments. Halfway reservoir bodies are stratigraphically isolated in updip areas, but pass southwestward into a broad, continuous shelf sandstone complex.

Halfway sandstone is primarily quartz arenite and sublitharenite, with local bioclastic (shell debris) sandstone and coquina. Grain sizes generally range from very fine to fine, as most clastic sediment was derived through aeolian (wind) transport from the craton. Major cements include silica, carbonate, and anhydrite. The best (and volumetrically dominant) reservoir facies in many pools in the updip Halfway are tidal channel fills. To the south and west, the reservoir quality generally deteriorates, although secondary solution of lithic and bioclastic grains can create significant reservoir sweet spots (NEBC Play Atlas, 2006).

Underlying the Halfway reservoirs are interbedded sandstone, siltstone and mudstone of the Doig Formation that act as a baffle or a stacked reservoir locally. The Doig and Halfway formations are from a similar lithological source (genetically-related) and depositional environment (Edwards et al, 1994). The Doig tends to be less permeable except for local reservoir development near the updip edge as noted in Geoscience BC Report 2021-14 (PRCL, 2021). The overlying tight (impermeable) mixed carbonates and clastics of the Lower Charlie Lake act as a baffle/seal to reservoirs in the Halfway *(figure 12.4)*. The Halfway, Doig and Charlie Lake formations are stratigraphically complex and will require more detailed analyses to characterize the CO_2 storage opportunities locally.

The Halfway structure map *(figure 12.5)* shows the topography of the top of the Halfway in the subsurface. Since the displacement of a CO_2 plume is governed by gravity and buoyancy, the plume tends to migrate up-structure during its injection period. As supercritical conditions for CO_2 comprise a temperature in excess of 31.1°C and a pressure greater than 7,500 kPa, the Halfway 7,500 kPa and 31°C contours indicate where CO_2 injection is expected to be in the supercritical phase.

Net reservoir maps are provided for the saline aquifers *(figure 12.6)* and depleted pools *(figure 12.7)*. These maps can indicate the most favourable areas for CO_2 injection within storage reservoirs; i.e. where the reservoir rock has the highest quality and most often the highest porosity and permeability. The net reservoir contours within the pools were provided by the BC Oil and Gas Commission (BC OGC). The net reservoir contours within the saline aquifers were sourced primarily from Geoscience BC Report 2021-14 (PRCL, 2021), with CDL providing geological support to fill in any gaps between previously existing datasets.

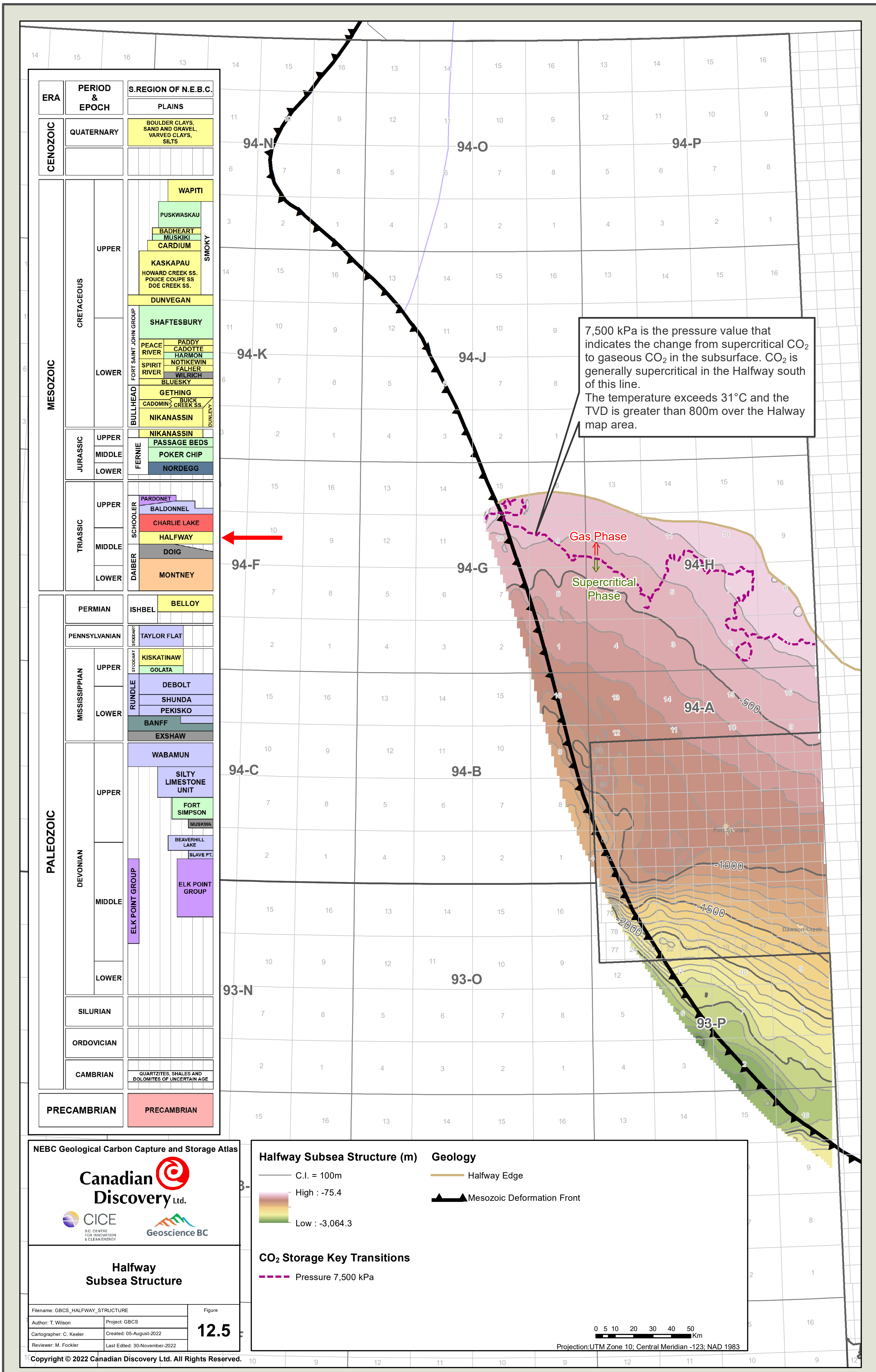

ERA
PERIOD & EPOCH
S.REGION OF N.E.B.C.
PLAINS
CENOZOIC
QUATERNARY
BOULDER CLAYS, SAND AND GRAVEL, VARVED CLAYS, SILTS
MESOZOIC
CRETACEOUS
UPPER
LOWER
WAPITI
PUSKWASKAU
BADHEART
MUSKIKI
CARDIUM
SMOKY
KASKAPAU
HOWARD CREEK SS. POUCE COUPE SS DOE CREEK SS.
DUNVEGAN
FORT SAINT JOHN GROUP
SHAFTESBURY
PEACE RIVER
PADDY
CADOTTE
HARMON
SPIRIT RIVER
NOTIKEWIN
FALHER
WILRICH
BLUESKY
BULLHEAD
GETHING
CADOMIN
BUICK CREEK SS.
NIKANASSIN
DUNLEVY
JURASSIC
UPPER
MIDDLE
LOWER
NIKANASSIN
FERNIE
PASSAGE BEDS
POKER CHIP
NORDEGG
TRIASSIC
UPPER
MIDDLE
LOWER
SCHOOLER
PARDONET
BALDONNEL
CHARLIE LAKE
HALFWAY
DAIBER
DOIG
MONTNEY
PALEOZOIC
PERMIAN
ISHBEL
BELLOY
PENNSYLVANIAN
STODDART
TAYLOR FLAT
MISSISSIPPIAN
UPPER
LOWER
KISKATINAW
GOLATA
RUNDLE
DEBOLT
SHUNDA
PEKISKO
BANFF
EXSHAW
DEVONIAN
UPPER
MIDDLE
LOWER
WABAMUN
SILTY LIMESTONE UNIT
FORT SIMPSON
MUSKWA
BEAVERHILL LAKE
SLAVE PT.
ELK POINT GROUP
ELK POINT GROUP
SILURIAN
ORDOVICIAN
CAMBRIAN
QUARTZITES, SHALES AND DOLOMITES OF UNCERTAIN AGE
PRECAMBRIAN
PRECAMBRIAN
94-N
94-O
94-P
94-K
94-J
94-F
94-G
94-H
94-C
94-B
94-A
93-N
93-O
93-P
7,500 kPa is the pressure value that indicates the change from supercritical CO_2 to gaseous CO_2 in the subsurface. CO_2 is generally supercritical in the Halfway south of this line.
The temperature exceeds 31°C and the TVD is greater than 800m over the Halway map area.
Gas Phase
Supercritical Phase
-500
-1000
-1500
-2000
Fort St. John
Dawson Creek
NEBC Geological Carbon Capture and Storage Atlas
Canadian Discovery Ltd.
CICE
B.C. CENTRE FOR INNOVATION & CLEAN ENERGY
Geoscience BC
Halfway Subsea Structure
Filename: GBCS_HALFWAY_STRUCTURE
Figure
12.5
Author: T. Wilson
Project: GBCS
Cartographer: C. Keeler
Created: 05-August-2022
Reviewer: M. Fockler
Last Edited: 30-November-2022
Copyright © 2022 Canadian Discovery Ltd. All Rights Reserved.
Halfway Subsea Structure (m)
C.I. = 100m
High : -75.4
Low : -3,064.3
Geology
Halfway Edge
Mesozoic Deformation Front
CO_2 Storage Key Transitions
Pressure 7,500 kPa
0 5 10 20 30 40 50
Km
Projection:UTM Zone 10; Central Meridian -123; NAD 1983

Figure 12.5

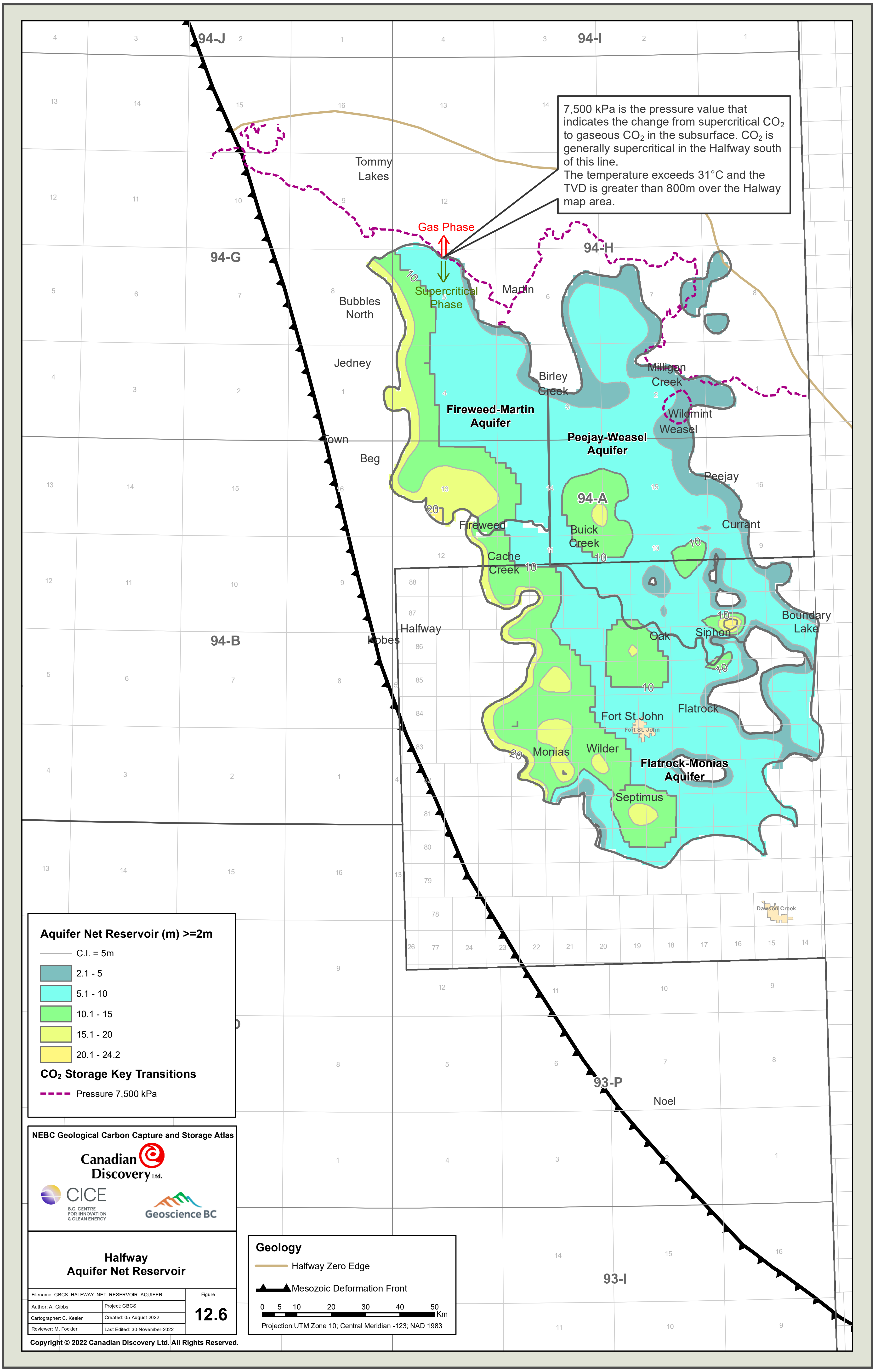

© Canadian Discovery Ltd. *Figure 12.6*

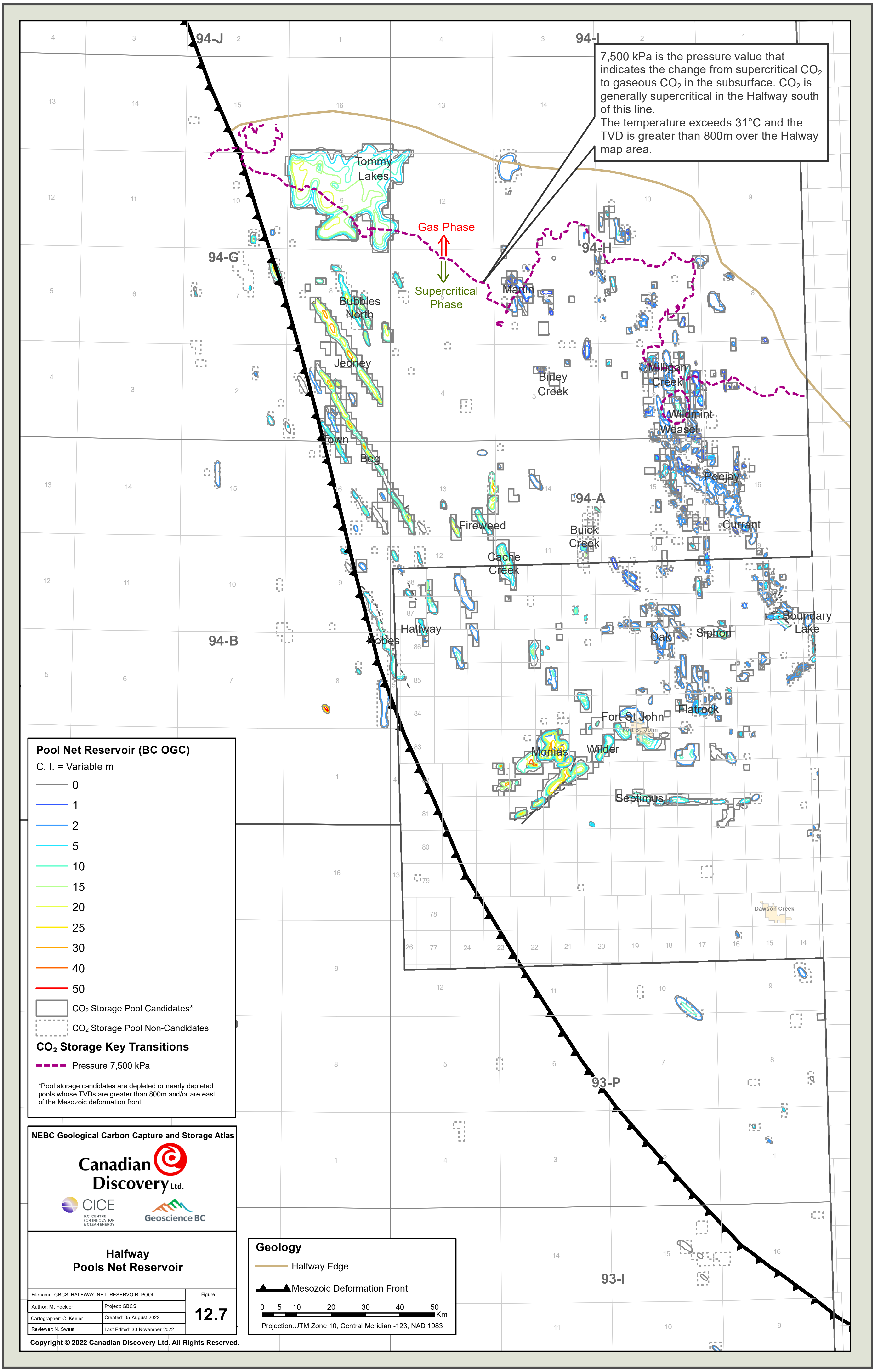

© Canadian Discovery Ltd.

Figure 12.7

Porosity-Permeability Correlations

Core data for the Halfway were obtained from geoLOGIC and filtered for better quality reservoir that is more conducive to carbon storage (greater than 6% porosity and 5 mD permeability) within the study area. These data were used to estimate porosity trends in the aquifers for storage calculations and to do a preliminary analysis of the multiple porosity-permeability trends that have been observed in the Halfway in past studies *(figure 12.8)*.

In the west, Halfway reservoirs are thick and continuous but have experienced more diagenesis due to deeper burial and less solution enhancement, so porosity values are generally less than 12% and permeabilities are generally less than 20 mD. This includes most of the Fireweed-Bubbles aquifer area and is represented by the West lower permeability trend (shown in blue). However, tidal inlet channel fills comprising coquinas and secondary solution of lithic and bioclastic grains can create significant reservoir sweet spots; for example at Tommy Lakes and Bubbles where porosities range from 12 to 19% and permeabilities range from 15 to 90 mD.

The South permeability trend (shown in yellow) represents the Flatrock-Monias aquifer area and pools, including the Boundary Lake, Oak, Flatrock, Buick Creek and Rigel pools. Reservoir porosity in these areas generally ranges from 10% to just over 20% with 50–500 mD permeability.

The East permeability trend (shown in orange) is located northwest of Boundary Lake toward Martin and includes Peejay, Wildmint, Weasel and Milligan Creek. There is a large data spread, particularly at Peejay, but it also comprises the best quality reservoir with porosity values exceeding 25% and permeabilities over 1 Darcy, due to many samples where reservoir quality has been enhanced by dissolution of shelly debris in the tidal channel facies (PRCL, 2021).

12.8 Halfway Porosity-Permeability Plot

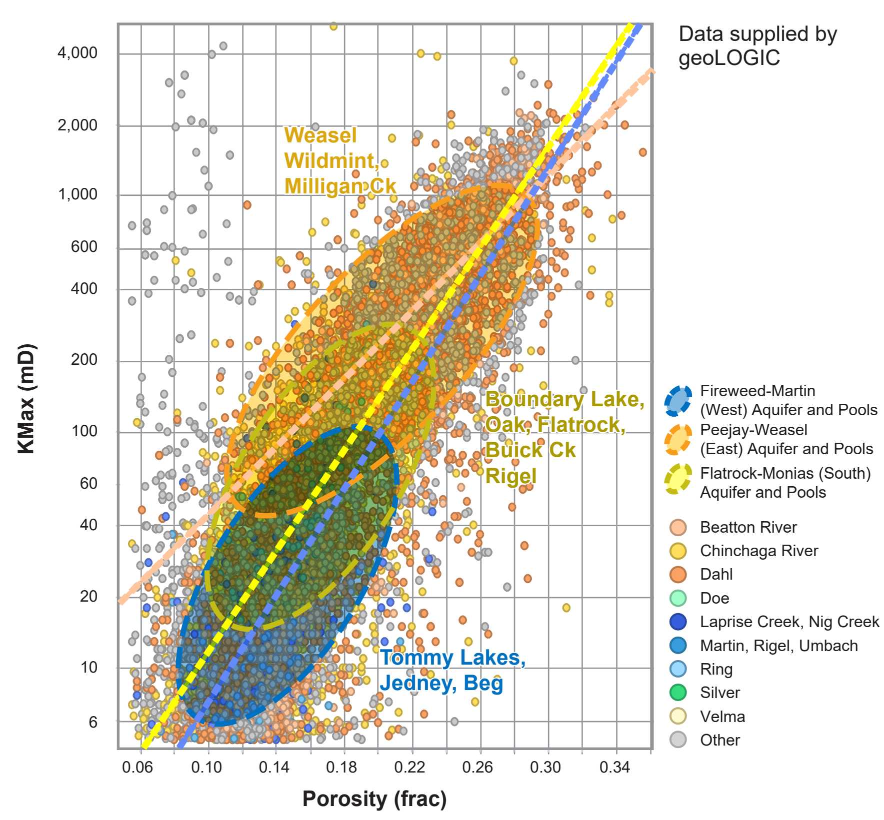

 Figure 12.8

Hydrodynamics

To delineate the extent of the aquifers and understand the relationship between the aquifers and the depleted pools, a high-level analysis was done on Halfway hydrodynamics *(figure 12.9)* using Hydrofax drillstem test (DST) data from within the aquifers and the initial pressure and datum depth of each depleted pool from the BC OGC reserves databases.

Halfway aquifers are relatively continuous throughout the study area, however several areas can be differentiated by variations in reservoir quality, pressure and temperature.

The western system, which is dominated by tighter reservoir and higher geothermal gradients, extends from the Fireweed pools in the south to the Martin area in the north. This region spans the lowest and highest pressure depth ratios within the study area. The lowest pressures are observed at Tommy Lakes, Martin and Birley Creek, where the pressures approach the transition out of the supercritical range (7,500 kPa). These low pressures may suggest potential connectivity with another zone, and therefore should be assessed in more detail for leakage risk. On the other hand, the western side of the aquifer is bounded by higher-pressured, deep basin style pools such as Kobes, Beg and Jedney, which display higher pressure-depth ratios (they fall to the right on the pressure vs elevation graph in *figure 12.9*) and have little to no water production. The tighter, higher-pressured reservoir should have good containment, provided that distance is maintained from observed faulting throughout this area. These pools also provide some of the best opportunities in terms of CO_2 storage potential, with storage capacities from 10 to 23 Mt.

The Flatrock-Monias (south) and Peejay-Weasel (east) regions have better reservoir quality within the aquifer (porosity from 10% to 22% and 25%, respectively) and exhibit more conventional behaviour on the pressure vs elevation graph *(figure 12.9)*. The Peejay-Weasel area appears to have a number of small depleted conventional pools directly overlying the aquifer (as suggested by their high water production) that may allow for a more open distribution of pressure between the pool/aquifer system, and therefore potentially higher storage potential locally than represented in the tables. This system extends from Boundary Lake in the south, through Peejay and Weasel north to Milligan Creek.

The Flatrock-Monias hydraulic system, at pressures of greater than 12,000 kPa, has the greatest combined storage opportunities between the aquifer and conventional pools in this area, including top 10 pools Cache Creek, Fort St. John, Wilder and Septimus. However, the Monias, Wilder, Fort St. John and Septimus areas have higher CO_2 storage risk due to faulting. Therefore candidates within the northern part of the Flatrock-Monias system, from Flatrock north to Oak and west to Cache Creek, may offer both good storage potential and more secure containment.

12.9 | Halfway Pressure vs Elevation Plot

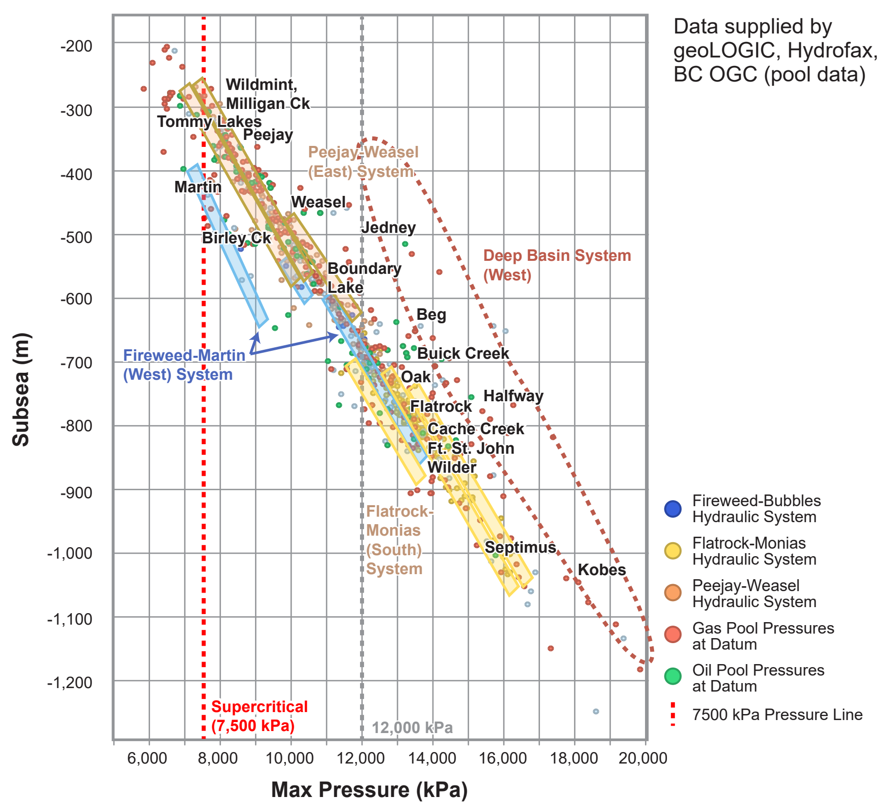

© Canadian Discovery Ltd. *Figure 12.9*

Carbon Storage Calculations

Depleted and Nearly Depleted Pools

The top 25 depleted and nearly depleted pool candidates for carbon storage potential within the Halfway Formation are shown in *table 12.2*.

The BC OGC defines depleted pools as ones that have no remaining reserves or production. The BC OGC also recognizes that there are nearly depleted pools that could become CO_2 storage candidates in the (relatively) near future. The nearly depleted CO_2 storage candidates include pools where 90%+ of the reserves have been recovered, or no production has occurred in over five years. Furthermore, CDL has excluded pools that are shallower than 800m TVD, or are west of the Mesozoic deformation front. See Depleted Pools Selection Criteria in *Chapter 4* for a more thorough discussion.

The theoretical CO_2 storage potential represents the mass of CO_2 that can be stored in the hydrocarbon reservoirs assuming that the volume occupied previously by the produced gas will be occupied entirely by the injected CO_2. These calculations have been provided by the BC OGC and are based on historical pool production.

The effective CO_2 storage potential represents the mass of CO_2 that can be stored in hydrocarbon reservoirs after taking into account intrinsic reservoir characteristics and flow processes, such as heterogeneity (how much variability there is in the rock), aquifer support, sweep efficiency, gravity override, and CO_2 mobility (Bachu, 2006). The effective CO_2 storage potential is calculated by CDL and reduces the theoretical storage potential by as little as 13% and as much as 75%. More detail is provided on the carbon storage calculations for depleted pools in *Appendix B*, and data are provided for all depleted pools included in this study in *Appendix C*.

The depleted and nearly depleted pools that are deemed to be CO_2 storage candidates by CDL are coloured by their effective storage potential mass on the summary map *(figure 12.10)*.

Aquifers

The Halfway aquifer parameters are summarized in *table 12.3*. Theoretical CO_2 storage potential can be calculated using the mapped pore volume of the reservoir and CO_2 density, and assumes that the pore volume will be occupied entirely by the injected CO_2. We know this is not the case however, since the pore space is already occupied by water and the water will need to be displaced in the process. As a result, a storage efficiency factor is introduced into storage potential calculations that accounts for the presence of both water and CO_2 in the aquifer. The storage efficiency factor is a function of reservoir and fluid properties and dynamics, including the geometry of the trap, gravity segregation, heterogeneity, permeability distribution and pressure, and may reduce the theoretical storage potential by 95 to 99%.

Aquifers considered favourable targets for CO_2 storage are indicated on the summary map *(figure 12.10)* and labelled with their estimated P10, P50 and P90 effective storage potential in Mt. More detail is provided on the aquifer carbon storage calculations in *Appendix B*.

Top 25 Depleted Halfway Pools

Pool Name	Pool Type	Well Count	Initial Pressure (kPa)	Temperature (˚C)	Average Porosity (%)	CO_2 Phase	Theoretical Storage Potential (Mt)	Effective Storage Potential (Mt)
Monias Halfway	Gas	93	14,457	46	15.3	Supercritical	51.1	44.6
Beg Halfway A	Gas	94	14,026	61	6.4	Supercritical	25.9	22.6
Jedney Halfway A	Gas	40	11,687	66	10.0	Supercritical	21.8	19.0
Tommy Lakes Halfway A	Gas	232	5,989	51	10.9	Gas	21.5	18.7
Fort St John Halfway A	Gas	10	13,983	55	6.4	Supercritical	7.2	6.3
Cache Creek Halfway A	Gas	14	13,355	60	8.7	Supercritical	6.3	5.5
Wilder Halfway A	Gas	11	14,028	58	11.3	Supercritical	7.8	4.9
Fort St John Southeast Halfway A	Gas	16	13,989	55	10.0	Supercritical	4.6	4.0
Town Halfway A	Gas	31	13,701	69	10.0	Supercritical	4.1	3.5
Septimus Halfway A	Gas	6	15,921	76	8.7	Supercritical	2.5	2.2
Flatrock West Halfway C	Gas	5	12,903	63	16.0	Supercritical	2.3	2.0
Oak Halfway A	Gas	15	12,759	54	13.4	Supercritical	7.4	1.8
Two Rivers Halfway A	Gas	4	14,465	54	11.9	Supercritical	2.8	1.7
Boundary Lake Halfway B	Gas	8	10,828	57	12.5	Supercritical	1.9	1.6
Willow Halfway A	Gas	4	8,143	55	18.0	Supercritical	1.8	1.5
Siphon Halfway A	Gas	6	11,852	59	14.2	Supercritical	2.4	1.5
Wilder Halfway D	Gas	12	13,951	44	11.4	Supercritical	2.3	1.5
Beg West Halfway C	Gas	17	13,352	71	10.8	Supercritical	2.1	1.3
Willow Halfway B	Gas	3	8,211	54	18.9	Supercritical	1.5	1.3
Lapp Halfway A	Gas	5	6,456	57	23.7	Gas	1.4	1.3
Halfway Halfway A	Gas	9	15,427	51	7.8	Supercritical	1.7	1.1
Beaverdam Upper Halfway A	Gas	5	9,287	58	17.1	Supercritical	1.2	1.1
Bubbles North Halfway C	Gas	29	10,194	67	9.8	Supercritical	1.5	1.0
Bear Flat Halfway B	Gas	6	13,883	68	12.1	Supercritical	1.1	0.9
Currant Halfway B	Gas	3	9,991	57	17.8	Supercritical	0.9	0.8

© Canadian Discovery Ltd. Data supplied by BC OGC and Canadian Discovery Ltd. *Table 12.2*

Halfway Aquifer Properties and Storage Potential

Aquifer Name	Type	Thickness Range (m)	Pressure Range (MPa)	Temperature Range (°C)	Porosity Range (%)	CO_2 Phase	P10 Effective Storage Potential at 0.5% (Mt)	P50 Effective Storage Potential at 2% (Mt)	P90 Effective Storage Potential at 5.4% (Mt)
Fireweed-Martin Regional System (West)	Aquifer	5-20	7.5-15	55-77	9-14%	Mostly Supercritical	5.6	22.5	60.8
Peejay-Weasel Regional System (East)	Aquifer	5-20	6-13	50-65	10-25%	Mostly Supercritical	7.6	30.3	81.8
Flatrock Monias Regional System (South)	Aquifer	5-20	12-17	42-70	10-22%	Mostly Supercritical	11.6	46.3	125.1

Table 12.3

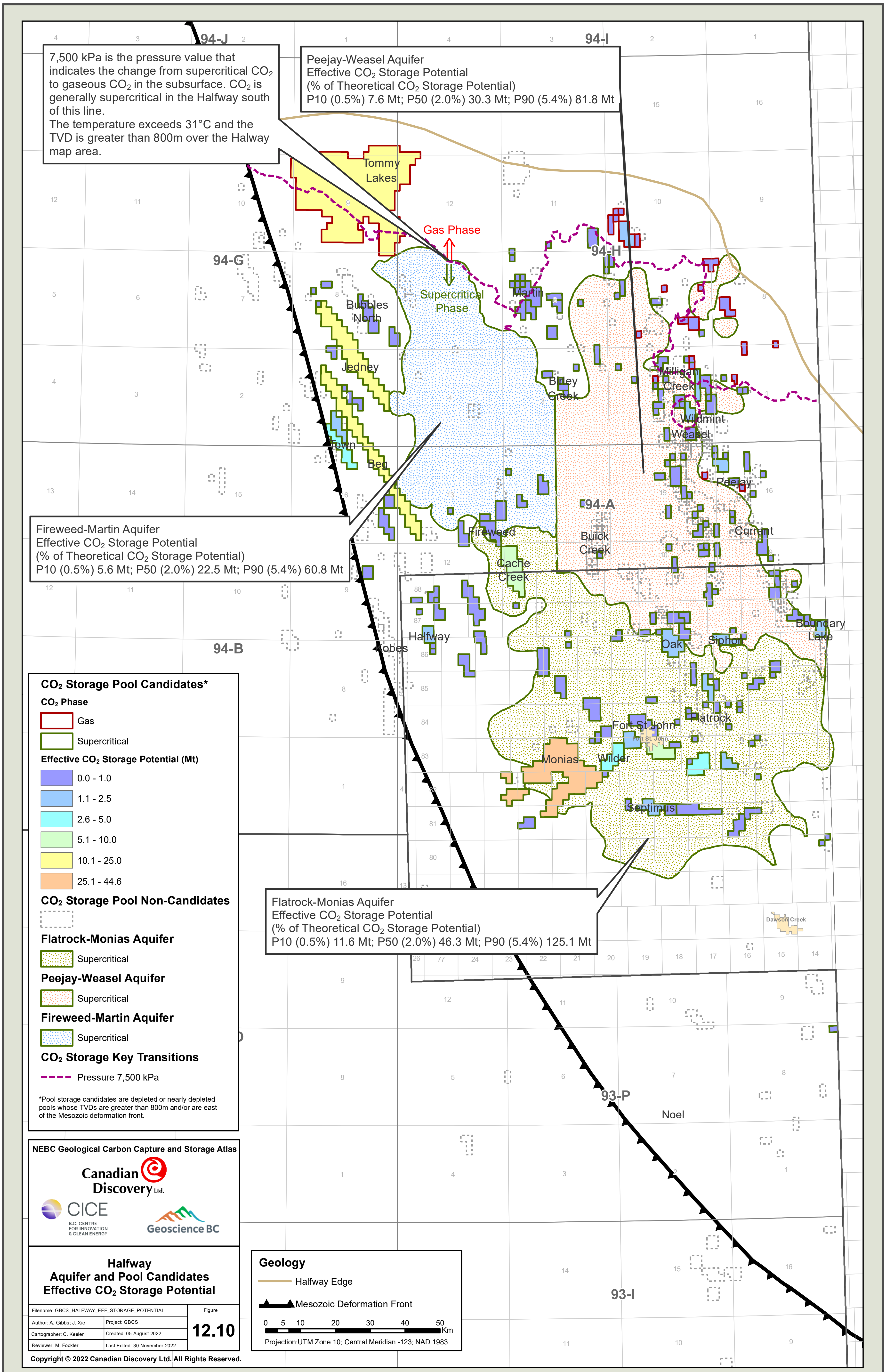

7,500 kPa is the pressure value that indicates the change from supercritical CO2 to gaseous CO2 in the subsurface. CO2 is generally supercritical in the Halfway south of this line.
The temperature exceeds 31°C and the TVD is greater than 800m over the Halway map area.
Peejay-Weasel Aquifer
Effective CO2 Storage Potential
(% of Theoretical CO2 Storage Potential)
P10 (0.5%) 7.6 Mt; P50 (2.0%) 30.3 Mt; P90 (5.4%) 81.8 Mt
Fireweed-Martin Aquifer
Effective CO2 Storage Potential
(% of Theoretical CO2 Storage Potential)
P10 (0.5%) 5.6 Mt; P50 (2.0%) 22.5 Mt; P90 (5.4%) 60.8 Mt
Flatrock-Monias Aquifer
Effective CO2 Storage Potential
(% of Theoretical CO2 Storage Potential)
P10 (0.5%) 11.6 Mt; P50 (2.0%) 46.3 Mt; P90 (5.4%) 125.1 Mt
Gas Phase
Supercritical Phase
94-J
94-I
94-G
94-H
94-A
94-B
93-P
93-I
Tommy Lakes
Bubbles North
Jedney
Town
Beg
Martin
Bivley Creek
Milligan Creek
Wildmint
Weasel
Peejay
Currant
Fireweed
Cache Creek
Buick Creek
Boundary Lake
Oak
Siphon
Halfway
Tobes
Flatrock
Fort St John
Wilder
Monias
Septimus
Dawson Creek
Noel
CO2 Storage Pool Candidates*
CO2 Phase
Gas
Supercritical
Effective CO2 Storage Potential (Mt)
0.0 - 1.0
1.1 - 2.5
2.6 - 5.0
5.1 - 10.0
10.1 - 25.0
25.1 - 44.6
CO2 Storage Pool Non-Candidates
Flatrock-Monias Aquifer
Supercritical
Peejay-Weasel Aquifer
Supercritical
Fireweed-Martin Aquifer
Supercritical
CO2 Storage Key Transitions
Pressure 7,500 kPa
*Pool storage candidates are depleted or nearly depleted pools whose TVDs are greater than 800m and/or are east of the Mesozoic deformation front.
NEBC Geological Carbon Capture and Storage Atlas
Canadian Discovery Ltd.
CICE
B.C. CENTRE FOR INNOVATION & CLEAN ENERGY
Geoscience BC
Halfway
Aquifer and Pool Candidates
Effective CO2 Storage Potential
Filename: GBCS_HALFWAY_EFF_STORAGE_POTENTIAL
Figure
12.10
Author: A. Gibbs; J. Xie
Project: GBCS
Cartographer: C. Keeler
Created: 05-August-2022
Reviewer: M. Fockler
Last Edited: 30-November-2022
Copyright © 2022 Canadian Discovery Ltd. All Rights Reserved.
Geology
Halfway Edge
Mesozoic Deformation Front
0 5 10 20 30 40 50 Km
Projection:UTM Zone 10; Central Meridian -123; NAD 1983

Figure 12.10

Belloy Formation

Belloy Overview

Storage potential in the Belloy *(figure 13.1)* occurs in the southern portion of the study area near Fort St. John and is proximal to many emitters and infrastructure. Favourability attributes are summarized in *table 13.1* with green and yellow circles indicating whether an attribute is considered generally favourable (green) or has risk and requires additional work (yellow). Both depleted pool reservoirs and saline aquifers are sequestration candidates and offer a range of storage opportunities. The top 10 depleted pools are shown in *figure 13.2*. *Figure 13.3* displays effective storage potential of the Belloy, as well as emitters and infrastructure in the NEBC study area.

Belloy Favourability Attributes

Top 10 Depleted Pool Total Potential	50 Mt	green
Aquifer Storage (P50)	158 Mt	green
Regional Seal Potential	Variable	yellow
Lithology	Dolomitic sandstone	green
Porosity	8-24%	green
Permeability	10-1,000 mD	green
Depth (TVD)	800-2,900m	green
Net Reservoir Thickness	5-45m	green

Table 13.1

13.1 Hydrostratigraphic Chart

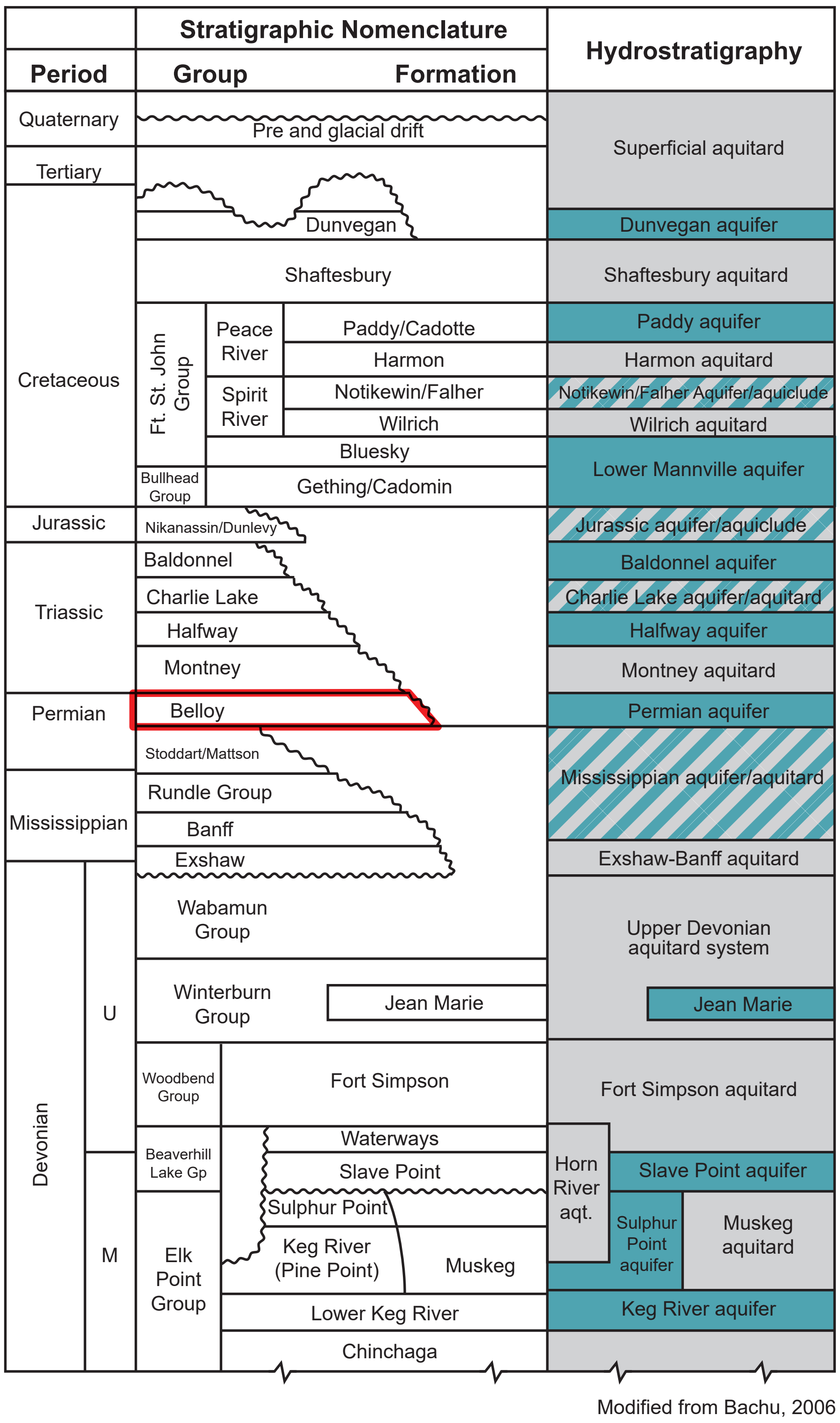

© Canadian Discovery Ltd. *Figure 13.1*

13.2 Top 10 Depleted Belloy Pools

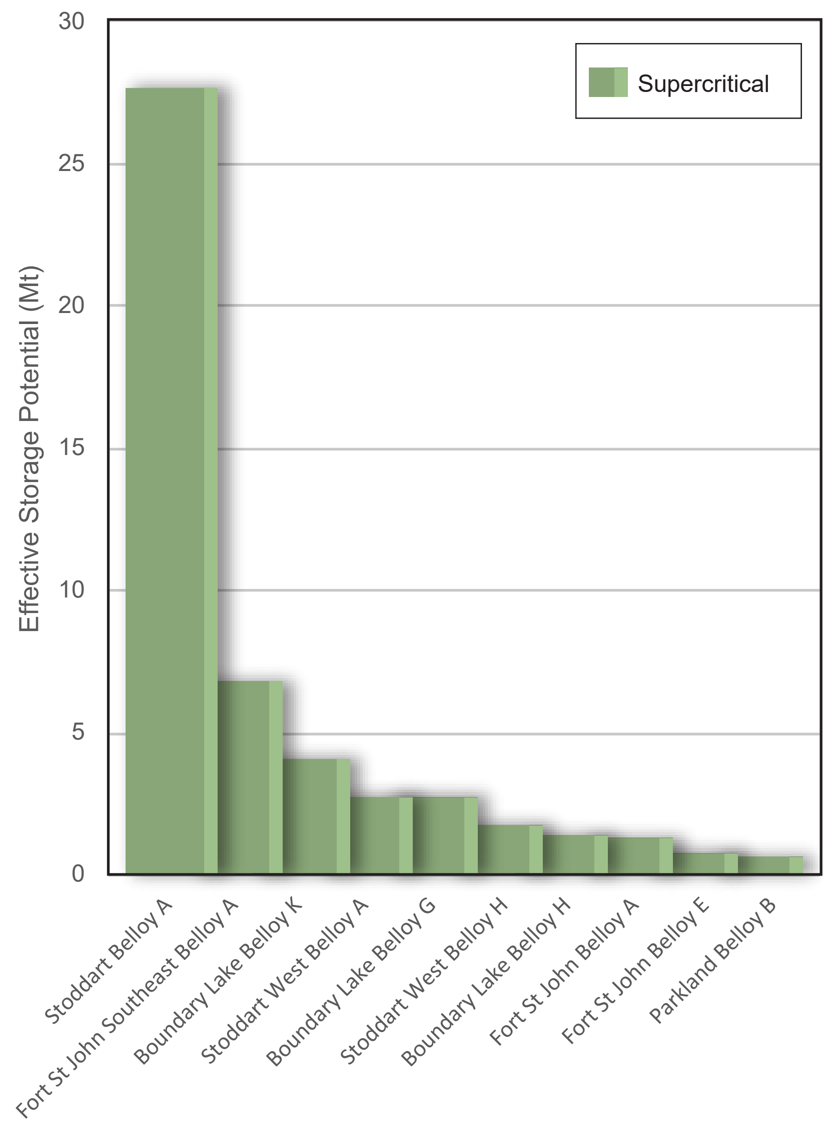

© Canadian Discovery Ltd. *Figure 13.2*

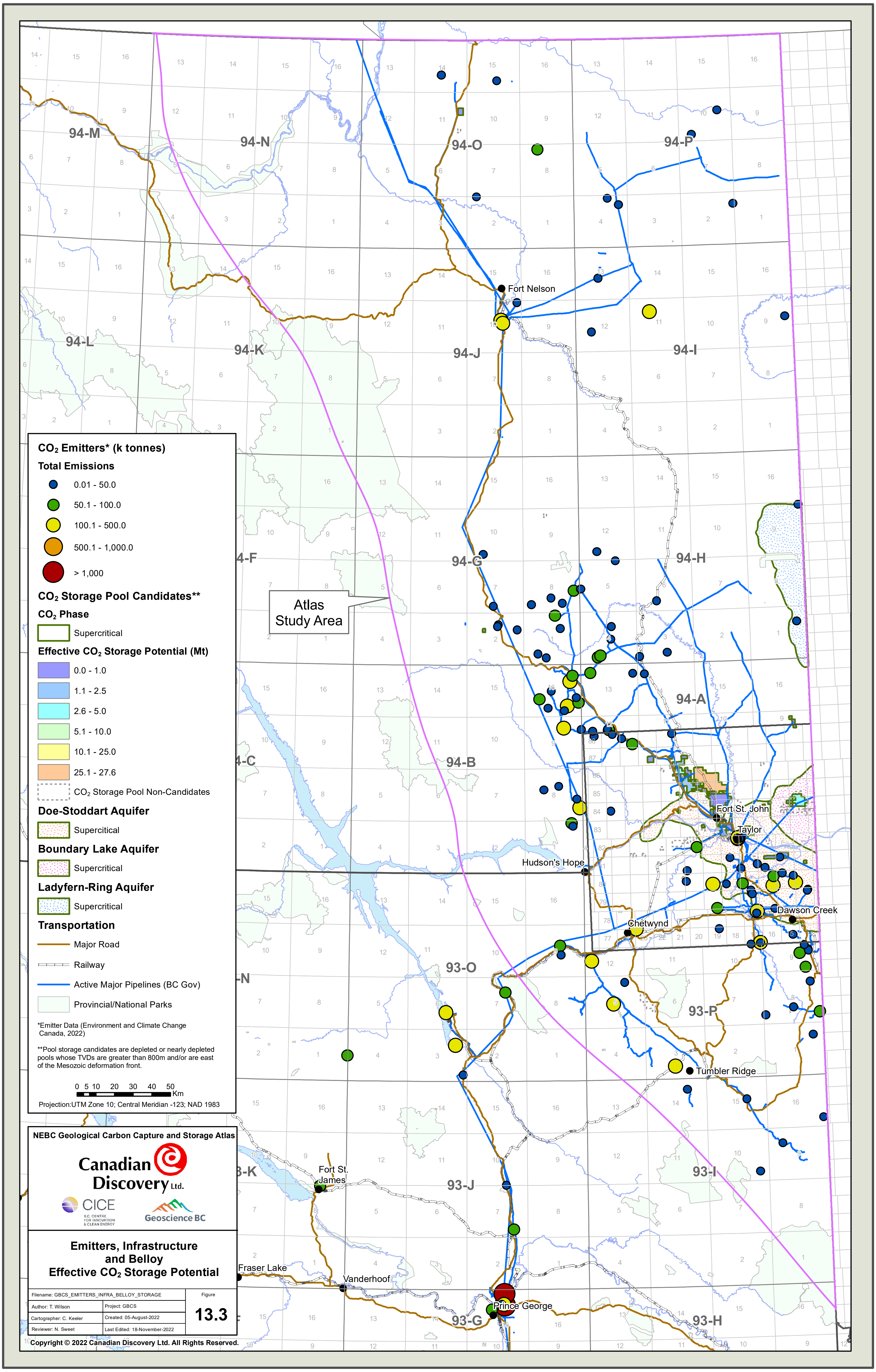

94-M
94-N
94-O
94-P
94-L
94-K
94-J
94-I
94-G
94-H
94-A
94-B
93-O
93-P
93-J
93-I
93-G
93-H
Fort Nelson
Atlas Study Area
Fort St. John
Taylor
Hudson's Hope
Chetwynd
Dawson Creek
Tumbler Ridge
Fort St. James
Fraser Lake
Vanderhoof
Prince George
CO_2 Emitters* (k tonnes)
Total Emissions
0.01 - 50.0
50.1 - 100.0
100.1 - 500.0
500.1 - 1,000.0
> 1,000
CO_2 Storage Pool Candidates**
CO_2 Phase
Supercritical
Effective CO_2 Storage Potential (Mt)
0.0 - 1.0
1.1 - 2.5
2.6 - 5.0
5.1 - 10.0
10.1 - 25.0
25.1 - 27.6
CO_2 Storage Pool Non-Candidates
Doe-Stoddart Aquifer
Supercritical
Boundary Lake Aquifer
Supercritical
Ladyfern-Ring Aquifer
Supercritical
Transportation
Major Road
Railway
Active Major Pipelines (BC Gov)
Provincial/National Parks
*Emitter Data (Environment and Climate Change Canada, 2022)
**Pool storage candidates are depleted or nearly depleted pools whose TVDs are greater than 800m and/or are east of the Mesozoic deformation front.
0 5 10 20 30 40 50 Km
Projection:UTM Zone 10; Central Meridian -123; NAD 1983
NEBC Geological Carbon Capture and Storage Atlas
Canadian Discovery Ltd.
CICE
B.C. CENTRE FOR INNOVATION & CLEAN ENERGY
Geoscience BC
Emitters, Infrastructure and Belloy Effective CO_2 Storage Potential
Filename: GBCS_EMITTERS_INFRA_BELLOY_STORAGE
Figure
13.3
Author: T. Wilson
Project: GBCS
Cartographer: C. Keeler
Created: 05-August-2022
Reviewer: N. Sweet
Last Edited: 18-November-2022
Copyright © 2022 Canadian Discovery Ltd. All Rights Reserved.

Figure 13.3

13.4 Belloy Play Schematic

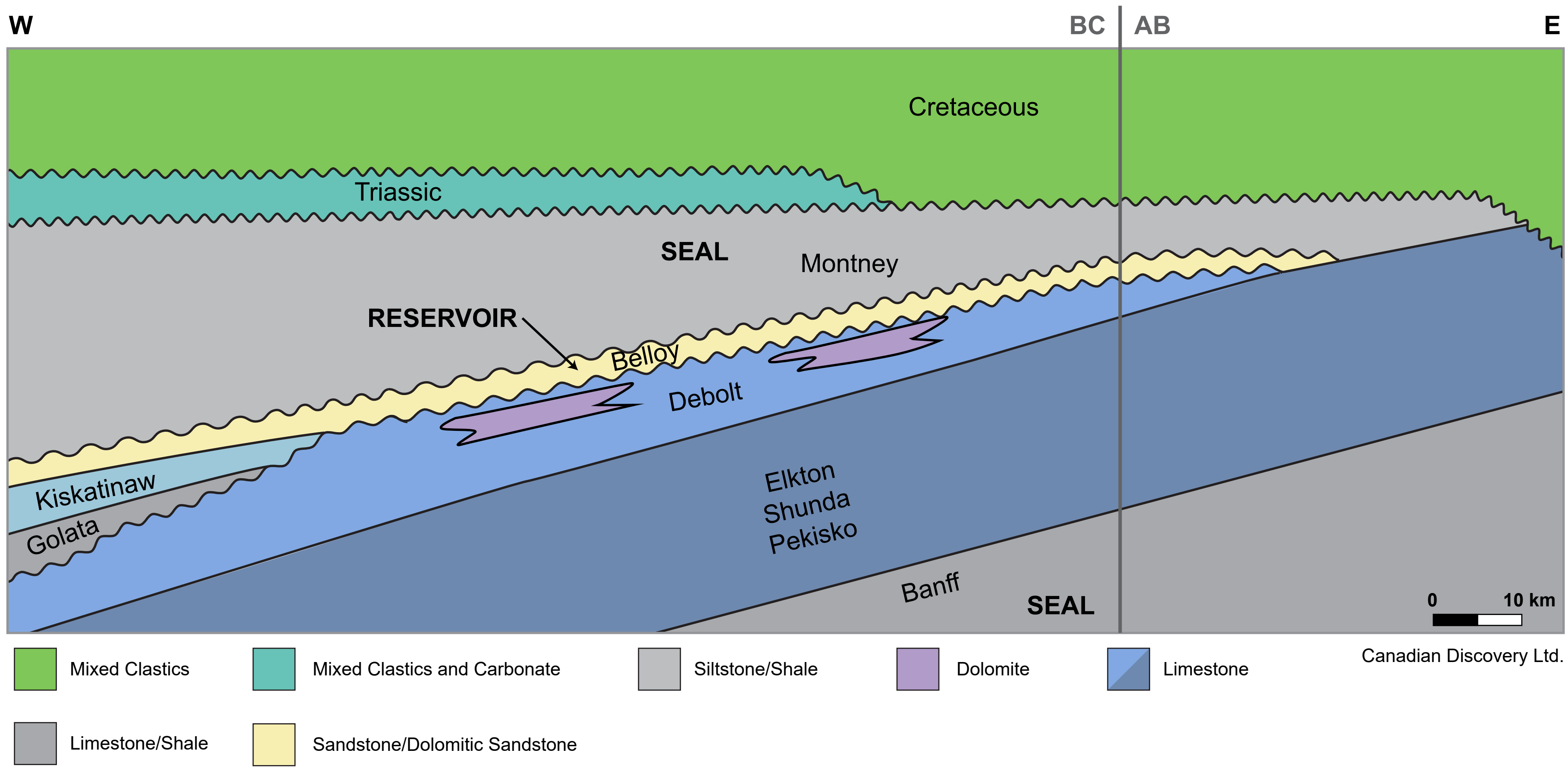

© Canadian Discovery Ltd.

Figure 13.4

Storage Complex

In the Peace River region of northeastern BC, the Permian Belloy Formation comprises porous and permeable interbedded carbonate, dolomitic sandstone and silica-rich sandstone. The Belloy is stratigraphically complex and lithologically variable as it was deposited within a broad west-east-trending Peace River embayment that had highly variable relief (Barclay et al, 1990).

In the southwest, the Belloy is unconformably underlain by dolomitic siltstone of the Mississippian Taylor Flat Formation; in the Fort St. John area, the Belloy is underlain by siltstone, limestone and shale of the Kiskatinaw and Golata formations *(figure 13.4)*; and in the north is underlain by the Mississippian Debolt Formation. The Belloy is unconformably overlain by shale and siltstone of the Triassic throughout most of the study area, except towards the depositional edges where the beds are unconformably overlain by Jurassic or Cretaceous strata.

Within the depleted pools, there is a diverse range of hydrocarbon-trapping styles. Structural traps result from drape over horst blocks related to the Dawson Creek Graben Complex in the Peace River Embayment. Unconformity traps form at the Belloy erosional edge and in isolated outliers contained by the tight shales and siltstones of the Montney Formation. Facies changes and diagenetic alteration provide reservoir that can be highly porous and permeable closer to the Alberta border.

The Belloy structure map *(figure 13.5)* shows the topography of the top of the Belloy in the subsurface. Since the displacement of a CO_2 plume is generally governed by gravity and buoyancy, the plume tends to migrate up-structure during its injection period. As supercritical conditions for CO_2 comprise a temperature in excess of 31.1°C and a pressure greater than 7,500 kPa, the Belloy 7,500 kPa and 31°C contours indicate where CO_2 injection is expected to be in the supercritical phase.

Net reservoir maps are provided for the saline aquifers *(figure 13.6)* and depleted pools *(figure 13.7)*. These maps can help indicate the most favourable areas for CO_2 injection within storage reservoirs; i.e. where the reservoir rock has the highest quality and most often the highest porosity and permeability. The net reservoir contours within the pools were provided by the BC Oil and Gas Commission (BC OGC). The net reservoir contours within the saline aquifers were sourced primarily from Geoscience BC Report 2021-14 (PRCL, 2021), with CDL providing geological support to fill in any gaps between previously existing datasets.

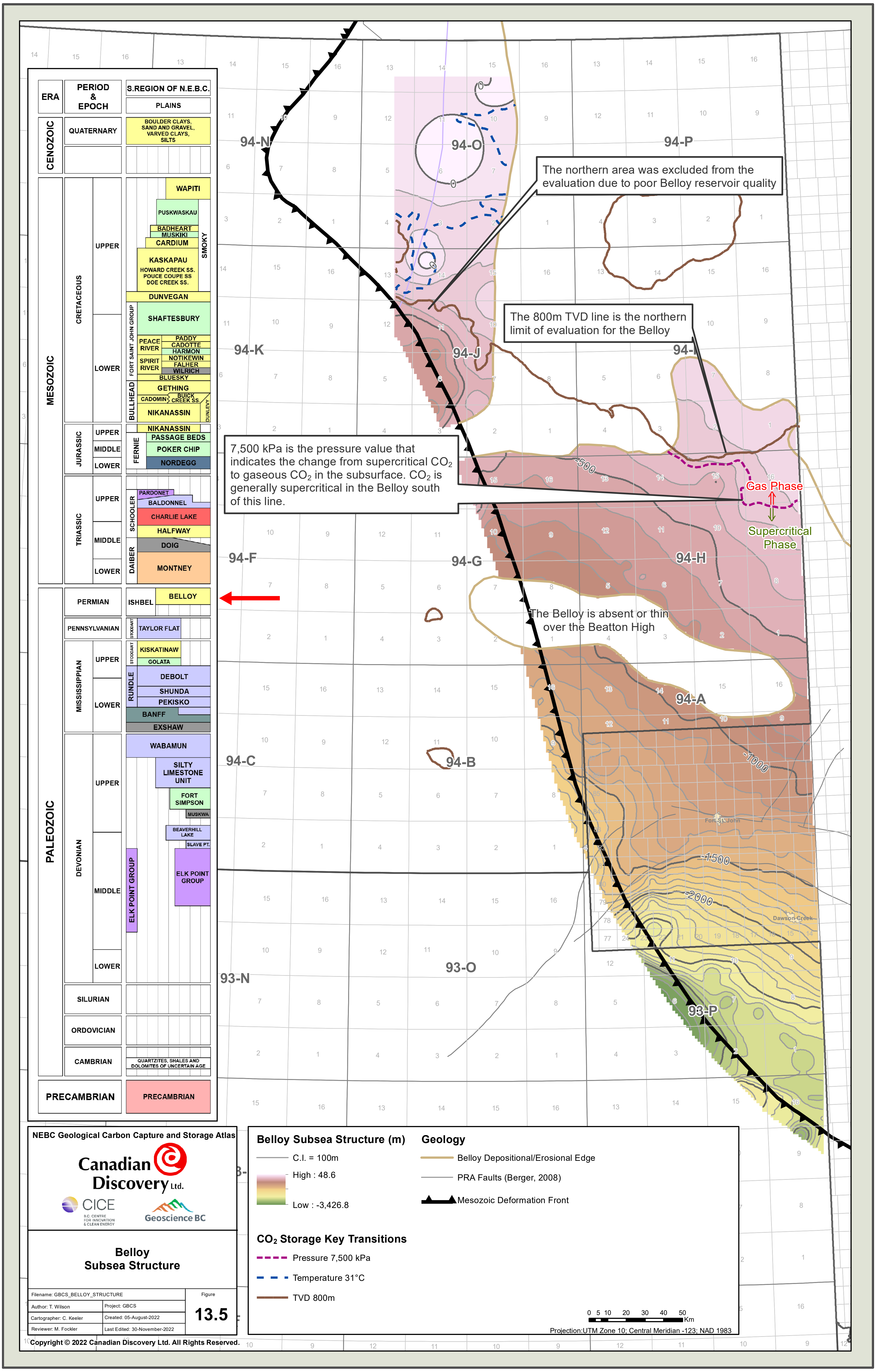

© Canadian Discovery Ltd.

Figure 13.5

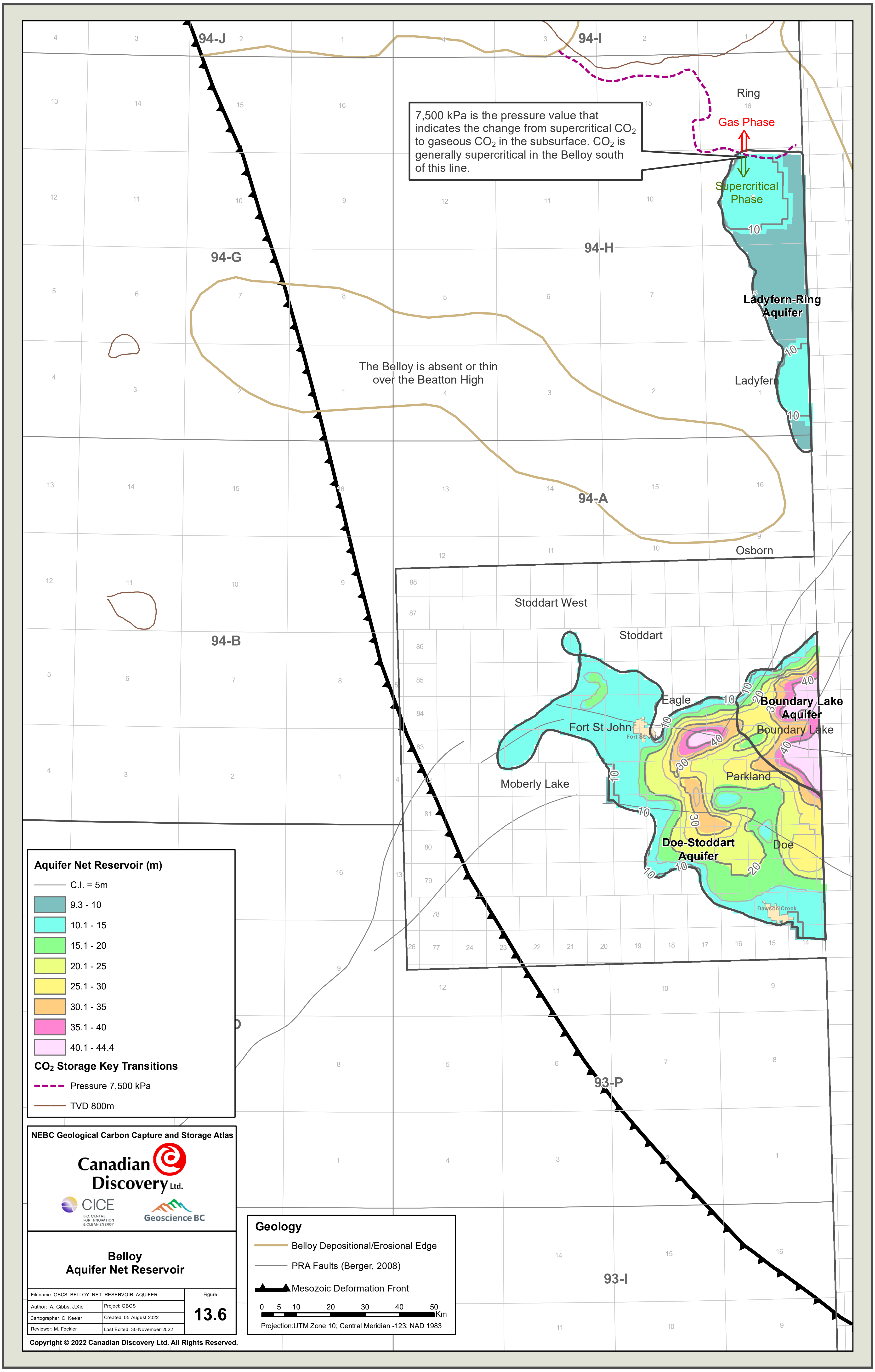

94-J
94-I
94-G
94-H
94-A
94-B
93-P
93-I
7,500 kPa is the pressure value that indicates the change from supercritical CO_2 to gaseous CO_2 in the subsurface. CO_2 is generally supercritical in the Belloy south of this line.
Ring
Gas Phase
Supercritical Phase
Ladyfern-Ring Aquifer
Ladyfern
The Belloy is absent or thin over the Beatton High
Osborn
Stoddart West
Stoddart
Eagle
Fort St John
Moberly Lake
Boundary Lake Aquifer
Boundary Lake
Parkland
Doe-Stoddart Aquifer
Doe
Aquifer Net Reservoir (m)
C.I. = 5m
9.3 - 10
10.1 - 15
15.1 - 20
20.1 - 25
25.1 - 30
30.1 - 35
35.1 - 40
40.1 - 44.4
CO_2 Storage Key Transitions
Pressure 7,500 kPa
TVD 800m
NEBC Geological Carbon Capture and Storage Atlas
Canadian Discovery Ltd.
CICE
Geoscience BC
Belloy
Aquifer Net Reservoir
Filename: GBCS_BELLOY_NET_RESERVOIR_AQUIFER
Figure 13.6
Author: A. Gibbs, J.Xie
Project: GBCS
Cartographer: C. Keeler
Created: 05-August-2022
Reviewer: M. Fockler
Last Edited: 30-November-2022
Copyright © 2022 Canadian Discovery Ltd. All Rights Reserved.
Geology
Belloy Depositional/Erosional Edge
PRA Faults (Berger, 2008)
Mesozoic Deformation Front
0 5 10 20 30 40 50 Km
Projection:UTM Zone 10; Central Meridian -123; NAD 1983

Figure 13.6

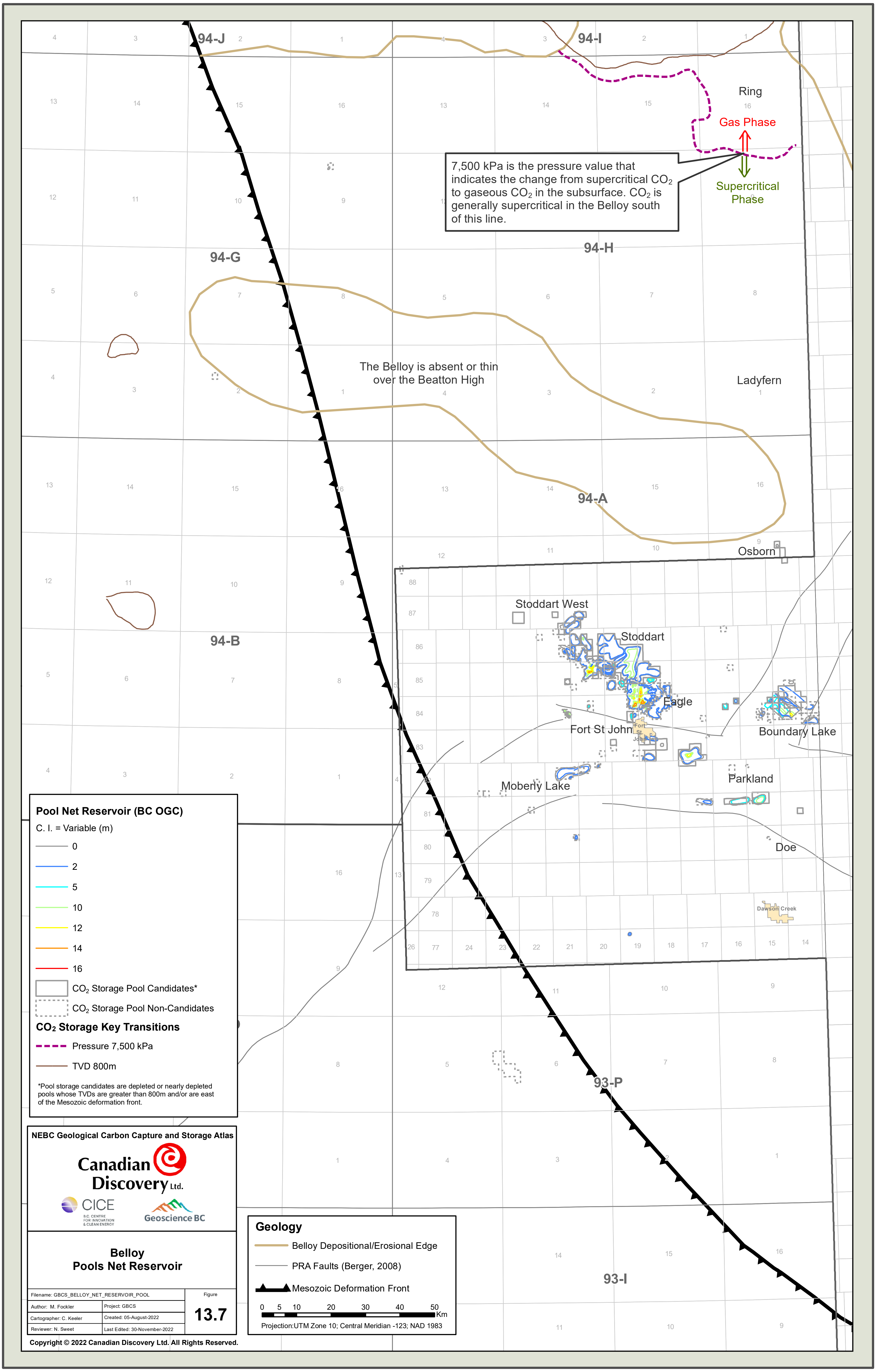

© Canadian Discovery Ltd.

Figure 13.7

Porosity-Permeability Correlations

Core data for the Belloy were obtained from geoLOGIC and filtered for better quality reservoir that is more conducive to carbon storage (greater than 6% porosity and 5 mD permeability) within the study area. These data were used to estimate porosity trends in the aquifers for storage calculations and to do a preliminary analysis of the multiple porosity-permeability trends that have been observed in the Belloy in past studies *(figure 13.8)*.

In the Boundary Lake area, shown in purple, Belloy reservoirs occur in stacked shoaling-upward successions capped by carbonate grainstones and sandstone (Bloy and Scott, 1993). The interbedded sandstone and carbonate reservoirs have high porosity but often more modest permeability. Local faulting controlled reservoir development (accommodation space), containment (structural trap) and preservation as post-Belloy erosion did not occur. In the Eagle and Stoddart areas, shown in orange, Leggett et al. (1993) documented sandstone-dominated shallow marine facies cut by a variety of channels filled with sandstone, exhibiting excellent reservoir quality in some areas.

The Ladyfern-Ring area hosts a regionally correlatable Belloy sand that ranges from 5 to over 15m in thickness, but has received little attention as it is not hydrocarbon-bearing. Drillstem tests have produced high volumes of water (500–800m of water recovery) and the zone is a successful water disposal zone at Ladyfern where 4.5 mmbbls of water have been injected into the b-17-I/94-H-01 well to date. The b-17-I/94-H-01 well has over 10m of net porous sand averaging 18% porosity and achieved initial injection rates of around 1,300 bwpd. Only one core was available for this area in the far north of the aquifer at Ring, but the core suggests that this zone may have high porosity and permeability, similar to what is observed at Stoddart, but not contained to areally limited channels.

13.8 Belloy Porosity-Permeability Plot

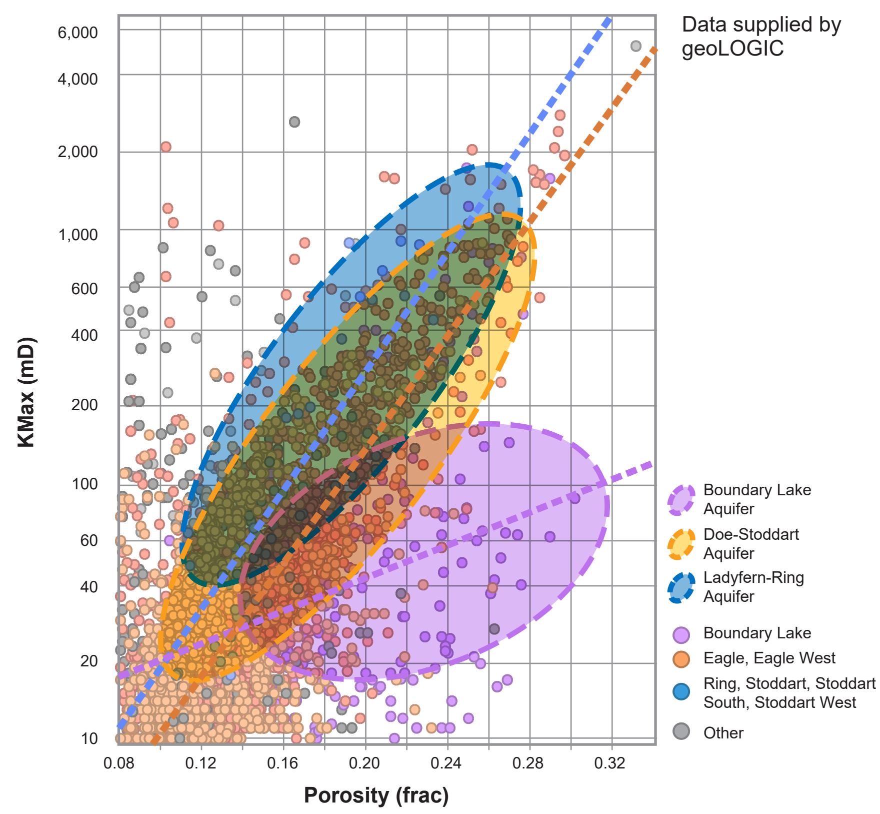

© Canadian Discovery Ltd. *Figure 13.8*

Hydrodynamics

To delineate the extent of the aquifers and understand the relationship between the aquifers and the depleted pools, a high-level analysis was done on Belloy hydrodynamics *(figure 13.9)* using Hydrofax drillstem test (DST) data from within the aquifers and the initial pressure and datum depth of each depleted pool from the BC OGC reserves databases.

In the northernmost aquifer at Ladyfern-Ring, the DSTs line up along the blue gradient on the Pressure versus Elevation (P/E) graph *(figure 13.9)*, suggesting good pressure continuity within the system. South of the Ring Field, the aquifer falls primarily within the supercritical range for CO_2, with pressures ranging from around 7,500 kPa to over 10,000 kPa in the south at Ladyfern.

In the Peace River block to the south, two conventional hydraulic systems, Boundary Lake and Doe-Stoddart, exist in close proximity and are likely interconnected to some extent. They have been separated into two systems due to the increasing amount of carbonate content in the Boundary Lake system, resulting in different reservoir properties (as discussed in the previous section). Both systems contain conventionally-trapped pools that qualify as depleted pool candidates for CO_2 storage. Many of the depleted pool options with the highest storage potential, including Boundary Lake, Stoddart, Stoddart West, and Fort. St. John, are indicated on the P/E graph. Pools with greater connection to the underlying aquifer (as suggested by higher water-gas ratios in *Appendix B*) may allow for a more open distribution of pressure between the pool/aquifer system, and therefore potentially higher variability in storage potential locally than represented in the tables. It must be noted that a significant amount of faulting exists throughout both these areas in the Fort St. John graben, and the risk of reactivating faults through injection should be investigated prior to pursuing any carbon storage project in this area.

13.9 Belloy Pressure vs Elevation Plot

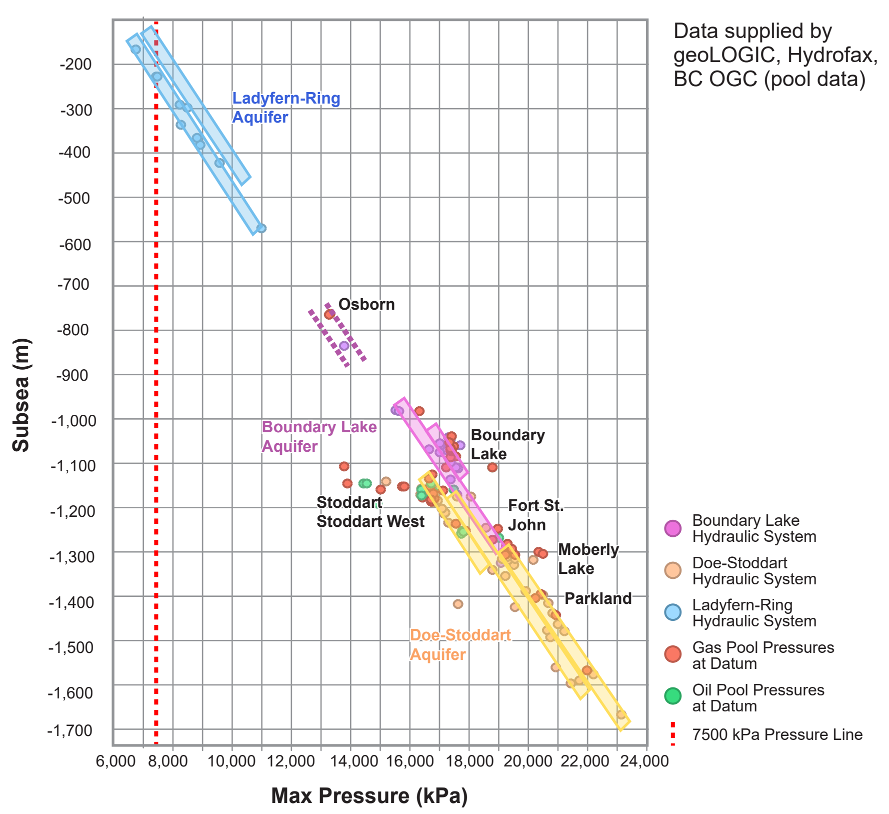

© Canadian Discovery Ltd. *Figure 13.9*

Carbon Storage Calculations

Depleted and Nearly Depleted Pools

The depleted natural gas pool candidates for carbon storage potential within the Belloy Formation are shown in *Table 13.2*.

The BC OGC defines depleted pools as ones that have no remaining reserves or production. The BC OGC also recognizes that there are nearly depleted pools that could become CO_2 storage candidates in the (relatively) near future. The nearly depleted CO_2 storage candidates include pools where 90%+ of the reserves have been recovered, or no production has occurred in over five years. Furthermore, CDL has excluded pools that are shallower than 800m TVD, or are west of the Mesozoic deformation front. See Depleted Pools Selection Criteria in *Chapter 4* for a more thorough discussion.

In the table, the theoretical CO_2 storage potential represents the mass of CO_2 that can be stored in the hydrocarbon reservoirs assuming that the volume occupied previously by the produced gas will be occupied entirely by the injected CO_2. These calculations have been provided by the BC OGC and are based on historical pool production.

The effective CO_2 storage potential represents the mass of CO_2 that can be stored in hydrocarbon reservoirs after taking into account intrinsic reservoir characteristics and flow processes, such as heterogeneity (how much variability there is in the rock), aquifer support, sweep efficiency, gravity override, and CO_2 mobility (Bachu, 2006). The effective CO_2 storage potential is calculated by CDL and reduces the theoretical storage potential by as little as 13% and as much as 75%. More detail is provided on the carbon storage calculations for depleted pools in *Appendix A*, and data are provided for all depleted pools included in this study in *Appendix B*.

The depleted and nearly depleted pools that are deemed to be CO_2 storage candidates by CDL are coloured by their effective storage potential mass on the summary map *(figure 13.10)*.

Aquifers

The Belloy aquifer parameters are summarized in *Table 13.3*. Theoretical CO_2 storage potential can be calculated using the mapped pore volume of the reservoir and CO_2 density, and assumes that the pore volume will be occupied entirely by the injected CO_2. We know this is not the case however, since the pore space is already occupied by water and the water will need to be displaced in the process. As a result, a storage efficiency factor is introduced into storage potential calculations that accounts for the presence of both water and CO_2 in the aquifer. The storage efficiency factor is a function of reservoir and fluid properties and dynamics, including the geometry of the trap, gravity segregation, heterogeneity, permeability distribution and pressure, and may reduce the theoretical storage potential by 95 to 99%.

Aquifers considered favourable targets for CO_2 storage are indicated on the summary map *(figure 13.10)* and labelled with their estimated P10, P50 and P90 effective storage potential in Mt. More detail is provided on the aquifer carbon storage calculations in *Appendix B*.

Depleted Belloy Pools

Pool Name	Pool Type	Well Count	Initial Pressure (kPa)	Temperature (˚C)	Average Porosity (%)	CO_2 Phase	Theoretical Storage Potential (Mt)	Effective Storage Potential (Mt)
Stoddart Belloy A	Gas	45	16,720	69	16.0	Supercritical	31.7	27.6
Fort St John Southeast Belloy A	Gas	10	19,512	69	9.0	Supercritical	7.8	6.8
Boundary Lake Belloy K	Gas	2	17,394	67	19.4	Supercritical	4.6	4.0
Stoddart West Belloy A	Gas	4	16,789	70	12.2	Supercritical	3.2	2.8
Boundary Lake Belloy G	Gas	1	17,429	75	23.1	Supercritical	3.1	2.7
Stoddart West Belloy H	Gas	2	16,869	73	13.0	Supercritical	2.1	1.8
Boundary Lake Belloy H	Gas	1	17,473	72	17.6	Supercritical	1.6	1.4
Fort St John Belloy A	Gas	3	19,050	68	12.0	Supercritical	1.5	1.3
Fort St John Belloy E	Gas	3	19,602	41	12.5	Supercritical	0.8	0.7
Parkland Belloy B	Gas	4	20,319	76	8.5	Supercritical	1.0	0.6
Stoddart West Belloy F	Gas	4	15,880	70	7.3	Supercritical	0.6	0.5
Boundary Lake Belloy E	Gas	1	17,427	73	21.5	Supercritical	0.6	0.5
Parkland Belloy A	Gas	2	20,491	77	7.4	Supercritical	0.8	0.5
Other Areas Belloy 16-10-087-22-W6M	Gas	1	17,653	84	11.7	Supercritical	0.5	0.4
Stoddart West Belloy B	Gas	2	16,759	70	14.0	Supercritical	0.3	0.3
Osborn Belloy A	Gas	1	13,348	67	17.0	Supercritical	0.3	0.2
Stoddart West Belloy E	Gas	2	16,470	71	12.2	Supercritical	0.9	0.2
Fort St John Belloy I	Gas	1	17,186	71	17.3	Supercritical	0.3	0.2
Stoddart West Belloy J	Gas	2	16,835	72	8.9	Supercritical	0.2	0.1
Osborn Belloy B	Gas	1	13,385	67	19.5	Supercritical	0.2	0.1
Flatrock Belloy A	Gas	1	18,843	72	9.9	Supercritical	0.2	0.1
Fort St John Lower Belloy A	Gas	2	19,301	69	12.9	Supercritical	0.1	0.1
Fort St John Belloy H	Gas	1	18,860	67	16.7	Supercritical	0.1	0.1

Table 13.2

Belloy Aquifer Properties and Storage Potential

Aquifer Name	Type	Thickness Range (m)	Pressure Range (MPa)	Temperature Range (˚C)	Porosity Range (%)	CO_2 Phase	P10 Effective Storage Potential at 0.5% (Mt)	P50 Effective Storage Potential at 2% (Mt)	P90 Effective Storage Potential at 5.4% (Mt)
Boundary Lake Hydraulic System	Aquifer	10-44	15.6-20.1	62-78	11-24%	Supercritical	12.2	48.7	131.4
Ladyfern-Ring Hydraulic System	Aquifer	10-15	7.4-10.8	53-62	16-20%	Supercritical	2.5	10.1	27.4
Doe-Stoddart Hydraulic System	Aquifer	10-45	15.5-29.7	58-104	10-22%	Supercritical	24.9	99.6	268.8

Table 13.3

13.10 | Belloy Aquifers and Pool Candidates Effective CO_2 Storage Potential

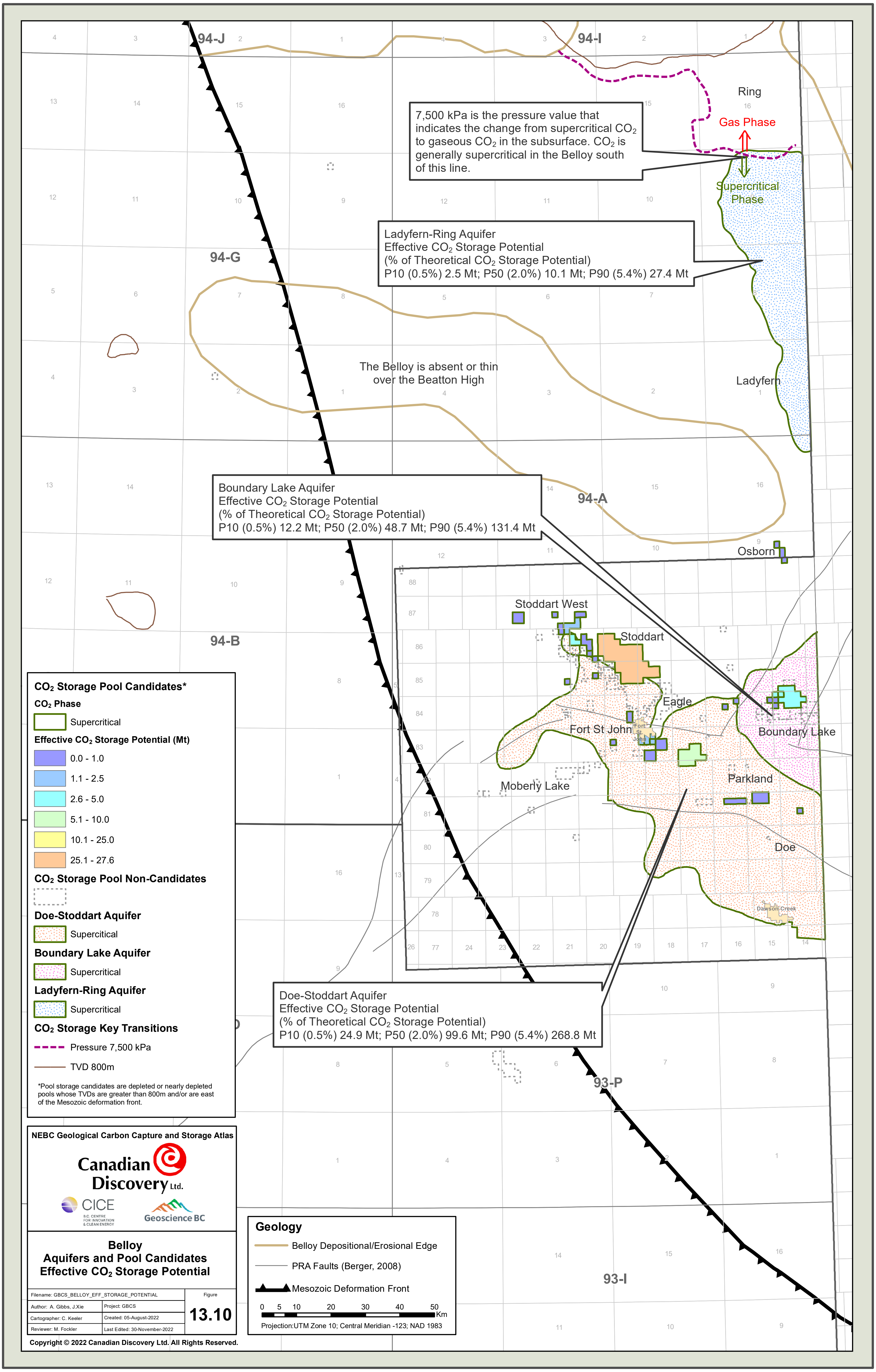

Figure 13.10

DEBOLT FORMATION

Debolt Overview

Storage potential in the Debolt *(figure 14.1)* occurs in the southern portion of the study area north of Fort St. John and is proximal to many emitters and infrastructure. Favourability attributes are summarized in *table 14.1* with green and yellow circles indicating whether an attribute is considered generally favourable (green) or has risk and requires additional work (yellow). Both depleted pool reservoirs and saline aquifers are sequestration candidates and offer a range of storage opportunities. The top 10 depleted pools are shown in *figure 14.2*. *Figure 14.3* displays effective storage potential of the Debolt, as well as emitters and infrastructure in the NEBC study area.

Debolt Favourability Attributes

Top 10 Depleted Pool Total Potential	4 Mt	yellow
Aquifer Storage (P50)	110 Mt	green
Regional Seal Potential	Variable	yellow
Lithology	Dolomite/limestone	green
Porosity	6-25%	green
Permeability	10-500 mD	green
Depth (TVD)	800-3,500m	green
Net Reservoir Thickness	2-30m	green

Table 14.1

14.1 Hydrostratigraphic Chart

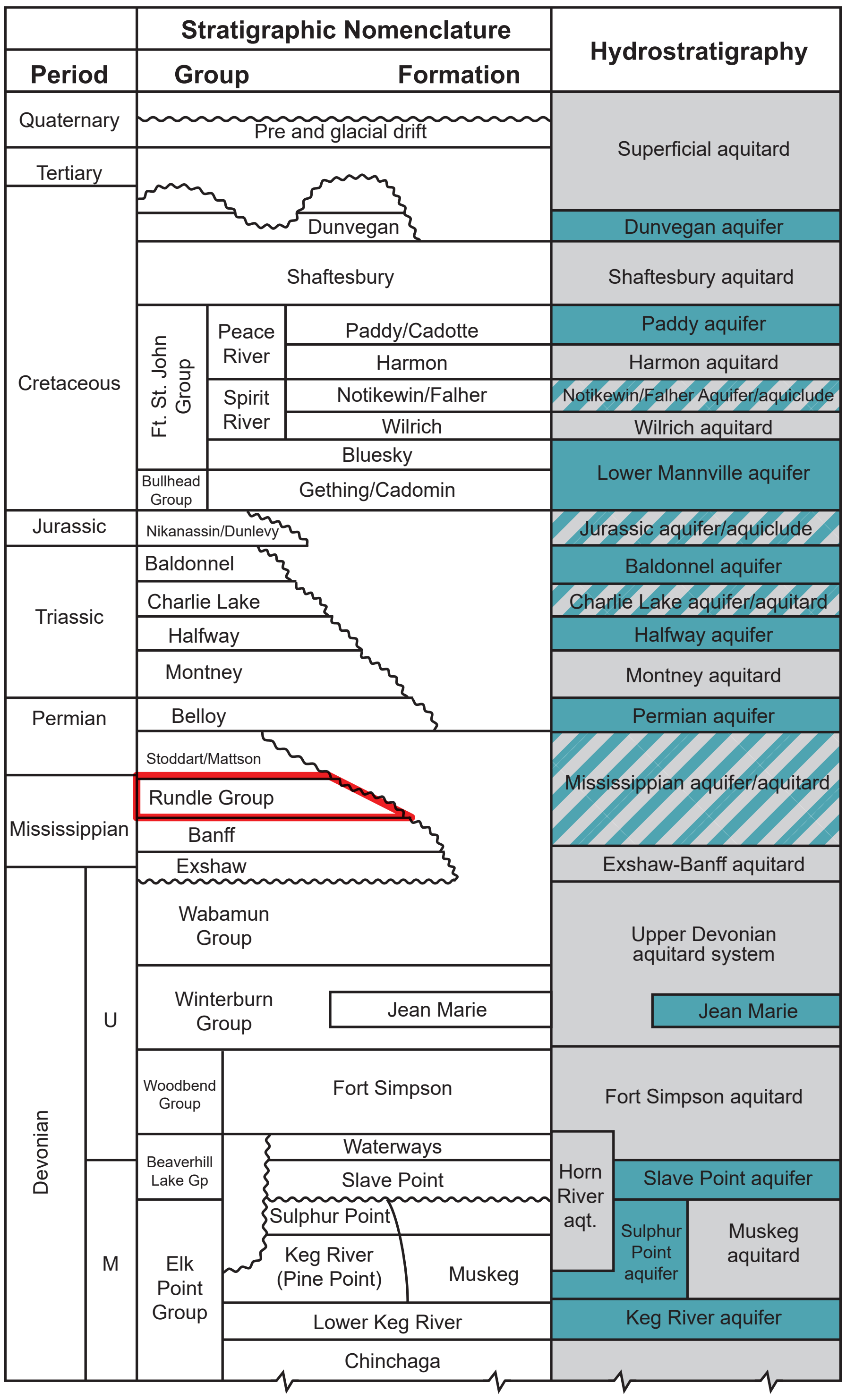

© Canadian Discovery Ltd. *Figure 14.1*

14.2 Top 10 Depleted Debolt Pools

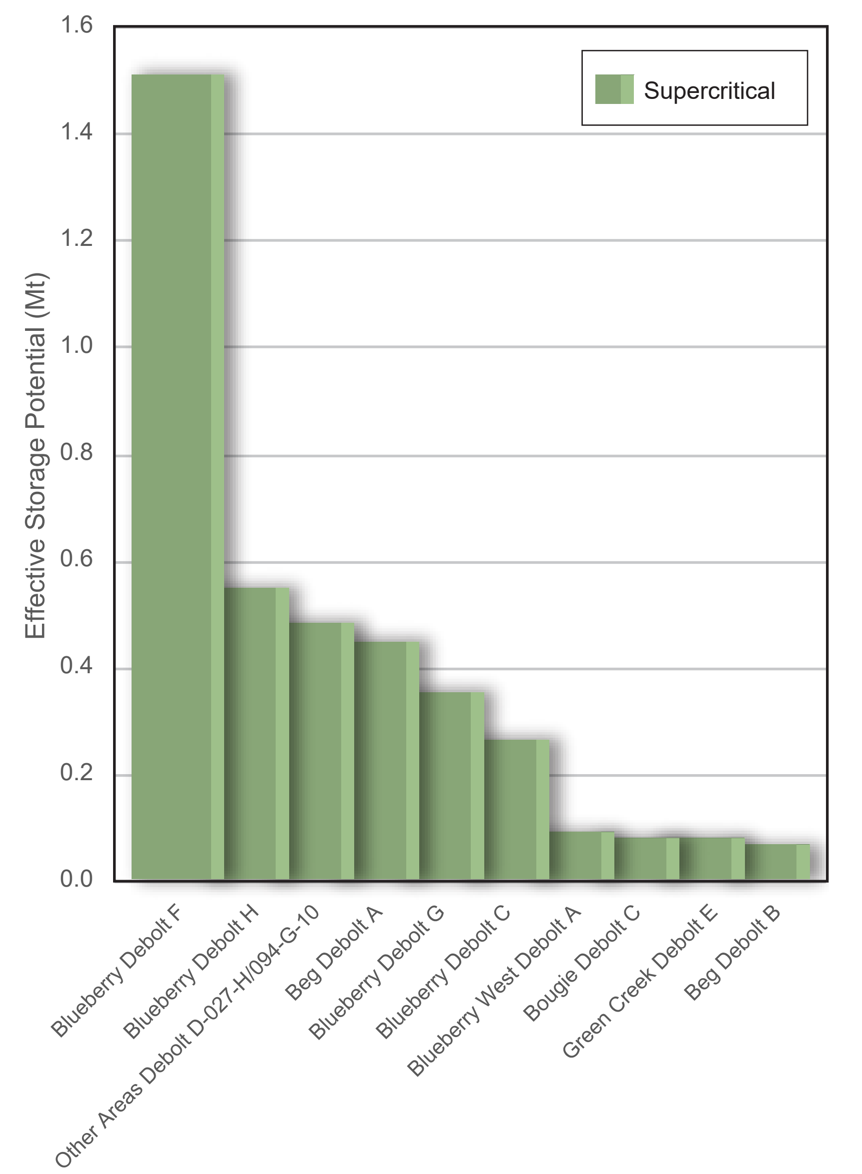

© Canadian Discovery Ltd. *Figure 14.2*

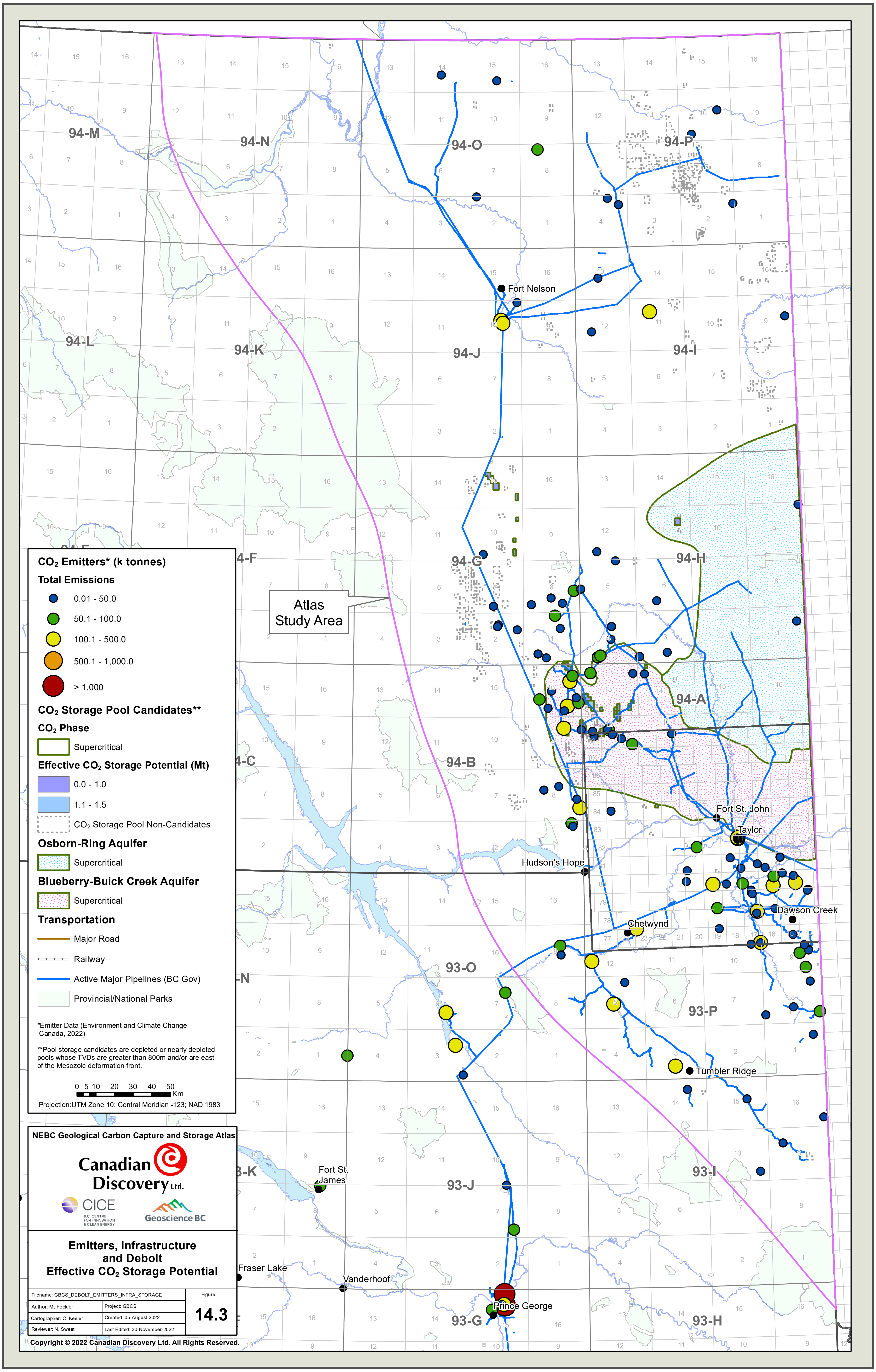

© Canadian Discovery Ltd.

Figure 14.3

14.4 Debolt Play Schematic

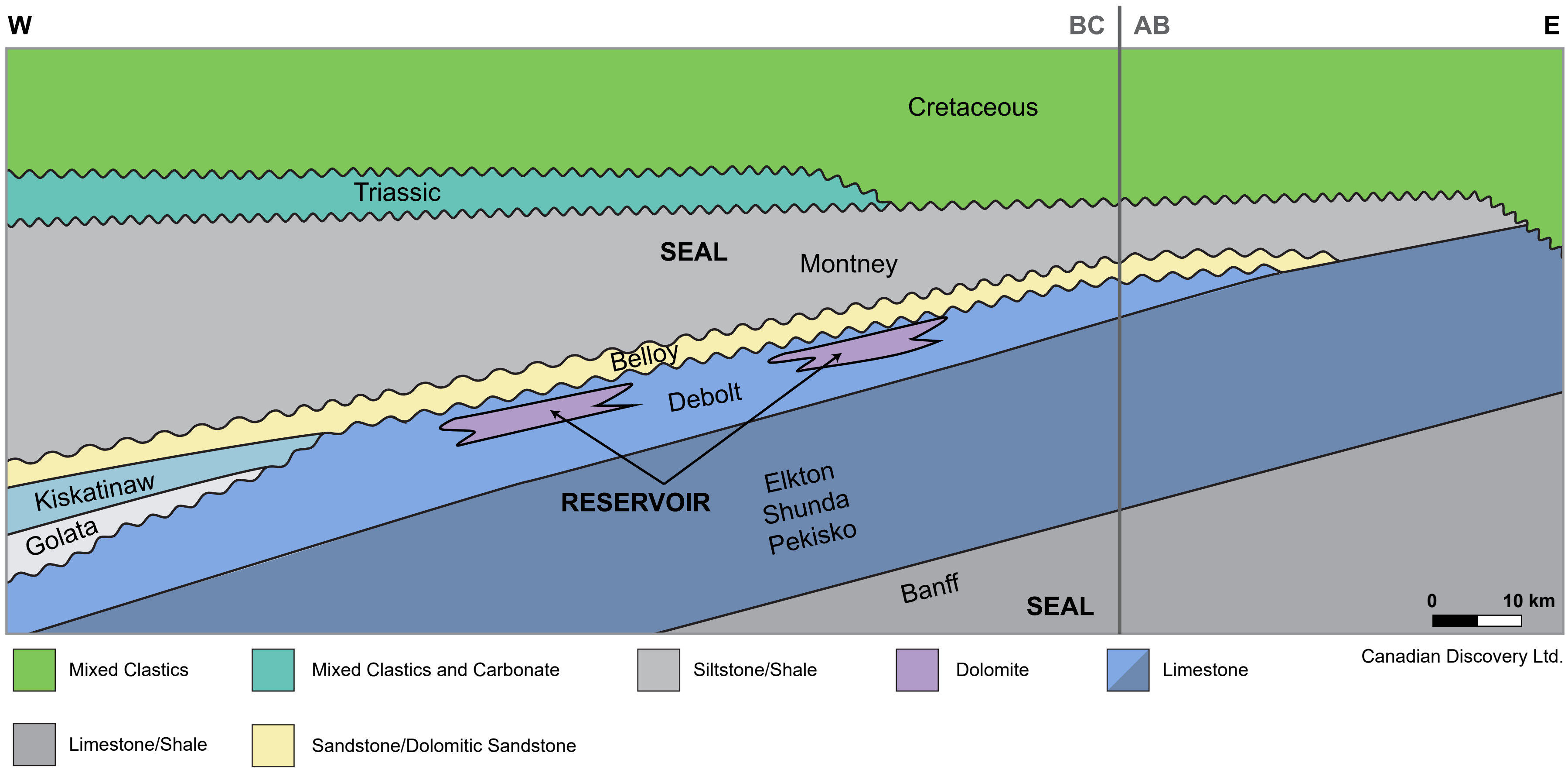

© Canadian Discovery Ltd. *Figure 14.4*

Storage Complex

The Debolt is the youngest of the three major Mississippian carbonate successions mappable throughout NEBC. Each was deposited during a long-term, basin-wide transgressive-regressive (sea level rise and fall) cycle, and all stack to form a carbonate ramp complex spanning the entire WCSB. Debolt lithologies range from intertidal dolomitic mudstones to open shelf packstones and wackestones, deposited within higher-order transgressive-regressive cycles. Reservoir occurs in dolomitized portions of the uppermost Debolt where porosity and permeability has been enhanced (NEBC Play Atlas, 2006). A large scale unconformity occurs at the top of the Debolt where it eventually subcrops in the northeast corner of BC. Although reservoir is present to the north, it is too shallow to be considered for carbon storage.

In the southwest, the Debolt is unconformably overlain by dolomitic siltstones of the Mississippian Taylor Flat Formation; in the Fort St. John area, the Debolt is overlain by the siltstones, limestones and shales of the Kiskatinaw and Golata formations *(figure 14.4)*; and in the north is overlain by the Permian Belloy Formation. Reservoirs are primarily low-temperature, fabric-selective dolomites that have formed below the unconformity at the top of the Debolt and are mappable over fairly broad areas as discussed in Durocher and Al-Asam (1997) and PRCL (2015). The Debolt is conformably underlain by tight limestone of the Mississippian Elkton and Shunda formations.

The Debolt structure map *(figure 14.5)* shows the topography of the top of the Debolt in the subsurface. Since the displacement of a CO_2 plume is governed by gravity and buoyancy, the plume tends to migrate up-structure during its injection period. As supercritical conditions for CO_2 comprise a temperature in excess of 31.1°C and a pressure greater than 7,500 kPa, the Debolt 7,500 kPa and 31°C contours indicate where CO_2 injection is expected to be in the supercritical phase.

Net reservoir maps are provided for the saline aquifers *(figure 14.6)* and depleted pools *(figure 14.7)*. These maps can help indicate the most favourable areas for CO_2 injection within storage reservoirs; i.e. where the reservoir rock has the highest quality and most often the highest porosity and permeability. The net reservoir contours within the pools were provided by the BC Oil and Gas Commission (BC OGC). The westernmost net reservoir contours within the saline aquifers were partially sourced from Geoscience BC Report 2021-14 (PRCL, 2021), while CDL did high level mapping of net reservoir to the east.

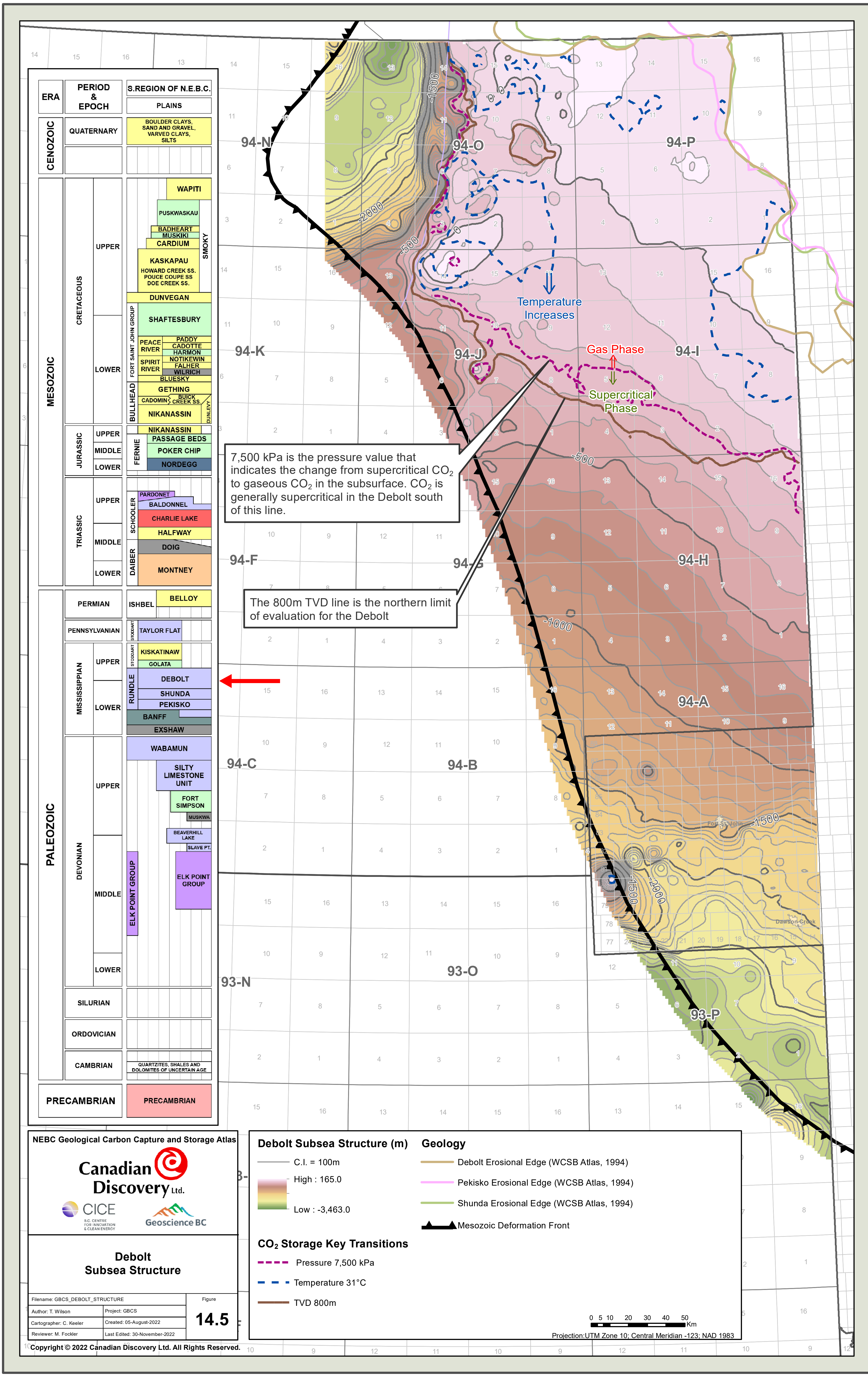

© Canadian Discovery Ltd. *Figure 14.5*

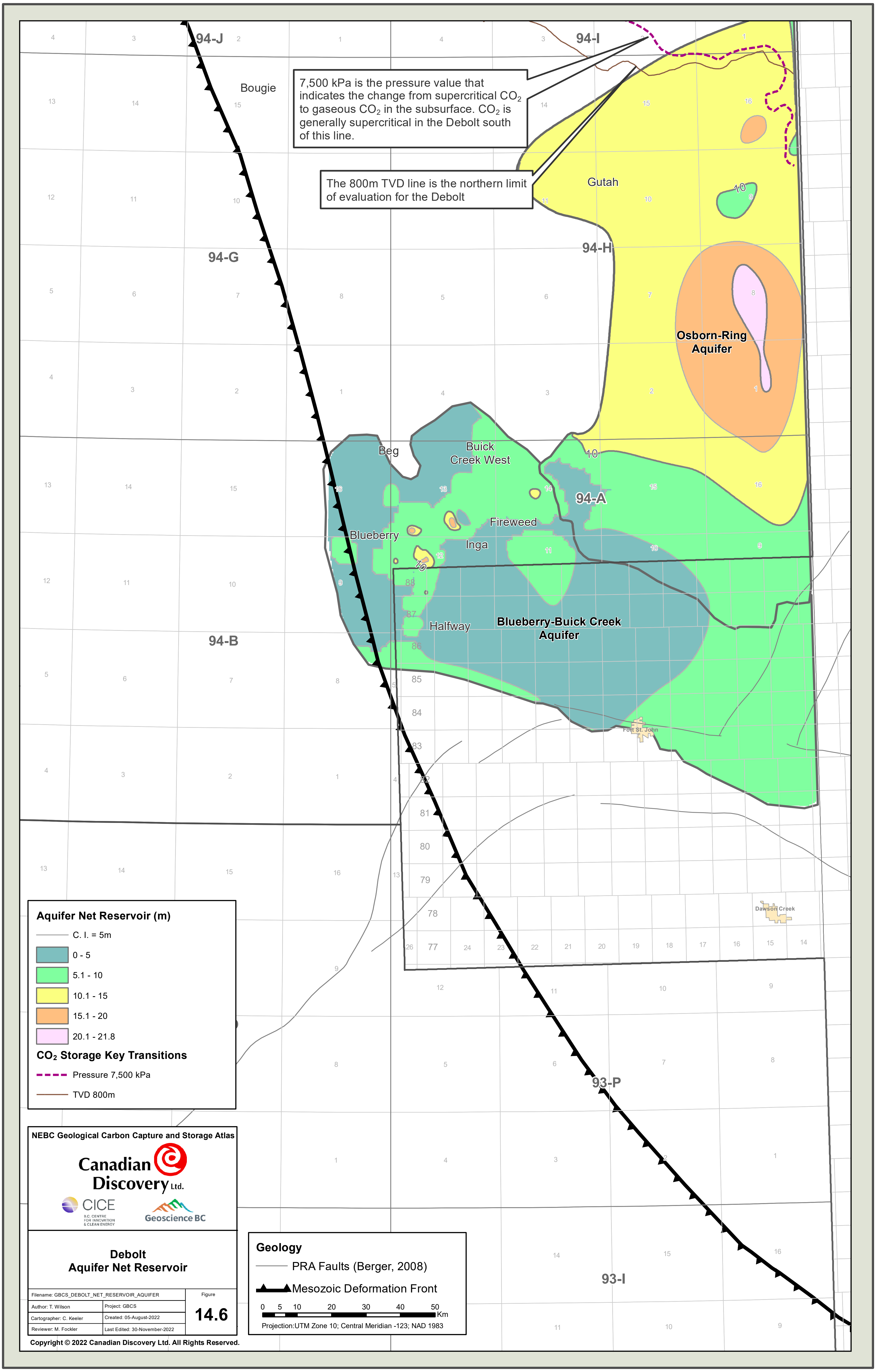
94-J
94-I
Bougie
7,500 kPa is the pressure value that indicates the change from supercritical CO_2 to gaseous CO_2 in the subsurface. CO_2 is generally supercritical in the Debolt south of this line.
The 800m TVD line is the northern limit of evaluation for the Debolt
Gutah
94-G
94-H
Osborn-Ring Aquifer
Beg
Buick Creek West
94-A
Blueberry
Fireweed
Inga
Halfway
Blueberry-Buick Creek Aquifer
94-B
Fort St. John
Dawson Creek
93-P
93-I
Aquifer Net Reservoir (m)
C. I. = 5m
0 - 5
5.1 - 10
10.1 - 15
15.1 - 20
20.1 - 21.8
CO_2 Storage Key Transitions
Pressure 7,500 kPa
TVD 800m
NEBC Geological Carbon Capture and Storage Atlas
Canadian Discovery Ltd.
CICE
Geoscience BC
Debolt Aquifer Net Reservoir
Filename: GBCS_DEBOLT_NET_RESERVOIR_AQUIFER
Author: T. Wilson
Project: GBCS
Cartographer: C. Keeler
Created: 05-August-2022
Reviewer: M. Fockler
Last Edited: 30-November-2022
Figure 14.6
Copyright © 2022 Canadian Discovery Ltd. All Rights Reserved.
Geology
PRA Faults (Berger, 2008)
Mesozoic Deformation Front
0 5 10 20 30 40 50 Km
Projection:UTM Zone 10; Central Meridian -123; NAD 1983

Figure 14.6

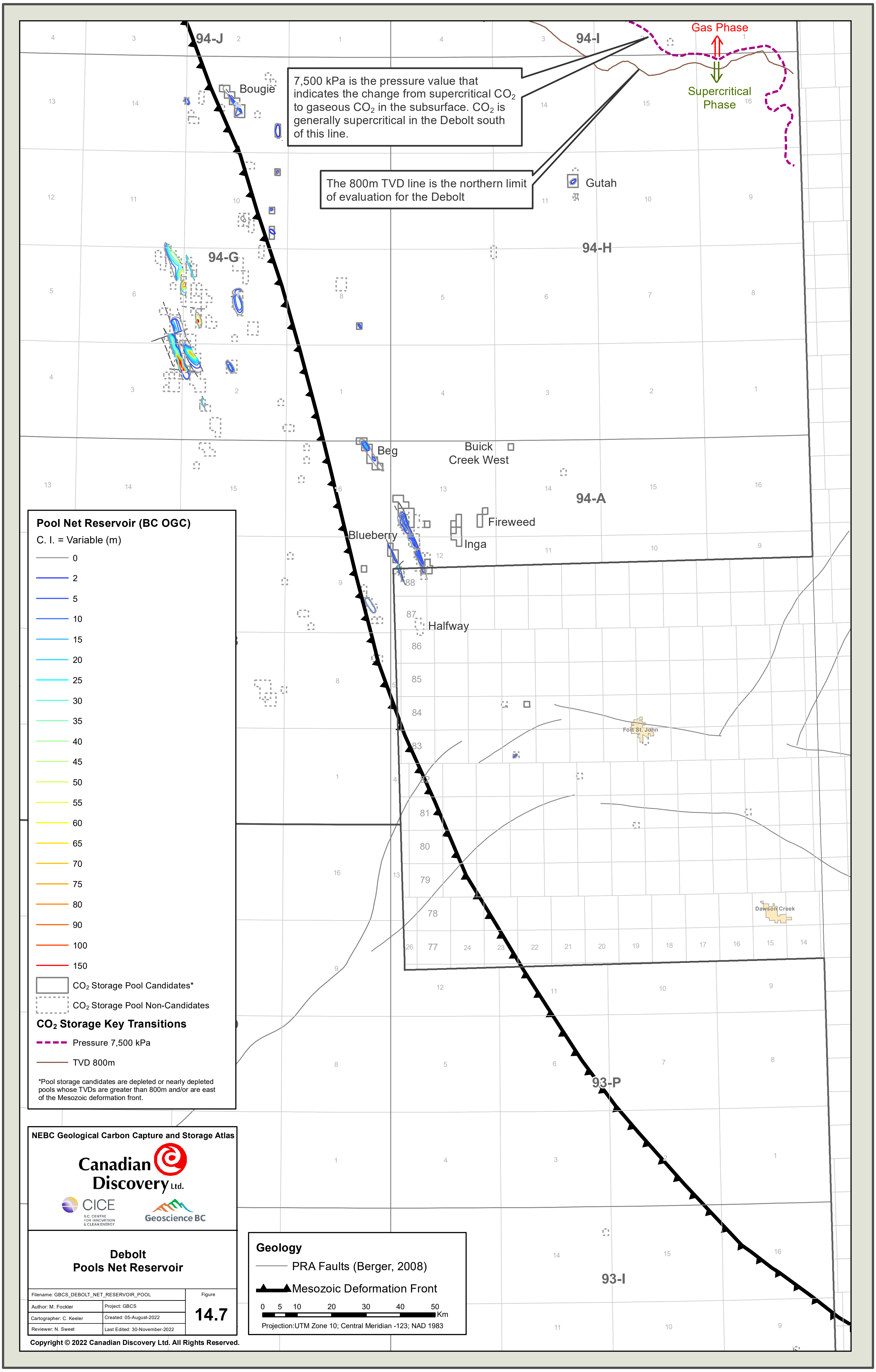
94-J
94-I
94-G
94-H
94-A
93-P
93-I
Gas Phase
Supercritical Phase
7,500 kPa is the pressure value that indicates the change from supercritical CO_2 to gaseous CO_2 in the subsurface. CO_2 is generally supercritical in the Debolt south of this line.
The 800m TVD line is the northern limit of evaluation for the Debolt
Bougie
Gutah
Beg
Buick Creek West
Fireweed
Blueberry
Inga
Halfway
Fort St. John
Dawson Creek
Pool Net Reservoir (BC OGC)
C. I. = Variable (m)
0
2
5
10
15
20
25
30
35
40
45
50
55
60
65
70
75
80
90
100
150
CO_2 Storage Pool Candidates*
CO_2 Storage Pool Non-Candidates
CO_2 Storage Key Transitions
Pressure 7,500 kPa
TVD 800m
*Pool storage candidates are depleted or nearly depleted pools whose TVDs are greater than 800m and/or are east of the Mesozoic deformation front.
NEBC Geological Carbon Capture and Storage Atlas
Canadian Discovery Ltd.
CICE
Geoscience BC
Debolt
Pools Net Reservoir
Filename: GBCS_DEBOLT_NET_RESERVOIR_POOL
Figure
14.7
Author: M. Fockler
Project: GBCS
Cartographer: C. Keeler
Created: 05-August-2022
Reviewer: N. Sweet
Last Edited: 30-November-2022
Copyright © 2022 Canadian Discovery Ltd. All Rights Reserved.
Geology
PRA Faults (Berger, 2008)
Mesozoic Deformation Front
0 5 10 20 30 40 50 Km
Projection:UTM Zone 10; Central Meridian -123; NAD 1983

Figure 14.7

Porosity-Permeability Correlations

Establishing detailed porosity trends requires examination of log suites and petrophysical models, which is beyond the scope of this phase of the Atlas. However, available core data can be used to provide a high level estimate of porosity trends, particularly within the aquifers, where this information is needed for storage potential estimates. Core data for the Debolt were obtained from geoLOGIC and filtered for better quality reservoir that is more conducive to carbon storage (greater than 6% porosity and 5 mD permeability) within the study area. Reservoirs are primarily low-temperature, fabric-selective dolomites, and data for these reservoirs were used to estimate porosity trends in the aquifers for storage calculations, and to do a preliminary analysis of the porosity-permeability trends *(figure 14.8)*.

14.8 Debolt Porosity-Permeability Plot

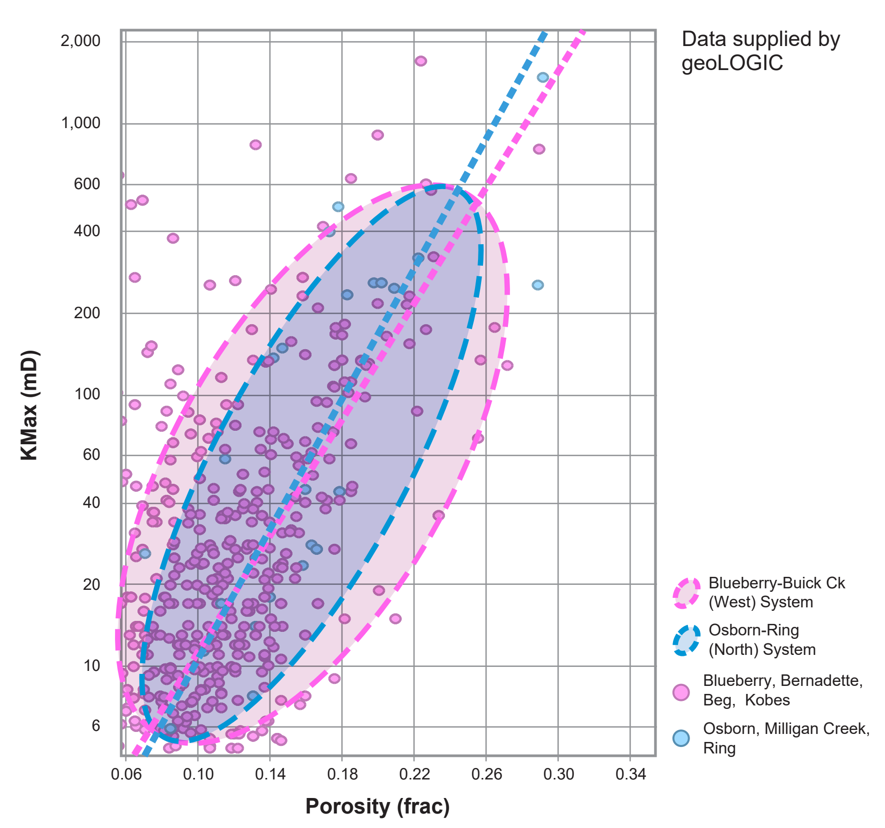

© Canadian Discovery Ltd. *Figure 14.8*

Hydrodynamics

To delineate the extent of the aquifers and understand the relationship between the aquifers and the depleted pools, a high-level analysis was done on Debolt hydrodynamics *(figure 14.9)* using Hydrofax drillstem test (DST) data from within the aquifers and the initial pressure and datum depth of each depleted pool from the BC OGC reserves databases.

Debolt aquifers that may be candidates for carbon storage are located in low-temperature dolomites along the northern border of the Peace River block, between Blueberry and Buick Creek (West system), and further north adjacent to the BC-Alberta border, between the Osborn and Ring areas (North system). Only the western aquifer hosts hydrocarbons within the prospective storage area, with most of the production occurring at Blueberry.

Aquifers within hydrothermal dolomites can also be found west of the Mesozoic deformation front around Pocketknife and Sikanni (PRCL, 2015); however, this area hosts considerable faulting and potential storage risk, so it was removed from consideration. The aquifers north of Ring were also removed from consideration due to their shallow depth.

In the Ring area, around 094-H-09 and 094-H-16, the Debolt aquifer is directly overlain by the Ladyfern-Ring Belloy aquifer, and the pressure regimes suggest that the aquifers may be in communication with each other. Detailed mapping is recommended to better characterize the extent of the connection between these aquifers, should a project be pursued in this area.

14.9 Debolt Pressure vs Elevation Plot

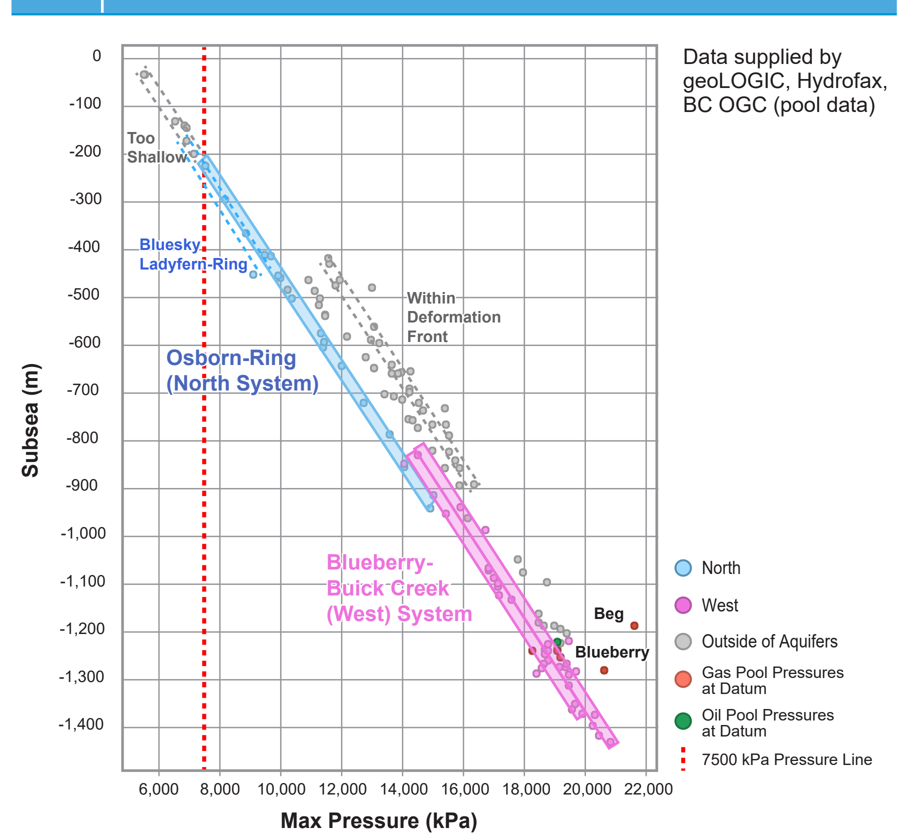

© Canadian Discovery Ltd. *Figure 14.9*

Carbon Storage Calculations

Depleted or Nearly Depleted Pools

The depleted and nearly depleted pool candidates for carbon storage potential within the Debolt Formation are shown in *table 14.2*.

The BC OGC defines depleted pools as ones that have no remaining reserves or production. The BC OGC also recognizes that there are nearly depleted pools that could become CO_2 storage candidates in the (relatively) near future. The nearly depleted CO_2 storage candidates include pools where 90+% of the reserves have been recovered, or no production has occurred in over five years. Furthermore, CDL has excluded pools that are shallower than 800m TVD, or are west of the Mesozoic deformation front. See Depleted Pools Selection Criteria in *Chapter 4* for a more thorough discussion.

In the table, the theoretical CO_2 storage potential represents the mass of CO_2 that can be stored in the hydrocarbon reservoirs assuming that the volume occupied previously by the produced gas will be occupied entirely by the injected CO_2. These calculations have been provided by the BC OGC and are based on historical pool production.

The effective CO_2 storage potential represents the mass of CO_2 that can be stored in hydrocarbon reservoirs after taking into account intrinsic reservoir characteristics and flow processes, such as heterogeneity (how much variability there is in the rock), aquifer support, sweep efficiency, gravity override, and CO_2 mobility (Bachu, 2006). The effective CO_2 storage potential is calculated by CDL and reduces the theoretical storage potential by as little as 13% and as much as 75%. More detail is provided on the carbon storage calculations for depleted pools in *Appendix B* and data are provided for all depleted pools included in this study in *Appendix C*.

The depleted and nearly depleted pools that are deemed to be CO_2 storage candidates by CDL are coloured by their effective storage potential mass on the summary map *(figure 14.10)*.

Aquifers

The Debolt aquifer parameters are summarized in *Table 14.3*. Theoretical CO_2 storage potential can be calculated using the mapped pore volume of the reservoir and CO_2 density, and assumes that the pore volume will be occupied entirely by the injected CO_2. We know this is not the case however, since the pore space is already occupied by water and the water will need to be displaced in the process. As a result, a storage efficiency factor is introduced into storage potential calculations that accounts for the presence of both water and CO_2 in the aquifer. The storage efficiency factor is a function of reservoir and fluid properties and dynamics, including the geometry of the trap, gravity segregation, heterogeneity, permeability distribution and pressure, and may reduce the theoretical storage potential by 95 to 99%.

Aquifers considered favourable targets for CO_2 storage are indicated on the summary map *(figure 14.10)* and labelled with their estimated P10, P50 and P90 effective storage potential in Mt. More detail is provided on the aquifer carbon storage calculations in *Appendix B*.

Depleted Debolt Pools

Pool Name	Pool Type	Well Count	Initial Pressure (kPa)	Temperature (˚C)	Average Porosity (%)	CO_2 Phase	Theoretical Storage Potential (Mt)	Effective Storage Potential (Mt)
Blueberry Debolt F	Gas	3	17,250	75	9.1	Supercritical	1.7	1.5
Blueberry Debolt H	Gas	4	17,029	80	5.9	Supercritical	0.9	0.6
Other Areas Debolt D-027-H/094-G-10	Gas	1	15,899	80	9.1	Supercritical	0.6	0.5
Beg Debolt A	Gas	2	21,622	87	10.0	Supercritical	0.7	0.5
Blueberry Debolt G	Gas	1	14,576	64	11.3	Supercritical	0.6	0.4
Blueberry Debolt C	Gas	1	20,631	74	6.8	Supercritical	0.4	0.3
Blueberry West Debolt A	Gas	1	18,270	75	11.9	Supercritical	0.2	0.1
Bougie Debolt C	Gas	6	12,408	63	8.7	Supercritical	0.1	0.1
Green Creek Debolt E	Gas	1	15,705	78	3.4	Supercritical	0.1	0.1
Beg Debolt B	Gas	1	20,196	89	7.6	Supercritical	0.1	0.1
Bougie Debolt E	Gas	2	12,600	67	6.2	Supercritical	0.1	0.1

Table 14.2

Debolt Aquifer Properties and Storage Potential

Aquifer Name	Type	Thickness Range (m)	Pressure Range (MPa)	Temperature Range (˚C)	Porosity Range (%)	CO_2 Phase	P10 Effective Storage Potential at 0.5% (Mt)	P50 Effective Storage Potential at 2% (Mt)	P90 Effective Storage Potential at 5.4% (Mt)
Osborn-Ring	Aquifer	4-22	6.6-15	39-82	5-17	Mostly Supercritical	19.7	78.9	213.1
Blueberry-Buick Creek	Aquifer	<2-30	15-25	42-99	4-17	Mostly Supercritical	7.7	30.7	82.8

Table 14.3

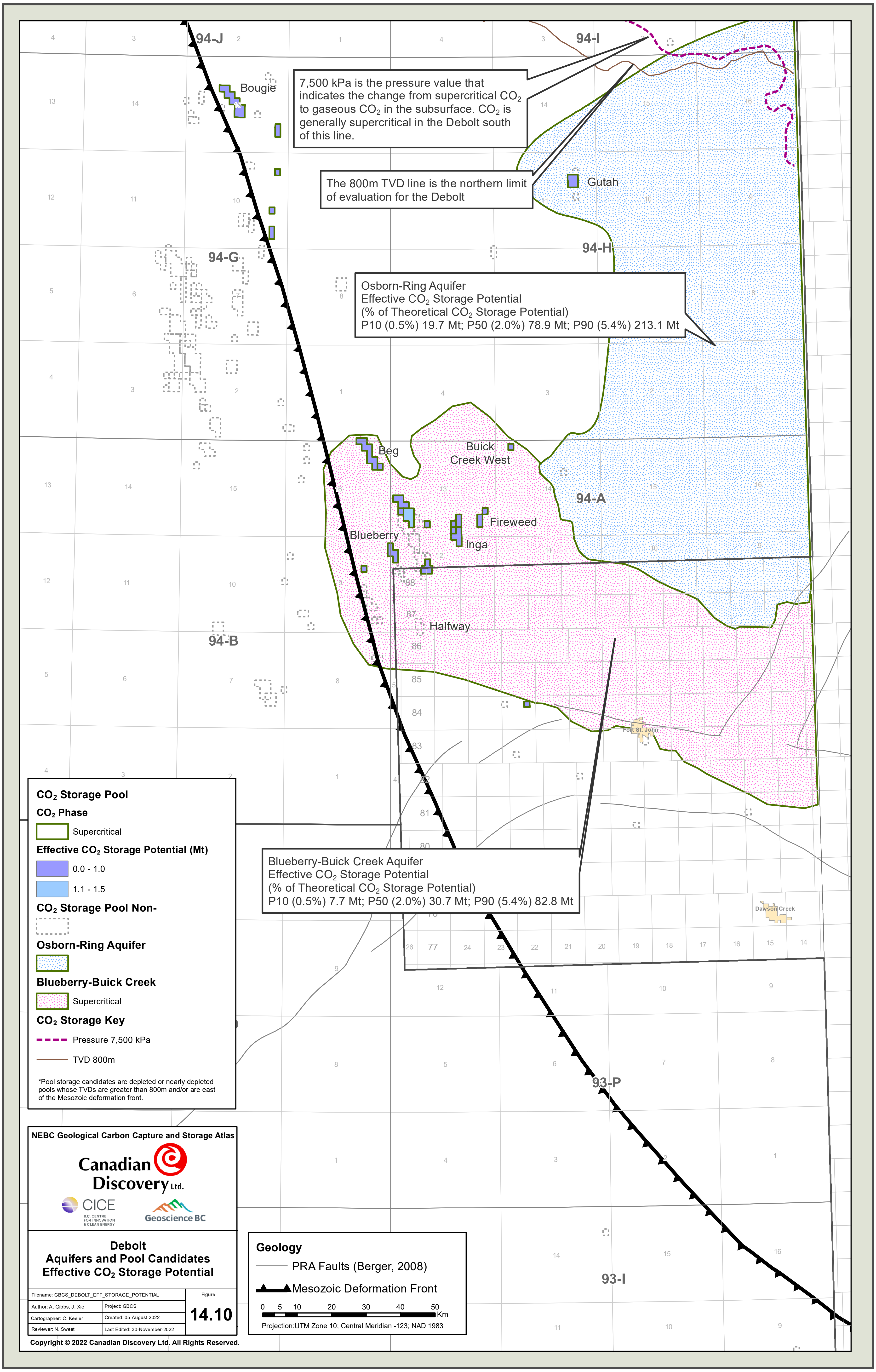

© Canadian Discovery Ltd.

Figure 14.10

Jean Marie Formation

Jean Marie Overview

Storage potential in the Jean Marie *(figure 15.1)* occurs northeast of Fort Nelson in the northernmost reaches of the study area. Favourability attributes are summarized in *table 15.1* with green and yellow circles indicating whether an attribute is considered generally favourable (green) or has risk and requires additional work (yellow). As there is no aquifer potential, only depleted pool reservoirs are candidates for storage opportunities. The areally large Jean Marie Helmet A Pool is the only depleted pool in this zone; the rest of the Jean Marie pools are still producing gas and therefore are not candidates for carbon storage at this time. The top (only) depleted pool is shown in *figure 15.2*. *Figure 15.3* displays the effective storage potential of the Jean Marie, as well as the emitters and infrastructure in the NEBC study area.

Jean Marie Favourability Attributes

Top 10 Depleted Pool Total Potential	80 Mt	yellow
Aquifer Storage (P50)	n/a	
Regional Seal Potential	High	green
Lithology	Limestone	green
Porosity	5-8%	yellow
Permeability	<10 mD	yellow
Depth (TVD)	1,000-1,700m	green
Net Reservoir Thickness	2-30m	green

Table 15.1

15.1 Hydrostratigraphic Chart

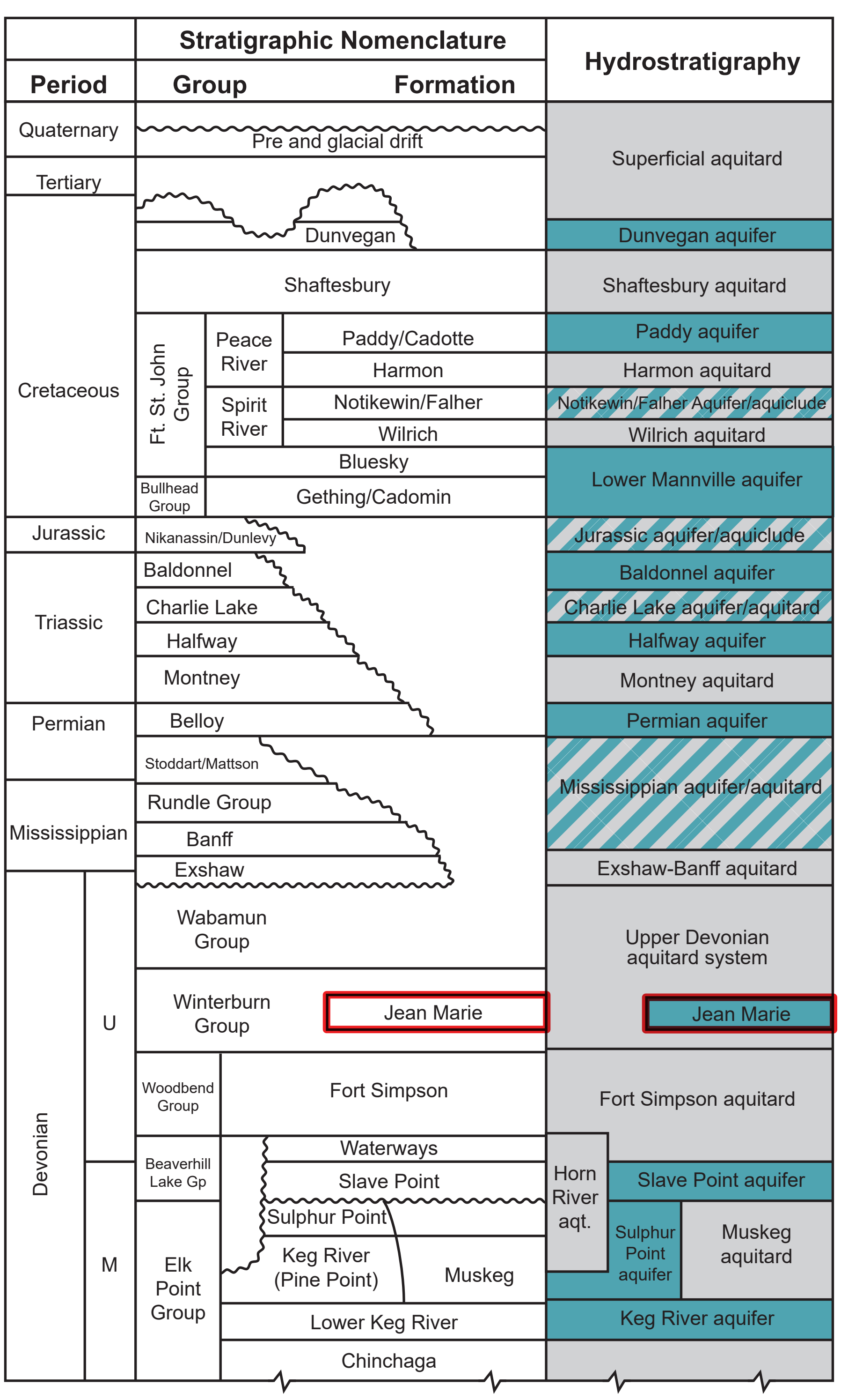

Modified from Bachu, 2006

© Canadian Discovery Ltd. *Figure 15.1*

15.2 Depleted Jean Marie Pools

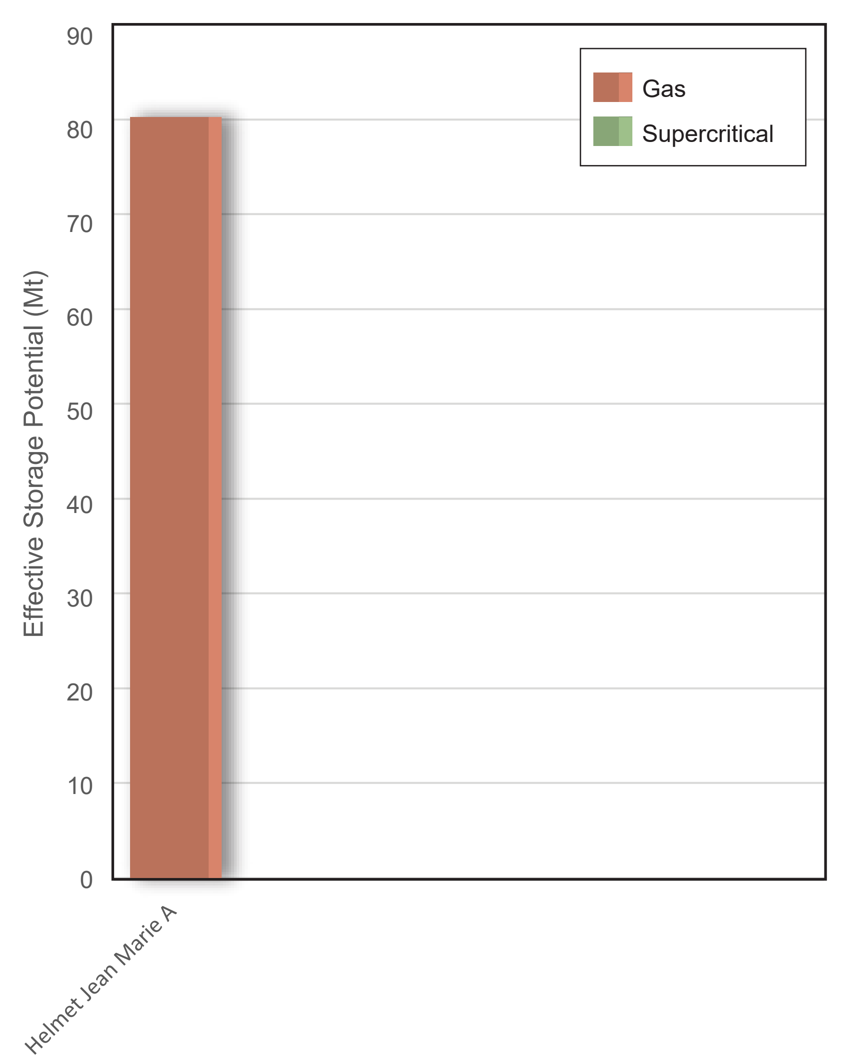

© Canadian Discovery Ltd. *Figure 15.2*

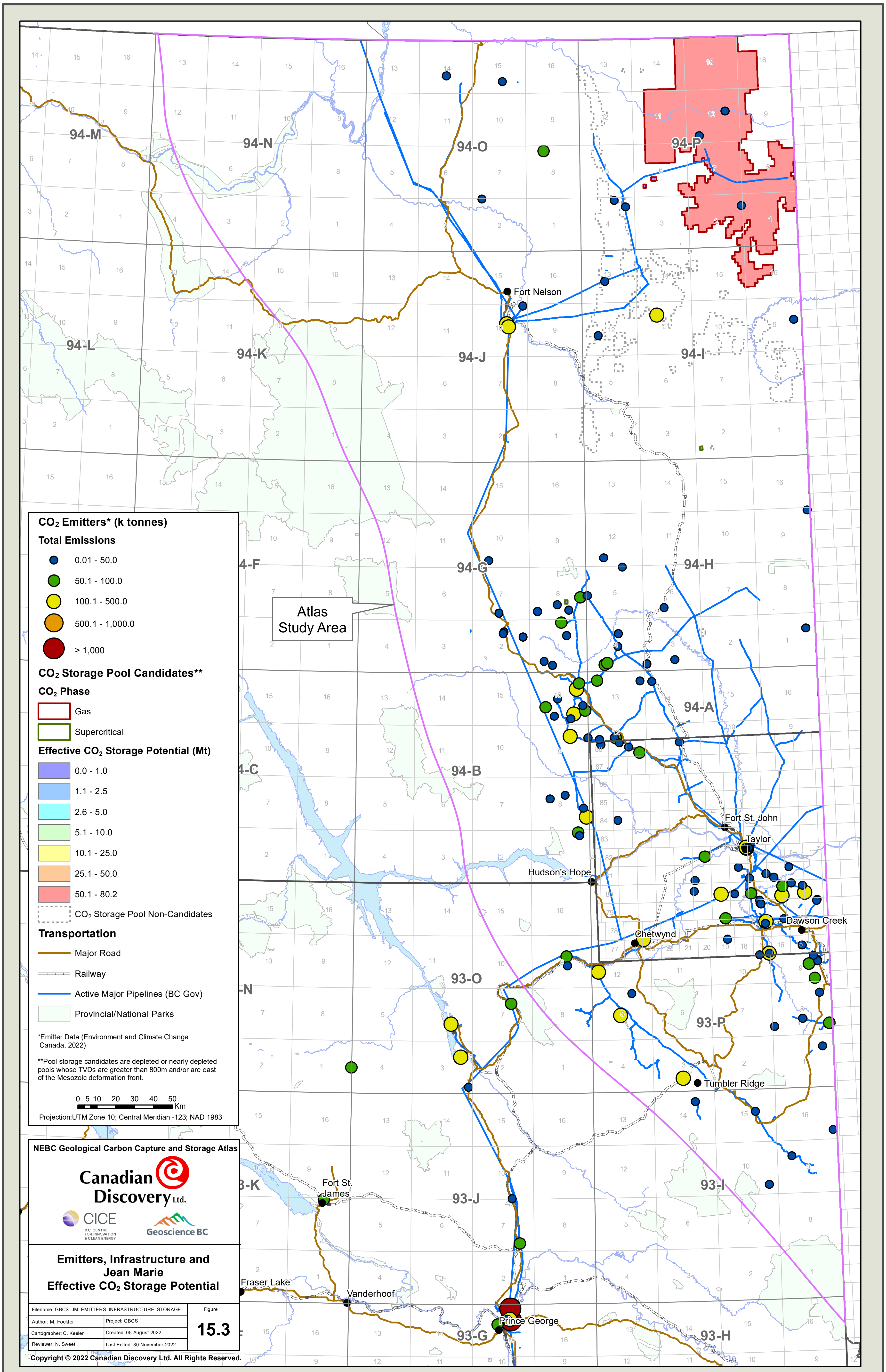

© Canadian Discovery Ltd.

Figure 15.3

15.4 Jean Marie Play Schematic

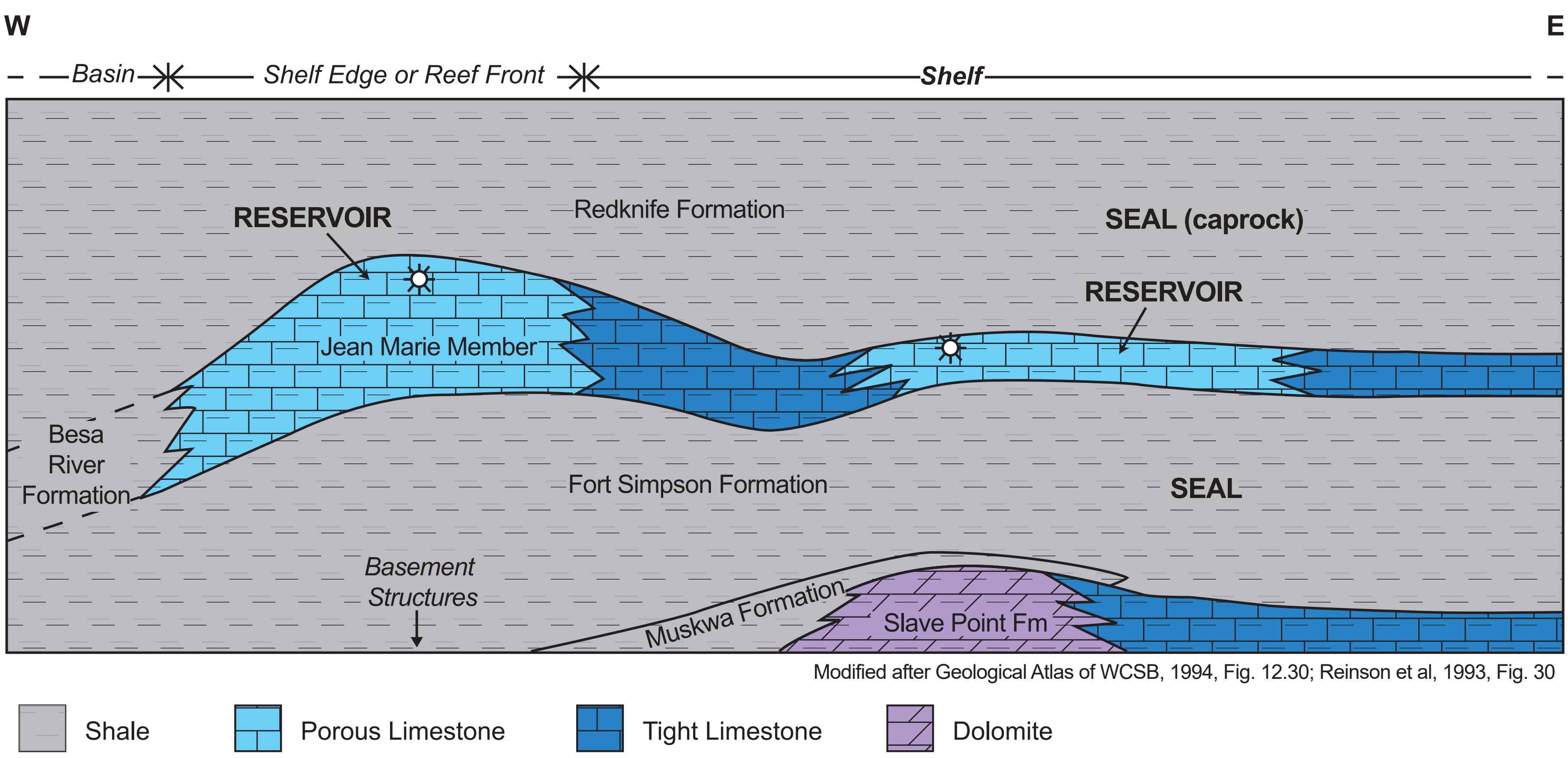

Figure 15.4

Storage Complex

The Late Devonian-age Jean Marie was deposited as a broad, shallow marine limestone shelf *(figure 15.4)* under moderate energy conditions (McAdam, 1993). It varies from 10–25m thick across NEBC and adjacent Alberta, thickening abruptly westward to a north-south-oriented shelf margin with a barrier reef that reaches over 90m in thickness. The Jean Marie shales out abruptly to the west of this reef. Overlying a basal crinoidal wackestone ramp, three transgressive-regressive (sea level rise and fall) cycles grade from relatively deep-water coralline limestones to shallower-water reefal facies.

Wackestone of the basal ramp thicken along the western margin of the Jean Marie platform, where it makes up the basal third to half of the formation. Above this, grainstone and broken reefal debris dominate the section, exhibiting relatively low-grade conventional to tight reservoir quality over a section ranging in excess of 50m. Although of lower quality than the platform reef "sweet spots", the platform margin reef detritus is consistently developed and highly mappable (NEBC Play Atlas, 2006). The entire Jean Marie is considered under-saturated with respect to water and therefore is not considered a saline aquifer candidate. Lateral, underlying and overlying shale of the Fort Simpson and Redknife formations, respectively, encase the Jean Marie and the formation is considered a closed system.

Net reservoir thickness in the depleted Helmet A Pool is relatively thin (up to 16m, but mostly in the 6–8m range) compared to the non-depleted pools along the Jean Marie shelf edge where net reservoir can reach 30m *(figure 15.5)*. The net reservoir map can help indicate the most favourable areas for CO_2 injection within storage reservoirs; i.e. where the reservoir rock has the highest quality and most often the highest porosity and permeability. The net reservoir contours within the pools were provided by the BC Oil and Gas Commission (OGC).

The Jean Marie is an underpressured system and the pressure does not reach the 7,500 kPa considered optimal for supercritical conditions for CO_2 storage.

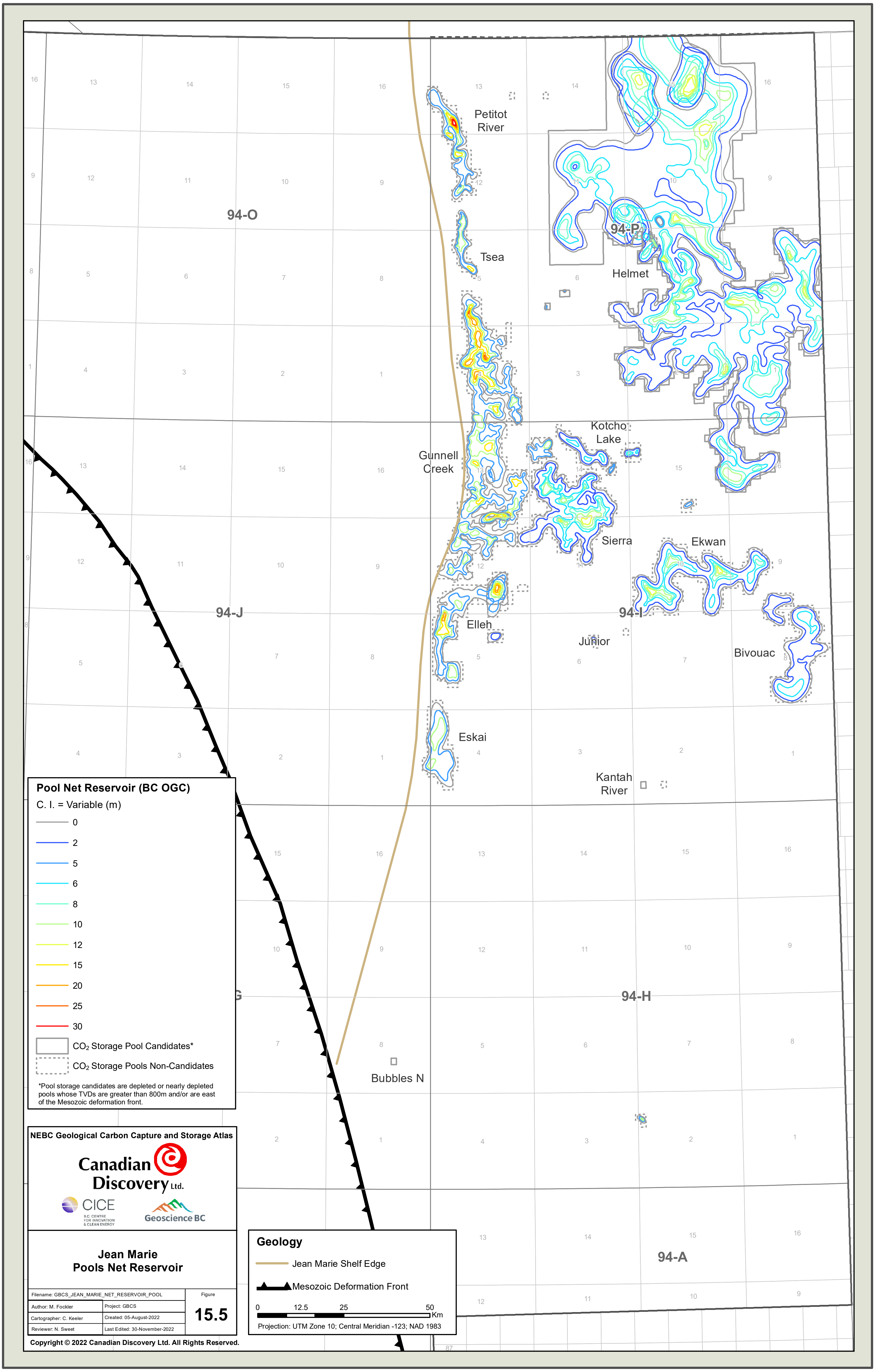

Petitot River
Tsea
Helmet
94-O
94-P
Kotcho Lake
Gunnell Creek
Sierra
Ekwan
94-J
94-I
Elleh
Junior
Bivouac
Eskai
Kantah River
94-H
Bubbles N
94-A
Pool Net Reservoir (BC OGC)
C. I. = Variable (m)
0
2
5
6
8
10
12
15
20
25
30
CO2 Storage Pool Candidates*
CO2 Storage Pools Non-Candidates
*Pool storage candidates are depleted or nearly depleted pools whose TVDs are greater than 800m and/or are east of the Mesozoic deformation front.
NEBC Geological Carbon Capture and Storage Atlas
Canadian Discovery Ltd.
CICE
Geoscience BC
Jean Marie Pools Net Reservoir
Filename: GBCS_JEAN_MARIE_NET_RESERVOIR_POOL
Figure
15.5
Author: M. Fockler
Project: GBCS
Cartographer: C. Keeler
Created: 05-August-2022
Reviewer: N. Sweet
Last Edited: 30-November-2022
Copyright © 2022 Canadian Discovery Ltd. All Rights Reserved.
Geology
Jean Marie Shelf Edge
Mesozoic Deformation Front
0 12.5 25 50 Km
Projection: UTM Zone 10; Central Meridian -123; NAD 1983

Figure 15.5

Carbon Storage Calculations

Depleted and Nearly Depleted Pools

The only depleted pool candidate for carbon storage potential within the Jean Marie Formation is shown in *table 15.2*.

The BC OGC defines depleted pools as ones that have no remaining reserves or production. The BC OGC also recognizes that there are nearly depleted pools that could become CO_2 storage candidates in the (relatively) near future. The nearly depleted CO_2 storage candidates include pools where 90%+ of the reserves have been recovered, or no production has occurred in over five years. Furthermore, CDL has excluded pools that are shallower than 800m TVD, or are west of the Mesozoic deformation front. See Depleted Pools Selection Criteria in *Chapter 4* for a more thorough discussion.

The theoretical CO_2 storage potential represents the mass of CO_2 that can be stored in the hydrocarbon reservoirs assuming that the volume occupied previously by the produced gas will be occupied entirely by the injected CO_2. These calculations have been provided by the BC OGC and are based on historical pool production.

The effective CO_2 storage potential represents the mass of CO_2 that can be stored in hydrocarbon reservoirs after taking into account intrinsic reservoir characteristics and flow processes, such as heterogeneity (how much variability there is in the rock), aquifer support, sweep efficiency, gravity override, and CO_2 mobility (Bachu, 2006). The effective CO_2 storage potential is calculated by CDL and reduces the theoretical storage potential by as little as 13% and as much as 75%. More detail is provided on the carbon storage calculations for depleted pools in *Appendix B*, and data are provided for all depleted pools included in this study in *Appendix C*.

The depleted and nearly depleted pools that are deemed to be CO_2 storage candidates by CDL are coloured by their effective storage potential mass on the summary map *(figure 15.6)*.

Aquifers

There are no aquifers associated with the Jean Marie Formation and the zone is considered under-saturated with respect to water.

Depleted Jean Marie Pool

Pool Name	Pool Type	Well Count	Initial Pressure (kPa)	Temperature (˚C)	Average Porosity (%)	CO_2 Phase	Theoretical Storage Potential (Mt)	Effective Storage Potential (Mt)
Helmet Jean Marie A	Gas	890	6,881	63	5.7	Gas	91.9	80.2

© Canadian Discovery Ltd. Data supplied by BC OGC and Canadian Discovery Ltd. *Table 15.2*

15.6 | Jean Marie Pool Candidates Effective CO_2 Storage Potential

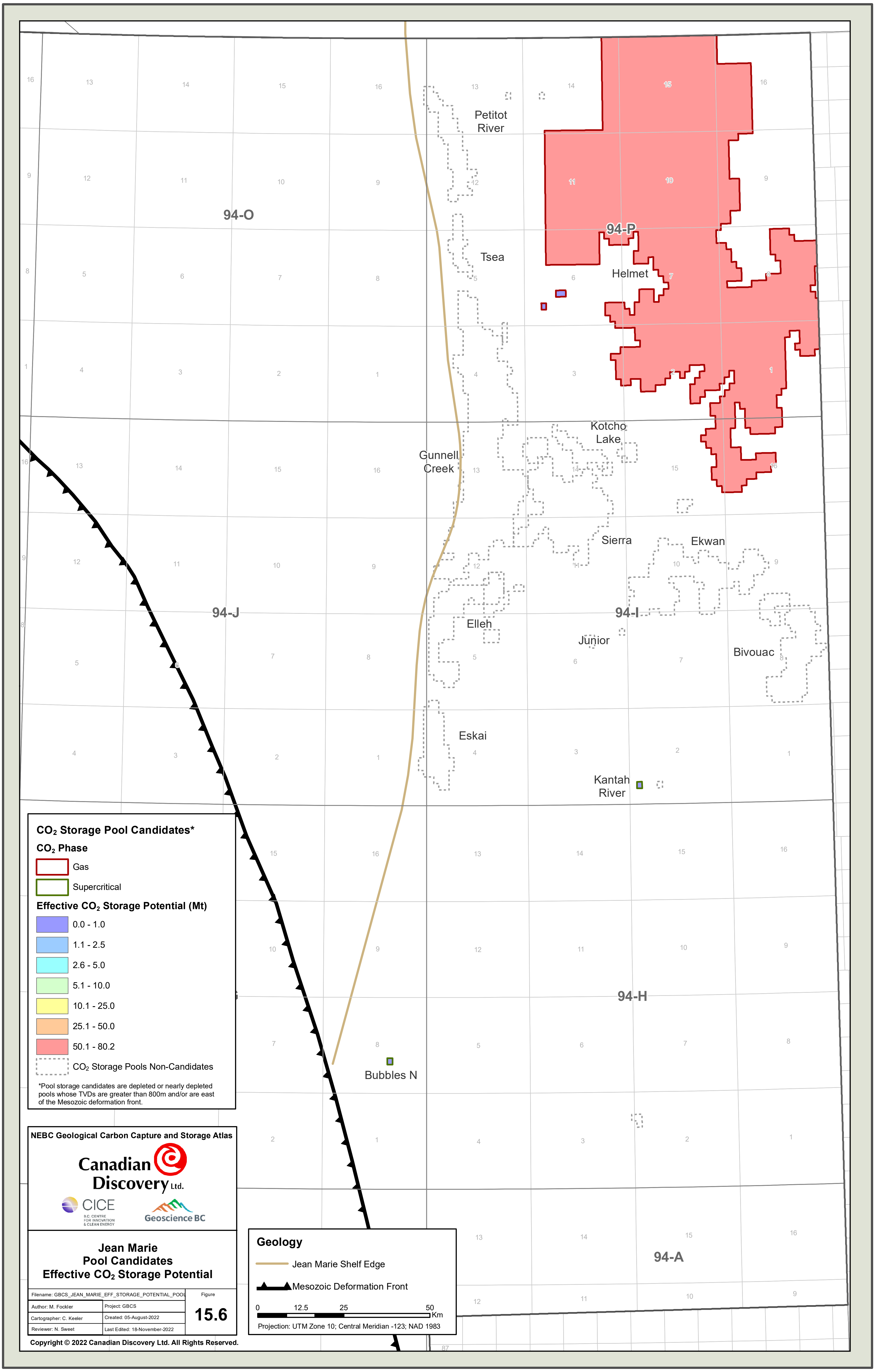

Figure 15.6

Middle Devonian Carbonates (Slave Point–Keg River) Overview

Storage potential in the Middle Devonian Carbonates *(figure 16.1)*, specifically the Slave Point to Keg River successions, extends from the Yukon border to north of Fort St. John. Favourability attributes are summarized in *table 16.1* with green and yellow circles indicating whether an attribute is considered generally favourable (green) or has risk and requires additional work (yellow). Both depleted pool reservoirs and saline aquifers are excellent candidates and offer a range of storage opportunities. The top 10 depleted pools are shown in *figure 16.2*. *Figure 16.3* displays the effective storage potential of the Middle Devonian Carbonates, as well as emitters and infrastructure in the NEBC study area.

Middle Devonian Carbonates Favourability Attributes		
Top 10 Depleted Pool Total Potential	295 Mt	●
Aquifer Storage (P50)	1,652 Mt	●
Regional Seal Potential	High	●
Lithology	Dolomite	●
Porosity	6-30%	●
Permeability	10-200 mD	●
Depth (TVD)	1,700-3,200m	●
Net Reservoir Thickness	5-275m	●

Table 16.1

16.1 Hydrostratigraphic Chart

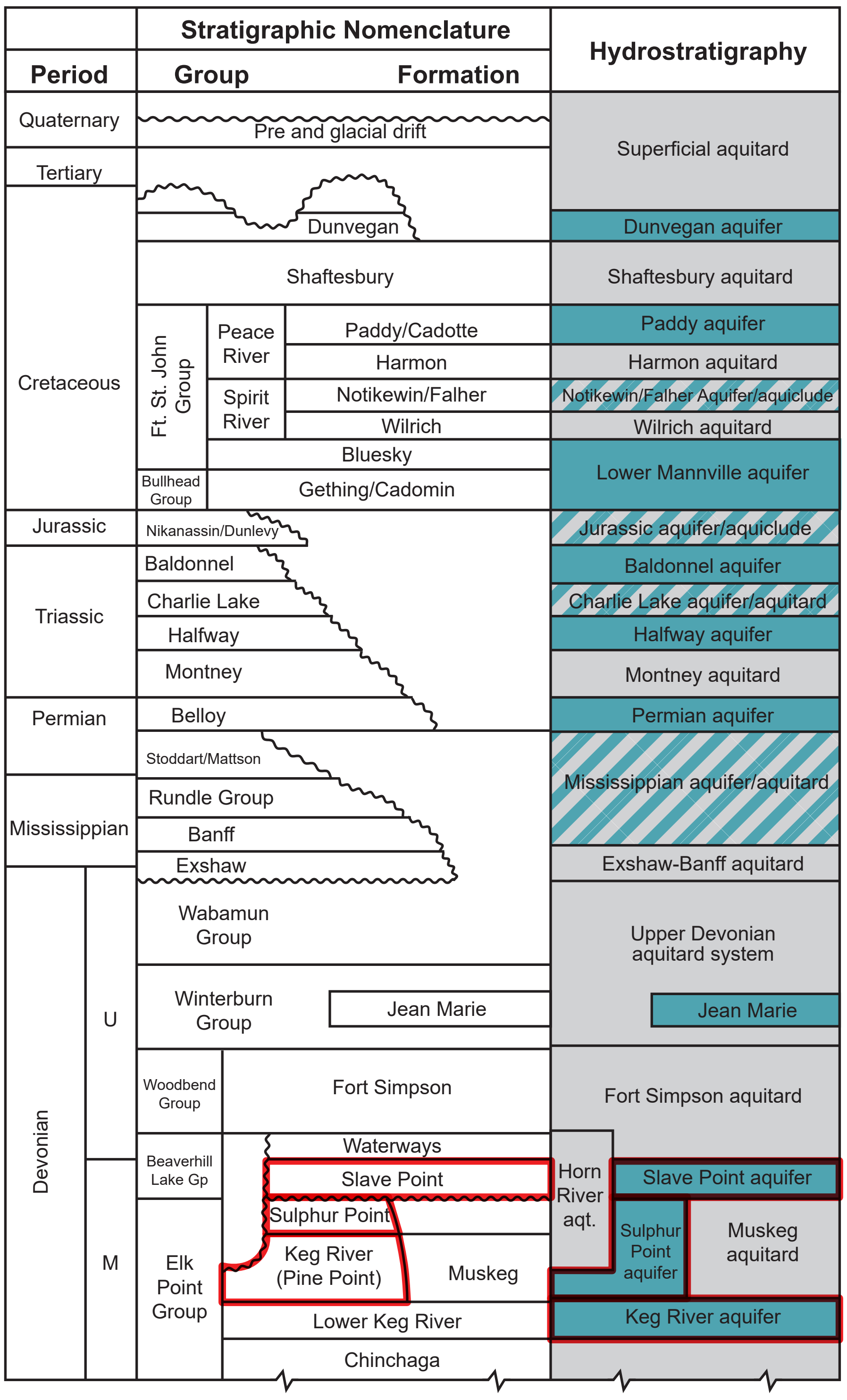

© Canadian Discovery Ltd. *Figure 16.1*

16.2 Top 10 Depleted Middle Devonian Carbonates Pools

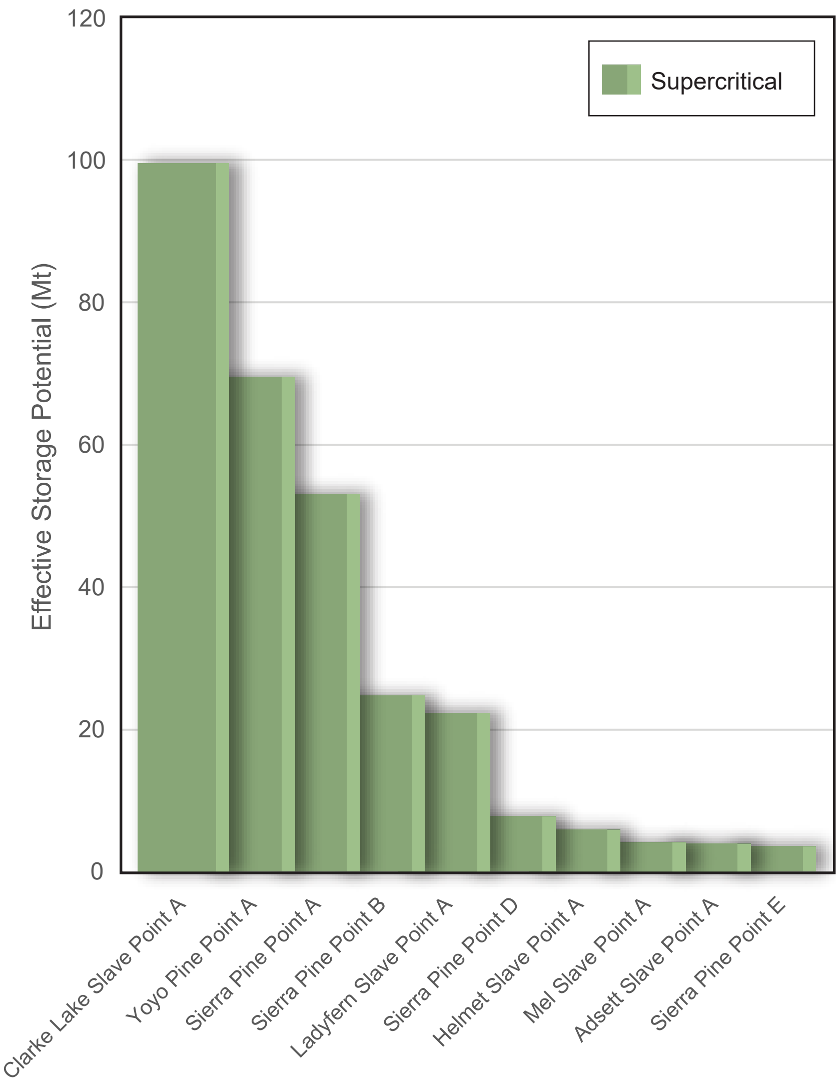

© Canadian Discovery Ltd. *Figure 16.2*

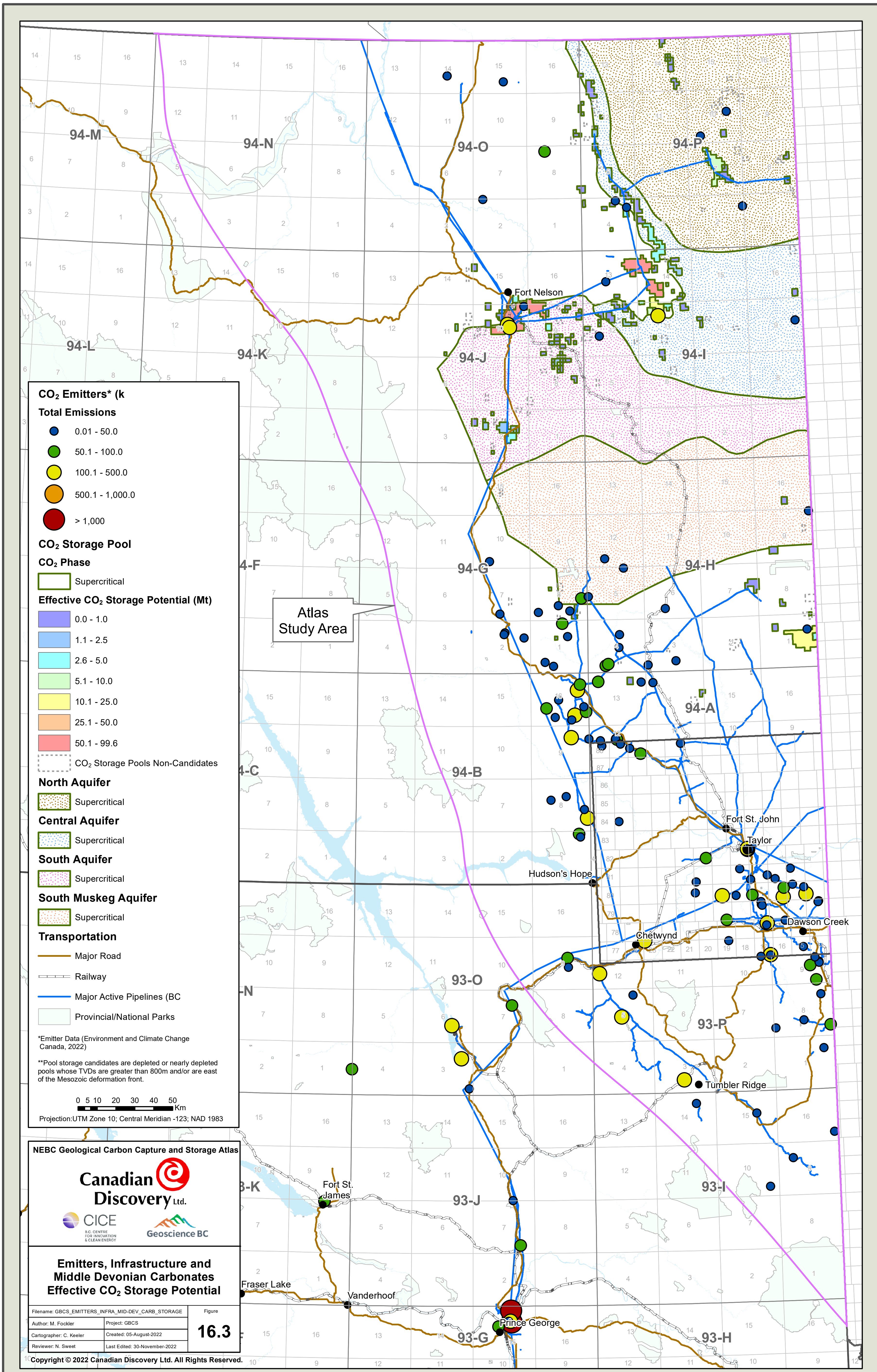

© Canadian Discovery Ltd.

Figure 16.3

16.4 Middle Devonian Carbonates Play Schematic

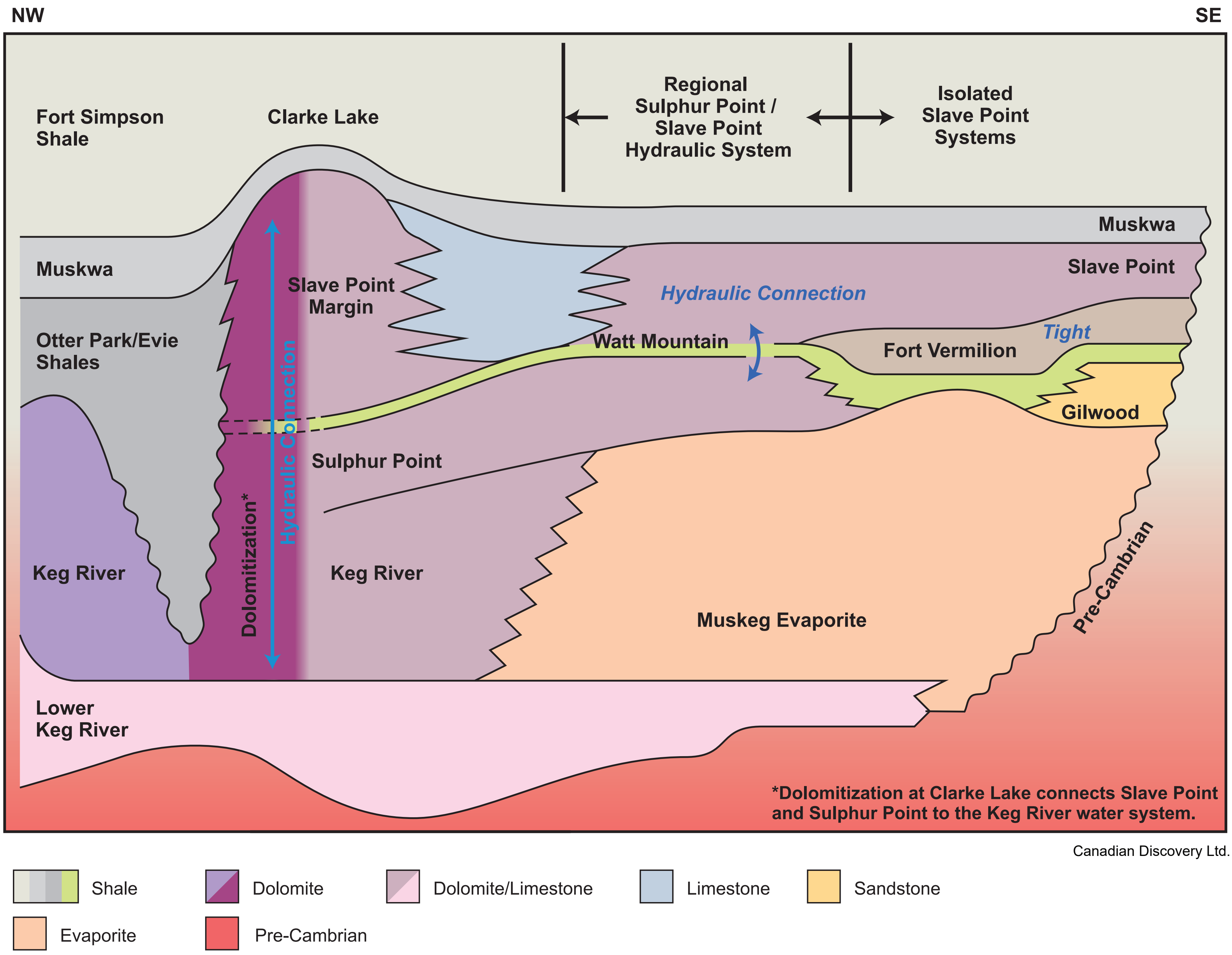

Figure 16.4

Storage Complex

The Middle Devonian Carbonate complex comprises the Slave Point, Sulphur Point and Keg River successions *(figure 16.4)*. Due to geological complexity, which leads to inconsistencies in the oil and gas industry's stratigraphic tops, the public tops database is not consistent and reliable. Because of these inconsistencies, the Slave Point, Sulphur Point, Keg River and Pine Point formations are mapped as one unit and referred to as "Middle Devonian Carbonates" for practicality and simplicity for this Atlas. These stacked carbonates are also in pressure communication over much of the area, supporting the approach of evaluating these units as one package.

Containment for CO_2 storage is provided by the overlying regional shales of the Fort Simpson and Muskwa formations. This shale package is over 500m thick, regionally widespread, and acts as a very competent caprock. Laterally, the Horn River Formation provides a thick and competent seal to the north and west of the main reef edge *(figure 16.4)*.

Geological Background

The carbonates, which were initially deposited as limestone and anhydrite, have undergone extensive dolomitization in some areas resulting in reservoirs that have high porosity and permeability. Because of this high porosity and permeability, drilling fluid losses were common, and therefore, not all wells have log suites or useful core, leading to sample bias.

Lower Keg River carbonates, which are typically dolomitized and underlie the entire carbonate complex, were deposited near the beginning of a widespread transgressive episode (sea level rise). Upper Keg River strata consist of stacked shoaling-upward carbonate cycles, capped by high-energy skeletal/reefal debris (Ministry of Energy and Mines, 2003). These banks reach thicknesses of more than 200m, and amalgamate with the Sulphur Point and Slave Point to form the dolomitized barrier reef at Clarke Lake. Isolated Upper Keg River buildups occur adjacent to the banks, their growth apparently nucleated over elevated fault blocks in the Horn River Shale Basin.

Slave Point strata form a thick and complex carbonate platform, comprising several stacked shallowing-upward cycles. High-energy reefal carbonate was deposited primarily along platform-margin banks in upper Slave Point cycles, although some banks are found on the margins of the Hotchkiss Embayment to the south, and along lesser embayments within the main platform. Otter Park marine shales accumulated during Slave Point time in the Horn River and Cordova embayments to the north, within the Hotchkiss Embayment and smaller platform embayments to the south (Meijer-Drees, 1994).

The Keg River interfingers southward with Muskeg Formation evaporites, and basinward with marine shales of the Evie Formation; both act as lateral seals for the Keg River. Overlying Fort Simpson and Muskwa shales are over 500m thick, regionally widespread, and act as very competent caprocks. Laterally the Horn River provides a thick and competent seal to the north and west of the main reef edge *(figure 16.4)*.

At the Clarke Lake reef complex, the very thick reservoir comprises stacked Slave Point, Sulphur Point and Keg River hydrothermal dolomites with good vertical reservoir continuity. Representative core data can be scarce because the vuggy and fractured nature of the hydrothermal dolomite makes it difficult to obtain a competent core for analyses — as the core tends to be rubble in the core barrel.

Previous studies have modeled the storage potential (Sorensen et al, 2014), and injectivity and flow potential (Sorensen et al, 2014, Walsh, 2013) of the Middle Devonian Carbonates near Fort Nelson. The studies showed that there is large storage potential, good injectivity and sufficient containment making this area a very good candidate for storage. Spectra (Sorensen et al, 2014) drilled a pilot injection well to attain detailed reservoir data and readers are directed to this study for further information. The Clarke Lake Pool updip from this pilot well is a depleted gas pool that is now being used as a geothermal energy project (Tu Dey-Kah Geothermal) and further work is required to prove that there would not be negative interference to this project.

Mapping the Complex

The Slave Point structure map *(figure 16.5)* shows the topography of the top of the Slave Point (the uppermost Middle Devonian Carbonate) in the subsurface. Since the displacement of a CO_2 plume is governed by gravity and buoyancy, the plume tends to migrate up-structure during its injection period. The entire Middle Devonian Carbonates area is within supercritical conditions for CO_2 injection as the temperature and pressure exceed 31.1°C and 7,500 kPa, respectively.

There was no regional net reservoir mapping available, so a net-to-gross mapping strategy was used to provide an estimation of net reservoir and available pore space within the aquifers *(figure 16.6)*. A gross isopach was mapped over the entire complex, from the top Slave Point to base Keg River. Net reservoir was estimated locally in several areas by targeting wells with good log data and well penetration through the entire section; these values, as well as general facies mapping to define trends, were used to calibrate net-to-gross values and to provide a high level estimate of net reservoir regionally. The paucity of wells that fully penetrate the entire storage complex leads to a poor distribution of data. The net reservoir map therefore requires more data to be truly reflective of actual reservoir potential. If planning a project in this zone, a more detailed assessment of stratigraphy is required to better delineate net reservoir trends and aquifer extent and connectivity. The net reservoir contours within the depleted pools were provided by the BC Oil and Gas Commission (BC OGC) *(figure 16.7)*.

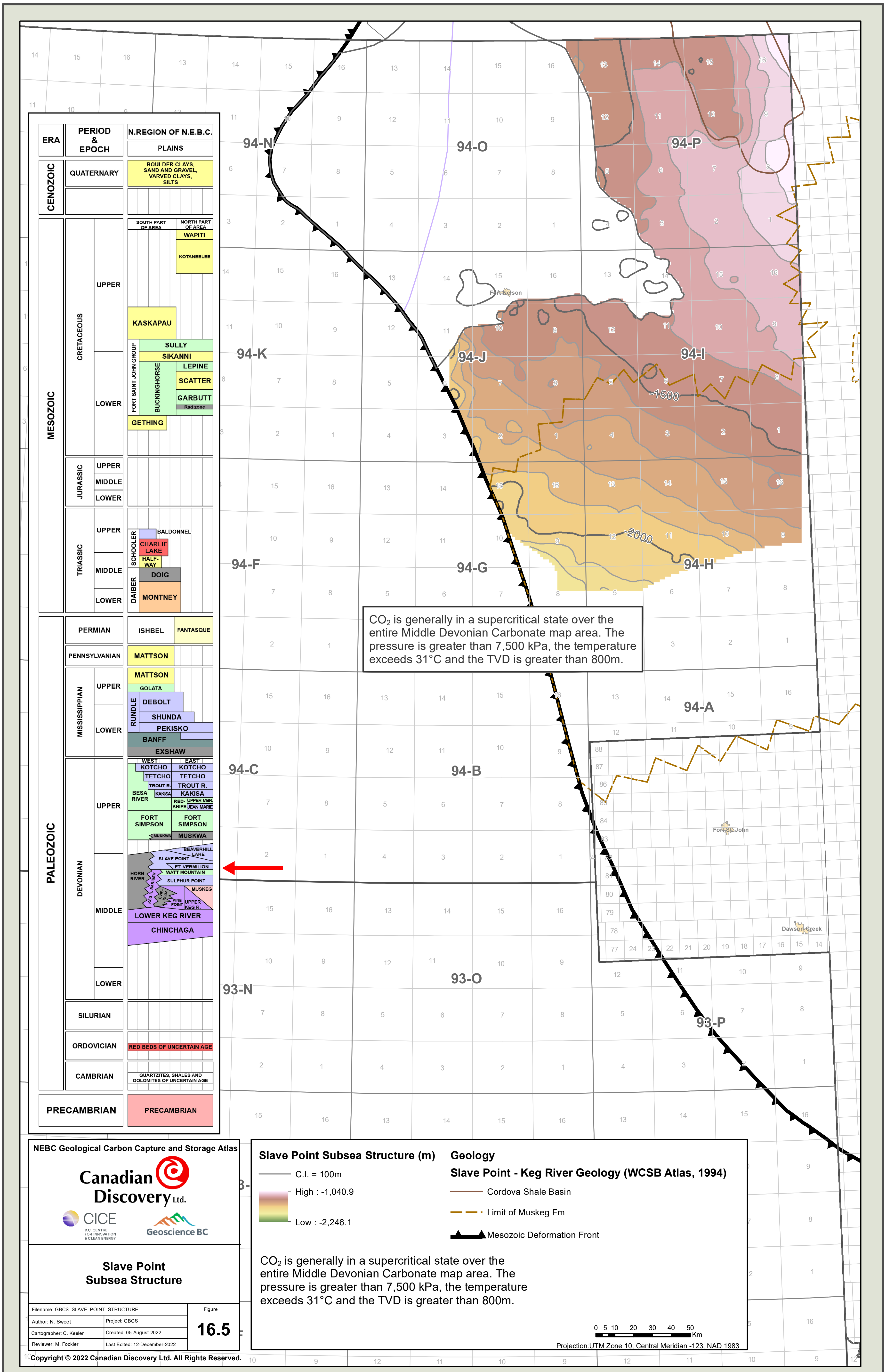

© Canadian Discovery Ltd.

Figure 16.5

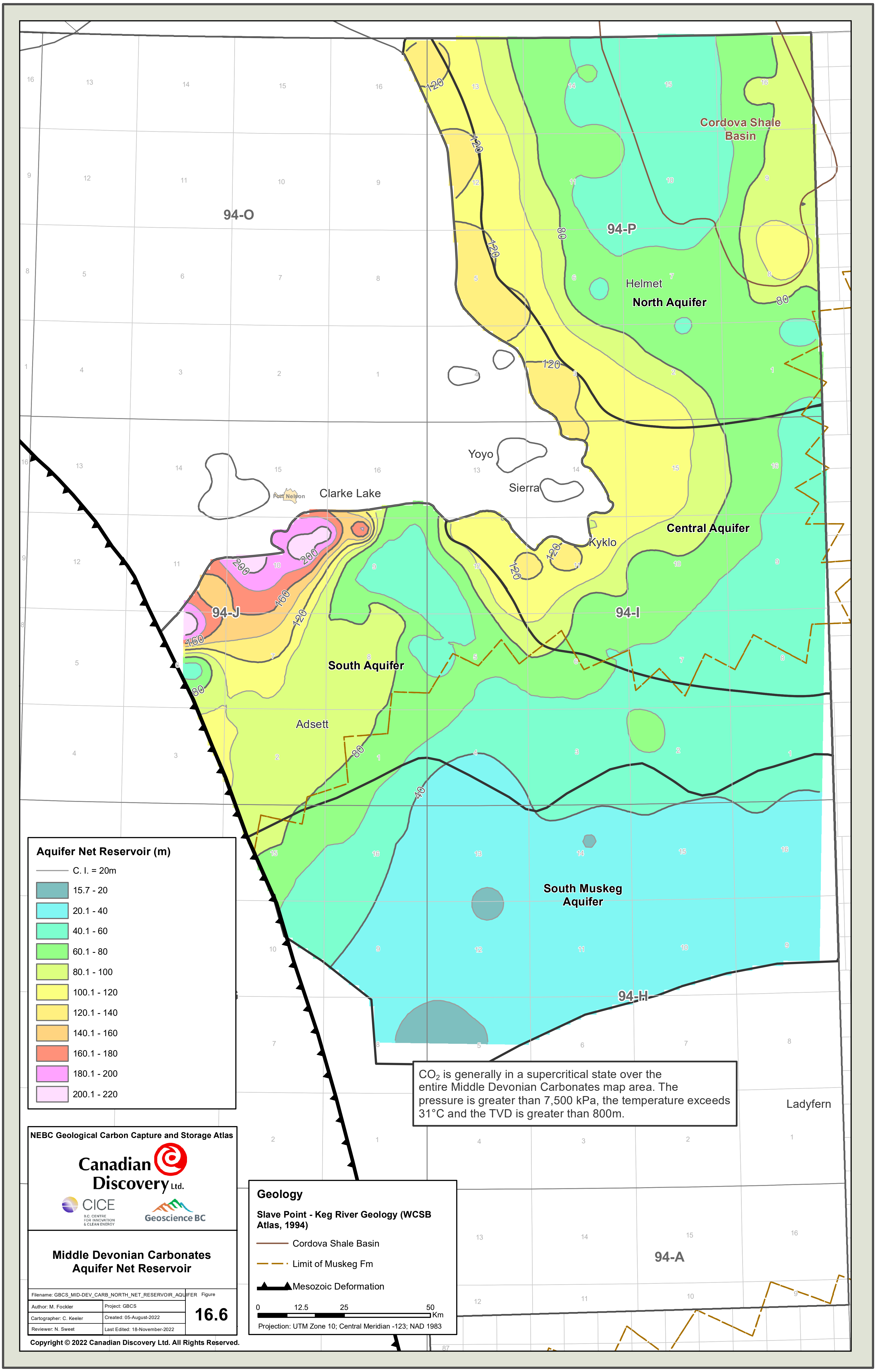

94-O
94-P
94-J
94-I
94-H
94-A
Cordova Shale Basin
Helmet
North Aquifer
Yoyo
Sierra
Clarke Lake
Fort Nelson
Kyklo
Central Aquifer
South Aquifer
Adsett
South Muskeg Aquifer
Ladyfern
Aquifer Net Reservoir (m)
C. I. = 20m
15.7 - 20
20.1 - 40
40.1 - 60
60.1 - 80
80.1 - 100
100.1 - 120
120.1 - 140
140.1 - 160
160.1 - 180
180.1 - 200
200.1 - 220
CO_2 is generally in a supercritical state over the entire Middle Devonian Carbonates map area. The pressure is greater than 7,500 kPa, the temperature exceeds 31°C and the TVD is greater than 800m.
NEBC Geological Carbon Capture and Storage Atlas
Canadian Discovery Ltd.
CICE
Geoscience BC
Middle Devonian Carbonates Aquifer Net Reservoir
Filename: GBCS_MID-DEV_CARB_NORTH_NET_RESERVOIR_AQUIFER
Figure 16.6
Author: M. Fockler
Project: GBCS
Cartographer: C. Keeler
Created: 05-August-2022
Reviewer: N. Sweet
Last Edited: 18-November-2022
Copyright © 2022 Canadian Discovery Ltd. All Rights Reserved.
Geology
Slave Point - Keg River Geology (WCSB Atlas, 1994)
Cordova Shale Basin
Limit of Muskeg Fm
Mesozoic Deformation
0 12.5 25 50 Km
Projection: UTM Zone 10; Central Meridian -123; NAD 1983

Figure 16.6

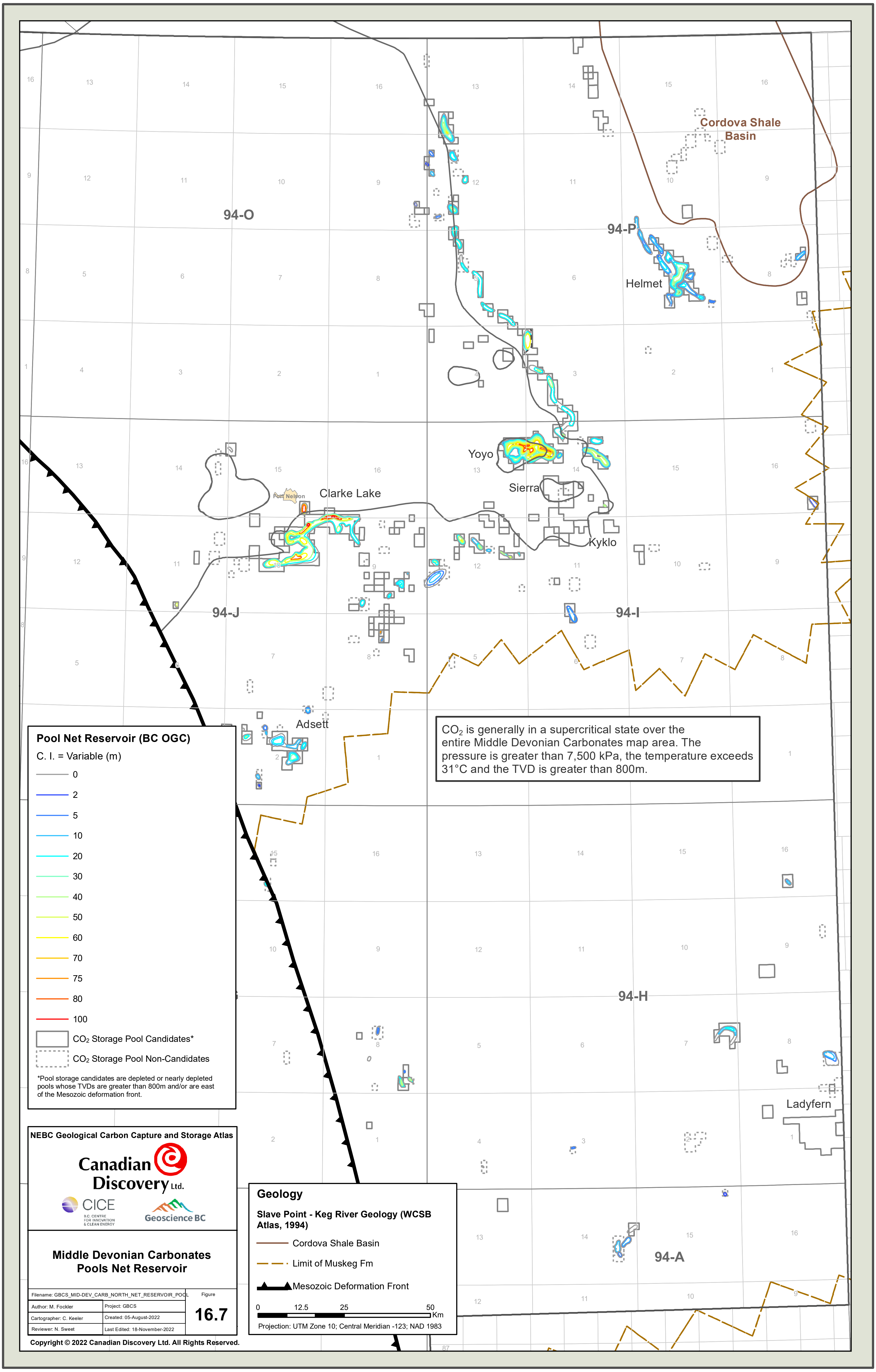

94-O
94-P
Cordova Shale Basin
Helmet
Yoyo
Sierra
Clarke Lake
Fort Nelson
Kyklo
94-J
94-I
Adsett
94-H
Ladyfern
94-A
CO_2 is generally in a supercritical state over the entire Middle Devonian Carbonates map area. The pressure is greater than 7,500 kPa, the temperature exceeds 31°C and the TVD is greater than 800m.
Pool Net Reservoir (BC OGC)
C. I. = Variable (m)
0
2
5
10
20
30
40
50
60
70
75
80
100
CO_2 Storage Pool Candidates*
CO_2 Storage Pool Non-Candidates
*Pool storage candidates are depleted or nearly depleted pools whose TVDs are greater than 800m and/or are east of the Mesozoic deformation front.
NEBC Geological Carbon Capture and Storage Atlas
Canadian Discovery Ltd.
CICE
Geoscience BC
Middle Devonian Carbonates Pools Net Reservoir
Filename: GBCS_MID-DEV_CARB_NORTH_NET_RESERVOIR_POOL
Figure
16.7
Author: M. Fockler
Project: GBCS
Cartographer: C. Keeler
Created: 05-August-2022
Reviewer: N. Sweet
Last Edited: 18-November-2022
Copyright © 2022 Canadian Discovery Ltd. All Rights Reserved.
Geology
Slave Point - Keg River Geology (WCSB Atlas, 1994)
Cordova Shale Basin
Limit of Muskeg Fm
Mesozoic Deformation Front
0
12.5
25
50
Km
Projection: UTM Zone 10; Central Meridian -123; NAD 1983

Figure 16.7

Porosity-Permeability Correlations

Establishing detailed porosity trends requires examination of log suites and petrophysical models, which is beyond the scope of this phase of the Atlas. Available core data can be combined with an examination of well logs to provide a high level estimate of porosity, particularly within the Middle Devonian Carbonate aquifers, where this information is needed for storage potential estimates.

Core data for the Middle Devonian Carbonates were obtained from geoLOGIC, and filtered for better quality reservoir that is more conducive to carbon storage (greater than 6% porosity and 5 mD permeability) within the study area *(figure 16.8)*. However, as mentioned previously, representative core data is scarce as the vuggy and fractured nature of the hydrothermal dolomite makes it very difficult to attain a competent core for analyses. The core analyses shown for the aquifers in *figure 16.8* rarely have porosities greater than 14–16%, whereas the Clarke Lake Gas Pool, for example, has over 275m of net reservoir with log porosity ranging from 8% to 30%.

Due to the nature of this reservoir, no clear porosity-permeability trends emerge on the plot, but the core analyses often show high permeability, with average permeabilities over 100 mD even at the average core porosity of about 9%. Log porosities average about 8%, so a range of 8–9% was used in storage potential estimates.

16.8 Middle Devonian Carbonates Porosity-Permeability Plot

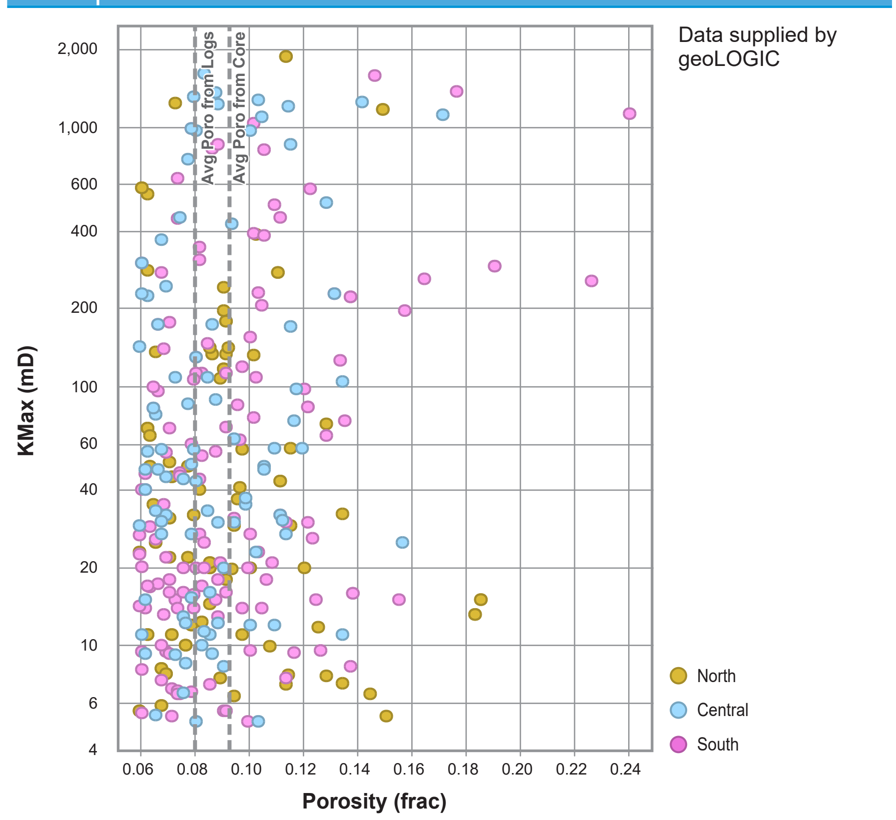

© Canadian Discovery Ltd. *Figure 16.8*

Hydrodynamics

To delineate the extent of the aquifers and understand the relationship between the aquifers and the depleted pools, a high-level analysis was done on Middle Devonian Carbonates hydrodynamics *(figure 16.9)* using Hydrofax drillstem test (DST) data from within the aquifers and the initial pressure and datum depth of each depleted pool from the BC OGC reserves databases.

While the Middle Devonian Carbonates aquifers are relatively continuous throughout the study area, several systems can be differentiated by variations in reservoir quality and pressure. Three main systems were identified, and line up quite well with the areas identified with variations in the net-to-gross mapping.

The North system is located northwest of Fort Nelson and consists of Slave Point and Keg River units, except in the Cordova Embayment where there is only Keg River overlain by shale. The Slave Point exists as a fringing reef and hosts conventionally trapped hydrocarbons in the Helmet pools.

The Keg River aquifer in the North System continues under the tight interior platform Slave Point limestones southwest towards the Cabin and Kyklo conventional pools within the Central system. Further west into the Horn River Basin there is a transition to more isolated systems, where the Sierra pools demonstrate the higher pressure trends associated with more contained and isolated pools.

The Clarke Lake Pool sits at the transition between the Central and South systems, where the Keg River, Sulphur Point and Slave Point stack to form the dolomitized barrier reef at Clarke Lake. To the south, the Adsett Pool approximates a transition to a larger spread in pressure data on the P/E graph, suggesting more isolated systems below a structural elevation of about -1800m subsea. This is where the Slave Point begins to experience separation from the underlying carbonates due to flow barriers in the Watt Mountain and Lower Slave Point. In the southernmost part of the study area, the Muskeg anhydrites also start to remove reservoir capacity from within the aquifer system.

The Ladyfern pools, in the southeastern part of the Middle Devonian Carbonate study area, exhibit an isolated system with good carbon storage potential in the pools, potentially accompanied by a small local aquifer.

16.9 Middle Devonian Carbonates Pressure vs Elevation Plot

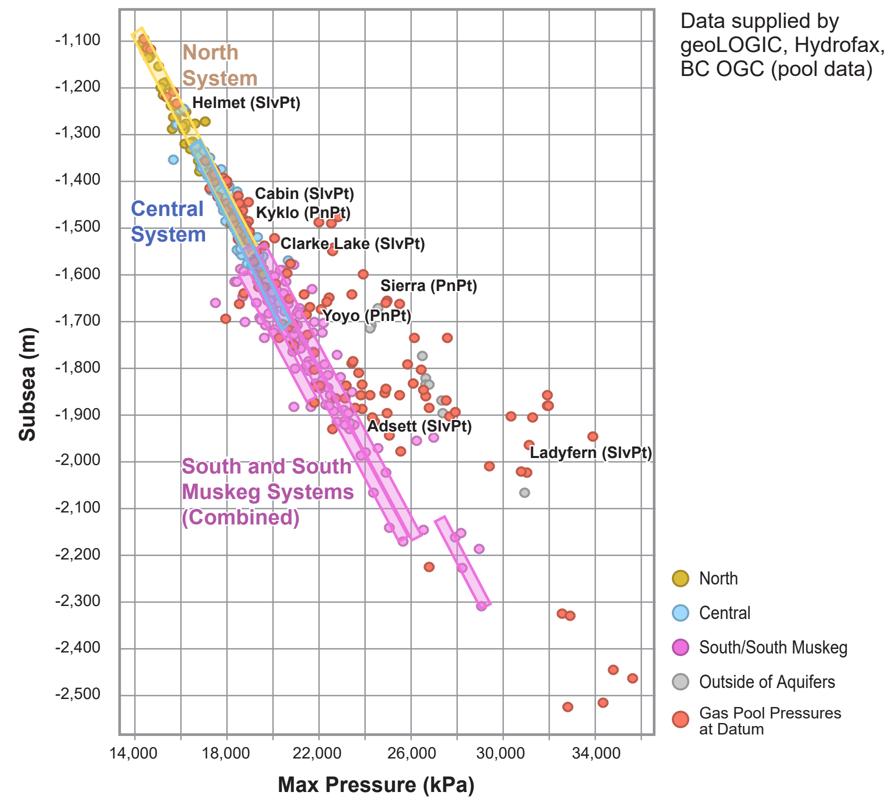

© Canadian Discovery Ltd. *Figure 16.9*

Carbon Storage Calculations

Depleted and Nearly Depleted Pools

The top 25 depleted and nearly depleted pool candidates for carbon storage potential within the Middle Devonian Carbonates are shown in *table 16.2*.

The BC OGC defines depleted pools as ones that have no remaining reserves or production. The BC OGC also recognizes that there are nearly depleted pools that could become CO_2 storage candidates in the (relatively) near future. The nearly depleted CO_2 storage candidates include pools where 90%+ of the reserves have been recovered, or no production has occurred in over five years. Furthermore, CDL has excluded pools that are shallower than 800m TVD, or are west of the Mesozoic deformation front. See Depleted Pools Selection Criteria in *Chapter 4* for a more thorough discussion.

The theoretical CO_2 storage potential represents the mass of CO_2 that can be stored in the hydrocarbon reservoirs assuming that the volume occupied previously by the produced gas will be occupied entirely by the injected CO_2. These calculations have been provided by the BC OGC and are based on historical pool production.

The effective CO_2 storage potential represents the mass of CO_2 that can be stored in hydrocarbon reservoirs after taking into account intrinsic reservoir characteristics and flow processes, such as heterogeneity (how much variability there is in the rock), aquifer support, sweep efficiency, gravity override, and CO_2 mobility (Bachu, 2006). The effective CO_2 storage potential is calculated by CDL and reduces the theoretical storage potential by as little as 13% and as much as 75%. More detail is provided on the carbon storage calculations for depleted pools in *Appendix B*, and data are provided for all depleted pools included in this study in *Appendix C*.

The depleted and nearly depleted pools that are deemed to be CO_2 storage candidates by CDL are coloured by their effective storage potential mass on the summary map *(figure 16.10)*.

Aquifers

The Middle Devonian Carbonates aquifer parameters are summarized in *table 16.3*. Theoretical CO_2 storage potential can be calculated using the mapped pore volume of the reservoir and CO_2 density, and assumes that the pore volume will be occupied entirely by the injected CO_2. We know this is not the case however, since the pore space is already occupied by water and the water will need to be displaced in the process. As a result, a storage efficiency factor is introduced into storage potential calculations that accounts for the presence of both water and CO_2 in the aquifer. The storage efficiency factor is a function of reservoir and fluid properties and dynamics, including the geometry of the trap, gravity segregation, heterogeneity, permeability distribution and pressure, and may reduce the theoretical storage potential by 95 to 99%.

Aquifers considered favourable targets for CO_2 storage are indicated on the summary map *(figure 16.10)* and labelled with their estimated P10, P50 and P90 effective storage potential in Mt. More detail is provided on the aquifer carbon storage calculations in *Appendix B*.

Top 25 Depleted Middle Devonian Carbonates Pools

Pool Name	Pool Type	Well Count	Initial Pressure (kPa)	Temperature (˚C)	Average Porosity (%)	CO_2 Phase	Theoretical Storage Potential (Mt)	Effective Storage Potential (Mt)
Clarke Lake Slave Point A	Gas	96	20,064	110	7.1	Supercritical	158.1	99.6
Yoyo Pine Point A	Gas	46	20,126	126	9.3	Supercritical	110.5	69.6
Sierra Pine Point A	Gas	19	23,925	126	10.0	Supercritical	84.4	53.1
Sierra Pine Point B	Gas	5	25,000	119	10.7	Supercritical	39.3	24.7
Ladyfern Slave Point A	Gas	47	31,138	111	9.9	Supercritical	35.4	22.3
Sierra Pine Point D	Gas	7	25,538	114	n/a	Supercritical	12.4	7.8
Helmet Slave Point A	Gas	17	16,134	109	8.6	Supercritical	9.5	6.0
Mel Slave Point A	Gas	1	20,752	117	8.0	Supercritical	4.8	4.2
Adsett Slave Point A	Gas	7	24,426	118	7.5	Supercritical	6.5	4.1
Sierra Pine Point E	Gas	1	23,453	119	8.3	Supercritical	5.6	3.5
Roger Pine Point A	Gas	3	20,684	130	7.4	Supercritical	5.5	3.5
Kotcho Lake Slave Point A	Gas	21	17,791	106	9.5	Supercritical	5.4	3.4
Sierra Pine Point J	Gas	1	26,151	122	8.8	Supercritical	5.1	3.2
Klua Slave Point B	Gas	1	19,636	111	8.1	Supercritical	4.4	2.7
Sierra Pine Point F	Gas	1	21,357	123	9.1	Supercritical	4.3	2.7
Ladyfern Slave Point B	Gas	1	30,818	110	5.8	Supercritical	4.1	2.6
Sextet Slave Point D	Gas	2	18,497	112	7.0	Supercritical	2.9	1.8
Adsett Slave Point B	Gas	10	24,311	116	6.9	Supercritical	2.8	1.7
Cabin Slave Point B	Gas	3	18,368	122	9.0	Supercritical	2.4	1.5
Klua Slave Point D	Gas	1	19,367	113	9.6	Supercritical	2.4	1.5
Adsett Slave Point I	Gas	3	24,214	105	6.7	Supercritical	2.4	1.5
Sierra Pine Point G	Gas	1	22,451	105	11.1	Supercritical	1.7	1.5
Kotcho Lake East Slave Point C	Gas	6	17,464	108	9.9	Supercritical	2.3	1.5
Klua Pine Point D	Gas	2	24,920	128	6.1	Supercritical	2.0	1.3
Milo Pine Point C	Gas	2	25,571	132	7.4	Supercritical	2.0	1.2

© Canadian Discovery Ltd. Data supplied by BC OGC and Canadian Discovery Ltd.

Table 16.2

Middle Devonian Carbonates Aquifer Properties and Storage Potential

Aquifer Name	Type	Thickness Range (m)	Pressure Range (MPa)	Temperature Range (°C)	Porosity Range (%)	CO_2 Phase	P10 Effective Storage Potential at 0.5% (Mt)	P50 Effective Storage Potential at 2% (Mt)	P90 Effective Storage Potential at 5.4% (Mt)
North Hydraulic System	Aquifer	41-122	11.6-19.1	74-119	8-9%	Supercritical	118.6	474.3	1,280.7
Central Hydraulic System	Aquifer	53-127	13.8-20.0	88-126	8-9%	Supercritical	95.2	381.0	1,028.6
South Hydraulic System	Aquifer	24-217	16.9-26.2	94-134	8-9%	Supercritical	137.2	548.9	1,482.0
South Muskeg Hydraulic System	Aquifer	16-87	18.5-30.5	105-161	8-9%	Supercritical	62.0	247.9	669.3

Table 16.3

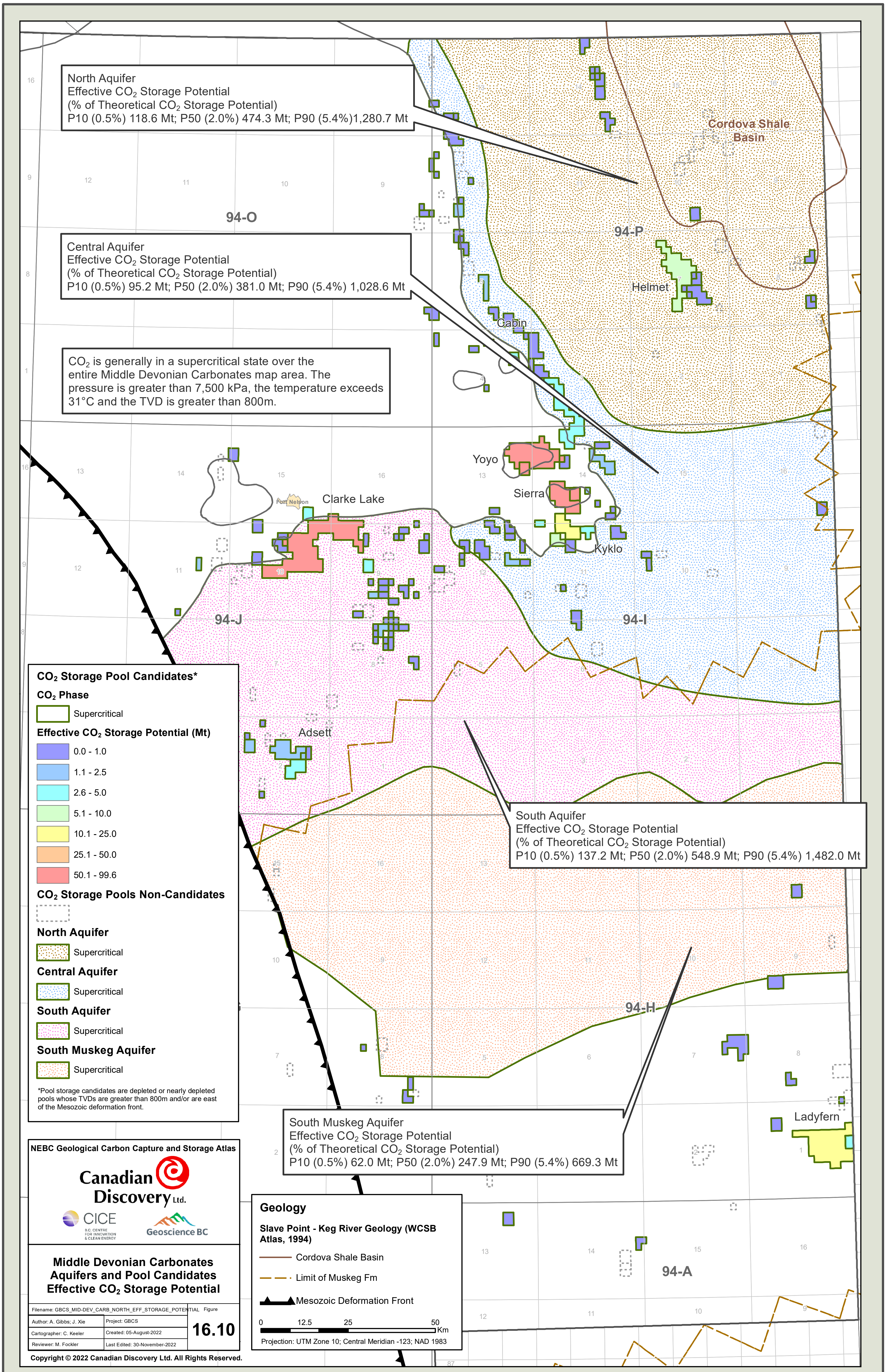

© Canadian Discovery Ltd.

Figure 16.10

RECOMMENDATIONS

Recommendations

This Atlas provides a high level assessment of geological storage potential in NEBC and identifies several saline aquifers and depleted pools as possible CO_2 storage targets. Further technical work is recommended to evaluate and advance identified potential CCS candidate sites to specific site selection and characterization stage, and to a stage suitable for regulatory approval application.

This chapter identifies focus areas from the study that are recommended for additional technical evaluation. Opportunities from specific pools and aquifer areas are identified and some key metrics are highlighted. The chapter also provides recommended next steps that address some identified knowledge gaps and metrics required for CCS site evaluation and some risks associated with CCS. Finally, recommendations are made for future CCS assessment projects in other areas of the province.

Focus Areas

Figure 17.1 shows recommended focus areas for further study, as they have large storage potential and are close to emitters and existing infrastructure.

The area within the solid blue lines indicates the thickest area of stacked aquifer potential. Aquifers tend to offer the best potential for CO_2 storage due to their thickness and lateral extent; they also tend to be penetrated by fewer wells than hydrocarbon reservoirs within pools, resulting in a lower risk of CO_2 leakage through legacy wellbores.

The lack of well control in aquifers however may present a risk in that the reservoir is not as well characterized as depleted pools. The benefit of having stacked aquifer targets is that the risk of local reductions in reservoir quality and injectivity are reduced by having multiple target options that can be prioritized once appraisal well drilling is completed. Should all targets continue to show good storage potential when examined in more detail, the storage potential can be additive, improving the conditions for a larger storage project within that region.

Depleted and nearly depleted pools with a storage potential of greater than 5 Mt have also been included in *figure 17.1*. These targets offer more certainty in terms of storage potential and injectivity, but some risk of containment lies in legacy wellbores within the hydrocarbon reservoirs. Further evaluation of depleted pools should include an assessment of the distribution of the storage potential within the pool (the provided pool net reservoir maps can be a tool in this process) as well as an evaluation of the distribution and vintage of legacy wellbores.

Dawson Creek to Fort St. John

Several storage options exist in the area between Dawson Creek and Fort St. John. There are five formations with saline aquifers that provide the potential for stacked storage within the Peace River Arch (i.e. PRA stacked aquifer fairway), as well as three large depleted pools in the region.

The PRA contains existing natural faults which should be evaluated for the risk of reactivation and the potential to breach overlying regional seals. If the faults are sealing in nature, these areas should be re-assessed with consideration of a potential decrease in lateral continuity and thus a decrease in lateral storage potential.

The opportunities within the Dawson Creek to Fort St. John region are as follows:

- Stacked aquifer fairway
  - Bluesky
    - Net reservoir thickens to the east and is 10–30m thick north of Dawson Creek.
    - Thick shale overlying reservoir
    - 36 Mt of estimated storage potential (P50)
  - Cadomin
    - 10–50m net reservoir thickness
    - 104 Mt of estimated storage potential (P50)
  - Nikanassin
    - Up to 100m of net reservoir in an extensive SE-NW trend
    - 40 Mt of estimated storage potential (P50)
  - Baldonnel
    - 5–16m net reservoir thickness
    - Local thick areas very close to Fort St. John
    - 62 Mt of estimated storage potential (P50)
  - Belloy
    - 20–40m net reservoir thickness just east of Fort St. John
    - 99 Mt of estimated storage potential (P50)
- Depleted pools
  - Belloy
    - North of Fort St. John
    - ~27 Mt of storage potential
  - Baldonnel
    - South of Fort St. John
    - ~10 Mt of storage potential
  - Halfway
    - West of Fort St. John
    - ~44 Mt of storage potential

94-A Block/Buick Creek

In the 94-A block/Buick Creek, storage of carbon emissions relating to oil and gas extraction may be available in stacked aquifers within four formations, as well as two areas with stacked depleted or nearly depleted pools. The Nikanassin-Dunlevy formations contain the majority of storage opportunities in this area. The Hay River Shear Zone extends into this region, and existing natural faults should be evaluated for risk of reactivation or sealing and compartmentalization of storage targets. Opportunities within this area are as follows:

- Stacked aquifer fairway
  - » Nikanassin-Dunlevy
    - 5–10m of net reservoir
    - 23 Mt of estimated storage potential (P50)
  - » Baldonnel
    - 5–10m of net reservoir
    - 36 Mt of estimated storage potential (P50)
  - » Halfway
    - 5–15m of net reservoir
    - 30 Mt of estimated storage potential (P50)
  - » Debolt
    - Extensive aquifer, but thinner and more variable target
    - 30 Mt of estimated storage potential (P50)
- Depleted pools
  - » Nikanassin-Dunlevy ~41 Mt of storage potential
  - » Stacked Nikanassin-Dunlevy and Bluesky east of Buick Creek ~20 Mt of storage potential
  - » Stacked Nikanassin-Dunlevy and Halfway in 94-A-13 ~16 Mt of storage potential

Fort Nelson

The stacked aquifer fairway in the Middle Devonian contains thick dolomitized carbonates that could provide a good opportunity for carbon storage. As discussed in Chapter 16, previous studies have shown that there is large storage potential, good injectivity and sufficient containment within these zones in the Fort Nelson area, provided an appropriate distance is maintained from the Tu Deh-Kah Geothermal project in the Clarke Lake Slave Point A Pool.

- Stacked aquifer fairway
  - » Middle Devonian Carbonates (Slave Point, Keg River)
    - 1.4 Gt of estimated storage potential (P50)
- Depleted pools
  - » Clarke Lake Slave Point A
    - Currently used for the Tu Deh-Kah Geothermal project
    - ~99 Mt of storage potential
    - Very thick overlying shale
  - » Yoyo-Pine Point
    - ~70 Mt of storage potential
    - Very thick overlying shale

Next Steps

For the CO_2 CCS candidate sites identified in this study, *(figure 17.1)*, knowledge gaps have been recognized, and further analyses of the pore space and surrounding seals are crucial next steps in determining the feasibility of CCS and the selection of potential sites. To fill these knowledge gaps, the following additional work is recommended on a regional, localized and site-specific scale.

Emissions and Infrastructure

Information on CO_2 emitters must be gathered, specifically, who, where, how much, and for how long? These data are necessary to allow the determination of both annual and project lifetime CO_2 storage needs. Infrastructure availability, as well as an assessment of existing pipelines and the potential to repurpose these existing pipelines should be undertaken to assist in project planning.

Containment Risk

Fault system characterization is required to understand leakage risks. The wastewater disposal study, Geoscience BC Report 2021-14 (Petrel Robertson, 2021) in the Peace River area, includes an evaluation of faults and fault systems. This information can assist in the delineation of high-risk areas for CO_2 storage and can be used to high-grade areas where additional work is recommended. The vertical and lateral extents of faults, the potential for fault reactivation, and critical stress directions are important risks that require detailed mapping and assessment. Seismic data are required to better understand faulting risk at a local level.

The potential for injection-induced earthquakes (seismicity) in NEBC has been investigated by Geoscience BC and several studies can be found on the Geoscience BC website data and projects portal. Further work is recommended to discern whether induced seismicity is a risk to containment of stored CO_2.

On a local and site-specific scale, legacy well bore integrity needs to be evaluated for potential CO_2 leakage risk.

Storage Risk

Storage risk refers to an identified reservoir's ability to accept all of the expected CO_2 injection volumes, and assessment requires further geological mapping, including detailed characterization of net reservoir, reservoir thickness, porosity and permeability, and mineralogical content of the reservoir and surrounding containment formations to better quantify the amount of pore space available to sequester CO_2. Reservoir variability needs to be evaluated to determine the size and character of the reservoir storage volume. Detailed hydrodynamics can provide insights pertaining to the existence of flow barriers and flow movement of an injected CO_2 plume within the reservoir.

Injectivity Risk

Quantifying reservoir injectivity is an important step as this will determine the capability of the reservoir to receive injected CO_2 into the pore spaces at sufficient rates. High level assessments can be gathered from production data and drillstem tests. Downhole injectivity tests and lab analyses on formation cores will provide additional data to further quantify injectivity parameters.

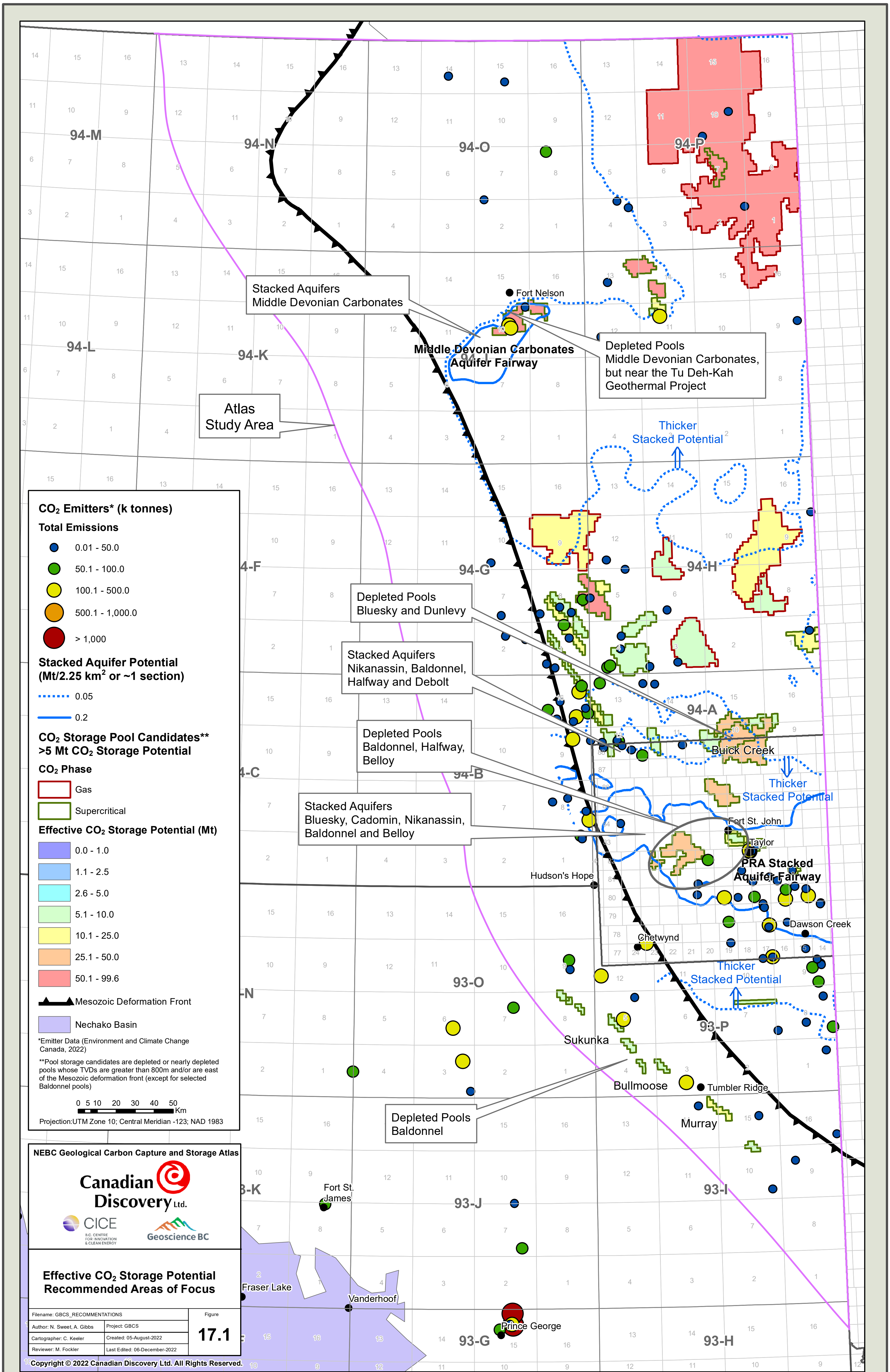

© Canadian Discovery Ltd. *Figure 17.1*

Proposed Future Areas of Study

Outside of NEBC, there are other areas of British Columbia that would benefit from identification and assessment of geological CCS potential, particularly near significant stationary CO_2 emitters. It is recommended that scoping projects to assess CCS suitability be undertaken in the following areas *(figure 17.2)*:

- Prince George Area
  - Examine the potential of CO_2 transport by rail or road to storage sites within depleted Baldonnel pools (Sukunka, Bullmoose and Murray) in the Tumbler Ridge area
  - Evaluate the nearby Nechako Basin for potential aquifer storage targets
- Lower Mainland
  - Evaluate the Georgia Basin for potential aquifer storage targets
- Southeast BC
  - Evaluate the Fernie Basin for potential aquifer storage targets

17.2 Basins for Future Evaluation

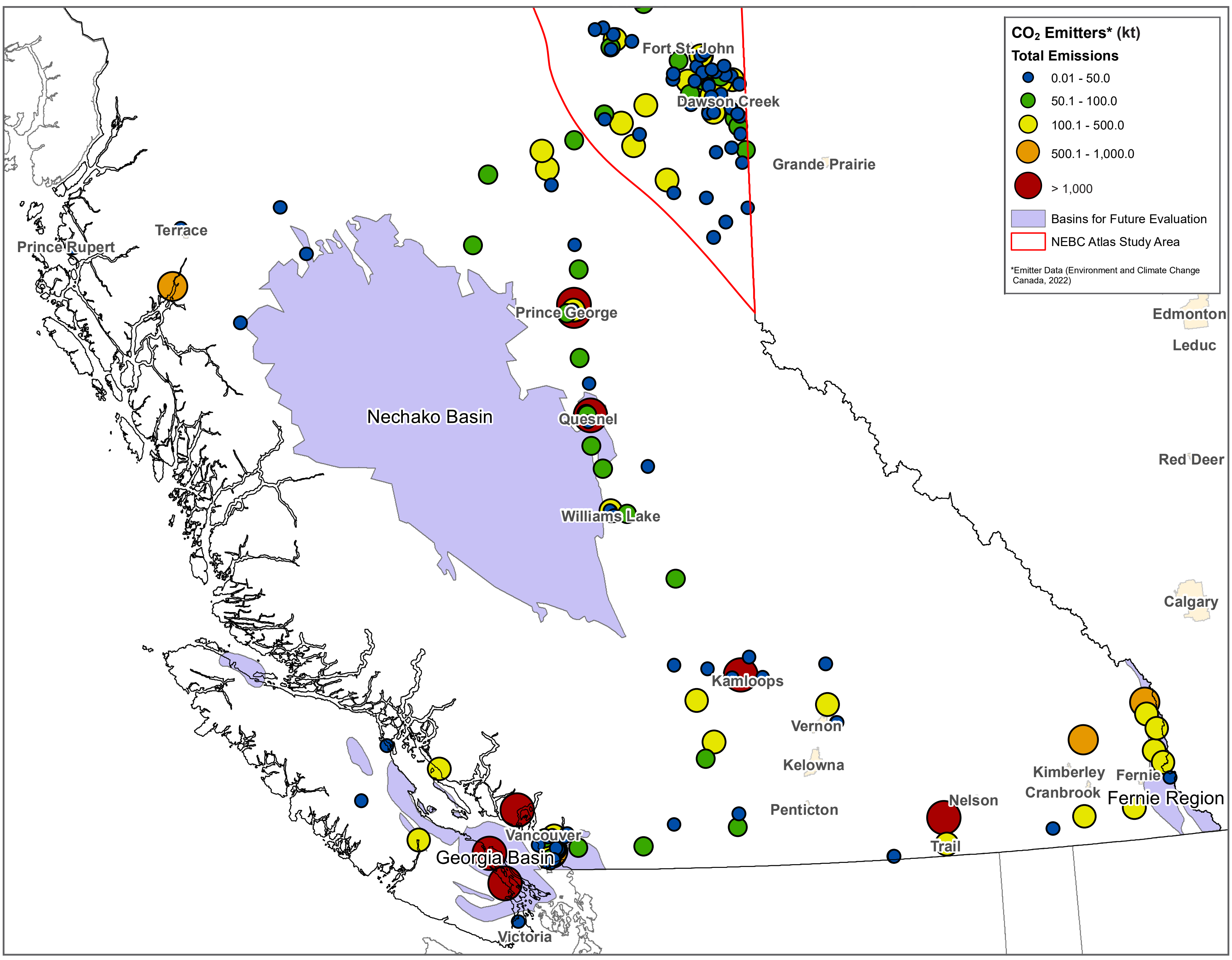

Figure 17.2

Introduction

The northeastern British Columbia (NEBC) region comprises part of the much larger Western Canadian Sedimentary Basin (WCSB). Here, rock strata are composed of stacked porous carbonates and sandstones (reservoirs), as well as impermeable shales and salt (seals). This regional stratigraphic summary is included to provide broader context to the geological stratigraphy in the study area, and as a high level discussion of the key reservoir units with the changing depositional environments through time. The NEBC Gas Play Atlas (2006) was a key reference for this summary. The formations that met the geological storage criteria are shown in this section with their corresponding chapter number where they are discussed in more detail. Formations that were excluded are discussed briefly for completeness.

For stratigraphic reference, *figure A.1*, shows the generalized stratigraphy in the southern area near Fort St. John and the northern area around Fort Nelson. The formations will be discussed from youngest to oldest to reflect the structure of the formation chapters.

Upper Cretaceous Cardium and Shaftesbury

The overall shallow depth of the Cardium (typically <750m) rules it out as a potential target for carbon storage.

Cardium strata comprise a northeast-prograding shoreface/alluvial plain complex, mappable along the western flank of the WCSB as far north as Twp. 75–77. In NEBC, Cardium reservoir potential is confined to a coarsening-upward sandstone succession from 15–50m thick. Upper shoreface/foreshore conglomerates cap the succession locally (NEBC Play Atlas, 2006). The overlying Cardium "zone" sands, which are productive in Alberta, are poorly developed in NEBC. Marine shales of the Shaftesbury Formation encase the Cardium and provide a thick overlying seal for deeper reservoirs in the study area. This shale acts as the top regional seal for all potential CCS reservoirs.

Upper Cretaceous Dunvegan

The Dunvegan is too shallow to provide effective carbon storage.

Dunvegan strata form a large, southeast-prograding wedge of deltaic and shoreface sediments, which originated in far northern BC and the Territories, and reached a distal edge in west-central Alberta. The Dunvegan lies between marine shales of the Shaftesbury Formation below and the Kaskapau Formation above. It comprises a series of 7 to 10 coarsening-upward successions separated by regionally extensive transgressive marine shales (NEBC Play Atlas, 2006). This progradational deposition corresponded to a global lowering of sea level, but it was also likely influenced locally by tectonic uplift associated with late stages of the Cordilleran orogeny (mountain building) to the west. Dunvegan sandstones were deposited in deltaic

A.1 NEBC Stratigraphic Columns

a. South Region b. North Region

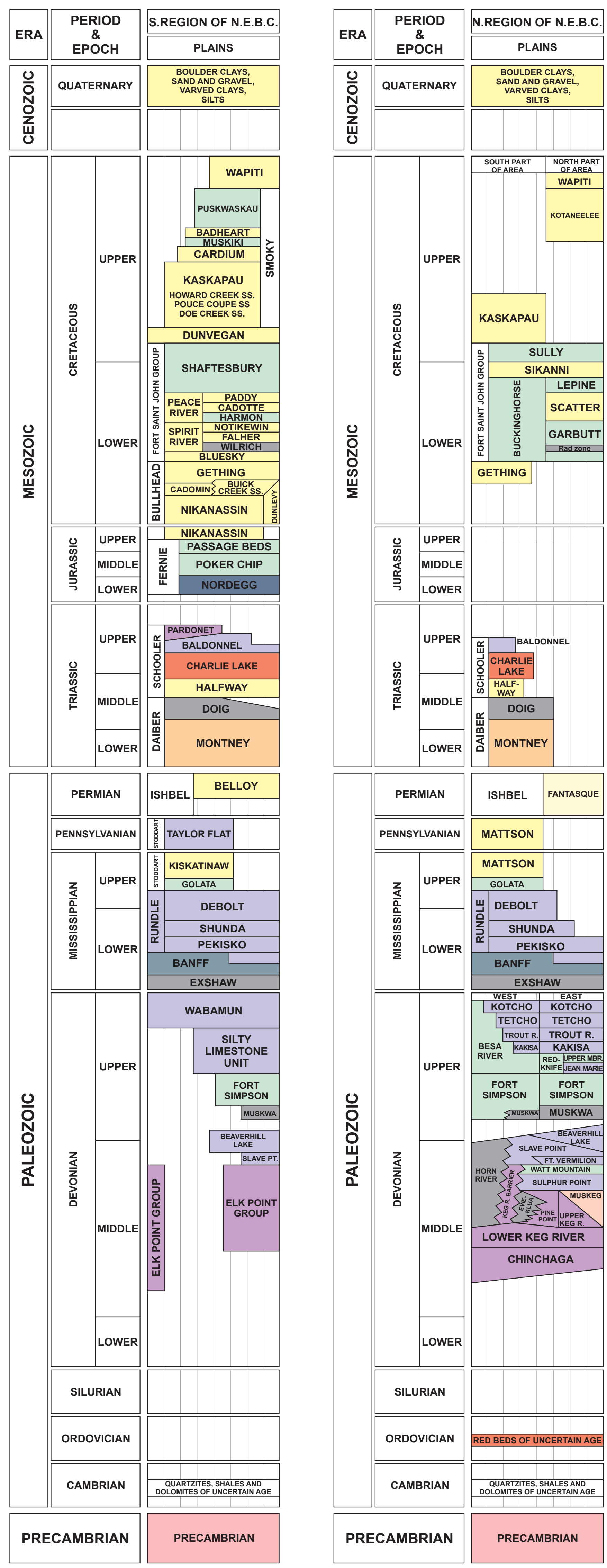

 Figure A.1

to shoreface settings at the seaward limit of several regressive subunits, and in associated distributary channels and valley fills.

Dunvegan hydrocarbon reservoirs produce over a broad area of west-central Alberta. Reservoir quality generally decreases westward into BC, largely as the result of compaction associated with significantly deeper burial in the past. North of the Deep Basin, Dunvegan strata crop out, or are at such shallow depths, that reservoir pressures and effective trapping become significant issues.

Lower Cretaceous Peace River Formation (Chapter 5)

The Paddy Member of the Peace River Formation in northwestern Alberta and NEBC is equivalent to the Viking Formation and was deposited in the upper Albian when the Peace River Arch (PRA) was a negative feature. The Paddy lies unconformably over the Cadotte and Harmon members of the Peace River Formation. Paddy strata were deposited across the southern Deep Basin in alluvial plain to bay/lagoonal environments at the culmination of a widespread regional transgressive-regressive (sea level rise and fall) cycle (NEBC Play Atlas, 2006). To the north, the Paddy grades into a regional, southwest-north-trending sandy shoreface/barrier that can be traced from outcrops in the BC foothills to the Peace River valley near Peace River, AB.

The Paddy section in the BC Deep Basin is dominated by fine-grained clastics and coals, and lacks regional stratigraphic markers. Locally, valleys incised from the top of the Paddy are filled with sand-dominated estuarine facies. Paddy strata cap Cadotte shoreface sandstones and related facies with a subtle unconformity that decreases in magnitude northward.

The Cadotte Member was deposited during northerly progradation of coarse clastic shorelines across the west-central portion of the WCSB. It comprises sandier- and coarsening-upward successions of sandstone and conglomerate. The northern limit is defined by a northerly facies change to more distal fine-grained clastics, approximately coincident with the Paddy northern barrier edge.

Cadotte reservoirs consist of moderately- to well-sorted granule to small pebble conglomerates, deposited in upper shoreface to foreshore environments. Reservoir quality is best in well-sorted upper shoreface to foreshore conglomerates.

Lower Cretaceous Spirit River (Chapter 6)

The Spirit River Formation is the product of a basin-wide progradational episode (sea level rise) during mid-Albian time. In the BC Deep Basin, it comprises six major stacked shoreface successions, termed (from the top down) Notikewin, Falher A, B, C, D, and F. An individual cycle typically consists of a coarsening-upward succession, passing from very fine-grained sandstones to coarse sandstone or conglomerate, capped by continental mudstones and coals. Subsequent work has illustrated more complex internal stratigraphic relationships that is important at a field development scale.

To the north, Spirit River shoreface sandstones grade to finer-grained, more distal facies. Individual Notikewin and Falher sub-members lose their identity, as capping conglomerates and coals pinch out to the north. Only the uppermost sandstone remains north of about Twp. 87, overlying a succession of siltstones and shales.

Spirit River sandstones grade up from underlying Wilrich Member marine shales, and are capped by transgressive marine shales of the Harmon Member in the south and Buckinghorse Formation in the north providing effective seals.

Lower Cretaceous Bluesky (Chapter 7)

The Bluesky Formation encompasses a wide variety of reservoir sandstone bodies associated with transgression and subsequent regression (sea level rise and fall) of the Boreal (northern) Sea across the WCSB.

Marine shoreface, deltaic, and estuarine reservoirs occur in discrete areas across NEBC. Excellent reservoir quality occurs in thin, well-sorted, coarse-grained, areally limited shoreface sandstones and conglomerates, while widespread deltaic and finer-grained shoreface sandstones generally exhibit poorer reservoir quality.

Lower Cretaceous Gething-Cadomin (Chapter 8)

Deposition of the Gething Formation took place in response to a rise in sea level and strong sediment supply from the Columbian Orogen (mountains) to the west. In the south, fine-grained clastics and coal were deposited in alluvial plain and coal-swamp settings, cut locally by fine- to medium-grained fluvial (river) channel sandstones. To the north, the lower Gething comprises sandy fluvial facies deposited in well-defined valleys, while the upper Gething includes deltaic to alluvial plain facies laid down over broader areas. Gething deposition was terminated with the first major Cretaceous transgression of the Boreal (northern) Sea (NEBC Play Atlas, 2006).

Cadomin strata were deposited as an outwash of alluvial fan to alluvial plain sedimentation in Early Cretaceous time, following renewed uplift of the Columbian orogenic highlands to the west (NEBC Play Atlas, 2006). Widespread sandstones and conglomerates range from 5m to more than 25m thick, thickening locally to 100m or more near depocentres in the Foothills. Cadomin sediments lie sharply on the pre-Mannville unconformity, and are sharply or gradationally overlain by Gething strata.

In the Liard Basin, the Chinkeh Formation occupies the same stratigraphic position atop the pre-Cretaceous unconformity. Conglomerates are limited to a basal lag unit, and as a component of overlying valley-fill and channel deposits. Existing production and most reservoir potential exists in the upper part of the Chinkeh, consisting of widespread coarsening- and sandier-upward marine shoreface successions, culminating in fine- to medium-grained sandstones with moderate to good reservoir quality. There are no depleted pools in the Chinkeh, and it is therefore not evaluated for CO_2 storage.

Upper Jurassic–Lower Cretaceous Nikanassin (Chapter 9)

Nikanassin strata comprise a thick, easterly-thinning wedge of clastics, deposited during latest Jurassic and earliest Cretaceous time. During Nikanassin time, the Jurassic Fernie

Sea retreated northward from the WCSB in response to sea level fall and immense volumes of sediment being shed from the rising Columbian Orogen (mountains) to the west (NEBC Play Atlas, 2006). With further marine retreat and orogenic uplift, deposition was terminated and uppermost Nikanassin strata were eroded.

Nikanassin strata grade up from marine Fernie shales at the base, and are capped by the basin-scale pre-Mannville unconformity. Blocky to fining-upward sandstone bodies are interbedded with siltstones, shales, and minor coal. Deposition took place in marginal marine to continental settings, resulting in an absence of regional stratigraphic markers and mappable depositional trends.

Upper Triassic Baldonnel-Pardonet (Chapter 10)

Baldonnel strata are widespread shallow marine to shelfal carbonates deposited during a regional transgression which drowned Charlie Lake arid coastline environments. Hydrocarbon reservoir rocks are primarily dolomitized skeletal calcarenites, with considerable variation in reservoir quality arising from the interplay of depositional facies, diagenesis and structural overprint. The Baldonnel can be mapped continuously from the southern Deep Basin to a northern subcrop edge in 94G and 94H. It lies more or less conformably on the Charlie Lake, whereas the Pardonet (and Baldonnel east of the Pardonet subcrop edge) is unconformably overlain by Jurassic marine shales.

Upper Triassic Charlie Lake (Chapter 11)

The Charlie Lake Formation comprises a thick succession of interbedded siliciclastic, carbonate, and evaporitic rocks, deposited at the culmination of a major transgressive-regressive (sea level rise and fall) cycle encompassing the Doig, Halfway and Charlie Lake. Reservoir units include very fine- to medium-grained sandstones, deposited in arid coastline to shallow marine settings, and crystalline to skeletal limestones and dolostones, primarily of shallow marine origin.

Stratigraphic markers can be correlated regionally with confidence in the Charlie Lake, reflecting very widespread, low-relief deposition. Several internal unconformity surfaces can also be traced throughout NEBC. One of these, the Coplin unconformity, serves as the boundary between Lower and Upper Charlie Lake. It progressively truncates all Lower Charlie Lake members, as well as the Halfway, Doig, and Montney, in a northeasterly direction and thus records a major early Late Triassic tectonic and erosional event (NEBC Play Atlas, 2006).

The Charlie Lake is overlain by the Baldonnel Formation. The contact is locally disconformable, but can be difficult to identify consistently on logs because of lithological similarities between the two units.

Charlie Lake reservoirs host both oil and gas in NEBC. Individual pools tend to be thin and areally small, reflecting low-relief environments of deposition and truncation by unconformities. Tight evaporitic facies provide effective seals throughout the formation.

Lower Charlie Lake sandstone and carbonate reservoirs occur below the Coplin unconformity. Like the Upper Charlie Lake, they consist of thin, arid coastline to shallow marine sandstones and restricted to shallow marine carbonates, occurring in highly-correlative stratigraphic successions. The Lower Charlie Lake overlies the Halfway Formation with a contact that is generally sharp in the east, but assumes a more interfingering nature to the west as the Lower Charlie Lake succession becomes sandier, and grades to more homogeneous marine facies.

Middle Triassic Halfway (Chapter 12)

The Halfway encompasses shallow marine sandstone sequences that were deposited along the western margin of the North American craton in barrier island, shoreface and tidal inlet channel environments. Halfway reservoir bodies are stratigraphically isolated in updip areas, but pass southwestward into a broad, continuous shelfal sandstone complex (NEBC Play Atlas, 2006).

Halfway sandstones are primarily quartz arenites and sublitharenites, with local bioclastic (shell debris) sandstones and coquinas. Grain sizes generally range from very fine to fine, as most clastic sediment was derived through aeolian (wind) transport from the craton. Major cements include silica, carbonates, and anhydrite. The best (and volumetrically dominant) reservoir facies in many pools in the updip "discontinuous Halfway" regime are tidal channel fills. To the south and west in the "continuous" Halfway, reservoir quality generally deteriorates, although secondary solution of lithic and bioclastic grains can create significant hydrocarbon reservoir sweet spots (NEBC Play Atlas, 2006).

Middle Triassic Doig–Lower Halfway

In places, it is difficult to separate the lower part of the Halfway from the Doig, so some strata may be genetically related to the Halfway, but grouped lithostratigraphically with the Doig. Westward, Doig and Halfway sandstones cannot be consistently differentiated as the section thickens; consequently, all Halfway and Doig prospects in the foothills are grouped within the Halfway.

The Doig and Halfway formations were deposited within a prograding clastic coastal system along the western margin of the North American craton, in proximal to distal marine environments. They are preserved across the southern Deep Basin and Peace River areas, thinning to a northeasterly subcrop edge. The Doig comprises offshore to lower shoreface shales, siltstones and sandstones, with thick, cleaner, more proximal sandstones in isolated bodies and linear trends. Doig sandstones are well-sorted, very fine- to fine-grained sublithic to quartz arenites, with interbedded bioclastic (coquinoid) packstones and grainstones. A complex diagenetic history has produced highly variable reservoir quality.

Lower Triassic Montney

Given that the Montney is deemed to be an unconventional reservoir (DPR Schedule 2), it was not assessed for this Atlas.

Montney strata accumulated on a broad continental ramp on the western flank of the North American craton. They comprise stacked, prograding highstand parasequences, interrupted by a medial transgressive (sea level rise) event. Aeolian (wind) processes provided most of the sediment supply (NEBC Play Atlas, 2006). Shoreface to subtidal facies in the east grade westward into more argillaceous basinal facies, cut by turbidite deposits associated with lowstand events. Major structural features, particularly within the Fort St. John Graben, exerted considerable influence upon transport and deposition of turbidite facies.

Montney hydrocarbon reservoirs are predominantly coarse siltstones to very fine-grained sandstones, with true shales being rare. Shoreface sandstones and associated dolomitic coquinas, to the east in Alberta), exhibit good conventional reservoir quality. Lower shoreface to shelfal equivalents of the uppermost parasequences, however, are buried sufficiently deeply in the west to form sand-dominated, low permeability reservoirs.

Permian Belloy (Chapter 13)

The Belloy Formation is best developed in the Peace River Embayment/Fort St. John Graben. It comprises several stacked regressive (sea level fall) sequences, grading from siltstones and fossiliferous carbonates typical of outer shelf to distal carbonate platform settings in the west, eastward to shoreface and tidal to fluvial (river) channel sandstones and dolostones. Reservoir quality is best developed on the embayment margins, where the section consists primarily of cleaner, better-sorted sandstones. Hydrocarbon prospectivity in the Belloy is focused within and on the margins of the Fort St. John Graben.

Pennsylvanian–Permian Belcourt–Taylor Flat

Due to the complexity of the Belcourt/Taylor Flat successions, and low carbon storage potential of the depleted pools, it is excluded from evaluation in this Atlas.

Pennsylvanian–Permian strata of the Belcourt/Taylor Flat succession exhibit highly variable depositional patterns and lithologies throughout NEBC. Although each formation is bounded by unconformities, regional correlations are generally questionable because of a lack of well and core control. The Taylor Flat accumulated within the Peace River Embayment as a poorly-developed carbonate ramp. Reservoir facies are relatively small skeletal carbonate and fine-grained sandstone bodies.

Upper Mississippian Mattson–Kiskatinaw

Due to the stratigraphic complexity of the Kiskatinaw, it is excluded from this evaluation. Likewise, the Mattson is excluded due to its shallow depth of burial and poor reservoir quality.

The Mattson Formation comprises a thick section of sandstones with minor shales and coals, deposited in deltaic to prodeltaic environments. Its depocentre is in the southwestern District of Mackenzie, NT, from which it grades westward to basinal shales of the Besa River Formation, and southward to more carbonate-rich, fine-grained strata of the Stoddart Group. However, it has not been described in detail in the subsurface. The Mattson truncates abruptly against the Bovie Lake structure in the east, and thus is confined to the Liard Basin and adjacent fold belt. The Mattson can be shallow with a depth of as little as 350m. Where it is deeper, reservoir quality is generally poor, and it is therefore not considered a CO_2 candidate.

In the Peace River area, the Kiskatinaw Formation was deposited in the Peace River Embayment in a variety of fluvial (river), estuarine, and marginal marine environments. The Kiskatinaw is unconformably underlain by shales of the Golata Formation and conformably overlain by carbonates of the Pennsylvanian Taylor Flat Formation (all of the Stoddart Group). The basal or lower Kiskatinaw was deposited as a sandy estuarine valley-fill complex, whereas the lower to upper Kiskatinaw records a shallow-shelf environment with interbedded tidal mudstones, sandstones, and lime mudstones. Kiskatinaw reservoirs have been influenced by fault development during deposition, and by continued subsequent fault movement associated with the Dawson Creek Graben Complex in the Peace River Embayment. Basal fluvial to estuarine channel fill sandstones are the primary reservoirs in the Kiskatinaw. Controls on hydrocarbon trapping can be stratigraphic, structural, or combination of both.

Lower–Upper Mississippian Debolt (Chapter 14)

The Debolt is the youngest of the three major Mississippian carbonate successions mappable throughout NEBC. Each was deposited during a long-term, basin-wide transgressive-regressive (sea level rise and fall) cycle, and all stack to form a carbonate ramp complex spanning the entire WCSB.

Debolt lithologies range from intertidal dolomitic mudstones to open shelf packstones and wackestones, deposited within higher-order transgressive-regressive cycles. Reservoir quality can be good and an aquifer potentially suitable for carbon storage has been mapped in the Inga area. Reservoir is present to the north, but it is too shallow for storage. The entire ramp grades northwestward to outer ramp to basin margin lime mudstones.

Lower Mississippian Banff–Pekisko–Shunda

The uppermost Banff, as well as the Pekisko and Shunda lie at shallow depths (<750m) in the north and are too shallow to host injected CO_2 in the supercritical phase. As well, reservoir quality is generally poor.

The Banff Formation is a basinal to slope assemblage of shales and muddy limestones, deposited in stacked shallowing-upward successions. The overlying Pekisko and Shunda formations were each deposited during a long-term, basin-wide transgressive-regressive (sea level rise and fall) cycle (NEBC Play Atlas, 2006). Lithologies range from intertidal dolomitic mudstones to open shelf packstones and wackestones, deposited within higher-order transgressive-regressive cycles mappable within each formation. The entire ramp grades northwestward to outer ramp to basin margin lime mudstones.

Upper Devonian Wabamun

There is minor production from Wabamun-age sediments in NEBC. Given that most of the strata, outside of the few hydrocarbon pools, have poor quality reservoir, the Wabamun was not assessed for CO_2 injection for this Atlas.

During Late Devonian time, the Wabamun carbonate ramp complex prograded (sea level rose) northwestwards across the WCSB, reaching a north-south margin in NEBC. Ramp facies consist of stacked cleaning- and shallowing-upward successions, deposited during repeated transgressive-regressive cycles (NEBC Play Atlas, 2006). Regionally, these facies grade from highly restricted, evaporitic facies in southeastern Alberta to subtidal/open marine carbonate sands and nodular skeletal mudstones/wackestones in the eastern part of NEBC. Further west, the ramp grades to basinal shales of the Kotcho Formation.

Hydrothermally dolomitized and karsted Wabamun reservoirs occur where reservoir quality within the carbonate ramp has been enhanced by hydrothermal fluids. Extensional faulting associated with creation of the Fort St. John Graben complex in Early Mississippian time provided both structural traps and routes for admission of hydrothermal fluids.

Upper Devonian Jean Marie (Chapter 15)

The Jean Marie was deposited as a broad, shallow marine limestone shelf, under moderate energy conditions. It varies from 10–25m thick across NEBC and adjacent Alberta, thickening abruptly westward to a north-south-oriented shelf margin with a barrier reef that reaches over 90m in thickness. The Jean Marie shales out abruptly to the west of this reef. Overlying a basal crinoidal wackestone ramp, three transgressive-regressive (sea level rise and fall) cycles grade from relatively deep-water coralline limestones to shallower-water reefal facies (NEBC Play Atlas, 2006; McAdam, 1993). Patch reefs up to 100m across grew with relief of about 7m above the sea floor.

Redknife and Fort Simpson marine shales encase the Jean Marie, producing a closed reservoir system for both hydrocarbons and CO_2 injection.

Middle Devonian Slave Point–Sulphur Point–Keg River (Chapter 16)

The Middle Devonian carbonate complex, comprising the Slave Point, Sulphur Point and Keg River successions, is evaluated together in this study due the hydrodynamic connectivity of the units and the difficulty extracting proper stratigraphy where the carbonate units stack.

The Slave Point Formation was deposited in the early stages of a basin-wide sea level rise which ultimately drowned the Middle Devonian carbonate platforms of NEBC and Alberta (NEBC Play Atlas, 2006). Slave Point strata form a thick and complex carbonate platform, comprising several stacked shallowing-upward cycles. The lower cycles can be correlated regionally, and consist of nodular brachiopod-crinoid mudstones and wackestones with local carbonate bank developments. High-energy reefal carbonates were deposited primarily along platform-margin banks in upper Slave Point cycles, although some banks are found on the margins of the Hotchkiss Embayment to the south, and along lesser embayments within the main platform. Otter Park marine shales accumulated during Slave Point time in the Horn River and Cordova Embayments to the north, and within the Hotchkiss Embayment and smaller platform embayments to the south. Slave Point gas reservoirs are hosted within dolomitized reefal buildups, which grew on platform- and embayment-margin banks. Dense back-reef limestones and basinal shales provide effective lateral and top seals. Muskwa shales provide an upper seal for the Keg River to Slave Point carbonate succession.

The term Pine Point is used inconsistently to refer to the stacked complex or dolomitized Sulphur Point and/or Keg River and is therefore included in the evaluation. The Keg River Formation can be subdivided into lower and upper units. The lower unit consists of relatively deep-water platform carbonates, deposited near the beginning of a widespread transgressive (sea level rise) episode. Lower Keg River carbonates are typically dolomitized and underlie the entire carbonate complex in the northern portion of the study area. Upper Keg River strata consist of stacked shoaling-upward carbonate cycles, capped by high-energy skeletal/reefal debris. These banks reach thicknesses of more than 200m, and amalgamate with the Sulphur Point and Slave Point to form the dolomitized barrier reef at Clarke Lake. Isolated Upper Keg River buildups occur adjacent to the banks, their growth apparently nucleated over elevated fault blocks in the Horn River shale basin. The Keg River interfingers southward with Muskeg Formation evaporites, and basinward with marine shales of the Evie Formation.

Middle Devonian Gilwood

The Gilwood Formation encompasses Middle Devonian sandstone and conglomerate reservoirs that drape the Peace River Arch (PRA). Depositional environments ranged from alluvial plain to fan delta and shallow marine. There are few penetrations and relatively poor regional knowledge making the Gilwood a poor candidate for carbon storage. It was not evaluated for this Atlas.

Cambrian (Basal Sand–Undivided)

Clastics resting upon crystalline Precambrian basement in NEBC within the Hay River Embayment, north of the Peace-Athabasca Arch, are interpreted as Middle Cambrian in age. Cambrian sediments are not major hydrocarbon producers in the WCSB, with gas production from the Waterfowl Formation at Ram River, AB and natural gas and helium production from the Deadwood and other zones in southern Alberta and Saskatchewan. Elsewhere in Alberta and Saskatchewan, these basal sands are primary targets for carbon storage, but are not considered viable targets in NEBC due to unknown geological parameters and depositional extent as a result of poor well control.

Carbon Storage Calculations

In each chapter, the CO_2 storage potential has been estimated for depleted pools and saline aquifers. For depleted pools, these estimates were based on previous fluid production. For aquifers, the estimates were based on a percentage of the aquifer pore volume, which requires net reservoir thickness maps and porosity estimates. This appendix provides more detail regarding these calculations, as well as the equations used and assumptions made.

Depleted and Nearly Depleted Pools

The BC Oil and Gas Commission (BC OGC) defines depleted pools as ones that have no remaining reserves or production. The BC OGC also recognizes that there are nearly depleted pools that could become CO_2 storage candidates in the (relatively) near future. The nearly depleted CO_2 storage candidates include pools where 90+% of the reserves have been recovered, or no production has occurred in over five years.

The BC OGC excludes depleted pools as candidates for CO_2 storage when:

- The zones are deemed unconventional (DPR Schedule 2), such as the Heritage Montney, Northern Montney, Deep Basin Cadomin and Horn River Muskwa Evie Otter pools
- All the wells have been decommissioned with surface reclamation completed
- The true vertical depth (TVD) is less than 600m.

Canadian Discovery (CDL) has further refined the depleted and nearly depleted pool candidates by excluding:

- Pools shallower than 800m TVD. As mentioned previously, at depths below about 800m, natural temperatures and pressures tend to exceed the critical point of CO_2. In areas where this transition is deeper than 800m, pressure and temperature transitions have been indicated on the maps.
- Hydrocarbon pools that produced greater than or equal to 20% oil. These pools were categorized as candidates for future evaluation for carbon capture and utilization (CCUS) studies and enhanced oil recovery. In these scenarios, the CO_2 may need to be produced and re-injected, rather than injected for permanent, dedicated storage.
- Pools that are west of the Mesozoic deformation front, as that area hosts considerable faulting and potential risk. Some exceptions were made for depleted pools in the southern part of the study area that were proximal to emitting areas where few other options for storage are currently available.

Theoretical CO_2 Storage

The *theoretical* CO_2 storage potential of a depleted or nearly depleted pool represents the mass of CO_2 that can be stored in the depleted pool assuming that the volume occupied previously by the produced gas will be occupied entirely by the injected CO_2. These calculations were provided by the BC OGC and are based on historical pool production.

1. Obtain the total net voidage of the pool from total production/injection
2. Calculate the density of CO_2 at the pool reservoir conditions (T,P) using the Peng-Robinson Equation of State
3. Calculate the mass (Megatonnes) of CO_2 that can be held in this void space.

Assumptions for the analysis:

- Reservoir temperature and pressure are equal to initial values
  - » Temperature should return to initial
  - » Project approval likely to set maximum storage pressure at initial pressure
- Reservoir and fluid variables based on published BC OGC Reserves tables values
- CO_2 is pure and does not interact with other phases (mix or dissolve)
- CO_2 density follows the Peng-Robinson Equation of State.

Estimated Effective CO_2 Storage

CDL used the theoretical estimates from the BC OGC (MCO_2) to calculate the estimated *effective* CO_2 storage potential, which represents the mass of CO_2 that can be stored in hydrocarbon reservoirs after taking into account intrinsic reservoir characteristics and flow processes, such as heterogeneity (how much variability there is in the rock), aquifer support, sweep efficiency, gravity override, and CO_2 mobility (Bachu, 2006).

$$M_{CO_{2eff}} = C_m \cdot C_b \cdot C_h \cdot C_w \cdot C_a \cdot M_{CO_2} \quad (3)$$

$$C_{eff} = C_m \cdot C_b \cdot C_h \cdot C_w \quad (4)$$

MCO_{2eff} is the estimated effective reservoir potential for CO_2 storage, and the subscripts of m, b, h, w and a represent the effects of mobility, buoyancy, heterogeneity, water saturation, and aquifer strength on the storage coefficient. For gas reservoirs, fingering and buoyancy effects would likely be very small to negligible, and the effect of water saturation is implicitly taken into account in the theoretical storage potential, therefore Cm, Cb and Cw will likely be close to one (Bachu, 2006). The degree of aquifer support, Ca, was estimated from the production data as per Bachu (2006). The estimated effective CO_2 storage potential reduces the theoretical storage potential by as little as 13% and as much as 75%.

At the end of each chapter, both the depleted and nearly depleted pools that are deemed to be CO_2 storage candidates by CDL are coloured by their estimated effective storage potential mass on a summary map. *Figure 1.5* in the *Executive Summary* shows the distribution of depleted and nearly depleted pools with greater than 5 Mt over the Atlas study area.

Aquifers

For aquifers, a *theoretical* CO_2 storage potential can be calculated using the mapped pore volume of the reservoir and CO_2 density, and assumes that the pore volume will be occupied entirely by the injected CO_2. We know this is not the case however, since the pore space is already occupied by water and the water will need to be displaced in the process. As a result, a *storage efficiency* factor is introduced into storage potential calculations that accounts for the presence of both water and CO_2 in the aquifer.

The NETL Carbon Storage Atlas (2015) uses the following method of estimating the CO_2 storage resource estimate potential in saline formations:

$$M_{CO2eff} = A_t \cdot h_g \cdot \phi_{est} \cdot \rho_{CO2}\ E_{saline}$$

Where MCO_{2eff} is the estimated effective CO_2 storage estimate, A_t is the total area, h_g is the formation thickness, ϕ_{est} is the total porosity, ρ_{CO2} is the CO_2 density at reservoir conditions, and E_{saline} is the storage efficiency factor. The storage efficiency factor is a function of reservoir and fluid properties and dynamics, including the geometry of the trap, gravity segregation, heterogeneity, permeability distribution and pressure, and may reduce the theoretical storage potential by anywhere from 95 to 99%.

It should be noted that aquifer storage estimates in this Atlas are extremely high level and intended for identifying areas in northeastern BC with the most storage potential. Many of the factors in this calculation currently contain significant uncertainty, and more work is required to properly quantify the storage in areas showing the most storage potential.

The *net reservoir* contours, which represent h_g within the saline aquifers, were primarily sourced from existing studies, and since CDL did not complete the mapping they cannot attest to the quality and consistency of all interpretations. CDL has gridded the contours from these datasets and provided geological support to fill in any gaps, using similar cutoffs to what was used in the existing data set. Due to time limitations, CDL correlations in gap areas were often limited to wells containing wet DSTs, which suggests that an aquifer is present in the area, and/or logs from nearby wells of sufficient quality to make correlations; therefore the extent and quality of the reservoir contains a high level of uncertainty.

The largest source of error is currently the *porosity distribution*. Detailed mapping of porosity trends requires examination of log suites and petrophysical models, both of which are beyond the scope of this phase of the Atlas. Available core data were used to provide a quick, high-level estimate of porosity trends, as an estimate is needed for storage potential calculations. The core data were filtered to avoid non-reservoir and then aggregated to estimate porosity trends in the aquifers. Note that uneven core distribution and biased sampling introduces error into these estimates. In areas showing good storage potential, detailed mapping of the porosity trends should be initiated to better quantify available pore volume within the reservoir and reservoir continuity.

Absolute pressure and temperature values are needed to determine the *CO_2 density* (ρ_{CO2}) at reservoir conditions from equations of state (Span and Wagner, 1996). The CO_2 densities were calculated using a web computation tool (Wischnewski, 2007). The temperature is determined by multiplying the total vertical depth for each formation by CDL's in-house geothermal gradient, assuming a surface temperature of 5°C. Hydrofax drillstem test (DST) data from within the aquifers and pressure-depth ratio mapping from previous studies were combined to create pressure-depth ratio maps. The pressure-depth ratio was multiplied by the total vertical depth to obtain an absolute pressure at depth.

Net reservoir, average porosity, and reservoir temperature and pressure were extracted to a 1500m x 1500m point grid within the study area, and a CO_2 density was determined for each grid cell point. Using the 225 ha area, a theoretical storage potential (M_{CO2}) was calculated for each cell using the equation:

$$M_{CO2} = A_t \cdot h_g \cdot \phi_{est} \cdot \rho_{CO2}$$

In areas where drillstem tests (DSTs) showed significant water recovery, and cells exhibited sufficient net reservoir and porosity, a theoretical CO_2 storage potential was calculated in Megatonnes (Mt).

To determine an estimated effective storage potential, an E_{saline} or storage efficiency factor was applied. The values used were similar to those in the Third, Fourth and Fifth editions of U.S. DOE-NETL CCS Atlas publications (2010, 2012, 2015) of 0.5% for the 10^{th} percentile, 2.0% for the 50^{th} percentile, and 5.4% for the 90^{th} percentile. It should be noted, however, that there are a wide range of static E_{saline} numbers available in literature; some are very small, which better reflect large-scale long term storage, and others are larger values that better represent local plume migration on a shorter timescale. Ideally, any numbers used in planning a project should be tested and verified by simulation, which is able to capture dynamic aspects of plume migration.

The total effective storage potential of each aquifer was then estimated (at the P10, P50 and P90 levels) by summing the effective storage potential for each cell point in the aquifer. ArcGIS was used to add all the aquifers from all the formations together, i.e. to stack the aquifers, to arrive at a total effective storage potential in Mt for each 1,500m x 1,500m cell in the NEBC study area *(figure 1.4 in the Executive Summary)*.

Aquifers considered favourable targets for CO_2 storage are indicated on the summary map in each chapter and labelled with their estimated P10, P50 and P90 estimated effective storage potential in Mt.

POOL STORAGE DATABASE (DIGITAL)

Digital Only

This Appendix is digital only, provided in Excel format, and includes the following:

- Current CO_2 Storage Candidates (Depleted, Nearly Depleted and Inactive Gas Pools included in Storage Estimates)
- Future CO_2 Storage Candidates (Gas Pools not yet 90% Depleted)
- Oil Pools for Future CO_2-EOR Evaluation
- Aquifer Storage Summary

Data provided by the BC OGC and Canadian Discovery Ltd.

Executive Summary, Carbon Capture and Storage and Hydrogen

- B.C. Hydrogen Strategy. 2021 https://www2.gov.bc.ca/assets/gov/farming-natural-resources-and-industry/electricity-alternative-energy/electricity/bc-hydro-review/bc_hydrogen_strategy_final.pdf
- BCOGC. 2010. Drilling and Production Regulation (DPR): Schedule 2.
- BCOGC. 2019. https://www.bcogc.ca/files/operations-documentation/Reservoir-Management/Subsurface-Disposal/activedisposalwellsoverview201918x24.pdf
- CleanBC. 2018. Cleaner Industry. https://www2.gov.bc.ca/gov/content/environment/climate-change/industry
- CleanBC. 2021. Provincial greenhouse gas emissions inventory. https://www2.gov.bc.ca/gov/content/environment/climate-change/data/provincial-inventory
- Donaldson, W.S. 2021. Carbon Capture and Storage: Criteria for Success Part I. https://digest.canadiandiscovery.com/article/8428
- Donaldson, W.S. 2021. Carbon Capture and Storage: Criteria for Success Part II. https://digest.canadiandiscovery.com/article/8429
- FECM. 2022 https://www.energy.gov/fecm/events/2022-carbon-management-project-review-meeting-0
- Global CCS Institute, 2018. Fact Sheet – Capturing CO_2. https://www.globalccsinstitute.com/resources/
- Government of Canada. 2022. Canada's climate plans and targets. https://www.canada.ca/en/services/environment/weather/climatechange/climate-plan/climate-plan-overview.html
- Gunnarsson, I., Aradóttir, E. S., Oelkers, E. H., Clark, D. E., Arnarson, M. Þ., Sigfússon, B., Snæbjörnsdóttir, S. Ó., Matter, J. M., Stute, M., Júlíusson, B. M., and Gíslason, S. R. 2018. The rapid and cost-effective capture and subsurface mineral storage of carbon and sulfur at the CarbFix2 site: International Journal of Greenhouse Gas Control, v. 79, p. 117-126
- Hares, R., McCoy, S., and Layzell, D. 2022. Review of Carbon Dioxide in Western Canada: Blue Hydrogen Roadmap to 2050. In Transition Accelerator Reports Volume 4, Issue 6
- International Energy Association Greenhouse Gas R&D Programme (IEAGHG). 2019. IEAGHG, "The Shell Quest Carbon Capture and Storage Project", 2019/04, September 2019.
- IPCC. 2005. Special Report on Carbon Dioxide Capture and Storage. Chapter 3 – Capture of CO_2.
- IPCC. 2005. Special Report on Carbon Dioxide Capture and Storage. Chapter 3 – Transport of CO_2.
- Keith, D.W. et al. 2018. A Process for Capturing CO_2 from the Atmosphere. Published in Joule, Volume 2, Issue 8.
- National Energy Technology Laboratory (NETL). 2021. Carbon Storage FAQS. Accessed August 2022 https://www.netl.doe.gov/coal/carbon-storage/faqs/carbon-storage-faqs
- National Petroleum Council. 2019a. Meeting the Dual Challenge. A Roadmap to At-Scale Deployment of Carbon Capture, Use, and Storage. Chapter Five – CO_2 Capture.
- National Petroleum Council. 2019b. Meeting the Dual Challenge. A Roadmap to At-Scale Deployment of Carbon Capture, Use, and Storage. Chapter Six – CO_2 Transport.
- National Energy Technology Laboratory (NETL). 2015. Carbon Storage Atlas, 5th Edition. 114p
- PCOR Partnership Atlas. 2021. 120p.
- Princeton University. 2022. Definition of viscosity. https://www.princeton.edu/~gasdyn/Research/T-C_Research_Folder/Viscosity
- Society of Petroleum Engineers (SPE). 2022. Carbon Dioxide Storage Resource Management System (SRMS) Guidelines.
- Swiss Federal Office of Energy (SFOE). 2021. Feasibility Study for Proposed CO_2 Circulation Test at the Aquistore Injection Site, Saskatchewan.
- US Department of Fossil Energy and Carbon Management. https://www.energy.gov/fecm/science-innovation/carbon-capture-and-storage-research/carbon-capture-rd/pre-combustion-carbon
- Vox. 2019. https://www.vox.com/energy-and-environment/2019/10/2/20838646/climate-change-carbon-capture-enhanced-oil-recovery-eor

Formation Chapters

Canadian Discovery Ltd. In-House Studies

- Canadian Discovery Ltd. 2019. Geothermics Internal Repository (GTIR)
- Canadian Discovery Ltd. 2019. Montney Hydrodynamics Project III (MRHS-III)
- Canadian Discovery Ltd. 2019. Montney Internal Repository (MNIR)
- Canadian Discovery Ltd. 2019. Geothermics Internal Repository (GTIR)
- Canadian Discovery Ltd. 2015. Characterization of Belloy/Debolt Water Disposal Zones in the Montney Fairway (GCWD)
- Canadian Discovery Ltd. 2015. Mid-Devonian Hydrothermal Evaluation (GCGT)
- Canadian Discovery Ltd. 2014. Charlie Lake Hydrodynamics (CLHS)
- Canadian Discovery Ltd. 2012. Hydrodynamic Study of the Upper Devonian Wabamun to Lower Mississippian Banff (DCDH)
- Canadian Discovery Ltd. 2009. Mid-Devonian Carbonate Bank Complex Hydrogeology (SPKR)
- Canadian Discovery Ltd. 2009. Doig Hydrogeology (DRHS)
- Canadian Discovery Ltd. 2006. Strategy 2005: Geology and Metrics for 108 Plays (S2K5)
- CDL. Rakhit Petroleum Consulting Ltd. 2005. Jean Marie Hydrodynamics II (JMHD-II)
- CDL. Rakhit Petroleum Consulting Ltd. 2002. Deep Basin Regional Hydrodynamics: Cardium to Cadomin (DBGR)
- CDL. Rakhit Petroleum Consulting Ltd. 2001. Cadomin Hydrodynamic Evaluation II (AXCN)
- CDL. Rakhit Petroleum Consulting Ltd. 2001. Deep Basin Hydrodynamics: Paddy/Cadotte, Bluesky and Cadomin (DBCR)
- CDL. Rakhit Petroleum Consulting Ltd. 1999. Baldonnel Geology and Hydrogeology (BCBL) BC Geological Carbon Storage Assessment 126 See the energy at TGS.com
- CDL. Rakhit Petroleum Consulting Ltd. 1999. Bluesky, Gething and Montney Hydrogeological Evaluation (BMCA)
- CDL. Rakhit Petroleum Consulting Ltd. 1995. Permocarboniferous Hydrogeology (BCPC)

Engineering References

- Bachu, S. 2006. The Potential for Geological Storage of Carbon Dioxide in NE British Columbia. BC Ministry of Energy, Mines and Petroleum Resources.
- Bachu, S. 2015. Review of CO_2 Storage Efficiency in Deep Saline Aquifers. International Journal of Greenhouse Gas Control.
- BCOGC. Pool Designation Areas [BCOGC-44631] https://databcogc.opendata.arcgis.com/datasets
- BCOGC. Pool Contours [BCOGC-44827] https://databcogc.opendata.arcgis.com/datasets
- BCOGC. 2020 Oil and Gas Reserves. https://www.bcogc.ca/data- reports/reservoirmanagement/reserves/
- British Columbia Ministry of Energy and Mines and Petroleum Resources, National Energy Board. Northeast British Columbia's Ultimate Potential for Natural Gas., Report 2006A.
- DOE-NETL. 2015. Carbon Storage Atlas, Fifth Edition. US Department of Energy Office of Fossil Energy, National Energy Technology Laboratory.
- DOE-NETL. 2012. The United States Carbon Storage Atlas, Fourth Edition. US Department of Energy Office of Fossil Energy, National Energy Technology Laboratory.
- DOE-NETL. 2010. The Carbon Sequestration Atlas of the United States and Canada, Third Edition. US Department of Energy Office of Fossil Energy, National Energy Technology Laboratory.
- Hartley, A., 2008. Carbon capture and storage in British Columbia; in Geoscience Reports 2008, BC Ministry of Energy, Mines and Petroleum Resources, pages 25-31.
- Plains CO_2 Reduction Partnership (PCOR). 2014. Fort Nelson Carbon Capture and Storage Feasibility Study.
- Span, R. and Wagner, W. (1996) A New Equation of State for Carbon Dioxide Covering the Fluid Region from the Triple Point Temperature to 1100 K at Pressures up to 800 MPa. Journal of Physical and Chemical Reference Data, 25, 1509-1596.
- Wischnewski, B. 2007. Calculation of thermodynamic state variables of carbon dioxide. https://www.peacesoftware.de/einigewerte/co2_e.html

- Barclay, J.E., G.D. Holmstrom, P.J. Lee, R.I. Campbell, and G.E. Reinson. 1997. Carboniferous and Permian gas resources of the Western Canada Sedimentary Basin, Interior Plains. Geological Survey of Canada Bulletin 515.
- Barclay, J.E., F.F. Krause, R.I. Campbell, and J. Utting. 1990. Dynamic casting and growth faulting: Dawson Creek Graben Complex, Carboniferous-Permian Peace River Embayment, western Canada. Bulletin of Canadian Petroleum Geology, v. 38A, p. 115-145.
- Barss, D.L. and Montanon, F.A. 1981. Sukunka-Bullmoose gas fields: models for a developing trend in the southern Foothills of northeast British Columbia. Bulletin of Canadian Petroleum Geology, v. 29, p. 293-333.
- Berger, Z., Boast, M., and Mushayandebvu, M., 2008. The Contribution of Integrated HRAM Studies to Exploration and Exploitation of Unconventional Plays in North America. CSPG Reservoir Issue 10, November 2008.
- Bloy, G. and Scott, B. 1993. Characterization of the Belloy Formation Reservoir, Bamdary Lake Pool, Northeastern British Columbia. Carboniferous to Jurassic Pangea=Core Workshop Guidebook.
- British Columbia Ministry of Energy, Mines and Petroleum Resources. Oil and Gas Division Resource Development and Geoscience Branch. Conventional Natural Gas Play Atlas, Northeast British Columbia. 2006. Petroleum Geology Publication 2006-01.
- Davies, G.R. 1997a. The Upper Triassic Baldonnel and Pardonet formations, Western Canada Sedimentary Basin. Bulletin of Canadian Petroleum Geology, v 45, #4, p. 643-674.
- Davies, G.R. 1997b. The Triassic of the Western Canada Sedimentary Basin: tectonic and stratigraphic framework, paleogeography, paleoclimate and biota. Bulletin of Canadian Petroleum Geology, v 45, #4, p. 434-460.
- Davies, G.R., T.F. Moslow and M.D. Sherwin. 1997. The Lower Triassic Montney Formation, west-central Alberta. Bulletin of Canadian Petroleum Geology, v. 45, #4, p. 474-505.
- Durocher, S., and I.S. Al-Aasm. 1997. Dolomitization and Neomorphism of Mississippian (Visean) Upper Debolt Formation, Blueberry Field, Northeastern British Columbia: Geologic, Petrologic and Chemical Evidence. AAPG Bulletin, v. 81, #6, p. 954-977.
- Dawson, F.M., C. Evans, R. Marsh, and B. Richardson. 1994. Uppermost Cretaceous and Tertiary strata of the Western Canada Sedimentary Basin. In: Geological Atlas of the Western Canada Sedimentary Basin. Mossop G. and Shetsen, I. (compilers). Calgary, Canadian Society of Petroleum Geologists, Alberta Research Council.
- Edwards, D., Barclay, J., Gibson, D., Kvill, G., and Halton, E. 1994. Triassic Strata of the Western Canada Sedimentary Basin Fig. 16.7. In: Geological Atlas of the Western Canada Sedimentary Basin. Mossop G. and Shetsen, I. (compilers). Calgary, Canadian Society of Petroleum Geologists, Alberta Research Council.
- Geological Atlas of the Western Canada Sedimentary Basin. G.D. Mossop and I. Shetsen (compilers). 1994. Calgary, Canadian Society of Petroleum Geologists / Alberta Research Council.
- Hayes, B., Christopher, J., Rosenthal, L., Los, G., and McKercher, B. 1994. Cretaceous Mannville Group of the Western Canada Sedimentary Basin. In: Geological Atlas of the Western Canada Sedimentary Basin. Mossop G. and Shetsen, I. (compilers). Calgary, Canadian Society of Petroleum Geologists, Alberta Research Council.
- Leckie, D.A., J.P. Bhattacharya, J. Bloch, C.F. Gilboy, and B. Norris. 1994. Cretaceous Colorado / Alberta Group of the Western Canada Sedimentary Basin. In: Geological Atlas of the Western Canada Sedimentary Basin. Mossop G. and Shetsen, I. (compilers). Calgary, Canadian Society of Petroleum Geologists, Alberta Research Council.
- Leckie, D.A., and C. Singh. 1991. Estuarine deposits of the Albian Paddy Member (Peace River Formation) and lowermost Shaftesbury Formation, Alberta, Canada. Journal of Sedimentary Petrology, v. 61, #5, p. 825-849.
- Leggett, S., R. Young, and D. Eibenschutz. 1993. Facies of the Belloy Formation (Lower Permian), northeastern British Columbia. Core workshop guidebook, Canadian Society of Petroleum Geologists Carboniferous to Jurassic Pangaea Conference, p. 88-108.
- McAdam, K., 1993. The Jean Marie Member in the Hossitl-Ring area, British Columbia. Petroleum Geology Branch; Ministry of Energy, Mines and Petroleum Resources, Special Paper 1993-1.
- Meijer-Drees, N.C. 1994. Devonian Elk Point Group of the Western Canada Sedimentary Basin. In: Geological Atlas of the Western Canada Sedimentary Basin. Mossop G. and Shetsen, I. (compilers). Calgary, Canadian Society of Petroleum Geologists, Alberta Research Council.
- Ministry of Energy and Mines Petroleum Geology. 2003. Exploration Assessment of Deep Devonian Gas Plays, Northeast British Columbia.
- Morrow, D.W., M. Zhao, and L.D. Stasiuk. 2002. The gas-bearing Devonian Presqu'ile Dolomite of the Cordova Embayment region of British Columbia, Canada: dolomitization and the stratigraphic template. American Association Petroleum Geologists Bulletin, v. 86, #9, p. 1609-1638.
- Mossop G. and Shetsen, I. (compilers) 1994. Geological Atlas of the Western Canada Sedimentary Basin. Canadian Society of Petroleum Geologists, Alberta Research Council.
- NEBC Play Atlas, 2006. British Columbia Ministry of Energy, Mines and Petroleum Resources. Oil and Gas Division Resource Development and Geoscience Branch Conventional Natural Gas Play Atlas Northeast British Columbia. Petroleum Geology Publication 2006.

- O'Connell, S. C., Dix, G. R., & Barclay, J. E. 1990. The origin, history, and regional structural development of the Peace River Arch, Western Canada. Bulletin of Canadian Petroleum Geology, 38(1), 4-24.
- Petrel Robertson Consulting Ltd. (PRCL) and Canadian Discovery Ltd. 2011. Deep subsurface aquifer characterization in support of Montney tight gas development; Geoscience BC Report 2011-11. http://www.geosciencebc.com/reports/gbcr-2011-11/
- Petrel Robertson Consulting Ltd. (PRCL) and Canadian Discovery Ltd. 2015. Characterization of Belloy and Debolt water disposal zones in the Montney play fairway, Northeast BC; Geoscience BC Report 2015-03. https://www.geosciencebc.com/majorprojects/deep-aquifer-fluid-disposal
- Petrel Robertson Ltd. (PRCL). 2021. Wastewater Disposal in the Maturing Montney Play Fairway of NEBC . Geoscience BC Report 2021-14: https://www.geosciencebc.com/projects/2019-004/
- Reinson, G.E., P.J. Lee, W. Warters, K.G. Osadetz, L.L. Bell, P.R. Price, F. Trollope, R.I. Campbell, and J.E. Barclay. 1993. Devonian gas resources of the Western Canada Sedimentary Basin. Geological Survey of Canada Bulletin 452.
- Reinson, G., Warters, W., Cox, J., and Price, P., 1994, Chapter 21: Cretaceous Viking Formation of the Western Canada Sedimentary Basin. In: Geological Atlas of the Western Canada Sedimentary Basin. Mossop G. and Shetsen, I. (compilers). Calgary, Canadian Society of Petroleum Geologists, Alberta Research Council
- Richards, B.C., J.E. Barclay, D. Bryan, A. Hartling, C.M. Henderson and R.C. Hinds. 1994. Carboniferous strata of the Western Canada Sedimentary Basin. In: Geological Atlas of the Western Canada Sedimentary Basin. Mossop G. and Shetsen, I. (compilers). Calgary, Canadian Society of Petroleum Geologists, Alberta Research Council.
- Smith, D.G., Zorn, C.E., and Sneider, R.M. 1984. The paleogeography of the Lower Cretaceous Mannville Group in Western Canada. In: Elmworth-Case Study of a Deep Basin Gas Field. Masters, J. (ed.). American Association of Petroleum Geologists, Memoir 38, p. 79-114.
- Sorensen, J., Gorecki, C., Steadman, E. 2014. Fort Nelson Test Site Characterization Report, Energy and Environmental Research Center, 2014-EERC-03-02.
- Stott, D.F. 1975. The Cretaceous System in northeastern British Columbia. In: The Cretaceous System of western North America, edited by W.G.E. Caldwell. Geological Association of Canada Special Paper 13, p. 441-467.
- Switzer, S.B., W.G. Holland, D.S. Christie, G.C. Graf, A.S. Hedinger, R.J. McAuley, R.A. Wierzbicki, J.A. Packard. 1994. Devonian Woodbend-Winterburn strata of the Western Canada Sedimentary Basin. In: Geological Atlas of the Western Canada Sedimentary Basin. Mossop G. and Shetsen, I. (compilers). Calgary, Canadian Society of Petroleum Geologists, Alberta Research Council.
- Walsh, W. 2013. Geothermal resource assessment of the Clarke Lake Gas Field, Fort Nelson, British Columbia. Bulletin of Canadian Petroleum Geology. 61. 241-251. 10.2113/gscpgbull.61.3.241.
- Warters, W., Cant, D., Tzeng, H., and Lee, P. 1997 Mannville Gas Resources of the Western Canada Sedimentary Basin. Geological Survey of Canada Bulletin 517 p.15-21.
- WCSB Atlas, 1994. Atlas of the Western Canada Sedimentary Basin, Downloadable Content/Atlas Shapefiles. https://ags.aer.ca/reports/atlas-western-canada-sedimentary-basin.
- Wright, G.N., McMechan, M.E. and Potter, D.E.G. 1994. Structure and Architecture of the Western Canada Sedimentary Basin. Chapter 3. In: Geological Atlas of the Western Canada Sedimentary Basin. Mossop G. and Shetsen, I. (compilers). Calgary, Canadian Society of Petroleum Geologists, Alberta Research Council. p. 25-40.

Appendix E MAPS, SHAPEFILES AND LIST OF FIGURES

All formation maps and shapefiles are provided digitally.

The following maps are provided:

- NEBC Atlas Study Area CO_2 Emitters and Transportation Infrastructure
- All Units Pool Candidates 5 Mt Effective CO_2 Storage Potential
- NEBC Atlas Study Area Stacked Aquifers P5 CO_2 Effective Storage Potential
- Effective CO_2 Storage Potential Recommended Areas of Focus

The following maps are provided for each formation chapter: (if applicable):

- Emitters, Infrastructure and Formation Effective CO_2 Storage Potential
- Subsea Structure (excluding Spirit River, Charlie Lake and Jean Marie)
- Aquifer Net Reservoir (excluding Spirit River, Charlie Lake and Jean Marie)
- Pools Net Reservoir
- Aquifers and Pool Candidates Effective CO_2 Storage Potential

Shapefiles provided for formations (if applicable):

- 7500 Kpa Absolute Pressure Line
- Isotherm 31 Degrees
- Aquifer Outlines
- Aquifer Net Reservoir
- Pool Candidates
- Pool Non-Candidates
- Commingles Pool Candidates
- Pool Net Reservoir
- Structure Elevation
- TVD 800m Line

List of Figures

Chapter 1 Executive Summary

Figure 1.1 NEBC Atlas Study Area, CO_2 Emitters and Transportation Infrastructure
Figure 1.2 Estimated Effective Storage Potential in Depleted Pools
Figure 1.3 Estimated Effective Storage Potential in Saline Aquifers
Figure 1.4 NEBC Study Area Stacked Aquifers P50 CO_2 Effective Storage Potential
Figure 1.5 All Units Pool Candidates >5 Mt Effective CO_2 Storage Potential

Chapter 2 Carbon Capture and Storage Basics

Figure 2.1 Direct Air Capture Plant
Figure 2.2 Post-Combustion Capture
Figure 2.3 CO_2 Transpotation via Pipeline
Figure 2.4 Options for Storing CO_2
Figure 2.5 Subsurface CO_2 Trapping Mechanisms
Figure 2.6 CO_2 Trapping Over Time in Saline Formations and Depleted Oil and Gas Reservoirs
Figure 2.7 Shell Quest Project Area
Figure 2.8 Aquistore Location Map

Chapter 3 Carbon Storage Project Considerations

Figure 3.1 Pressure Effects on CO_2
Figure 3.2 NEBC Atlas Study Area Major Faults and Structural Elements

Chapter 4 Atlas Overview

Figure 4.1 Hydrostratigraphic Chart

Chapter 5 Peace River

Figure 5.1 Hydrostratigraphic Chart
Figure 5.2 Top 10 Depleted Peace River Pools
Figure 5.3 Emitters, Infrastructure and Peace River Effective CO_2 Storage Potential
Figure 5.4 Peace River Play Schematic
Figure 5.5 Peace River Subsea Structure
Figure 5.6 Peace River Aquifer Net Reservoir
Figure 5.7 Peace River Pools Net Reservoir
Figure 5.8 Peace River Porosity-Permeability Plot
Figure 5.9 Peace River Pressure vs Elevation Plot
Figure 5.10 Peace River Aquifers and Pool Candidates Effective CO_2 Storage Potential

Chapter 6 Spirit River

Figure 6.1 Hydrostratigraphic Chart
Figure 6.2 Top 10 Depleted Spirit River Pools
Figure 6.3 Emitters, Infrastructure and Spirit River Effective CO_2 Storage Potential
Figure 6.4 Spirit River Play Schematic
Figure 6.5 Spirit River Pools Net Reservoir
Figure 6.6 Spirit River Pool Candidates Effective CO_2 Storage Potential

Chapter 7 Bluesky

Figure 7.1 Hydrostratigraphic Chart
Figure 7.2 Top 10 Depleted Bluesky Pools
Figure 7.3 Emitters, Infrastructure and Bluesky Effective CO_2 Storage Potential
Figure 7.4 Bluesky Play Schematic
Figure 7.5 Bluesky Subsea Structure
Figure 7.6 Bluesky Aquifer Net Reservoir
Figure 7.7 Bluesky Pools Net Reservoir

Figure 7.8 Bluesky Porosity-Permeability Plots
Figure 7.9 Bluesky Pressure vs Elevation Plot
Figure 7.10 Bluesky Aquifers and Pool Candidates Effective CO_2 Storage Potential

Chapter 8 Cadomin-Gething

Figure 8.1 Hydrostratigraphic Chart
Figure 8.2 Top 10 Depleted Cadomin-Gething Pools
Figure 8.3 Emitters, Infrastructure and Cadomin-Gething Effective CO_2 Storage Potential
Figure 8.4 Cadomin-Gething Play Schematic
Figure 8.5 Cadomin Subsea Structure
Figure 8.6 Cadomin Aquifer Net Reservoir
Figure 8.7 Cadomin-Gething Pools Net Reservoir
Figure 8.8 Cadomin-Gething Porosity-Permeability Plot
Figure 8.9 Cadomin-Gething Pressure vs Elevation Plot
Figure 8.10 Cadomin Aquifers and Cadomin-Gething Pool Candidates Effective CO_2 Storage Potential

Chapter 9 Nikanassin-Dunlevy

Figure 9.1 Hydrostratigraphic Chart
Figure 9.2 Top 10 Depleted Nikanassin-Dunlevy Pools
Figure 9.3 Emitters, Infrastructure and Nikanassin-Dunlevy Effective CO_2 Storage Potential
Figure 9.4 Nikanassin-Dunlevy Play Schematic
Figure 9.5 Nikanassin Subsea Structure
Figure 9.6 Nikanassin-Dunlevy Aquifer Net Reservoir
Figure 9.7 Nikanassin-Dunlevy Pools Net Reservoir
Figure 9.8 Nikanassin-Dunlevy Porosity-Permeability Plot
Figure 9.9 Nikanassin-Dunlevy Pressure vs Elevation Plot
Figure 9.10 Nikanassin-Dunlevy Aquifer and Pool Candidates Effective CO_2 Storage Potential

Chapter 10 Baldonnel-Pardonet

Figure 10.1 Hydrostratigraphic Chart
Figure 10.2 Top 10 Depleted Baldonnel-Pardonet Pools
Figure 10.3 Emitters, Infrastructure and Baldonnel-Pardonet Effective CO_2 Storage Potential
Figure 10.4 Baldonnel-Pardonet Play Schematic
Figure 10.5 Baldonnel Subsea Structure
Figure 10.6 Baldonnel Aquifer Net Reservoir
Figure 10.7 Baldonnel-Pardonet Pools Net Reservoir
Figure 10.8 Baldonnel-Pardonet Porosity-Permeability Plot
Figure 10.9 Baldonnel-Pardonet Pressure vs Elevation Plot
Figure 10.10 Baldonnel-Pardonet Aquifer and Pool Candidates Effective CO_2 Storage Potential

Chapter 11 Charlie Lake

Figure 11.1 Hydrostratigraphic Chart
Figure 11.2 Top 10 Depleted Charlie Lake Pools
Figure 11.3 Emitters, Infrastructure and Charlie Lake Effective CO_2 Storage Potential
Figure 11.4 Charlie Lake Play Schematic
Figure 11.5 Charlie Lake Pools Net Reservoir
Figure 11.6 Charlie Lake Pool Candidates Effective CO_2 Storage Potential

Chapter 12 Halfway

Figure 12.1 Hydrostratigraphic Chart
Figure 12.2 Top 10 Depleted Halfway Pools
Figure 12.3 Emitters, Infrastructure and Halfway Effective CO_2 Storage Potential
Figure 12.4 Halfway Play Schematic
Figure 12.5 Halfway Subsea Structure
Figure 12.6 Halfway Aquifer Net Reservoir

Figure 12.7 Halfway Pools Net Reservoir
Figure 12.8 Halfway Porosity-Permeability Plot
Figure 12.9 Halfway Pressure vs Elevation Plot
Figure 12.10 Halfway Aquifer and Pool Candidates Effective CO_2 Storage Potential

Chapter 13 Belloy

Figure 13.1 Hydrostratigraphic Chart
Figure 13.2 Top 10 Depleted Belloy Pools
Figure 13.3 Emitters, Infrastructure and Belloy Effective CO_2 Storage Potential
Figure 13.4 Belloy Play Schematic
Figure 13.5 Belloy Subsea Structure
Figure 13.6 Belloy Aquifer Net Reservoir
Figure 13.7 Belloy Pools Net Reservoir
Figure 13.8 Belloy Porosity-Permeability Plot
Figure 13.9 Belloy Pressure vs Elevation Plot
Figure 13.10 Belloy Aquifers and Pool Candidates Effective CO_2 Storage Potential

Chapter 14 Debolt

Figure 14.1 Hydrostratigraphic Chart
Figure 14.2 Top 10 Depleted Debolt Pools
Figure 14.3 Emitters, Infrastructure and Debolt Effective CO_2 Storage Potential
Figure 14.4 Debolt Play Schematic
Figure 14.5 Debolt Subsea Structure
Figure 14.6 Debolt Aquifer Net Reservoir
Figure 14.7 Debolt Pools Net Reservoir
Figure 14.8 Debolt Porosity-Permeability Plot
Figure 14.9 Debolt Pressure vs Elevation Plot
Figure 14.10 Debolt Aquifers and Pool Candidates Effective CO_2 Storage Potential

Chapter 15 Jean Marie

Figure 15.1 Hydrostratigraphic Chart
Figure 15.2 Depleted Jean Marie Pools
Figure 15.3 Emitters, Infrastructure and Jean Marie Effective CO_2 Storage Potential
Figure 15.4 Jean Marie Play Schematic
Figure 15.5 Jean Marie Pools Net Reservoir
Figure 15.6 Jean Marie Pool Candidates Effective CO_2 Storage Potential

Chapter 16 Middle Devonian Carbonates

Figure 16.1 Hydrostratigraphic Chart
Figure 16.2 Top 10 Depleted Middle Devonian Carbonates Pools
Figure 16.3 Emitters, Infrastructure and Middle Devonian Carbonates Effective CO_2 Storage Potential
Figure 16.4 Middle Devonian Carbonates Play Schematic
Figure 16.5 Middle Devonian Carbonates Subsea Structure
Figure 16.6 Middle Devonian Aquifer Net Reservoir
Figure 16.7 Middle Devonian Pools Net Reservoir
Figure 16.8 Middle Devonian Carbonates Porosity-Permeability Plot
Figure 16.9 Middle Devonian Carbonates Pressure vs Elevation Plot
Figure 16.10 Middle Devonian Carbonates Aquifers and Pool Candidates Effective CO_2 Storage Potential

Chapter 17 Recommendations

Figure 17.1 Effective CO_2 Storage Potential Recommended Areas of Focus
Figure 17.2 Basins for Future Evaluation

Figure A.1 NEBC Stratigraphic Columns